A Burning Question:

Structural and Isotopic Studies of Cremated Bone in Archaeological Contexts

Christophe Snoeck

Merton College

Research Laboratory for Archaeology and the History of Art

University of Oxford

Trinity Term 2014

A Thesis presented to the University of Oxford in partial fulfilment of

the requirements for the Degree of Doctor of Philosophy

To Kristin Bartik

Who sparked my *Burning Question*

&

To my parents, Karine and Georges, and my sisters, Charlotte and Laurence

For believing in me

Acknowledgments

I owe a great debt of gratitude to my supervisors, Rick Schutling and Julia Lee-Thorp. Without their guidance, encouragements, and expertise, this thesis would not have been written.

I have also greatly benefitted in the course of my DPhil from the advice and help of Fiona Brock, Maura Pellegrini, Richard Staff, Mark Pollard, Tom Higham, Christopher Bronk Ramsey, Peter Ditchfield, Mike Dee, Angela Bowles, Barbara Emery and Jane Davies from the Research Laboratory of Archaeology and the History of Art, University of Oxford. I offer special thanks to Nadine Mattielli, Wendy Debouge and Jeroen de Jong for receiving me at the G-Time Laboratory (Géochimie: Traçage isotopique, minéral et élémentaire) of the Université Libre de Bruxelles (Belgium) where I could carry out strontium isotope analyses on their MC-ICP-MS. I am extremely grateful to Antoine Zazzo, Matthieu Lebon, Denis Fiorillo and Joël Ughetto from the Muséum National d'Histoire Naturelle (Paris, France), for giving me access to their mass spectrometry facilities in order to carry out the stable carbon and oxygen isotope analyses, and discussing the results with me. I am grateful to John Pouncett for his help and advice with the creation of maps using ArcGIS. Colleagues met at various conferences throughout my DPhil provided valuable comments and suggestions.

Some results presented in this thesis have already been presented at various conferences and parts have been submitted for publications (Snoeck et al. 2014a; 2014b; 2015). I am grateful to the co-authors of these papers for their help and advices.

For access to archaeological samples, I thank C. Jones (Parknabinnia), G. Eogan and K. Cleary (Knowth), G. Ramsey and S. McCartan on behalf of the Ulster Museum (Annamghare, Legland, Ballynahatty, Clontygora Cairn and Ballymacaldrack), S. Walsh (Church Lawton, Whitelow Cairn and Green Howe), R. Crellin on behalf of the Manx National Heritage (Isle of Man), W. Jarvis of ULAS on behalf of Jelson Homes ltd. and English Heritage (Asfordby), and C. Willis, M. Parker-Pearson and P. Marshall on behalf of UCL and English Heritage (Stonehenge). I am grateful to the National Museum of Ireland for permitting analysis of the Parkbabinnia and Knowth material, and to English Heritage for permission to use the excess material from Haddenham Causewayed Enclosure, Wally Corner (Berinsfield) and Imperial College Sports Ground, Sipson Lane (Brock et al. 2007; 2010a). I also thank M. Pellegrini for the modern horse tooth samples, D. Miles for the

dendrochronologically dates wood, and the butchers (Hedges, and John Lindsey and Son) from the Covered Market, Oxford, for the animal joint samples.

I thank Petra, Francisca and Chelsea for their help and laughter in the DPhil room. My warmest and deepest thanks go to my friends Pauline, Sophie, Violette, Henry, Aurélie, Marie-Noëlle, Julia, Daisy, Sébastien, Stephan and Florence who have brought emotional and social balance to this academic journey. I would also like to thank my Grandmothers, Gilberte and Simone, and my Godmother, Kristin, for their emotional support. I am grateful to Merton College for providing a social, sportive and academic environment where I met numerous eminent scholars and made many friends.

I am grateful for the financial support of the Sigma Xi Grant-in-Aid of Research (G20120315161475), the Quaternary Research Association, the Meyerstein Fund of the School of Archaeology, the Research Laboratory for Archaeology and the History of Art and Merton College towards research and travel expenses incurred during this DPhil. Some of the samples were also analysed as part of the British Academy grant (SG130690) 'Coming to Knowth'. I am also grateful to Edward Hall Memorial Fund for providing funding towards my tuition fees for the academic year 2011/2012.

Last but not least, I am forever indebted to the Philippe Wiener - Maurice Anspach Foundation for their financial support towards my DPhil. I am grateful to Nicole Bosmans and Francesca Spinelli for their help. I would also like to thank the current and out-going Presidents, Pierre Francotte and Jean-Victor Louis, the Vice-President, Catheline Périer-D'Ieteren, and the executive director, Kristin Bartik, for believing in my project and encouraging me throughout my time in Oxford.

Table of Contents

List of Figures

Chapter 2

Chapter 3

Chapter 4

Chapter 5

Chapter 6

Chapter 7

Chapter 8

Appendices

List of Tables

Chapter 6

Chapter 7

Chapter 8

Appendices

Lexicon

ATR	Attenuated Total Reflectance mode used with FTIR
Bone apatite	Inorganic/mineral fraction of bone with a similar composition and structure to hydroxyapatite
Burned bone	Bone heated in the presence of flames (N.B. all burned bone fragments are heated but not all heated bone fragments are burned)
Calcination	The term calcination refers to the process of heating or burning bone until it is fully calcined (white).
Calcined bone	Bone submitted to such high temperatures (typically temperature above 700°C – in laboratory conditions or on a natural fire) that all its structural water and organic matter have been removed; such bone will be completely white
Charred bone	Bone submitted to temperatures (typically temperature between 400 and 600°C) leading to a decrease in structural water and organic content but still contains significant amount of both; such bone will be black or grey
Cremated bone	Bone that has been burned on a natural fire (modern or archaeological)
Crystallinity	Crystallinity is an indication of crystal size and defects (or distortions) in apatite; apatite samples with large crystals and low distortions have higher crystallinity than those with smaller crystals and high distortions
Cyanamide	$–CN_2H$; functional group believed to be present in calcined bone apatite when heated in ammonia-rich atmosphere

Diagenesis	'*Diagenesis is a general term for any kind of alteration or change subsequent to original definition of a mineral matrix. Thus, it may include recrystallization in place, solution and recrystallization of the same or a different phase, secondary deposition of phases extraneous to the original matrix, sorption of ions or phases onto the surface of the existing matrix, exchange of material with the existing matrix, and any number of the other introductions or alterations. All of these processes can be reduced to two basic types, the addition of new material to the existing matrix, and the alteration of the existing matrix itself'* (Krueger, 1991, p. 356)
Heated bone	Bone that has been submitted to high temperatures (in the presence or absence of flames)
FTIR	Fourier Transform Infrared Spectroscopy
IRMS	Isotope-Ratio Mass Spectrometry
Structural water	Water that is 'locked' within the structure of bone apatite

Abstract

A Burning Question:
Structural and Isotopic Studies of Cremated bone in Archaeological Contexts

Christophe Snoeck, Merton College
D.Phil., Research Laboratory for Archaeology and the History of Art
Trinity Term 2014

Cremated bone occurs in many archaeological sites as small grey and white fragments. The high temperatures reached during heating induce structural, chemical and isotopic changes to bone apatite (the inorganic fraction of bone). These changes are investigated here by infrared spectroscopy and mass spectrometry ($\delta^{13}C$, $\delta^{18}O$ and $^{87}Sr/^{86}Sr$) in both modern heated bone and archaeological cremated specimens. The results of various heating experiments (in laboratory and natural conditions) highlight the significant carbon and oxygen exchanges with the fuel used as well as with bone organic matter (mainly collagen). While not informing on dietary practice and hydrology as is the case with unburned bone, the $\delta^{13}C$ and $\delta^{18}O$ values of calcined samples together with infrared results provide information on the conditions in which the bone was heated (e.g. presence of fuel, size of the pyre, temperatures reached, dry or fresh bone, etc.). In parallel, the effect of heat on the strontium present in bone is minimal, if not undetectable. Furthermore, as observed through artificial contamination experiments, post-burial alterations also appear to be extremely limited, which is to be expected due to the higher crystallinity of calcined bone apatite compared to tooth enamel and unburned bone. These experiments demonstrate that calcined bone provides a reliable substrate for mobility studies using its strontium isotope composition. The application of these results to the study of six Neolithic and one Bronze Age sites from Ireland showed the possibility of discriminating cremated individuals that ate food originating from different regions, as well as highlighting possible variations in cremation practices between different sites. The results of this thesis greatly extend the application of strontium isotopes to places and periods in which cremation was the dominant mortuary practice, or where unburned bone and enamel do not survive. They also provide insights into the reconstruction of ancient cremation practices.

Chapter 1 – Introduction

Burned bones are frequently observed in the archaeological record, resulting from cooking practices, accidental exposure to fire, use of bone as fuel, or mortuary practices, i.e. cremation, a common rite in many cultures and civilisations throughout pre/history. Whether burning took place accidentally or purposefully, the material residue includes calcined bone fragments. In many situations where soil conditions are not conducive to the preservation of unburned bone (e.g. acid soils), they are all that survive. Gathering more information about these remains will help scholars to better understand societies where cremation took place as well as the use of fire in past cultures.

The *Burning Question* of this thesis was sparked by the results showing that comparable radiocarbon dates could be obtained from charcoal and calcined bone from the same contexts (Lanting et al. 2001). Scholars started to discuss the reasons why radiocarbon dating of calcined bone was possible even though no collagen survives in such bone (e.g. Zazzo et al. 2009; Hüls et al. 2010). This work was born from that discussion but goes well beyond radiocarbon dating: it investigates other potential sources of information that could be extracted from the structural, compositional and isotopic properties of calcined bone in archaeological contexts.

1 The challenge of heated bone

The complex and variable structure of bone, as well as its variable chemical and isotope composition make burned bone a very difficult material to understand. As a consequence, burned remains have until today often been excluded from isotopic studies. The introduction of calcined bone for radiocarbon dating in the last decade, however, created a new interest and raised many questions. Why should such complex and variable material be considered

suitable for radiocarbon dating when even unburned bone apatite (the inorganic fraction of bone; the only one that survives after calcination) is not; and if reliable radiocarbon dates can be obtained, why then should other isotopic measurements be devoid of information? Might there be more reliable bioarchaeological information locked into burned bone remains than previously thought?

Bone is one of the most important sources of information about the past. It contains information about the lives of past populations, their diet, the climate and environment in which they lived, where they came from, and much more, providing knowledge about the lives of individuals, populations and societies. Chemical analyses of unburned ancient bone, including those of stable isotopes and radiocarbon dating on bone collagen, are well established techniques that have provided crucial archaeological information over the last fifty years. The study of bone is of crucial importance for archaeologists who aim at a better understanding of how, where, and when humans lived, and interacted with each other as well as with their surrounding environment.

When bone is heated, its colour changes to black (charred) and then to white (calcined), the latter representing the colour of bone that has been most intensively heated and in which no collagen remains. Bone may be heated for many different reasons: animal bones are often burned to reduce waste or during cooking, while humans are burned in funeral rites. Indeed, of the various funeral rites used by humans, cremation is one of the most common today and in the past. Depending on the period and the region, cremation may be the normative burial practice of an entire population but it may also be reserved for a subset of a population. Contrarily to common belief, cremation, and more generally, the heating of bone leaves behind bone fragments and not just ash. As a consequence, burned bone fragments are often recovered in a wide range of archaeological contexts.

Cremated human bone fragments from different periods – from the Mesolithic to the present day – occur in many parts of the world, forming an important testimony of the human past. Excluding them from isotope analyses reduces significantly the amount of available material from which information can be obtained, leaving many blank pages in the archaeological record. In the long term, it will not only be possible to, hopefully, gather chronological, dietary, funerary and migratory information on ancient populations but also enhance the current knowledge on the relation between humans and fire, how it changed in time and space, and how these changes were the consequence of social and cultural factors or induced by the environment.

The following section presents the main arguments of the thesis. It is followed by a brief presentation of the research strategy and the main archaeological sites of interest for this study. An overview of the chapter structure of this thesis closes the chapter.

2 Aims

The focus of this thesis is to extract as much information as possible from calcined bone to increase the current knowledge of archaeological sites where calcined bone fragments have been recovered. More specifically, the present study aims to understand its structural modifications due to heating, as well as the changes in the carbon, oxygen and strontium isotope ratios. It assesses the extent to which reliable dietary (C & O), chronological (C), and mobility (O & Sr) information can be extracted from archaeological cremated bone. Furthermore, the impact of different heating regimes (time, temperature, presence of fuel, etc.) will be investigated to look into the possibility of reconstructing ancient cremation practices.

The use of calcined bone for radiocarbon dating and palaeodietary studies has been interrogated by many scholars. Studies have shown that the carbon isotope composition of

calcined bone apatite (the inorganic fraction) differs from its original composition and that different fractionation and/or exchange processes occur when bone is heated. The final carbon isotope composition of calcined bone apatite can be explained by four different hypotheses: (1) carbon exchanges between bone apatite carbonates and the fuel combustion gases, (2) loss of endogenous apatite carbonates accompanied by a potential time/temperature dependent fractionation, (3) admixture of carbon originating from the combustion of the organic fraction of bone (e.g. collagen, flesh, fats, etc.), and (4) contamination with atmospheric CO_2. Only a combination of these four possibilities could explain the observed modification of the isotope composition of bone apatite after heating (Olsen et al. 2008; Zazzo et al. 2009; 2012; Van Strydonck et al. 2005; 2010; Hüls et al. 2010). During earlier MSc research, I explored some of these possibilities. Its results confirmed the significant influence of the combustion gases on the carbon isotope content of bone apatite (Snoeck 2011), but also raised many questions. Is there any information regarding cremation practices that could be extracted from calcined bone fragments? Are there any other isotopes than carbon that could provide information about the lives of cremated individuals? These gaps are addressed here, extending the research framework to include infrared analyses, oxygen and strontium isotopes. Indeed, when studying burned bone, it is important to understand what it is composed of and how its structure evolves from an unburned to a fully calcined state. It is also important to be able to discriminate post-burial alterations from the effects of the actual heating. One possible way to assess this is using infrared spectroscopy (FTIR – e.g. Thompson et al. 2009; Lebon et al. 2010). Oxygen isotopes of the carbonate fraction of bone apatite, generally used for palaeoclimatic reconstructions, have been studied in heated bone only in a cursory manner (Munro et al. 2008). Strontium isotopes too, increasingly used in mobility studies, have been examined only incidentally in heated bone (Harbeck et al. 2011; Harvig et al. 2014). Nevertheless, calcined bone is more crystalline than unburned bone, and

even tooth enamel, and should be more stable and less subject to post-burial alterations than unburned bone (Zazzo & Saliège 2011). This potentially eliminates one of the main constraints for using unburned bone for strontium isotope mobility studies.

If it is possible to prove that the isotopic and structural information contained in bone is conserved or altered in a predictable way during heating, the results will contribute towards the study of archaeological sites where calcined bone fragments were excavated. In regions where only burned bone has survived from a certain period, for example, the ability to gather isotopic information would allow scholars to understand better aspects of populations' funerary practices and lifestyles. At some archaeological sites, both cremations and inhumations were practiced side by side. This could be the result of differences in social status, sex, age, or geographical origin. Stable isotopes and structural analyses may provide the key that could enable archaeologists to answer these questions.

The present research addresses three main questions: (1) what isotopic, chemical and structural changes occur in bone apatite during and after heating? (2) Which isotopes and structural infrared indices can provide reliable information about archaeological calcined bone, and what information can be obtained from them? (3) How can the information gathered from calcined bone increase the current knowledge about past populations?

3 Research strategy

Since the use of calcined bone for isotope studies is still a controversial topic, much research has to be undertaken before the results of such studies can be fully understood and considered reliable. This work represents a new step towards that end.

The research strategy has three main orientations. First, the compositional and structural changes that occur in bone apatite during heating are investigated. This is mainly assessed by Fourier Transform Infrared Spectroscopy (FTIR). Second, the effects of heating

on the carbon and oxygen isotope content of bone apatite carbonates are monitored by Isotope Ratio Mass Spectrometry (IRMS). Radiocarbon dating is also studied in this section as the carbon isotopic changes will impact on both ^{13}C and ^{14}C concentrations. Third, the possibility of obtaining reliable strontium isotope measurements from calcined bone is investigated by Multi-Collector Induced Coupled Plasma Mass Spectrometry (MC-ICP-MS). Because of the increasing crystallinity in bone during heating, it is likely that bone apatite behaves similarly to tooth enamel regarding strontium isotopes; if so, it could be used to obtain reliable strontium isotope ratios from calcined bone.

Up until now, various infrared studies have been carried out by FTIR on modern and archaeological bone, both heated and unburned. Many indices have been proposed, yet many of these represent similar structural and/or compositional characteristics of bone apatite. The first step of the present work is to assess which indices provide useful information and allow the discrimination of modern, archaeological and burned bone, as well as bone heated in different conditions (time, temperature, presence of fuel, etc.).

The compositional information obtained by infrared analyses shows the amount of carbon and oxygen remaining in bone apatite after heating. As the origin of the carbon and oxygen remaining in the bone after calcination is still unknown, it is necessary to question which carbon and oxygen is actually being measured (endogenous, atmospheric, fuel, etc.). It is important to propose a model for carbon and oxygen exchanges and losses during heating and test the different possibilities both in laboratory and outdoor experiments.

The structural information obtained by infrared analyses provides a first idea of the extent to which calcined bone apatite becomes more crystalline compared to unburned bone and therefore more resistant to post-burial alterations. This, however, is only the first step towards showing that reliable strontium isotopic measurements can be obtained from calcined bone. Further experiments are carried out to test whether there is any intake or loss of

strontium into or from the burial environment of calcined bone using a ‘spiked’ strontium carbonate solution of known isotope composition.

All these experiments allow for the design of new models of exchanges, losses, and intakes of carbon, oxygen, and strontium isotopes; they provide an understanding of what exactly is being measured and which measurements can be considered reliable and, more importantly, meaningful. These results are tested on human archaeological cremated bone from Irish Neolithic and Bronze Age sites.

4 Applied study – Irish Neolithic and Bronze Age

In the final section of this work, several archaeological Irish Neolithic and Bronze Age sites will be studied including the megalithic passage tombs of Knowth. The main mound at Knowth is the largest megalithic passage tomb of the Middle Neolithic period (c. 3200–2900 cal. BC) in Western Europe and is situated along the river Boyne (County Meath, Ireland) (Eogan 1973). In this megalithic passage tomb, and in the smaller tombs around it, both unburned and cremated bone fragments were discovered. One of the most interesting hypotheses explaining this dual burial practice is that those living close to Knowth were initially inhumed while those living further away were cremated as it would have been easier to carry an urn or bowl containing calcined bone fragments and ashes than an entire corpse. This hypothesis relies on the observation that the stones used to build the megalithic passage tomb from Knowth originate from different places (Cooney 2000; Meighan 2011).

Provided that sufficient geological variability exists, strontium isotopes would allow the discrimination of individuals originating from the different regions around Knowth. A previous examination of the biologically available strontium at Knowth and its surrounding areas is required as no map of the Irish biologically available strontium currently exists. Stable carbon isotopes could, in combination with the mobility information obtained through

strontium isotopes, provide further information about the diet of the people buried at Knowth, or as suggested by Zazzo et al. (2013), fuel management. The unburned remains of Knowth have already been studied through carbon stable isotopes (on collagen), indicating a terrestrial C_3-plant based diets typical of the Neolithic (Schulting et al. forthcoming) but the cremated bone fragments have not yet been analysed biochemically except for radiocarbon dating.

In addition to Knowth, six other sites dating from the Neolithic to the Middle Bronze Age feature in the case study: four Neolithic court tombs (Annaghmare, Co. Armagh, Clontygora, Co. Armagh, Legland, Co. Tyrone and Parknabinnia, Co. Clare), a megalithic circular chamber close to the Ballynahatty timber circle and the Giant's Ring henge monument, Co. Down, and Middle Bronze Age urns found near the Neolithic court tomb of Ballymacaldrack, Co. Antrim. The archaeological study of these sites is currently incomplete because of the lack of isotopic information from burned bone. The present work aims at understanding better how the isotope content (carbon, oxygen and strontium) and structure are modified during heating and at assessing the extent to which reliable information can be obtained from them. This, in turn, will allow archaeologists to enhance their knowledge of many archaeological sites of which only a very small fraction have been presented above.

5 Thesis structure

This study is divided into nine chapters. The introductory chapter concerns itself with the importance of studying calcined bone isotopically and structurally. It further summarises the thesis outline and the research design. The second presents an overview of the relevant background information, beginning with the structure and composition of bone before and after heating. The characteristics that will be studied in calcined bone are also summarized: structural information obtained by Fourier Transform Infrared Spectroscopy (FTIR) and

isotopic information by Mass Spectrometry (MS). This is followed by a chapter detailing the materials and methods used in this work. Chapters 4, 5, and 6 are concerned with scientific analyses of heated bone. Chapter 4 focusses on the compositional and structural changes that occur in bone during heating using infrared analyses. In chapters 5 and 6 the results of the isotope analyses by Mass Spectrometry (MS) are presented. In order to gather more information about the effects of heat on the different isotope ratios, several experiments were carried out in controlled conditions in laboratory furnaces as well as in more realistic conditions on outdoor pyres. Chapter 5 focusses on carbon and oxygen isotopes including ^{14}C – ^{13}C – ^{12}C and ^{18}O – ^{16}O; strontium isotopes (^{87}Sr – ^{86}Sr) are considered in chapter 6. Chapter 7 focusses on establishing a map of the biologically available strontium isotopes for Ireland that could then be used for the study of archaeological samples from that region. To this effect, modern plants are included in the study to assess the biologically available strontium in present-day Ireland. The study of archaeological calcined human bone is detailed in chapter 8. This applied study focusses on human remains from seven Irish Neolithic and Bronze Age sites. It should be possible to study the remains' geographical origins through strontium isotopes, provided it can be demonstrated that calcined bone preserves an *in situ* signal. Chapter 9 summarises all the results and details the main discussions and conclusions. Suggestions for further research are also outlined in the final chapter. A number of appendices can be found at the end of this volume.

Chapter 2 – Background

1 Introduction

This thesis aims at assessing the structural, compositional and structural changes that occur in bone apatite when bone is heated. This chapter starts by summarizing the current state of knowledge about the chemistry of unburned and heated bone. This is followed by a section on Fourier Transform Infrared Spectroscopy (FTIR) and its uses in the study of unburned and heated bone. The isotopes of interest in bioarchaeological studies – carbon, oxygen, and strontium – are discussed in the last sections of this chapter.

2 Bone

Bone is composed of three main parts: a poorly crystalline inorganic mineral fraction, an organic fraction, mainly collagen, and water (Vaughan 1970). On average, dry bone is composed of 70% of inorganic and 30% of organic material (Posner et al. 1984; LeGeros 1991). Here, since it is the only one that survives after calcination, the focus is on the inorganic mineral fraction of bone, a highly substituted hexagonal calcium phosphate apatite commonly called bone apatite (LeGeros 1991). Calcium phosphate apatites are composed of four essential elements: calcium, phosphate, oxygen and an appropriate channel-filling ions such as chlorides, fluorides or hydroxyl groups: $Ca_5(PO_4)_3(Cl/F/OH)_2$. The composition of apatite is characteristically much more flexible than that of most minerals: it accommodates chemical substitution relatively easily. The most symmetric apatite is fluoroapatite as fluoride (F^-) is smaller than both chlorides and hydroxyl groups and it fits easily into space between the Ca columns at the centre of the unit cell (Figure 2.1). When hydroxyl groups occupy this space, distortions are created because of their size, non-spherical form and charge arrangement (Wopenka & Pasteris 2005).

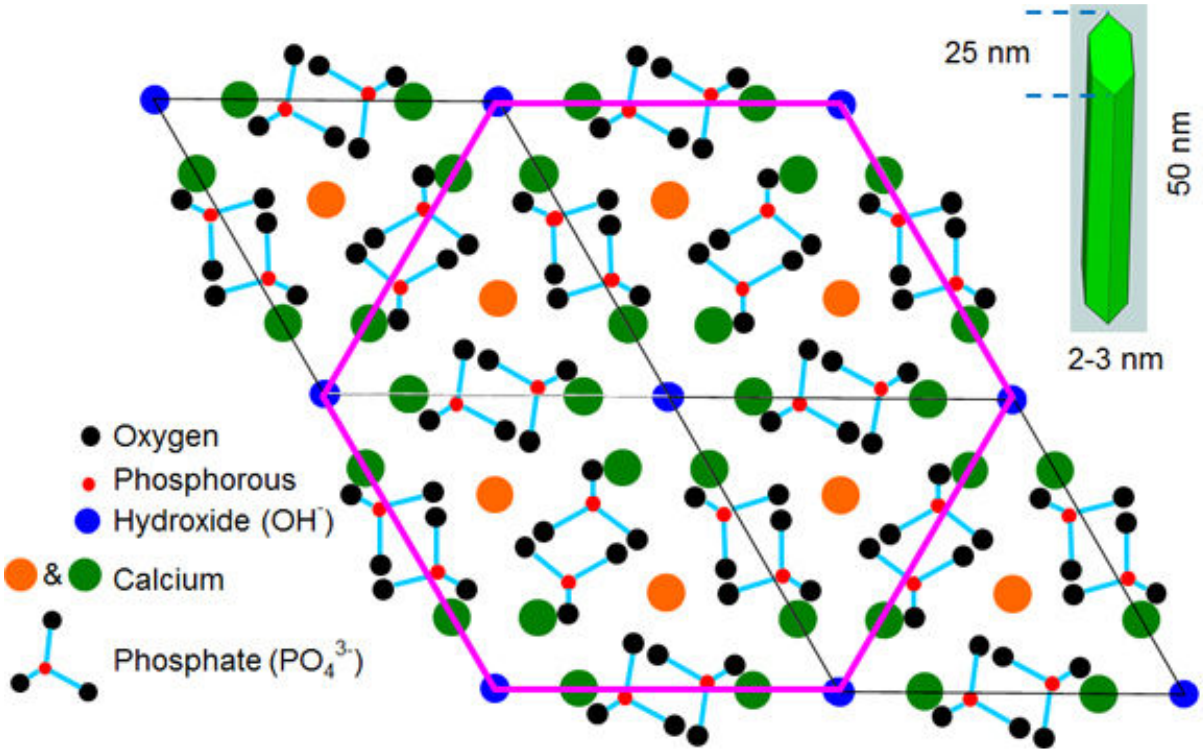

Figure 2.1 – Hexagonal crystal lattice of hydroxyapatite (HAP) highlighting the two different positions of the phosphates (from Bone Biology and Mechanics Lab – IUPUI)

Bone apatite is similar, but not identical, to hydroxyapatite (HAP – $Ca_5(PO_4)_3(OH)_2$ – Figure 2.1) in which non-stoichiometric substitutions are possible (Lee-Thorp 2002). Phosphates (PO_4^{3-}) are partially replaced by carbonates (CO_3^{2-}) and most hydroxyl groups (OH^-), if not all, also replaced by carbonates (Pasteris et al. 2004; Skinner 2005; Wopenka & Pasteris, 2005). Carbonate is the third most concentrated element in bone apatite after calcium and phosphate (Rey et al. 1989), accounting for c. 5 % of its weight (Pasteris et al. 2004; Leventouri 2006). The carbonates that replace hydroxyl groups and phosphates are known as type A and B carbonates respectively (LeGeros et al. 1969; LeGeros 1991). Carbonates not only substitute for phosphates and hydroxyl groups within the crystal structure of bioapatite ('structural carbonate') but can also be adsorbed onto the surface of crystals and hydration layers ('adsorbed carbonate') (LeGeros 1981). Other minor and trace elements such as strontium can also substitute in bone apatite (LeGeros 1991). Water is found adsorbed on the bone crystallites (hydration layers) but can also be found within the structure

of bone apatite, probably replacing the channel filling ions (Yoder et al. 2012). The composition of bone apatite can be approximated with the following formula where [ ] represents potential vacancies in the structure (LeGeros et al. 1986; Skinner 2005; Wopenka & Pasteris 2005; Yoder et al. 2012):

$$(Ca, Na, Mg, Ba, Fe, Sr, Zn[\,])_{10}(PO_4, HPO_4, CO_3)_6(OH, F, Cl, CO_3, O, H_2O\ [\,])_2$$

Since carbonates have a different geometry and charge to phosphates and as they are larger than hydroxyl groups, their presence in the crystal structure of bone apatite leads to lattice distortions of the hexagonal structure, and to smaller crystal size compared to HAP (LeGeros 1991; LeGeros 2008). The crystallinity – indication of defects (or distortions and strains) and crystal sizes of apatite (LeGeros 1991) – of bone apatite is therefore lower than that of HAP. Because of the small crystal sizes, the area/mass ratio is very high, resulting in a higher reactivity and solubility of bone apatite compared to HAP (LeGeros 1991). Bone apatite is therefore susceptible to post-mortem alterations or diagenesis. Furthermore, it has been suggested that when the organic fraction of bone has been degraded, bone apatite is less protected and more prone to diagenesis (Hu et al. 2006). Indeed, the porosity levels after the disappearance of organic matter tends to increases the liability to possible post-burial alterations (Lee-Thorp 2002). As bone apatite, tooth enamel is similar to HAP, but has fewer substitutions, less distortions and larger crystals than bone apatite (LeGeros 1991) rendering it more stable to post-mortem alterations than bone apatite (Lee-Thorp and Sponheimer 2003).

It is important at this stage to discriminate post-mortem alterations (or diagenesis) and post-burial alterations. The former corresponds to *all* possible alterations following the death of an individual, including decomposition and fossilization, all post-burial alterations as well

as potential alterations related to heating. Post-burial alterations, however, cover only those alterations following burial in an urn, soil, etc.

During post-mortem alterations the size of bone apatite crystals increases while the internal defects or distortions are reduced (Kyle 1986; Lee-Thorp 2002; Trueman et al. 2004; Lee-Thorp 2008) making bone apatite less reactive (LeGeros 1991). At ambient temperature, bone crystals are altered and larger crystals that are more thermodynamically stable tend to grow instead of smaller ones (*Ostwald ripening*) (Pollard et al. 2007). This is a very slow process that can take up to several millennia by fossilization, or can proceed more quickly, in a period as short as several months, in case of weathering. At higher temperatures (> 550°C) changes in crystal size are much faster occurring while the bone is heated.

While bone crystals are altered, they may incorporate and exchange elements such as carbonates (Lee-Thorp & Sponheimer 2003) and strontium (Sealy et al. 1991; Sillen and Sealy 1995) with their surrounding environment. During fossilization and weathering, these exchanges can take place with the burial environment, while during calcination these exchanges can occur first with the combustion atmosphere (e.g. Zazzo et al. 2012), and then, potentially, with the burial environment.

3 Heated bone

During heating, bone undergoes a series of changes. Macroscopically, the colour changes to black in charred bone (300 – 500°C) and then to white in calcined bone (above 600 – 700°C). The temperature at which bone is completely calcined is still the topic of some debate. Some scholars have suggested temperatures above 650°C (Stiner et al. 1995), others that bone is already calcined at 600°C (Lanting et al. 2001; Naysmith et al. 2007), at 625°C (Person et al. 1996), or only at 725°C (Van Strydonck et al. 2009). It is likely that these different results are

the results of different exposure times and/or rates of heating, as well as different bone fragment sizes used in the experiments.

A colour code was developed to assess the degree of heating of bone: the 'Burn Colour Code' (Table 2.1 – Stiner et al. 1995). This approach is commonly used to gather an initial impression of the damages caused to bone by heating. The method does have limitations: the boundaries between each category are ill-defined and require individual judgement so there is an element of subjectivity. In addition to colour changes, further macroscopic changes can occur such as shrinkage and appearance of cracks (Shipman et al. 1984; Nicholson 1993).

Table 2.1 – The 'Burn Colour Code' by Stiner et al. 1995

Burn Colour Code	**Description**
0	Not burned - cream/tan
1	Slightly burned - localised and less than half carbonised
2	Lightly burned - more than half carbonised
3	Fully carbonized - completely black
4	Localized less than half calcined - more black than white
5	More than half calcined - more white than black
6	Fully calcined - completely white

Microscopically, the structure and composition of the mineral phase are modified: carbonate content decreases while hydroxyl group content increases compared to unburned bone. Thus, bone apatite becomes more crystalline and more similar to HAP (Stiner et al. 1995). These changes are related to the loss of water, organic matter and CO_2. First, water evaporates below 225°C. A first fraction of CO_2 is then lost, between 225 and 500°C, as a consequence of the combustion of the organic phase of the bone. Finally, above 500°C, the decomposition of structural carbonates and secondary carbonates results in the loss of a second fraction of CO_2. Laboratory experiments have shown that the carbonate content decreases from ca. 5% in raw bone to 0.5 to 1 % in calcined bone (Van Strydonck et al. 2005; Zazzo et al. 2009). These experiments also demonstrated that the loss of CO_2 is not only

dependent on temperature but also on time (Van Strydonck et al. 2005). Finally, it has been suggested that the structure and crystallography of calcined bone apatite is similar to tooth enamel apatite, and therefore, should be more resistant to post-burial alterations than unburned bone (Zazzo et al. 2009; Lebon et al. 2010 Zazzo & Saliège 2011; Quarta et al. 2013). This concluding observation together with the observation that comparable results could be obtained from paired dates of charcoal and calcined bone from the same contexts (Lanting et al. 2001) is the reason why calcined bone is now generally considered to produce reliable radiocarbon dates. Furthermore, the enhanced crystallinity and hence lower reactivity of calcined bone, more akin to enamel, raises the question as to whether calcined bone may represent a good substrate for the preservation of the original strontium concentration and strontium isotopes. Experiments are designed to explore this possibility in this thesis.

4 Fourier Transform Infrared spectroscopy (FTIR)

Fourier Transform Infrared spectroscopy is one of the main tools used in this study to understand the structural and compositional modifications of bone apatite during heating, as well as the possible changes in archaeological calcined bone that has been exposed for long periods to external soils and water. The three polyatomic ions of interest for the infrared study of bone apatite are phosphates (PO_4^{3-}), carbonates (CO_3^{2-}) and hydroxyl groups (OH^-).

An important parameter of bone apatite that can be monitored using infrared spectroscopy is its crystallinity: the infrared splitting factor (IRSF) is used to evaluate it. While it is clear that high IRSF is associated with bone fossilization (e.g. Sillen & Parkington 1996; Lebon et al. 2010; King et al. 2011), it can also be linked to heating (e.g. Munro et al. 2007; Olsen et al. 2008; Zazzo et al. 2009; Lebon et al. 2010). Consequently, its reliability as sole arbiter of diagenesis has been questioned (Trueman et al. 2008). It remains difficult to

discriminate bone heated at low temperatures (< 550°C) from bone that underwent fossilization based only on the IRSF (Stiner et al. 1995; Lebon et al. 2010).

Further information can be gathered by measuring the carbonate content of bone apatite (using a carbonate to phosphate ratio – C/P). During heating, the C/P ratio of bone apatite decreases with intensity as carbonates are lost preferentially compared to phosphates since calcium-phosphate bonds are much stronger than the calcium-carbonate bonds. In Figure 2.2 the infrared spectra of heated and unburned bones show the decrease of the bands characteristic of carbonates (1456, 1417 and 872 cm^{-1}) with the degree of calcination (burn colour code: 0, unburned, to 6, fully calcined). At the same time, the IRSF (indicator of crystallinity) increases as the crystals become larger and the atomic order increases (Stiner et al. 1995).

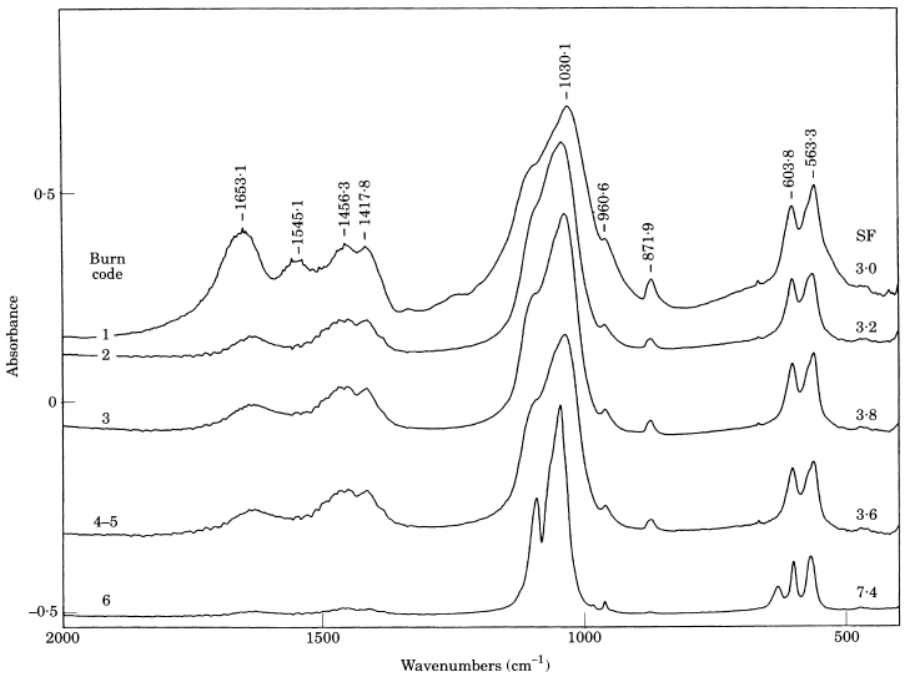

Figure 2.2 - Infrared spectra of modern bone fragments burned in fire experiments (Figure 3 from Stiner et al. 1995)

Combining IRSF and C/P ratio improves the understanding the modifications undergone by bone: low C/P ratio and high IRSF are characteristic of bone that underwent

diagenesis (Wright & Schwarcz 1996) or heat alterations (Stiner et al. 1995). Once again, C/P ratio and IRSF alone are not sufficient to discriminate fossil bone from bone heated at low temperatures (< 550ºC). Many other infrared indices have consequently been developed over the last twenty years to characterize heated bone, some of which appear to be temperature dependent (Thompson et al. 2009). In addition to these indices, it is also possible to check for bone alteration by looking for the presence of organic matter (e.g. collagen) and non-apatitic domains (e.g. calcite, aragonite) (Hassan et al. 1977; Lee-Thorp & van der Merwe 1991; Wright & Schwarcz 1996).

5 Isotope composition

When bone is heated to full calcination, only its inorganic fraction survives. Firstly, all organic matter is destroyed during intense heating, so none of the isotopes present in bone collagen (N, C, H, O) survives. Furthermore, the isotope composition of bone apatite carbonates is strongly modified to such an extent that it has been argued that these modifications are unpredictable and consequently $^{13}C/^{12}C$ and $^{18}O/^{16}O$ ratios obtained from carbonate in calcined bone are unlikely to yield useful information (Lanting et al. 2001; Van Strydonck et al. 2005; Olsen et al. 2008; Zazzo et al. 2009). The carbon and oxygen isotope ratios are, by convention, expressed relative to a standard (usually vPDB – Vienna Pee Dee Belemnite). Both are expressed in per mil (‰ – 1/1000):

$$\delta^{13}C = \frac{\left(^{13}C/^{12}C\right)_{sample} - \left(^{13}C/^{12}C\right)_{vPDB}}{\left(^{13}C/^{12}C\right)_{vPDB}} \times 1000 \quad \& \quad \delta^{18}O = \frac{\left(^{18}O/^{16}O\right)_{sample} - \left(^{18}O/^{16}O\right)_{vPDB}}{\left(^{18}O/^{16}O\right)_{vPDB}} \times 1000$$

As it is much heavier than carbon and oxygen, and much less volatile, strontium substituted for calcium in the crystal structure should be less affected by high temperatures.

The strontium isotope ratio seems to be unaltered by heating, although this has not been convincingly demonstrated so far. The present work focuses on investigating the fate of carbon and oxygen isotopes from the carbonate fraction, and strontium isotopes of bone apatite.

5.1 Stable carbon isotopes – ^{13}C & ^{12}C

Stable carbon isotopes (^{13}C and ^{12}C) have been used by archaeologists for decades in order to gather dietary information about past populations (Vogel & van der Merwe, 1977). The carbon isotope values range from 0 ‰ for marine water bicarbonate (HCO_3^-) and -6 to -8‰ for atmospheric carbon dioxide to -35 ‰ in some terrestrial plants (Tauber 1981). There are two main types of terrestrial plants that form the basis of the terrestrial foodwebs: C_3 and C_4-plants assimilating carbon from the environment in different ways. The $\delta^{13}C$ values of C_4-plants are less negative (-9/-16 ‰) than those of C_3-plants (-22/-35 ‰). A large variation can, however, be observed within each group though there is very limited, if any, overlap between the two (Vogel & van der Merwe 1977; Lee-Thorp 2008).

The use of unburned bone apatite for stable isotope analyses has been the topic of some controversy, partly because of its greater susceptibility to diagenesis and partly because of different pre-treatment methods designed to eliminate secondary carbonates which in turn affect the chemical and isotope compositions (Lee-Thorp & van der Merwe 1991; Koch et al. 1997; Garvie-Lok et al. 2004). It was earlier suggested that archaeological bone apatite $\delta^{13}C$ values cannot provide reliable dietary information (Schoeninger & DeNiro 1982). Further experiments, however, have suggested that appropriately treated bone apatite can provide reliable isotopic information in bone apatite up to 100,000 years of age (Krueger 1991; Lee-Thorp & Sponheimer 2003). While concerns about diagenesis have diminished, the remaining unsettled issue is that of the variable effects of different pre-treatment protocols

(Lee-Thorp & van der Merwe 1991; Krueger 1991; Koch et al. 1997; Lee-Thorp & Sponheimer 2003; Ambrose & Krigbaum 2003; Garvie-Lok et al. 2004; Pestle et al. 2014).

When bone is heated, its crystallinity increases and appears to be less susceptible to post-burial alterations. Nevertheless, calcination has an effect on the isotope composition of bone apatite carbonates. It was first observed in radiocarbon experiments: unburned bone with C_3-based diets showed less negative $\delta^{13}C$ values (c. -15 ‰) than burned C_3-bone (c. -24 ‰) (Lanting et al. 2001). In parallel, the $\delta^{13}C$ values of archaeological cremated bones varied between different fragments of a single individual and also from one laboratory to another (Lanting et al. 2001; Naysmith et al. 2007; Olsen et al. 2008). The main goal of subsequent studies was to understand the observed variations in the context of radiocarbon dating (Zazzo et al. 2009; Hüls et al. 2010; Van Strydonck et al. 2010; Zazzo et al. 2012).

The modifications of the $\delta^{13}C$ values of bone apatite carbonates during calcination are problematic if one wants to assess the diet of an archaeological population from cremated bone. Measurements on calcined bone from humans and animals with more or less known diets showed that there is an overlap in the $\delta^{13}C$ values of calcined bones with C_3 and C_4-based diets. Nevertheless, calcined bone fragments with terrestrial C_3-based diets still generally display more negative values than those with C_4-based diets (Zazzo et al. 2009). While not information directly on the diet, recent work does suggest the possibility that stable carbon isotopes measured in calcined bone apatite carbonates could be used to highlight variations in heating conditions (Zazzo et al. 2013).

5.2 Radiocarbon dating – ^{14}C

Many radiocarbon studies have been carried out on calcined bone over the last decade since it was shown that comparable results could be obtained from paired dates of charcoal and calcined bone from the same contexts (Lanting et al. 2001). However, because of the variations observed in the $\delta^{13}C$ values between raw bone and calcined bone, some doubts

remained regarding the validity of radiocarbon dating (Lanting et al. 2001; Naysmith et al. 2007; Olsen et al. 2008). Many scholars have worked on this issue over the last decade, struggling to explain what is modified in the bone structure and composition during heating and how this affects the results of radiocarbon dating (Olsen et al. 2008; 2012; Zazzo et al. 2009; 2012; 2013; Van Strydonck et al. 2005; 2010; 2013; Hüls et al. 2010; Harbeck et al. 2011).

Potentially, carbon exchanges between bone apatite carbonates and fuel gases could create an "old-wood effect" (Olsen et al. 2008): if there were a large difference in age between the fuel used and the body being cremated, the resulting calcined bone would appear older than it really is. Indeed, when comparing the radiocarbon date obtained from calcined bone fragments to the age of a dendrochronologically dated coffin, the bones fragments appeared to be about 70 years older (Olsen et al. 2012).

Experiments on the exchange between bone apatite carbonates and old carbon sources have so far been carried out only in laboratories (e.g. Van Strydonck et al. 2005; Hüls et al. 2010) or with dry archaeological bones burned on modern wood (Zazzo et al. 2012). Heating of a modern animal bone in a muffle furnace in the presence of coal showed that the amount of modern carbon was much lower after heating compared to another piece of the same bone heated in the same conditions but without coal (Van Strydonck et al. 2010). Other laboratory heating experiments were realised in a controlled atmosphere with old CO_2. Bone fragments heated in the presence of old CO_2 contained less modern carbon than those heated without old CO_2 (Hüls et al. 2010). Although the importance of outdoor experiments in natural conditions in validating the previously obtained results has been emphasised, no outdoor burning of modern bone with old fuel (e.g. coal) has been yet reported (Van Strydonck et al. 2010; Zazzo et al. 2011). More recently, archaeological bone was burned on an outdoor fire using modern wood as fuel. The archaeological bones were dated before and after burning,

and they all appeared younger after burning, indicating that carbon from the modern fuel had been taken up by the calcined bone (Zazzo et al. 2012). Burning archaeological bone which has lost all flesh and part of its collagen is, however, not comparable to the burning of a corpse that still possesses flesh and fresh collagen, and has an unaltered bone apatite fraction.

5.3 Oxygen isotopes – ^{18}O & ^{16}O

Oxygen isotopes from calcified tissues are of interest as they archive information about hydrological conditions. Oxygen occurs in both phosphates and carbonates within the bone apatite structure. However, bone apatite is rarely used to study oxygen isotope distributions in archaeological material owing to concerns about diagenesis mentioned above.

Phosphates and carbonates precipitate into apatite from body water, the composition of which depends on drinking water and food water, and can be approximated to the isotope value of precipitation. Both phosphates and carbonates are precipitated in equilibrium with body water (Podlesak et al. 2008). The isotope values of phosphates and carbonates of bone apatite are therefore linked although offset by a relatively consistent amount, of about 8–10‰. In this work, only the oxygen of the carbonate fraction will be investigated as its isotope ratio is measured alongside the carbon isotope ratio and is thus more easily available.

The effect of heating on the $\delta^{18}O$ values of bone apatite carbonates has been studied in step heating experiments. The $\delta^{18}O$ values of a modern deer bone decreased gradually with temperature (Munro et al. 2008). A study on cattle bone confirmed these results; $\delta^{18}O$ decreased from ca. -8 ‰ before heating to ca. -17 ‰ above 800°C (Harbeck et al. 2011). Munro et al. (2008) suggested that the decrease in $\delta^{18}O$ during heating was the consequence of exchange with water vapour, as well as of fractionation linked to the loss of CO_2.

Carbonate oxygen is more susceptible to exchange than carbonate carbon as oxygen is more exposed and has a known propensity to exchange with water (Wang & Cerling 1994), and there are many more oxygen sources surrounding bone during heating (e.g. atmospheric

dioxygen and water, oxygen in organic compounds such as collagen, lipids, etc.). Consequently, the $\delta^{13}C$ values of structural carbonates in bone apatite should be less affected by external changes than $\delta^{18}O$ values (Hu et al. 2006). Thus extracting endogenous information from $\delta^{18}O$ values of calcined bone apatite carbonates may prove to be a chimera, but could, together with the $\delta^{13}C$ values, highlight differences in heating conditions.

5.4 Strontium isotopes – ^{87}Sr & ^{86}Sr

Two isotopes of strontium, ^{86}Sr and ^{87}Sr, are widely used in mobility studies of humans and fauna. Strontium-87 is the product of the radioactive decay of Rubidium-87 (^{87}Rb), so strontium isotope ratios ($^{87}Sr/^{86}Sr$) vary between different types of bedrock, depending on the initial Rb-Sr ratio and the age of the bedrock (Faure & Powell 1972). The older and more Rb-enriched the bedrock, the more enriched it is in ^{87}Sr. $^{87}Sr/^{86}Sr$ values higher than 0.710 and up to 0.740 may be observed for older rocks and going as high as 0.9 in some granites of the Mourne Mountains in Northern Ireland (Meighan et al. 1988) and of South-Africa (Sillen et al. 1998). Younger geological formations generally have values below 0.706, and those with very low initial Rb/Sr ratios, such as basalt, typically have values of 0.703–0.704 (GEOROC). Modern ocean water has a $^{87}Sr/^{86}Sr$ ratio of 0.7092, an important value as it is imparted to world-wide precipitation and to marine calcareous deposits.

Strontium isotopes can be measured in bone and teeth in order to track the place of origin of animals and humans. Bone apatite and tooth enamel contain trace amounts of strontium that substitute for calcium (LeGeros et al. 1969; Wopenka & Pasteris 2005). Strontium in biological systems ultimately derives from a combination of inputs from the underlying bedrock geology, precipitation and air-borne particles (e.g. Saharan dust), and groundwater, entering the foodchain initially through uptake by plants and into the tissues of consumers. Therefore, $^{87}Sr/^{86}Sr$ values provide a reflection of the location in which an individual lived during the time of tissue formation. Measurements on tooth enamel relate to

the time during which the tooth crown formed, and so present an indication of conditions during infancy through to early adolescence, depending on the tooth. They cannot, however, inform on residence in adulthood. Bone on the other hand continues to remodel, and so it provides information relating to the last decade or more of adult life (Dempster 1999; Hedges et al. 2007; Robins & New 2002). An important exception to this is the inner part of the petrous bone, which forms during late gestation to infancy and does not remodel thereafter (Jeffery & Spoor 2004; Jørkov et al. 2009).

When studying archaeological remains that have been in contact with soil for centuries and millennia, an important issue to consider is the exchange and/or intake of strontium by bone and teeth from the burial environment (Sillen 1989; Tuross et al. 1989; Sealy et al. 1991). Attempts to remove post-depositional strontium have relied largely on leaching with solutions of buffered or non-buffered acetic acid (Sillen 1986; Sillen & LeGeros 1991; Budd et al. 2000). It has been shown that successive leaching with acetic acid leave up to 80% non-biogenic strontium in bone compared to less than 5% in tooth enamel (Hoppe et al. 2003). Tooth enamel has been shown to be more resistant to post-depositional strontium absorption due largely to its higher crystallinity and stability compared to bone and tooth dentine, which are both far more reactive. In bone, apatite crystallites are heavily substituted and therefore extremely tiny and distorted (LeGeros 1991). Because of these problems, currently only tooth enamel is considered to provide reliable results with archaeological material, while bone and tooth dentine may incorporate variable amounts of strontium in solution from the soil in which they were buried (e.g. Tuross et al. 1989; Budd et al. 2000).

Due to its higher crystallinity compared to unburned bone and tooth enamel, calcined bone is far less susceptible to post-burial alterations. In principle, then, this raises the possibility that calcined bone might retain an original *in vivo* strontium isotope composition,

but to date, only two studies included strontium isotope analyses of calcined bone. In the first it was shown that no modification of strontium isotope ratios occurred before and after heating without fuel in a furnace (Harbeck et al. 2011). This experiment, however, did not consider the possibility of the uptake of strontium from fuel wood or the burial environment. The second study compared the strontium isotope ratios of tooth enamel and calcined petrous bone from a cremated individual, which, unusually, had retained its enamel. These tissues gave similar results suggesting that the calcined petrous bone provides a reliable *in vivo* strontium isotope signal (Harvig at al. 2014). As noted in that study, the otic capsule (the portion of the petrous bone that was sampled) is composed of uniquely dense bone, whereas most calcined fragments would originate from less dense bone.

In addition to the issues related to diagenesis, a difficulty arising when interpreting strontium isotope results in the frame of mobility studies is the identification of the biologically available strontium (hereafter referred to as BASr) in the landscape. Strontium in biological systems originates mainly from the underlying bedrock geology but also from other sources (see above). Therefore, before being able to carry out migration studies based on strontium isotopes, it is important to assess the BASr that can be considerably different than the strontium isotope ratios of the rocks (Sillen et al.1998; Evans et al. 2009). Bone and tooth enamel of small mammals have proven to show a narrow range of $^{87}Sr/^{86}Sr$ values than plants: small mammals sample and integrate the local vegetation and water, while plants can only incorporate the strontium available for their roots and, therefore, are not such good integrators. It has consequently been suggested that archaeological teeth of small mammals should be used to determine the BASr: dental enamel because it is more resistant to diagenesis than bone; archaeological teeth because they will not be influenced by present-day pollution (fertilizers, polluted rainfalls, etc.); and small mammals because these would remain within a small area and probably within the same geological context (Price et al. 2002;

Bentley et al. 2004). However, archaeological samples are not always available and modern specimens present other issues: they are difficult to obtain and it would be ethically unacceptable to trap and kill small animals for this kind of study (Evans et al. 2009).

Another way of measuring the BASr is measuring the isotope ratio of modern plants assuming that modern contamination (e.g. pesticides, fertilisers, etc.) is not a major issue (Porder et al. 2003; Evans et al. 2009; 2010; Kusaka et al. 2009; 2011; Copeland et al. 2010; 2011; Laffoon et al. 2012). A large study aiming at mapping the biologically available strontium on the Isle of Skye, Scotland, used mainly plants, including also a few small mammal bones, snails and river water. While plant samples are the easiest and most convenient type of samples to collect, small mammal bones should not be neglected when readily available (Evans et al. 2009).

An additional difficulty encountered when interpreting strontium isotopes measured in human populations is that of mixing. First, individuals may move more than once during their lifetime, and they could have moved between two geologically similar regions. Second, the residence time of strontium in the body can be up to several months and even years (Dahl et al. 2001) and the individual would need to have lived in a specific region for a certain amount of time before its strontium isotope composition reflects the 'new' local BASr value. In addition, the food they consume could originate from different geologies. Also the large animals consumed by humans are unlikely to have remained in the same geological area. Since the strontium present in bone and teeth comes from the diet, the isotope ratio is more likely to actually reflect the region(s) where the food and water were collected (catchment area) than those region(s) where humans lived (Bentley et al. 2004; Evans et al. 2010). Nevertheless, plants being more enriched in strontium compared to animal meat are likely to contribute more to the strontium isotope composition of human remains than animal food (Elias 1980; Burton et al. 1999).

Chapter 3 – Materials and methods

1 Introduction

The samples selected for the different parts of this thesis are listed here together with the various analytical methods used in their study. Laboratory heating and outdoor burning experiments are detailed.

2 Samples

A wide range of samples were selected for structural, chemical and isotopic characterization, including heated and burned bone of both archaeological and modern origin. Several samples of dental enamel were also included (Table 3.1).

Table 3.1 – Bone and tooth samples

Code (#)	Type	Age	Location
LAB1 (8)	Heated Bone	Modern	Oxford, England
LAB2 (80)			Oxford, England
LAB3 (32)			Oxford, England & Cape Cross, Namibia
OUT (15)	Burned Bone		Oxford, England
Asf (2)		Mesolithic	Asforby, England
St (31)		Neolithic	Stonehenge, England
K (33)			Knowth, Ireland
A (2)			Annaghmare, N. Ireland
BN (4)			Ballynahatty, N. Ireland
C (3)			Clontygora, N.Ireland
L (2)			Legland, N. Ireland
P (4)			Parknabinnia, Ireland
IoM (10)		Late Neolithic, early BA	Isle of man
CLN (5)		Early BA	Church Lawton North, England
WC (5)			Whitelow Cairn, England
GH (2)			Green Howe, England
BM (6)		Middle Bronze Age	Ballymacaldrack, N. Ireland

Table 3.1 (*continued*)

Code (#)	Type	Age	Location
MB (11)	Unburned Bone	Modern	England
AB (52)		Neolithic to Anglo-Saxon	England (provided by F. Brock)
En (1)	Unburned Teeth	Modern horse tooth	Italy (provided by M. Pelligrini)
KT (8)		Neolithic	Knowth, Ireland
PT (4)			Parknabinnia, Ireland
BNT (3)			Ballynahatty, N. Ireland

3 Heating experiments and outdoor burnings

In order to better understand the changes that occur structurally, chemically and isotopically during calcination it was necessary to carry out several laboratory heating and outdoor burning experiments. The laboratory heating experiments were carried out in a Carbolite muffle furnace (RHF 1500) and Haldenwanger porcelain crucibles of 50 and 100 mL.

3.1 Laboratory heating experiments

3.1.1 Laboratory heating experiments 1 (LAB 1)

The first set of laboratory heating experiments (LAB 1) was carried out on small fragments of lamb bone obtained from a butcher at the Covered Market, Oxford. The samples were heated at 700°C in a muffle furnace (Table 3.2 with data from Snoeck 2011). Some of the samples were wrapped in aluminium foil and placed into a crucible which was then filled with sand to separate the sample from the atmosphere limiting oxygen availability. Furthermore, millet (C_4-plant) and barley seeds (C_3-plant) were placed in the furnace next to some of the bone samples. Part of these experiments aimed at assessing the impact of additional carbon and oxygen sources on the isotope composition of calcined bone.

Table 3.2 – List of lamb bone sections heated in a muffle furnace at 700ºC (Snoeck 2011)

	Time	Heating environment
L1	30 min	Open crucible
L2	1h	Open crucible
L3	2h	Bone placed in aluminium foil, and crucible filled with sand
L4	4h	Bone placed in aluminium foil, and crucible filled with sand
L5	4h	5g of millet seeds added into the open crucible
L6	4h	Bone placed together with 5g of millet seeds in aluminium foil, and crucible filled with sand
L7	4h	5g of barley seeds added into the open crucible
L8	4h	Bone placed together with 5g of barley seeds in aluminium foil, and crucible filled with sand

3.1.2 Laboratory heating experiments 2 (LAB 2)

For the second set of laboratory heating experiments (LAB 2), a cow tibia obtained from a butcher at the Covered Market, Oxford, was selected. It was cut into 80 fractions of similar size – twenty 1-cm-slices divided into quarters. The heating experiments had durations from half an hour to 24 hours (0.5, 1, 2, 4, 8, 12, 18 and 24 h), with temperatures ranging from 500 to 900°C (8 durations * 5 temperatures = 40 experiments). Two bone fractions were randomly selected for each of the 40 experiments.

3.1.3 Laboratory heating experiments 3 (LAB 3)

The third set of laboratory heating experiments (LAB 3) involved two fresh ribs from the same pig obtained from the Covered Market, Oxford, and a dried leg of juvenile Cape fur seal (*Arctocephalus pusillus*) from Cape Cross, Namibia. The two samples were selected to observe the difference between the heating of fresh and dry bone. The samples were cut in small fragments of about one gram for the pig ribs and about three grams for the seal bone. The fragments were then randomly selected and treated in four different ways followed by calcination for four hours at 800°C, with or without additives including lard, barley seeds (C_3) and cornflour (C_4) (Table 3.3). Lard was used to mimic the effects of fat.

Table 3.3 – Laboratory heating experiments 3 (LAB 3) samples

	No calcination	**Calcination**	**Calcination + lard**	**Calcination + barley**	**Calcination + corn**
No treatment	A0	A1	A2	A3	A4
Lipid removal	B0	B1	B2	B3	B4
Organic matter removal	C0	C1	C2	C3	C4
Lipid and organic matter removal	D0	D1	D2	D3	D4

Lipids were removed by soaking the unburned bone in a mixture of methanol and chloroform (2:1), and ultrasonication. It was done several times until no visible lipid residue was left. Organic matter (e.g. collagen) was removed using hydrazine hydrate (95%) following the protocol designed by Termine et al. (1973).

3.2 Outdoor burnings

Several animal joints were burned on outdoor pyres (OUT). Four pyres were prepared, each surrounded by a small brick wall on three sides to protect it from wind and to minimise CO_2 cross-contamination (Figures 3.1). The pyres were fuelled with manufactured coal briquettes, modern and dendrochronologically dated wood. The modern wood fire and the one fuelled with manufactured coal briquettes were carried out on the same day, and those fuelled with dendrochronologically dated wood on another. Some millet seeds (C_4-plant) were also added to the coal fire for the burning of two samples in order to observe the effects of fuel on the isotope composition.

Animal joints obtained from local butchers and supermarkets were placed on the four pyres once they were burning well (Table 3.4). Some of the animal joints were specially chosen to represent as closely as possible the remains of a recently deceased individual. The pig foot and scapula, as well as the whole corn-fed chicken, still retained all flesh and skin.

Figure 3.1 – (from left to right) Coal fire 1, modern wood fire 3, old wood fires 1 & 2

Table 3.4 – List of samples burned on outdoor pyres

	Sample	Fuel (Appendix 6.10)	Time
L1_A	Defleshed lamb leg	Wood 3	1h
L1_B	Defleshed lamb leg	Coal 1	50 min
L1_D	Defleshed lamb leg	Coal 1 + millet seeds	2h
L2_A	Defleshed lamb leg	Coal 1	1h 30 min
L3	Defleshed lamb leg	Wood 1	1h 30 min
P1	Defleshed and dried pig scapula	Coal 2	4h
P2	Defleshed pig rib	Wood 2	1h 15 min
P3	Defleshed pig rib	Wood 1	1h
P4	Defleshed pig rib (within the corn fed chicken)	Wood 2	2h 30 min
P5	Defleshed pig leg with lard	Wood 2	1h 45 min
P6	Pig trotter with flesh and skin	Wood 1	1h 30 min
P7	Pig scapula with flesh and skin	Wood 1	1h 30 min
C1	Defleshed cow tibia	Wood 2	1h 15 min
C2	Defleshed cow tibia	Wood 1	1h
Ch1	Whole corn-fed chicken	Wood 2	2h 30 min

It is important to note the extreme variability in the temperatures which were recorded during the burnings on Wood 1 and 2 via a thermocouple: from 600 to 900ºC. Temperatures above 900ºC were also recorded locally, but only for a few seconds at any given time – such temperatures would be reached and maintained much more readily in a larger pyre. The hottest point of the fire shifted over time. In general, small fragments (for example the phalanges of a pig foot) were fully calcined, while larger ones (for example the cow tibia)

were only partially calcined, with their outer parts mostly white and the inner parts partially grey and black (charred).

The temperature of the Wood 3 as well as the 'Coal' fires 1 and 2 were evaluated using pieces of calcite wrapped in aluminium foil and placed in the fires. The thermal degradation of calcite occurs at between 700°C and 750°C which is the temperature that has to be reached in order to achieve completely calcined bone. All the piece of calcite underwent thermal transformation, showing that the temperature of the fires reached at least 700–750°C, but may have reached even higher temperatures (Rodriguez-Navarro et al. 2009).

4 Chemical pre-treatments

4.1 Collagen extraction

For bone collagen $\delta^{13}C$ measurements of modern unburned bone, skin and flesh were removed mechanically. Lipids were removed by soaking the bone in a mixture of methanol and chloroform (2:1), and ultrasonication. The bone was then demineralised with HCl (0.5M at 4°C). The collagen was subsequently extracted by adding pH3 water at 75°C. The supernatant solution containing the dissolved collagen was then freeze-dried (O'Connell et al. 2001).

4.2 Radiocarbon dating of calcined bone

For radiocarbon dating, the burned bone fragments were treated with sodium chlorite (1.5% at pH3) for 48 hours to remove any remaining organic matter. This was followed by a treatment with acetic acid (1M) of 24 hours to eliminate calcite and adsorbed carbonates. Some samples only underwent a 24 hour treatment with 1M acetic acid (Appendix 3). The bones were then reacted with phosphoric acid (85%), and the CO_2 released was trapped cryogenically and converted into graphite before being radiocarbon dated (Lanting et al.

2001; Brock et al. 2010b). A fragment of the manufactured coal briquettes ('Coal' 1) used for the outdoor burning was also dated, after having been treated with HCl (1M) in order to demineralize it, NaOH (0.2M) to remove any humic acid, and with HCl (1M) for a second time to remove dissolved atmospheric CO_2 from the preceding base wash (Brock et al. 2010b). The dates were obtained by AMS at the Oxford Radiocarbon Accelerator Unit.

4.3 Stable carbon and oxygen isotopes from apatite carbonates

For stable carbon and oxygen isotope measurements, heated bone fragments were treated with sodium hypochlorite (1% NaClO) for one hour to remove any remaining organic matter (if any) followed by a four-hour treatment with 1M acetic acid (CH_3COOH) to remove any adsorbed carbonates and diagenetic apatites. Tooth enamel samples were pre-treated the same way but left for only 30 minutes in a 1M solution of calcium acetate buffered acetic acid. Unburned modern bone samples were treated with hydrazine hydrate (95%) following the protocol designed by Termine et al. (1973) to remove all organic matter. This was followed by 30 minutes in a 1M solution of calcium acetate buffered acetic acid. All samples were then left in the freeze-dryer overnight. The use of hydrazine hydrate instead of sodium hypochlorite is justified by lower impact of hydrazine on the $\delta^{13}C$ and $\delta^{18}O$ values of unburned bone apatite carbonates compared to NaClO (Pellegrini and Snoeck in prep). The use of calcium acetate-buffered acetic acid limited the losses of material for unburned bone and tooth enamel.

4.4 Pre-treatment for strontium isotope measurements

For strontium isotope analyses, tooth enamel and calcined bone samples were rinsed three times with milliQ water. For each rinsing, the samples were placed for 10 min in an ultrasonication bath. The samples were then treated with 1M acetic acid (1 mL per 10 mg of sample) for 3 min in an ultrasonication bath and then rinsed once more with milliQ water and

10 min ultrasonication. All samples were then dried in a freeze-dryer overnight. The limit of three minutes in the ultrasonication bath was chosen in order to limit sample loss. This protocol is detailed and justified in Chapter 6.

4.5 Acid digestion and strontium purification for isotope analyses

The entire acid digestion process and subsequent strontium purification was achieved under a class 100 laminar flow hood in a class 1000 clean room (Université Libre de Bruxelles, Belgium). About 50 mg of sample was dissolved in closed ®Savillex containers overnight using 14M HNO_3 on a heating plate at 110°C. Once dissolved the samples were dried and left to cool to room temperature, before being redissolved in 2M HNO_3 and ultrasonicated for 20 minutes. Strontium was extracted by column chromatography using successive acid elution on a Sr-Spec resin following a similar protocol to that described in Míková & Denková (2007). The sample was charged onto the column with 4x0.5mL of 2M HNO_3. The column was then rinsed with 2x0.5mL 2M HNO_3, 6x0.5mL 7M HNO_3 and 1x0.5mL 3M HNO_3. Finally, the column was eluted and the strontium collected with 4x0.5mL 0.05M HNO_3. The purified sample was then evaporated and dried.

5 Fourier Transform Infrared spectroscopy (FTIR)

For infrared analyses, the samples were first crushed using a mortar and pestle and then analysed by Fourier Transform Infrared spectroscopy with Attenuate Total Reflectance (FTIR-ATR – Agilent Technologies Cary 640 FTIR with GladiATR™ from Pike Technologies). Each sample was measured three times. The background was subtracted and a baseline correction was carried out using Agilent Resolution Pro software. The spectra were normalised and all three spectra of each sample were averaged before calculation of the various infrared indices. To ensure better reproducibility of the measurements carried out by

FTIR-ATR, only spectra with a minimum absorbance of 0.06 for the highest phosphate band at c. 1035 cm^{-1} were taken into account (Appendix 5).

Most FTIR-ATR are limited to a 4000–600 cm^{-1} range while the one used here can go up to 400 cm^{-1} which is of particular interest for the study of bone apatite since two of the main phosphate absorbance bands (used to measure the IRSF and other indices) are located at 605 and 565 cm^{-1}.

6 Mass spectrometry

6.1 Elementary analyses of calcined bone and isotope analyses of fuels and collagen

For collagen and fuel isotope measurements, two or three aliquots of approximately 1 mg of dried collagen or crushed fuel were placed in a tin capsule and analysed by mass spectrometry (Sercon Geo 2022 IRMS coupled to Sercon Europa EA–GSL running with continuous flow mode with helium carrier gas 80 mL/min; alanine was used as standard). The same spectrometer was used to analyse calcined bone for elementary carbon and nitrogen composition. While FTIR allows for sample recovery, IRMS requires between 5 to 10 mg of sample, and was therefore only carried out on experimentally heated samples (LAB 2). The limit of detection is 2 µg nitrogen and 5 µg of carbon. The values are reported in % weight.

6.2 Isotope analyses of apatite carbonates

6.2.1 Common acid bath

Some calcined bone samples were measured in the Department of Earth Sciences of the University of Oxford using a VG Isoglas Prism II mass spectrometer with an on-line Isocarb common acid bath preparation system. Between 2 and 5mg of samples were required.

6.2.2 Carbonate device

Because of the isotopic memory effect observed in the common acid bath (Appendix 4), it was decided to measure all the samples using a carbonate device. The $\delta^{13}C$ and $\delta^{18}O$ values of tooth enamel and calcined bone samples were measured at the Muséum National d'Histoire Naturelle, Paris, France. Between 600µg and 5mg were reacted with 100% phosphoric acid at 70°C for 4 min in a Kiel IV carbonate device, interfaced with a Delta V Advantage isotope ratio mass spectrometer. An internal laboratory carbonate standard (LM marble) was used to check the accuracy of the data. Its isotope values, normalized to the international standard NBS 19, are +2.08 ‰ for carbon and +1.70 ‰ for oxygen. Analytical precision was ± 0.04 ‰ for $\delta^{13}C$ (1SD) and ± 0.05 ‰ for $\delta^{18}O$ (1SD) (n = 78) over the period of analysis.

6.3 Strontium isotope analyses

The dried residues of purified strontium samples were dissolved in 100 µl of concentrated HNO_3, evaporated and finally dissolved in 1.5 mL of 0.05M HNO_3. Strontium isotope compositions were measured on a Nu Plasma Multi-Collector Inductively Coupled Plasma Mass Spectrometer (Nu015 MC-ICP-MS from Nu Instruments) at Université Libre de Bruxelles, Belgium. Particular attention was paid to the purity of the Ar gas used inside the MC-ICP-MS in order to avoid any interference (from Kr for instance) on Sr isotope masses. Strontium isotopes were analysed by static multi-collection. Each analysis consisted of 60 ratio measurements (3 blocks of 20 cycles), resulting in a data collection duration for each individual sample of 12–13 minutes. All strontium isotopes (84, 86, 87, 88) were measured, while the masses 85 (Rb) and 83 (Kr) were simultaneously monitored, allowing for interference corrections on masses 84, 86 (Kr) and 87 (Rb). Sr isotope ratios were automatically normalized to $^{86}Sr/^{88}Sr = 0.1194$ using an exponential law except for the 'spiked' samples (see Chapter 6) for which the internal normalization does not apply. During

the course of this study, repeated measurements of the NBS987 standard yielded $^{87}Sr/^{86}Sr$ = 0.710249±26 (2SD for 37 analyses – standard deviations reported in this work refer to the fifth and sixth decimal places), which is consistent with the mean value of 0.710252±13 obtained on TIMS (Weis et al. 2006). All the sample measurements were normalised using a standard bracketing method with the recommended value of $^{87}Sr/^{86}Sr$ = 0.710248 (Weis et al. 2006). For each sample a 2σ error (absolute error value of the individual sample analysis – internal error) was calculated.

7 Statistical analyses

Statistical analyses were carried out using *Microsoft Excel 2010*. To compare two groups of samples, two-tailed t-tests were carried out using the equal or unequal variance mode depending on the variance observed in each group. An ANOVA was carried out when more than two groups were being compared. For all tests, the *p*-values are reported in the text. In many cases, correlations were observed between two characteristics and a regression analysis was carried out (the R^2 values are reported in the text and in the graphs with *p*-values only if above 0.01).

Chapter 4 – Compositional and structural changes of bone during and after calcination

1 Introduction

During heating, the chemical and isotope compositions as well as the structure of bone apatite are modified. This chapter deals with the chemical and structural changes as observed by infrared and elementary analyses. I begin by describing the infrared spectra of unburned, charred and calcined bone. The current infrared indices used in the literature are then comprehensively reviewed. The following part outlines the experimental design for the study of compositional and structural changes. The results are presented and discussed in the final sections, followed by preliminary conclusions.

The compositional and structural modifications of bone apatite during calcination have already been assessed using a combination of infrared indices, mostly on experimentally heated bone (e.g. Thompson et al. 2009; Lebon et al. 2010; Thompson et al. 2013). However, due to the different experimental conditions used (time, temperature), the relative effects of temperature and exposure time remain unclear. Furthermore, although the higher crystallinity observed in calcined bone likely makes it more resistant to diagenesis (Zazzo & Saliège 2011; Quarta et al. 2013), the impact of burial environment on the composition and structure of calcined bone fragments has not yet been investigated. These gaps will be addressed in this chapter.

2 Infrared spectra of unburned, charred and calcined bone

The use of infrared spectroscopy for the analysis of heated bone is of particular interest since both compositional and structural information can be obtained with a minimal amount of sample (2 to 5 mg) and time (less than 10 minutes/sample measured in triplicates). Indeed by

looking at the spectra of unburned, charred and calcined bone (Figure 4.1) it is already possible to extract useful information such as the loss of organic matter and water once bone is fully calcined (disappearance of the broad band B and band D).

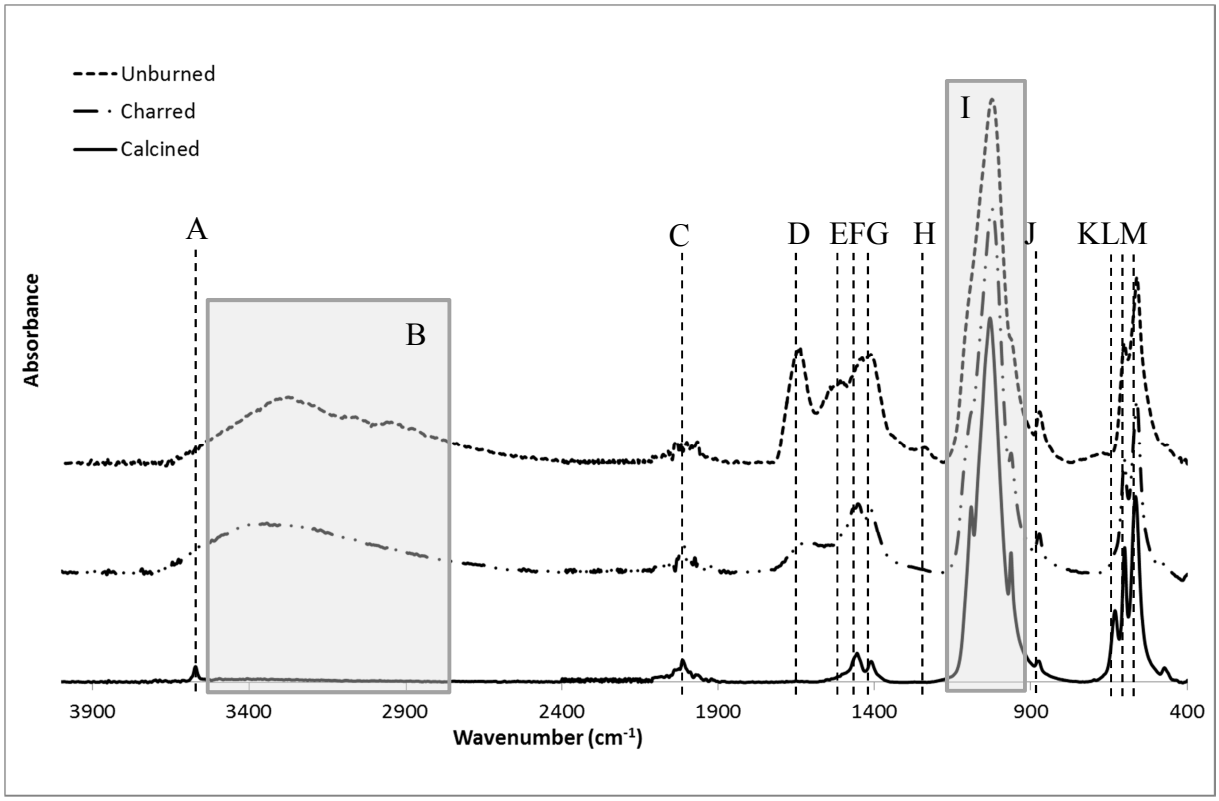

Figure 4.1 – FTIR spectra of unburned, charred and calcined bone with the important bands highlighted

In the infrared spectra, several bands can be seen. Each band corresponds to a specific vibration mode (e.g. stretching, bending) of a particular polyatomic ion or molecule (e.g. CO_3^{2-}, PO_4^{3-}). When infrared photons interact with ions, vibrational excitation of the chemical bonds between the atoms can occur. Each ion can have several vibration modes depending on its nature. The most common are stretching (changes on the length of the chemical bond) and bending (changes in angle between two chemical bonds). For each of these vibration modes to be excited, a specific energy is required that corresponds to a specific wavenumber. The infrared photons having that energy will be absorbed creating the bands that can be seen in the infrared spectra. The exact wavenumber at which a specific

chemical bond will absorb infrared photons depends not only on the nature of the bond (singe, double, triple) and the atoms involved in it (C, N, O, etc.) but also on the other elements present in the vicinity of the bond as well as its position in, for example, a crystalline structure such as bone apatite. For example, the bands L and M (Figure 4.1) both correspond to the bending mode of phosphates in bone apatite ($\nu_4PO_4^{3-}$). The two bands correspond to phosphates located in two different positions in the structure of bone apatite (Figure 2.1).

Table 4.1 – List of infrared bands of interest for the structural and compositional study of bone

Band	Functional Group(s)	Mode	Wavenumber (cm^{-1})	References
A	Apatitic hydroxyl groups (ν_SOH^-)	O-H stretching	3570	1, 2, 5
B	Organic fraction	C-H and O-H stretching	3600–2700	9, 10
	Water	O-H stretching		13
C	Cyanamide (ν_SCN)	C-N stretching	2010	3, 7,12
D	Amide I (C=O)	C-O stretching	1650	8, 9
	Water	H-O-H bending		13
E	Amide II (N-H)	N-H bending	1550	8, 9
	Type A carbonates ($\nu_3CO_3^{2-}$)	C-O stretching	1540	1
F	Type A + B carbonates ($\nu_3CO_3^{2-}$)	C-O stretching	1450	6, 10, 11
G	Type B carbonates ($\nu_3CO_3^{2-}$)	C-O stretching	1415	1, 4
H	Amide III (N-H)	N-H bending	1250	8, 9
I	Phosphates ($\nu_1\nu_3PO_4^{3-}$)	Symmetric (ν_1) and anti-symmetric (ν_3) P-O stretching	1200–900	1
J	Type A + B carbonates ($\nu_2CO_3^{2-}$)	Out-of-plane bending	870	1, 4
K	Apatitic hydroxyl groups (ν_LOH^-)	Librational	630	2
L	Phosphate ($\nu_4PO_4^{3-}$)	P-O bending	605	1, 4
M	Phosphate ($\nu_4PO_4^{3-}$)	P-O bending	565	1, 4

[1]LeGeros et al. 1969; [2]González-Díaz & Santos 1977; [3]Dowker & Elliott 1979; [4]LeGeros & LeGeros 1983; [5]Rey et al. 1995; [6]Sønju Clasen & Ruyter 1997; [7]Habelitz et al. 2001; [8]Paschalis 2009; [9]Rajendran 2011; [10]Holcomb & Young 1980; [11]Suetsugu et al. 1998; [12]Duvernay et al. 2005; [13]Praprotnik & Dušanka Janežič 2005

When studying the structural and compositional changes occurring in bone during heating, there are 14 bands of interest (A to M on Figure 4.1 – Table 4.1) that correspond to different polyatomic ions or molecules. The changes observed in the intensity and/or exact position of these bands are linked to heat damage and/or post-burial alterations. Indeed, experiments carried out on more than 500 samples obtained from cow and sheep bones showed that the variability seen in the infrared spectra throughout the skeletal element is small compared to the changes caused by heating and other external conditions (Thompson et al. 2011).

In this work, bands around 2300–2400 cm^{-1} are observed in most of the infrared spectra. These correspond to the presence of atmospheric carbon dioxide in the working area which increases with time due to the breathing of the operator, which is a particular problem of the ATR mode. Fortunately, no band of interest is present in that spectral region, except, potentially, for some carbon dioxide released during the decomposition of bone apatite carbonates that could still be within the structure of bone apatite (Holcomb & Young 1980). It is not possible in ATR mode to discriminate these from the atmospheric carbon dioxide.

3 Current infrared indices for the study of bone apatite

Infrared spectra provide information on the vibrations between atoms in molecules and ions, and these vibrations are influenced by the chemical and crystalline environment. As a way of deciphering and cataloguing this information, calcified tissue researchers have developed a series of ratios, or indices based on the intensity and position of various bands of the infrared spectra (e.g. Roche et al. 2010). However, there is still a large debate on how significant they are, and how the information given by each of these indices varies from other indices.

3.1 Carbonate to phosphate ratios

The most commonly used infrared indices in the study of bone are the carbonate to phosphate ratios that evaluate the relative amount of carbonates (of type A and/or B) compared to phosphates. Several carbonate to phosphate ratios exist (Table 4.2) and all compare one or more carbonate bands to one or more phosphate bands (Figure 4.2).

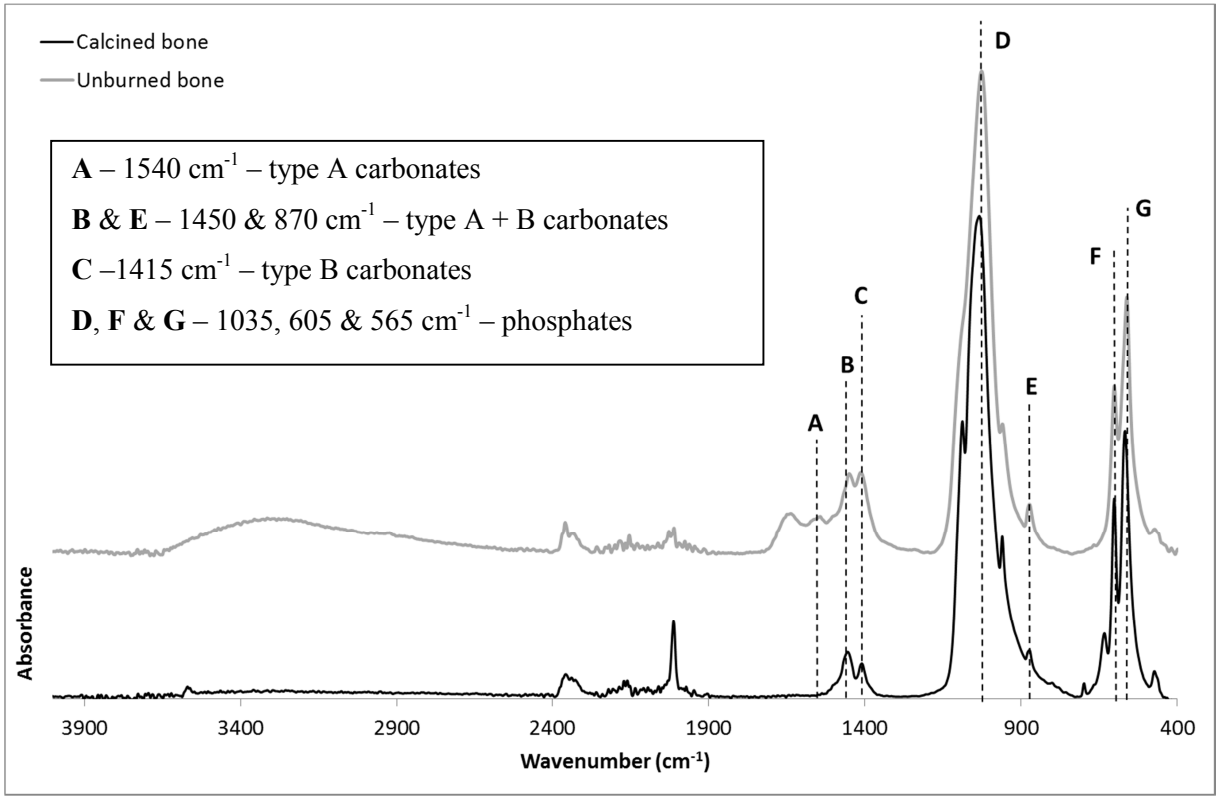

Figure 4.2 – FTIR spectra of archaeological calcined and unburned bone; the bands used for the measurements of the various carbonate to phosphate ratios are highlighted

Table 4.2 – List of carbonate to phosphate ratios

Name	Measurement	Significance	Reference
C/P 1 or BPI	A_{1415}/A_{605}	Amount of type B carbonates	1,2
C/P 1_a	A_{1415}/A_{1035}		3
C/P 2_a	A_{870}/A_{565}	Amount of type A + B carbonates	4
C/P 2	A_{870}/A_{605}		1
API	A_{1540}/A_{605}	Amount of type A carbonates	2
CO_3/PO_4	$(A_{1415} + A_{1450}) / (A_{605} + A_{565})$	Amount of type A + B carbonates	5

[1]LeGeros & LeGeros 1983; [2]Sponheimer & Lee-Thorp 1999; [3]Wright & Schwarcz 1996; [4]Stiner et al. 1995; [5]Pucéat et al. 2004

The C/P 1 (or BPI – type B carbonate to phosphate index) and C/P 1_a are the most commonly used in the literature to assess the relative concentration of type B carbonates. Both use the same type B carbonate band at 1415 cm^{-1} but different phosphate bands (605 and 1035 cm^{-1} respectively). It has been shown that C/P 1 is linearly related to the carbonate content of carbonated apatite (Featherstone et al. 1984), but the use of C/P 1_a instead of C/P 1 allows the carbonate to phosphate ratio to be independent from the infrared splitting factor (Wright & Schwarcz 1996; Lebon et al. 2010). The different C/P 2 (C/P 2 and C/P 2_a) compare another carbonate band (870 cm^{-1}) corresponding to a combination of type A and B carbonates to different phosphate bands. In spite of the contribution of HPO_4^{2-} around 870 cm^{-1}, when organic matter is present, such as in unburned bone, the use of a C/P 2 ratio is recommended as the band at 1415 cm^{-1} is affected by organic components (LeGeros & LeGeros 1983; Stiner et al. 1995). The CO_3/PO_4 ratio, such as the C/P 2 ratios, evaluates the amount of type A and B carbonates as the band at 1450 cm^{-1} accounts for both types of carbonates (Holcomb & Young 1980; Sønju Clasen & Ruyter 1997; Suetsugu et al. 1998).

Type A carbonates are evaluated using the API (type A carbonate to phosphate index). In modern bone, in which there is still a large amount of organic matter, the band at 1540 cm^{-1} overlaps with the amide band at 1550 cm^{-1}. Even in archaeological bone containing some remaining organic matter, the API will be affected. In calcined bone, it is generally possible to detect the presence of type A carbonates, even if the band is very small. In the latter, the API will not be affected by the presence of organic matter since all have been destroyed.

3.2 Phosphate indices

The most common indices relying only on phosphate bands are the indicators of crystallinity and mineral maturity, two different characteristics of bone apatite. Crystallinity is defined as the degree of order within a crystal lattice and provides information about the relative sizes of

crystals (LeGeros 1991; Farley et al. 2010) while mineral maturity describes the change from non-apatitic domains into well-crystallised apatites (Farley et al. 2010). The transformation of a non-apatitic domain into an apatitic one refers to an increase in symmetry within the structure and the loss of tension in the crystal lattice due to the removal of carbonates and other ions. More details on the difference between crystallinity and mineral maturity can be found elsewhere (Farley et al. 2010). Several indices have been developed to characterize both properties of calcined bone (Table 4.3) all based on different phosphate bands (Figure 4.3).

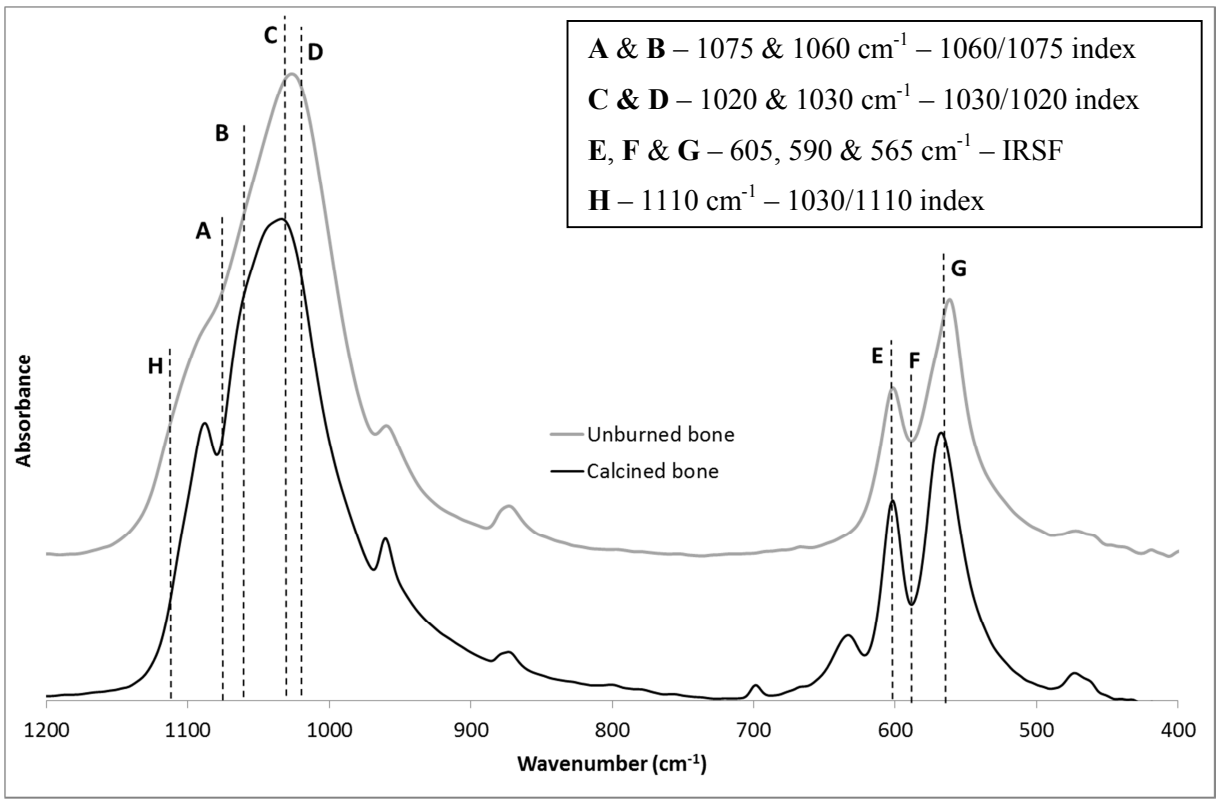

Figure 4.3 – FTIR spectra of archaeological calcined and unburned bone; the bands and specific wavenumbers used for the measurements of the various crystallinity and mineral maturity indices are highlighted

The Infrared Splitting Factor (IRSF) has been intensively used in bone studies. To calculate it, the intensity of the bands at 605 and 565 cm^{-1} are summed and then divided by the absorbance of the valley between these two bands (Weiner & Bar-Yosef 1990). The average IRSF measured in transmission mode (Appendix 5) for modern fresh bone is 2.50–

3.25, but this may increase up to 7 when bone is altered (Olsen et al. 2008; Thompson et al. 2009). Other indices use the broad phosphate band between 900 and 1100 cm^{-1}, composed of several overlapping bands. The ratio of the absorbance intensity at 1030 cm^{-1} to the intensity at 1020 cm^{-1} (1030/1020) is used as an index of variation in crystal perfection: this ratio increases as crystal size increases (Paschalis et al. 1996; 1997; Lebon et al. 2010; Farlay et al. 2010). A further index evaluates crystallinity: 1060/1075 (Lebon et al. 2010). Finally, mineral maturity can be assessed by using the 1030/1110 index (Farley et al. 2010). The bands at ca. 1020 cm^{-1} (and 1110 cm^{-1}) and 1030 cm^{-1} (and 1092 cm^{-1}) are characteristic of non-apatitic and apatitic phosphates respectively.

Another index is found by comparing the different phosphate bands: the phosphate to phosphate index or PPI (Lee-Thorp & Sponheimer 2003). This index comparing the phosphate bands at 565 and 605 cm^{-1} is believed to be sensitive to the changes in alignment of the phosphates in apatite. A final index, the PSF or phosphate splitting factor, was developed in this study especially for the study of calcined bone by analogy to the IRSF: the resolution of the various phosphate bands around 1035 cm^{-1} increase significantly when bone apatite is subjected to high temperatures (Table 4.3 and Figure 4.4).

Table 4.3 – List of phosphate indices

Name	Measurement	Significance	Reference
IRSF	$(A_{605} + A_{565}) / A_{590}$	Crystallinity	1
1030/1020	A_{1030} / A_{1020}		2,3
1060/1075	A_{1060} / A_{1075}		3
1030/1110	A_{1030} / A_{1110}	Mineral maturity	4
PPI (605/565)	A_{605} / A_{565}	Indication of the realignment of phosphate ions in apatite	5
PSF	$(A_{960} + A_{1035} + A_{1090}) / (A_{1000} + A_{1070})$	new index: its significance has not yet been assessed	This study

[1]Weiner & Bar-Yosef 1990; [2]Paschalis et al. 1996; [3]Lebon et al. 2010; [4]Farley et al. 2010; [5]Lee-Thorp & Sponheimer 2003

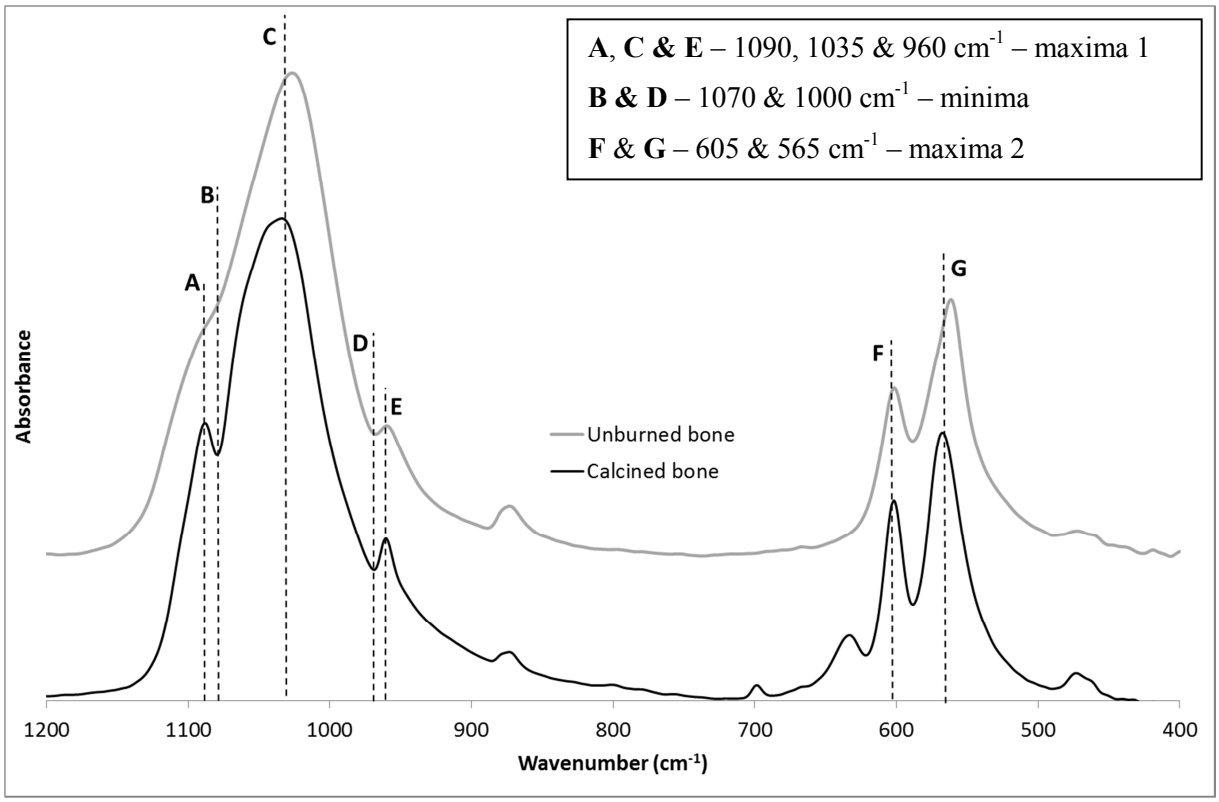

Figure 4.4 – FTIR spectra of archaeological calcined and unburned bone; the bands and specific wavenumbers used for the measurements of the various phosphate to phosphate ratios are highlighted

3.3 Carbonate to carbonate ratios

Two types of carbonates are present in apatite: type A carbonates replacing hydroxyl groups, and type B carbonates replacing phosphates. The BAI (type B to type A carbonate index) evaluates the proportion of each type of carbonates in the apatite using the bands at 1415 and 1540 cm^{-1} for type B and A respectively (Sponheimer & Lee-Thorp 1999; Trueman et al. 2008; Roche et al. 2010). The AB index compares the amounts of type A and B carbonates as it has been demonstrated that the band around 870 cm^{-1} could be separated between a first band at 878 cm^{-1} and another at 871 cm^{-1} corresponding to type A and B carbonates respectively (Rey et al. 1989). The AB index can be used to assess the amount of each type of carbonate, but one ought to be cautious as there is a potential overlap with the HPO_4^{2-} band at 870 cm^{-1} (Paschalis et al. 1996). The C/C ratio compares two different absorbance wavelengths associated with carbonates (Table 4.4 and Figure 4.5). The band at 1450 cm^{-1} is

associated with both types of carbonates while the band at 1415 cm^{-1} only with type B. This index has been shown to be temperature dependent, and is therefore of particular interest to a study of heated bone (Thompson et al. 2009).

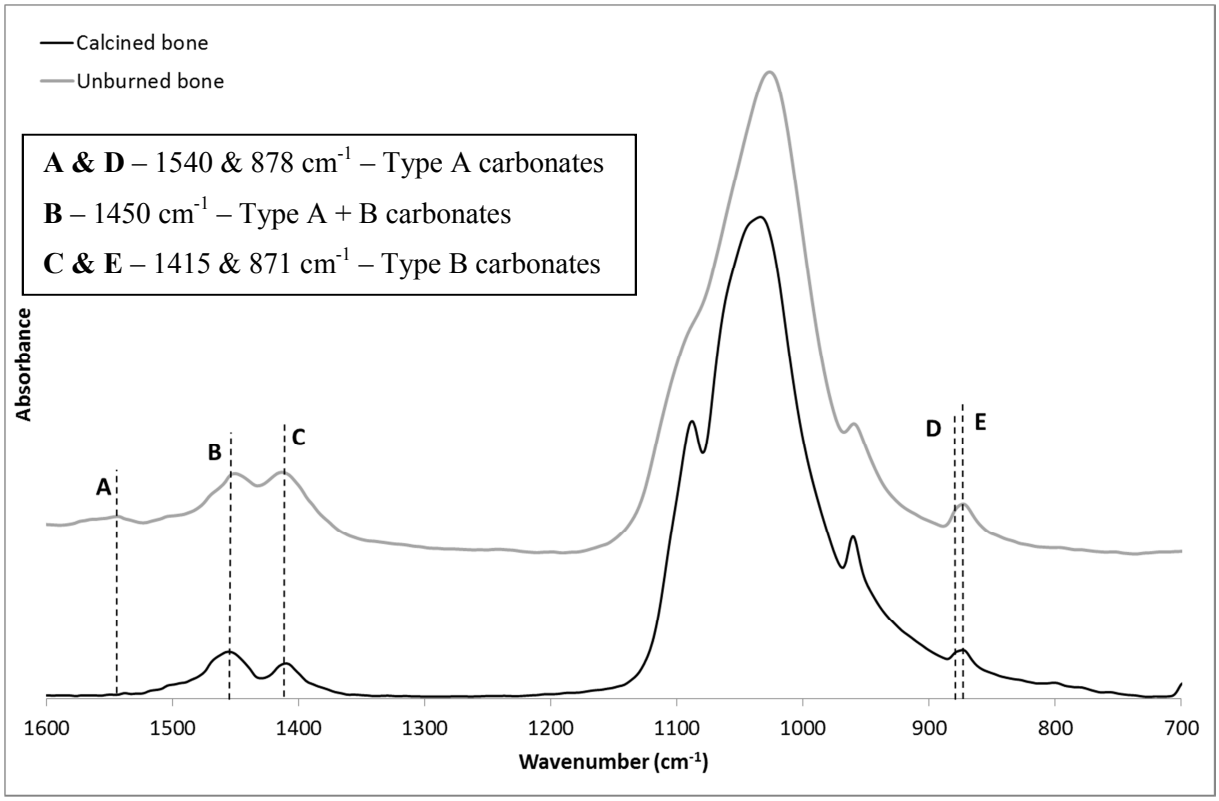

Figure 4.5 – FTIR spectra of archaeological calcined and unburned bone; the bands and specific wavenumbers used for the measurements of the various carbonate to carbonate ratios are highlighted

Table 4.4 – List of carbonate to carbonate ratios

Name	Measurement	Significance	Reference
BAI	A_{1415} / A_{1540}	Assesses the relative amount of type A & B carbonates	1
AB	A_{878} / A_{871}		2
C/C	A_{1450} / A_{1415}	Compares two carbonate bands : (A+B)/B	3

[1]Sponheimer & Lee-Thorp 1999; [2]Rey et al. 1989; [3]Thompson et al. 2009

3.4 Organic content and structural water

When unburned bone is analysed by infrared spectroscopy, its organic fraction is often still present, mainly in the form of collagen. Its presence is reflected in the occurrence of three main bands: Amide I (c. 1650 cm^{-1}), Amide II (c. 1550 cm^{-1}) and Amide III at 1650 cm^{-1},

1550 cm^{-1} and 1350 cm^{-1} respectively (Paschalis 2009; Rajendran 2011; Paschalis et al. 2011). The presence of an organic fraction in bone can also be detected by a broad band from 3600 to 2700 cm^{-1} (Figure 4.6). Structural water (H_2O) is also present within the structure of bone apatite and has characteristic bands similar to those of organic matter around 1650 cm^{-1} and 3600–2700 cm^{-1} (Table 4.1).

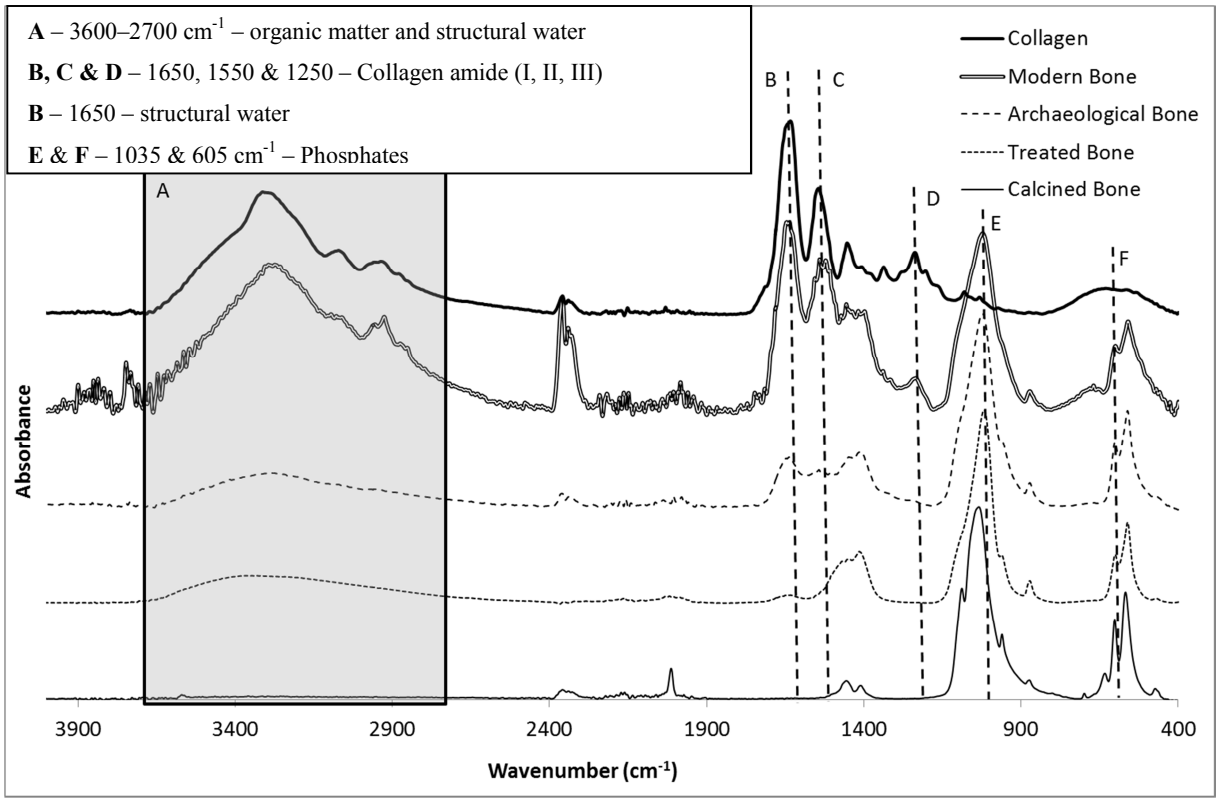

Figure 4.6 – FTIR spectra of collagen, modern and archaeological bone both containing organic matter, a treated (with NaClO) archaeological bone with no organic matter left, and a fully calcined archaeological bone with no organic matter left; the bands used for the measurements of the various organic content indices are highlighted

Several indices have been proposed for the evaluation of the organic content of bone apatite (Table 4.5). The water-amide on phosphate index (WAMPI) evaluates the amount of collagen present in bone apatite using the amide I band of collagen at 1650 cm^{-1} and the phosphate band at 605 cm^{-1}. Similarly, the 1650/1035 ratio evaluates the concentration of collagen by using the phosphate band at 1035 cm^{-1} instead of 605 cm^{-1}. The amount of organic matter (in %wt.) can be evaluated using this 1650/1035 ratio but is only valid if the

bone still contains more than 15% of collagen (modern bone contains about 30% collagen). One of the problems that occur when using these indices is that water also adsorbs around 1650 cm^{-1}, making it difficult to discriminate the presence of organic matter and structural water within the structure of bone apatite.

Table 4.5 – List of organic content indices

Name	Measurement	Significance	Reference
WAMPI	A_{1650}/A_{605}	Amount of water/amide	1
1650/1035	A_{1650}/A_{1035}		2
% Organic	$11.06*\ln(A_{1650}/A_{1035}) + 32.43$	Weight of organic component in bone (%)	2

[1]Roche et al. 2010; [2] Trueman et al. 2004

3.5 Hydroxyl group content

The presence of hydroxyl groups in unburned bone apatite is still the topic of much debate (e.g. Mkukuma et al. 2004; Leventouri 2006; Pasteris et al. 2004; Wopenka & Pasteris 2005) but it is generally agreed that the amount of hydroxyl groups increases when bone is heated (Figure 4.7). When heated in air at 300°C, the infrared spectrum is modified and a band corresponding to the apatitic hydroxyl groups appears at 3570 cm^{-1} (Rey et al. 1995; Biltz & Pellegrino 1983). This was confirmed by further heating experiments up to 1200°C. Furthermore, the occurrence of hydroxyl group bands, first around 3570 cm^{-1} at lower temperature, and then around 630 cm^{-1} from 700–850°C onwards is accompanied by a loss of carbonates (Mkukuma et al. 2004; Rajendran 2011). The 630 cm^{-1} band caused by high temperatures was observed in further experiments (Berna et al. 2012) and has been shown to originate mostly from the decomposition of phosphate by liberation of hydroxyl groups (Rajendran 2011) and another small fraction from the reaction of bone apatite carbonates with water (Holcomb & Young 1980).

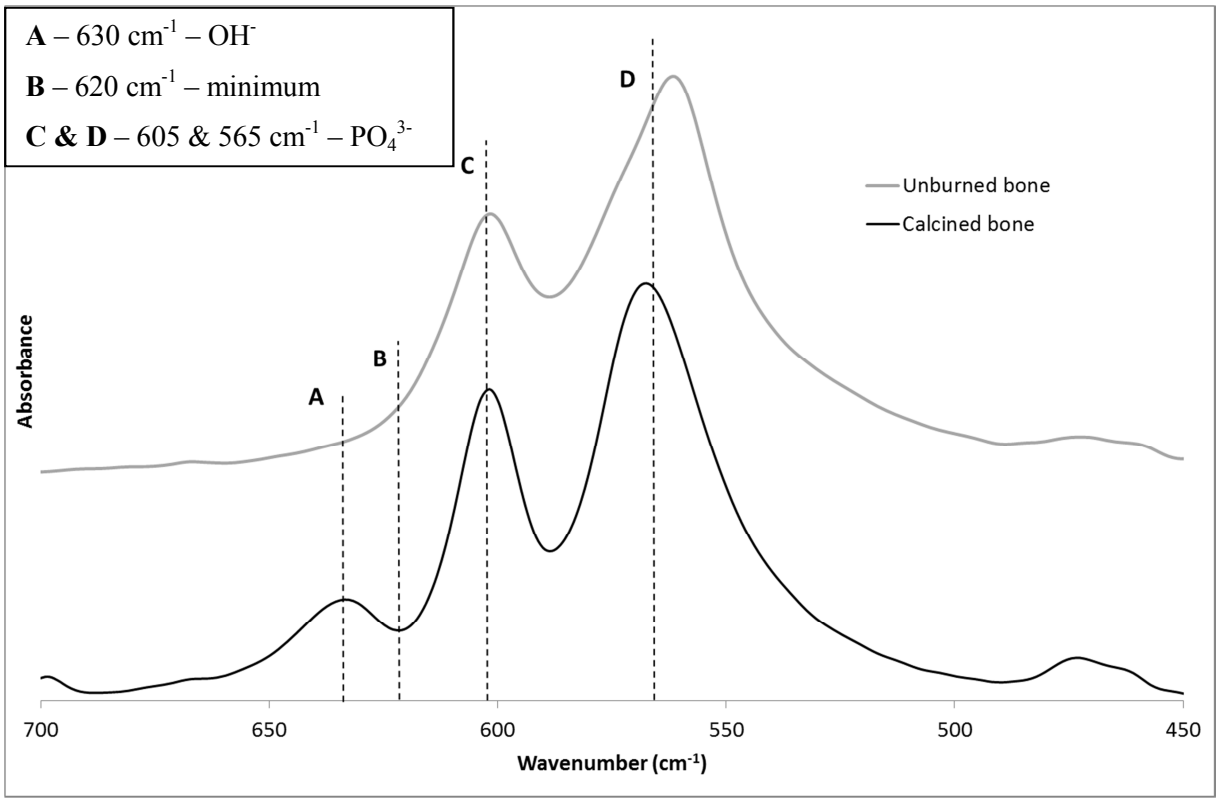

Figure 4.7 – FTIR spectra of archaeological calcined and unburned bone; the bands used for the measurements of the various hydroxyl group content indices are highlighted

New indices were developed in this study to observe the changes in composition and structure caused by the introduction of hydroxyl groups in apatite (Table 4.6). The OH/P ratio (hydroxyl group to phosphate ratio) describes the changes in hydroxyl group content in bone apatite using the band at 630 cm^{-1} and phosphate band at 605 cm^{-1}. The OHSF (hydroxyl splitting factor), such as the PSF, was developed by comparison to the IRSF. The two new indices are especially introduced here for the study of calcined bone as the hydroxyl group bands are only visible in heated bone.

Table 4.6 – List of hydroxyl group content indices

Name	Measurement	Significance	Reference
OH/P	A_{630} / A_{605}	Amount of hydroxyl groups	1
OHSF	(A_{630} + A_{605}) / A_{620}	new index: its significance has not yet been assessed	This study

[1]Snoeck et al. 2014b

3.6 Cyanamide content

Infrared spectra of calcined bone reveal the frequent presence of a band around 2010 cm^{-1} (Figure 4.8). This particular band characteristic of the C≡N stretching has been attributed to the presence of cyanamide ($–CN_2H$) together with a minor band, around 700 cm^{-1}. The incorporation of cyanamide in calcined bone apatite is the consequence of heating in an atmosphere which contains ammonia (Habelitz et al. 2001). The origin of ammonia in the combustion atmosphere is still debated: burning of organic matter (collagen, flesh, skin, fat, etc.) or combustion of fuels/graphite (Habelitz et al. 2001; Hüls et al. 2010; Van Strydonck et al. 2010; Zazzo et al. 2013). A similar cyanamide to phosphate ratio (CN/P) as the one proposed by Zazzo et al. (2013), is proposed here to reflect the presence of cyanamide in heated bone (Table 4.7).

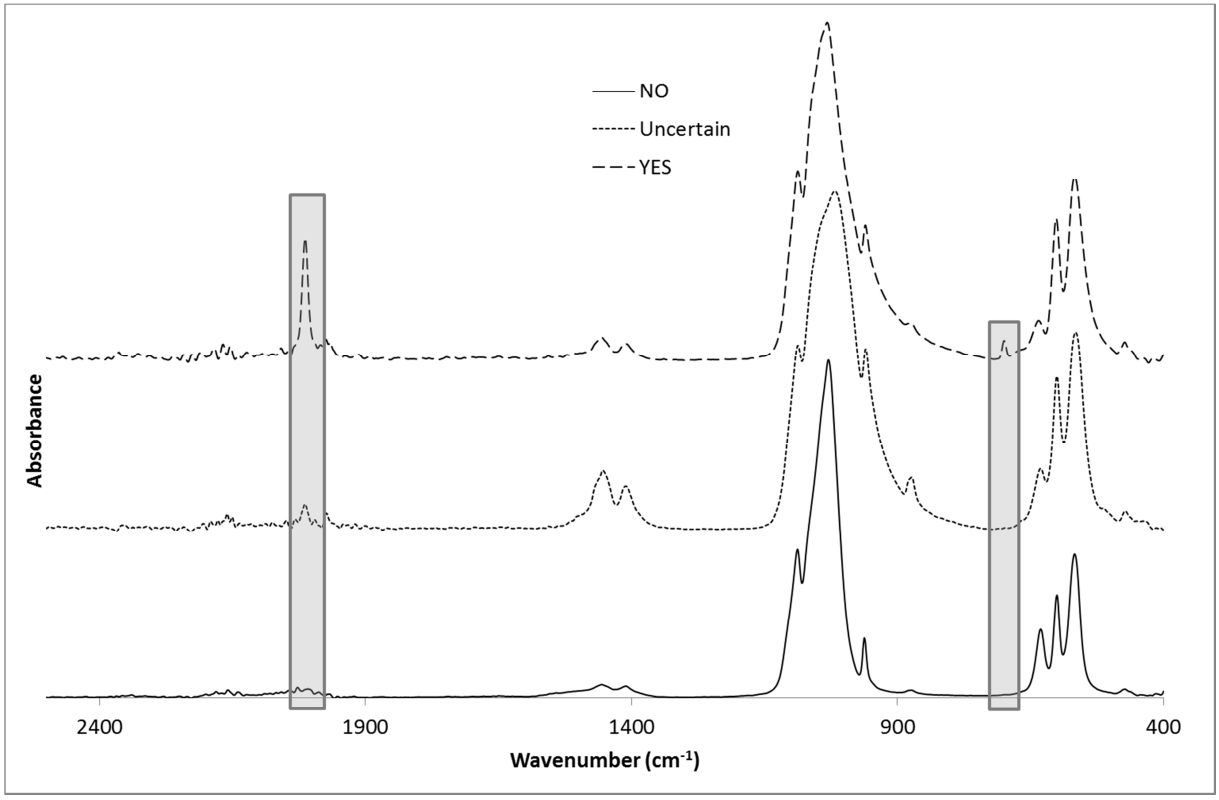

Figure 4.8 – Presence or absence of cyanamide on the FTIR spectra of calcined bone apatite observed through the presence or absence of bands at 2010 and 700 cm^{-1}

Table 4.7 – List of cyanamide to phosphate ratios

Name	Measurement	Significance	Reference
CN_2/PO_4	A_{2010} / A_{1035}	Amount of cyanamide	1
CN/P	A_{2010} / A_{605}		2

[1]Zazzo et al. 2013; [2]Snoeck et al. 2014b

3.7 Potential contaminants

In samples that have been buried in soil, the presence of calcite can be detected based on the sharp C-O band at 710 cm^{-1} and aragonite based on a sharp band at 710 cm^{-1} and another at 1080 cm^{-1} (Hassan et al. 1977; Lee-Thorp & van der Merwe 1991; Wright & Schwarcz 1996). Additionally, quartz is detected by the presence of a Si-O doublet at 796 and 779 cm^{-1} (Bosch Reig et al. 2002). This indicates contamination originating from the soils in which the calcined bone was buried (e.g. quartz in sandstone environments; calcite in chalk and limestone environments).

3.8 Summary of infrared indices

Compositional indices evaluating the amount of carbonates, cyanamide or hydroxyl groups are always comparing a specific band (or two) to one (or two) of the three major phosphate bands (565, 605 or 1035 cm^{-1}). As shown in Appendix 1, due to the presence of quartz in many archaeological samples, compositional indices using the phosphate band at 1035 cm^{-1} are discarded. Furthermore, the relation between indices using a same specific band and comparing it to the 565 or 605 cm^{-1} phosphate bands are strongly linearly correlated ($R^2 > 0.96$), indicating that the same information is obtained when using one or the other index. Finally, the information obtained by calculating indices based on band intensity and band area is the same (Appendix 2). Hereafter, for compositional indices, only those using the phosphate band at 605 cm^{-1} will be considered (Table 4.8). These indices will be investigated in order to highlight those that are of potential interest for the study of heated bone.

Table 4.8 – Infrared indices for the study of bone

Name	Measurement	Significance	Reference
C/P 1 or BPI	A_{1415}/A_{605}	Amount of type B carbonates	1,2
C/P 2	A_{870}/A_{605}	Amount of type A + B carbonates	1
API	A_{1540}/A_{605}	Amount of type A carbonates	2
CO_3/PO_4	$(A_{1415} + A_{1450}) / (A_{605} + A_{565})$	Amount of type A + B carbonates	5
IRSF	$(A_{605} + A_{565}) / A_{590}$	Crystallinity	6
1030/1020	A_{1030} / A_{1020}		7,8
1060/1075	A_{1060} / A_{1075}		8
1030/1110	A_{1030} / A_{1110}	Mineral maturity	9
PPI	A_{605} / A_{565}	Indication of the realignment of the phosphate ions in apatite	10
PSF	$(A_{960} + A_{1035} + A_{1090}) / (A_{1000} + A_{1070})$	new index: its significance has not yet been assessed	This study
BAI	A_{1415} / A_{1540}	Assesses the relative amount of type A & B carbonates	2
AB	A_{878} / A_{871}		11
C/C	A_{1450} / A_{1415}	Compares two carbonate bands : (A+B)/B	12
OH/P	A_{630} / A_{605}	Amount of hydroxyl groups	13
OHSF	$(A_{630} + A_{605}) / A_{620}$	new index: its significance has not yet been assessed	This study
CN/P	A_{2010} / A_{605}	Amount of cyanamide	13
WAMPI	A_{1650}/A_{605}	Amount of water/amide	14
% Organic	$11.06*\ln(A_{1650}/A_{1035}) + 32.43$	Weight of organic component in bone (%)	15

[1]LeGeros & LeGeros 1983; [2]Sponheimer & Lee-Thorp 1999; [3]Wright & Schwarcz 1996; [4]Stiner et al. 1995; [5]Pucéat et al. 2004; [6]Weiner & Bar-Yosef 1990; [7]Paschalis et al. 1996; [8]Lebon et al. 2010; [9]Farley et al. 2010; [10]Lee-Thorp & Sponheimer 2003; [11]Rey et al. 1989; [12]Thompson et al. 2009; [13]Snoeck et al. 2014b; [14]Roche et al. 2010; [15]Trueman et al. 2014

4 Experimental design

To investigate the compositional and structural changes occurring in bone apatite caused by heating and/or post-burial alterations, both Fourier Transform Infrared Spectroscopy in attenuated total reflectance mode (FTIR-ATR) and elementary analysis mass spectrometry (MS) were used. While infrared spectroscopy enables a first assessment of the structure and composition of bone through various ratios, the use of mass spectrometry allows a better evaluation of the amount of carbon and nitrogen present in the samples (%C and %N), useful

in the detection of small amounts of organic matter remaining in bone after heating. Furthermore, the amount of CO_2 released per gram of sample can also be calculated using the data obtained during isotope analyses of the carbonate fraction of bone apatite. The %C and %N were measured on untreated samples while the pCO_2/g of sample was measured after pre-treatment with sodium hypochlorite and acetic acid.

For my purposes here, it is first necessary to assess which FTIR indices provide reliable information and which are superfluous. To do so, unburned, charred, and calcined bone fragments, both archaeological and modern, have been analysed. Having identified the most appropriate indices, they are used to compare unburned and heated bone as well as modern and archaeological calcined bone and to observe compositional and structural changes caused by calcination and post-burial alterations on bone apatite.

All modern samples were also pre-treated using sodium hypochlorite (NaClO) and acetic acid (CH_3COOH) for isotope measurements. For logistical reasons, it was only possible to pre-treat the archaeological samples from Ireland. Infrared spectra were recorded before and after pre-treatment to observe their effect on the composition and structure of calcined bone.

5 Results

5.1 Identification of useful infrared indices for the study of calcined bone

To identify the useful infrared indices for the study of calcined bone, the indices calculated from the infrared spectra of unburned, charred and calcined bone will be compared. The infrared data can be found in appendix 6.

5.1.1 Carbonate to phosphate ratios

There is a strong correlation between the BPI and the CO_3/PO_4 ratio ($R^2 = 0.98$) but both will still be investigated further since the former evaluates the amount of type B carbonates while the latter, the amount of type A + B carbonates. Since the amount of type A carbonates is much lower than the amount of type B in unburned and charred bone, such correlation between both indices is not altogether surprising. The correlations are much lower between the other indices ($R^2 < 0.70$). When comparing the C/P 2 ratio to the BPI (Figure 4.9), two different clusters can be observed, one following an 'upper' correlation and the other, a 'lower' correlation. The first group ('upper') is composed mainly of calcined bone while the latter ('lower') is made of charred and unburned bone. The differences observed between the results of these four indices (API, BPI, CO_3/PO_4, C/P 2) suggests that they highlight different compositional and/or structural characteristics of bone apatite, and will therefore be studied in calcined bone.

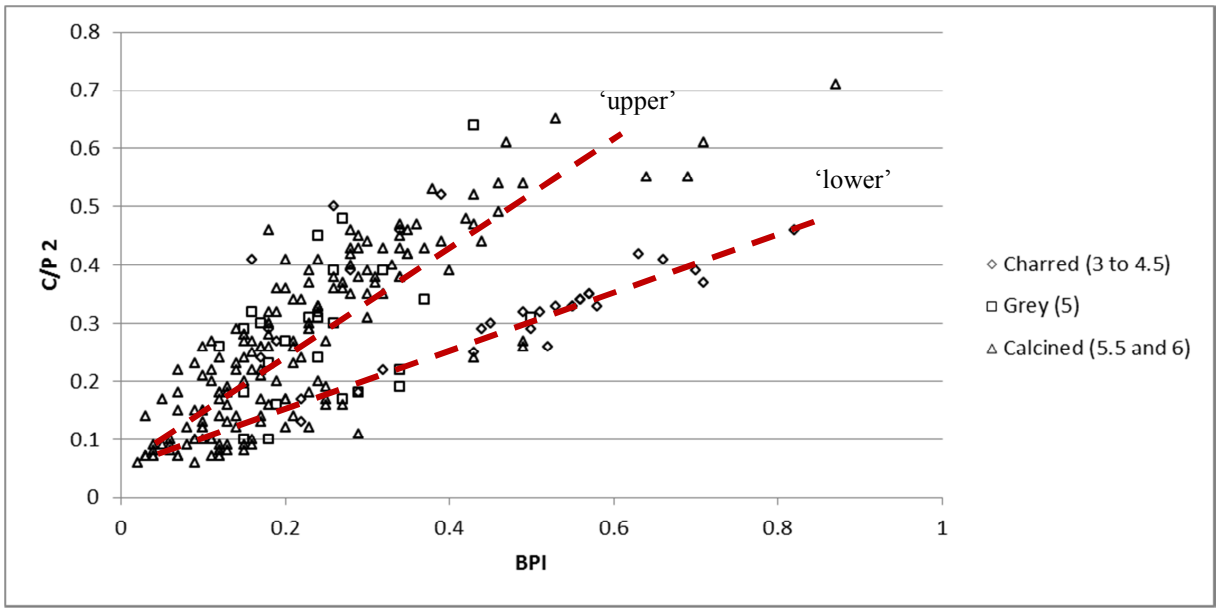

Figure 4.9 – C/P 2 versus BPI showing two possible correlations (dotted lines): an 'upper' and a 'lower' one; charred samples mainly follow the lower correlation while calcined samples follow the upper one

5.1.2 Phosphate indices

The first index that can be discarded from the list of phosphate indices is the 1030/1020 ratio. Because of the ATR mode used in this work, some 'artefacts' make it impossible to extract useful information from that index (Lebon, pers comm). There is good correlation between the IRSF and the 1060/1075 ratio (R^2 = 0.77), confirming previous observations that these two indices provide similar information about crystallinity of bone apatite (Lebon et al. 2010) but both indices still seem to provide slightly different information. The correlation between IRSF and the 1030/1110 ratio is quite similar to its relation to the 1060/1075 ratio (R^2 = 0.71), however, the correlation between 1060/1075 and 1030/1110 is not as good (R^2 = 0.61), suggesting that mineral maturity and crystallinity are indeed two distinct characteristics of bone apatite and that the relation between the two is not straightforward but an increase of crystallinity is associated with an increase in mineral maturity. Even though the 1030/1110 and the 1060/1075 ratios can be influenced by the presence of quartz, all three indices will be investigated to characterise the impact of heating on the structure of bone apatite, as at this stage it is not clear which provide useful and different information.

Additionally, there is only a small correlation between the PPI and the PSF (R^2 = 0.20) suggesting that these two indices highlight different properties of bone apatite. Nevertheless, there is a correlation between the PSF and IRSF (R^2 = 0.73) which is to be expected since it was calculated similarly to the IRSF using the phosphate bands around 1035 cm^{-1} instead of the bands at 565 and 605 cm^{-1}. Both PPI and PSF will be investigated further.

5.1.3 Carbonate to carbonate ratios

The BAI is no more than a combination of the API and BPI and does not provide additional information when studying the compositional changes of bone apatite. The C/C allows for the comparison of the different types of carbonates and has already been shown to be temperature-dependent and is therefore of particular interest for the study of calcined bone.

Increases in the C/C ratio reflect a change in the proportion of type A compared to type B carbonates which can be achieved by an increase in type A carbonates due perhaps to a transfer of carbonates from the B to the A site (as was observed in heated enamel, Holcomb & Young 1980), or a decrease in type B carbonates. Finally the AB ratio could provide useful information additionally to the C/C ratio ($R^2 = 0.67$ for C/C and AB).

5.1.4 Organic content and structural water

The measurement of % organic content is obsolete in the study of calcined bone. Indeed, the infrared spectrum itself provides more information about the presence of organic matter. The absence of bands at 1650 and 2700–3600 cm^{-1} is sufficient indication of the absence of organic matter in calcined bone (Figure 4.6). Nevertheless, the WAMPI is used to compare unburned, charred, and calcined bone, and confirm the absence of organic matter and structural water in calcined samples (WAMPI < 0.05).

5.1.5 Hydroxyl group content

No strong correlation could be found between the OH/P and OHSF ($R^2 = 0.21$) and OHSF and IRSF ($R^2 = 0.05$); though when considering only calcined bone fragments, for which the OHSF was specifically designed, the correlation increases ($R^2 = 0.81$). Interestingly, there is a moderate correlation between the OH/P ratio and IRSF ($R^2 = 0.64$) as the crystallinity increases when the amount of hydroxyl groups increases. Both OH/P and OHSF will be investigated here.

5.1.6 Cyanamide content

As shown on Figure 4.8, it is sometimes difficult to detect the presence of cyanamide but CN/P values above 0.25 clearly indicate its presence. Values between 0.18 and 0.25 were classified as ‘uncertain’, and values below 0.18 as unlikely to contain observable amounts of cyanamide. This ratio will be used to screen for the presence of cyanamide in calcined bone.

5.1.7 Summary of useful infrared indices

Fifteen potentially useful infrared indices were selected for the study of burned bone (Table 4.9). These were measured on all heated bone samples (modern and archaeological) and are discussed in the following sections. Some infrared indices such as the API and the CO_3/PO_4 are used to assess compositional changes while others, such as the IRSF, are used to study the structural changes undergone by bone apatite during heating.

Table 4.9 – Potentially useful infrared indices for the study of heated bone

Name	Measurement	Significance	Reference
C/P 1 or BPI	A_{1415}/A_{605}	Amount of type B carbonates	1,2
C/P 2	A_{870}/A_{605}	Amount of type A + B carbonates	1
API	A_{1540}/A_{605}	Amount of type A carbonates	2
CO_3/PO_4	$(A_{1415} + A_{1450}) / (A_{605} + A_{565})$	Amount of type A + B carbonates	3
IRSF	$(A_{605} + A_{565}) / A_{590}$	Crystallinity	4
1060/1075	A_{1060} / A_{1075}		5
1030/1110	A_{1030} / A_{1110}	Mineral maturity	6
PPI	A_{605} / A_{565}	Indication of the realignment of the phosphate ions in apatite	7
PSF	$(A_{960} + A_{1035} + A_{1090}) / (A_{1000} + A_{1070})$	new index: its significance has not yet been assessed	This study
AB	A_{878} / A_{871}	Assesses the relative amount of type A & B carbonates	8
C/C	A_{1450} / A_{1415}	Compares two carbonate bands : (A+B)/B	9
OH/P	A_{630} / A_{605}	Amount of hydroxyl groups	10
OHSF	$(A_{630} + A_{605}) / A_{620}$	new index: its significance has not yet been assessed	This study
CN/P	A_{2010} / A_{605}	Amount of cyanamide	10
WAMPI	A_{1650}/A_{605}	Amount of water/amide	11

[1]LeGeros & LeGeros 1983; [2]Sponheimer & Lee-Thorp 1999; [3]Pucéat et al. 2004; [4]Weiner & Bar-Yosef 1990; [5]Lebon et al. 2010; [6]Farley et al. 2010; [7]Lee-Thorp & Sponheimer 2003; [8]Rey et al. 1989; [9]Thompson et al. 2009; [10]Snoeck et al. 2014b; [11]Roche et al. 2010

5.2 Compositional and structural changes of experimentally heated bone

The compositional changes that can be observed in bone apatite through infrared spectroscopy are the changes in carbonate, phosphate and hydroxyl group content. Bone is not only composed of bone apatite, but also contains large amounts of organic matter (mainly in the form of collagen) and water. The elimination of water as well as the decrease and destruction of organic matter after heating can also be monitored. Furthermore, the infrared spectra allow the detection of cyanamide ($-CN_2H$) in the structure of heated bone. The main structural change that can be observed is a change in crystallinity but it is also possible to observed changes in mineral maturity.

In this section, the results of the laboratory heating experiments 2 and 3 (LAB 2 and LAB 3) will be detailed. The LAB 2 samples have also been analysed for elementary analyses (%C and %N) and LAB 2 and LAB 3 samples have been investigated isotopically giving additional information about their carbonate content via the pCO_2/g. The raw data can be found in Appendices 6.2 and 6.3.

5.2.1 Laboratory heating experiments 2 (LAB 2)

The laboratory heating experiments 2 (LAB 2) included the heating of bone samples from the same cow tibia for different times and at different temperatures. Some samples were still charred while others were calcined. For each a colour code was assigned according to the burn colour code (Table 2.1 – Chapter 2). In some cases it was difficult to assign a colour code and 'half-codes' have sometimes been assigned (e.g. 4.5 if the bone was between category 4 and 5).

5.2.1.1 Phosphate content

Most indices used to assess the compositional changes rely on one of the phosphate bands as reference, making it difficult, if not impossible, to assess the effect of heating on the

phosphate content in bone through infrared spectroscopy but it is generally assumed that phosphate content is not altered by heating. Variations in the relative intensity of phosphate bands are generally associated with structural changes (e.g. crystallinity).

5.2.1.2 Organic content and structural water

As mentioned above, there is no real need to use an infrared index to observe the decrease in organic content in charred bone or their complete disappearance in fully calcined bone. The use of the WAMPI, however, enables rapid analysis of the data, allowing the detection of samples that still contain organic matter or adsorbed and structural water after heating without having to analyse each spectrum individually. The band at 1650 cm^{-1}, characteristic of amides in collagen, completely disappears after full calcination (Figure 4.6). In the same Figure 4.6, it is possible to observe a band at 1650 cm^{-1} in an archaeological unburned sample treated with sodium hypochlorite for organic removal prior to isotope analyses (treated bone – the absence of organic matter in that sample was confirmed by elementary analyses – %N below level of detection), showing that even when all organic matter has been removed, a certain amount of structural water remains in unburned bone. The heating process appears to remove not only organic matter but also all structural water, as no such band at 1650 cm^{-1} can be observed in calcined bone.

5.2.1.3 Carbonate content

During the heating of bone, the overall carbonate content (measured using the CO_3/PO_4 ratio) decreases drastically with time and temperature (Figure 4.10a), and it is possible to roughly assess the amount of carbonates left by simply observing the colour. Bone fragments heated at 500 and 600°C for less than 4 hours are completely black, characteristic of charred bone, and still contain significant amounts of carbonates and organic matter; samples heated for longer and/or at higher temperatures are fully white, contain less carbonates and no detectable amount of organics (%N below level of detection).

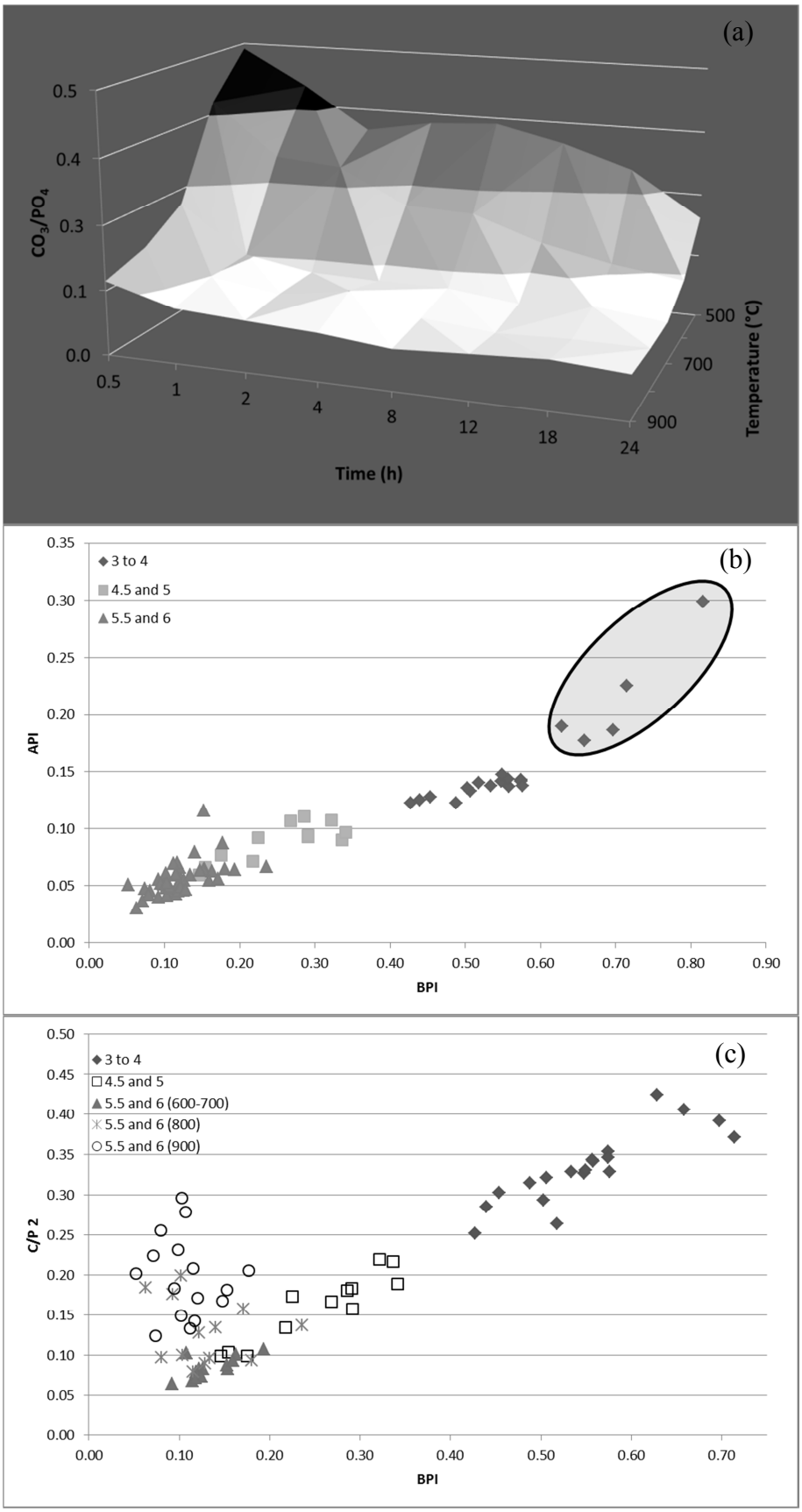

Figure 4.10 – (a) Effect of time and temperature on the colour and amount of carbonates (CO_3/PO_4) left in laboratory heated bone; (b) API versus BPI in experimentally heated bone (LAB2); the charred samples with high %N are highlighted; (c) C/P 2 versus BPI in experimentally heated bone (LAB2) for samples with different colour codes (3 to 6) and heated at different temperature for calcined bone (colour codes 5.5 and 6)

The amount of type A and B carbonates measured with the API and BPI respectively decreases with heating intensity (Figure 4.10b). There is a strong correlation between the decrease in A and B carbonates ($R^2 = 0.90$) with a potential overestimation of the API for the charred bone since there is some organic matter left that has an infrared absorbance at 1550 cm^{-1} close to the carbonate A one at 1540 cm^{-1}. Indeed, the charred samples still show significant amount of organic matter which is also observed through the %N.

The C/P 2 compared to the BPI (Figure 4.10c) highlights that the BPI differentiates charred from calcined samples: the charred samples follow the 'lower' correlation observed in Figure 4.9 and the calcined specimens follow the 'upper' correlation. The C/P 2 differentiates calcined bone (colour code 5.5 and 6) heated at different temperatures with samples heated at 600–700ºC having much lower C/P 2 ratios than those heated at 900ºC.

When comparing measurement taken with FTIR and MS, the best correlation between the amount of carbon dioxide emitted per gram of sample (pCO_2/g sample) and a carbonate to phosphate ratio is found with the CO_3/PO_4 ratio ($R^2 = 0.95$) confirming that this ratio is indeed evaluating the total amount of carbonates (A + B) present in bone apatite. The correlation between the amount of carbon (%C) and the CO_3/PO_4 ratio is lower ($R^2 = 0.71$) which is to be expected since there is still degraded organic matter left in charred bone which is included in the measurement of the %C during elementary analyses. When removing charred bone (colour codes 3 and 3.5), the correlation increases ($R^2 = 0.89$) but the correlation limited to only calcined bone (colour code 5.5 and 6) is much lower ($R^2 = 0.11$). This can be explained by the very low amounts of carbonates left in calcined bone: the %C values measured in calcined bone are close to the level of detection of the mass spectrometer. The correlation between the pCO_2/g of sample and CO_3/PO_4 ratio remains significant even when only looking at calcined bone ($R^2 = 0.52$). This suggests that the pCO_2/g of sample is a much better indicator of the amount of carbonates present in bone apatite than %C and is not

influcenced by the presence of organic matter in the sample (as these have been removed with sodium hypochlorite prior to the measurements and phosphoric acid used in order to release CO_2 by reaction with the carbonates of bone apatite should not react with the organic matter).

The two last indices giving information about the carbonate content are the carbonate to carbonate ratios: the AB and C/C ratios. The latter has already been shown to be temperature dependent (Thompson et al. 2009). For calcined bone (Figure 4.11) both indices are influenced by the heating temperature with lower values at lower temperature but there is more overlap between the different temperature groups when using the AB ratio while there is only very limited overlap when using the C/C ratio.

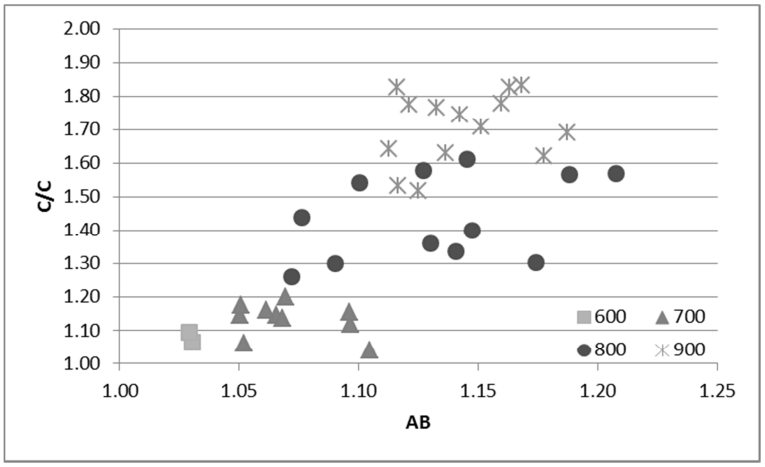

Figure 4.11 – C/C versus AB for calcined bone only

Looking at the API and BPI in calcined samples heated at different temperatures, there is no obvious difference between the temperature groups. There seem, however, to be a subtle difference between the samples heated at 900ºC and the others: those heated at 900ºC seem to have generally lower BPI and higher API (Figure 4.12a and b). This difference is significant for the BPI (t-test *p*-value = 0.013) but not in the case of API (*p*-value = 0.099).

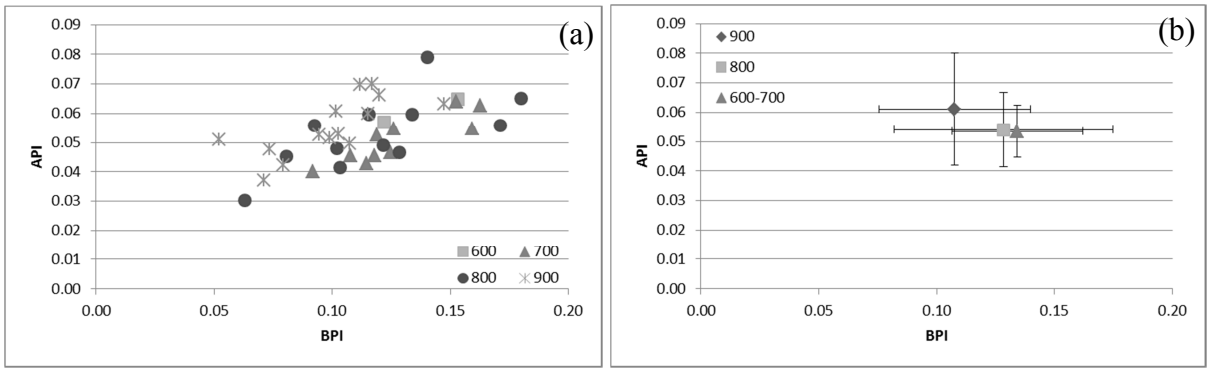

Figure 4.12 – API versus BPI for calcined bone (a) for each sample (b) averaged for each temperature group (1SD)

5.2.1.4 Hydroxyl group content

The amount of hydroxyl groups, undetectable by FTIR in unburned bone, increases with heating intensity (i.e. time and temperature) and OH/P values seem to stabilise around 0.60–0.75 when heated for more than one hour and at a temperature equal to or above 700°C (Figure 4.13). Furthermore, there is a strong inverse correlation between OH/P and CO_3/PO_4 ($R^2 = 0.89$): the amount of hydroxyl groups increases as the amount of carbonates decreases. When considering only calcined bone, however, that correlation drops ($R^2 = 0.33$).

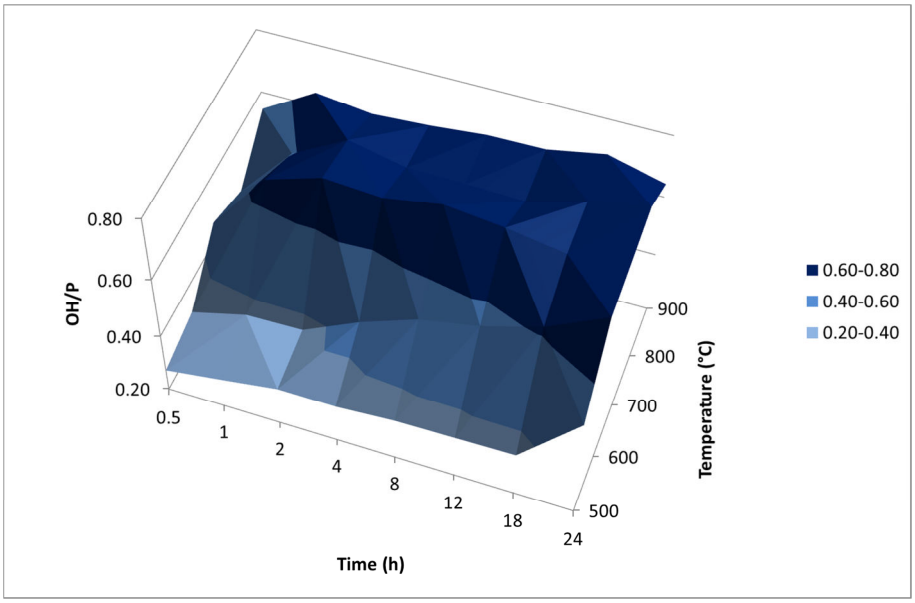

Figure 4.13 – Effect of time and temperature on the amount of hydroxyl groups present in laboratory heated bone

5.2.1.5 Cyanamide content

Only two samples clearly show the presence of cyanamide (CN/P $\geq$ 0.25). Four further samples could contain some cyanamide (0.18 $\leq$ CN/P < 0.25). All the others do not contain detectable amounts of cyanamide (CN/P < 0.18). Both samples containing cyanamide were heated for only 30 minutes; three of those potentially containing cyanamide were also heated for 30 minutes and the last one for one hour. It seems that, in these laboratory settings, if present in heated bone, cyanamide is only present in bone fragments heated for maximum one hour.

5.2.1.6 Structural changes

The most important structural change observed in the heated cow tibia samples is a change in crystallinity highlighted by the IRSF. The IRSF increases from charred to calcined and, once calcined, decreases with temperature. The 1030/1110 ratio, indicator of mineral maturity, and the newly introduced PSF behave similarly (with both $R^2 = 0.87$). The OHSF that can only be measured in calcined bone also decreases with temperature and is correlated to the IRSF ($R^2 = 0.81$ for calcined bone only). The PPI, describing the alignment of the phosphates in the structure of bone apatite, does not change as long as the bone is not calcined but then suddenly decreases in calcined bone heated at 700ºC and goes back to its original value (of charred bone) in calcined bone heated at 900ºC. Of all these indices the IRSF is the one showing the least overlap between the calcined samples heated at different temperatures.

While both 1060/1075 and IRSF are indicator of crystallinity, they do not change in the same way (Figures 4.14a and b). While the IRSF increases until 700ºC and then decreases again at higher temperatures going back to values observed in charred bone, the 1060/1075 also increases with temperature until 700ºC and then decreases again at higher temperatures but does not go back to the lower values observed in charred bone. It remains higher allowing

the discrimination of charred and calcined bone which is not possible by only looking at the IRSF value (though bone colour would directly indicate if it is charred or calcined).

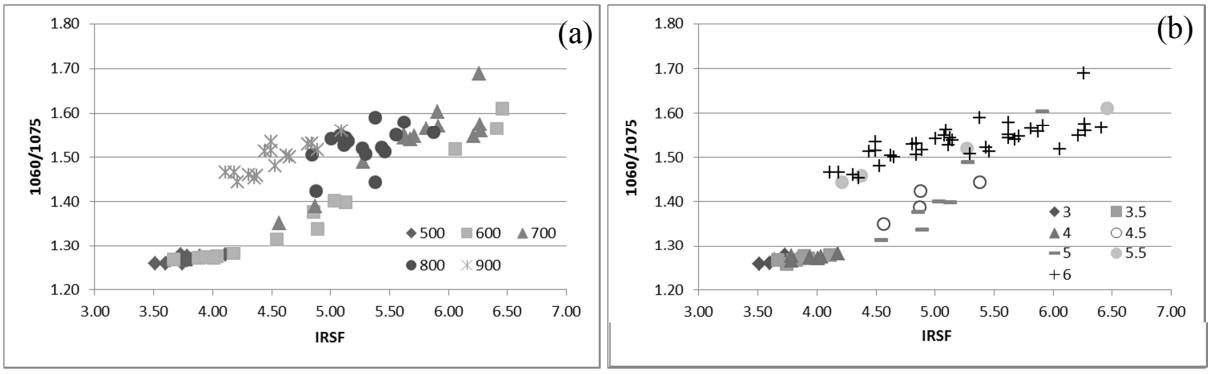

Figure 4.14 – 1060/1075 versus IRSF for experimentally heated cow tibia (LAB2) highlighting (a) samples heated at different temperatures and (b) samples with different burn colour codes

When comparing the IRSF and the C/C ratio (Figures 4.15a and b), it is clear that calcined bone samples heated at different temperature cluster in different parts of the graph. It seems that by combining both indices, it is possible to assess the heating temperature. Grouping the samples heated at 600 and 700ºC together, all three temperature groups (600–700, 800 and 900ºC) are statistically different (ANOVA *p*-values for IRSF and C/C < 0.001). The main interest of using these two indices is that one relies on the carbonates bands (C/C ratio) while the other uses phosphate bands (IRSF).

While temperature seems to have a significant impact on many infrared indices, in calcined bone (colour codes 5.5 and 6) it was not possible to identify any effects of time on any of the indices studied here once bone fragments were calcined.

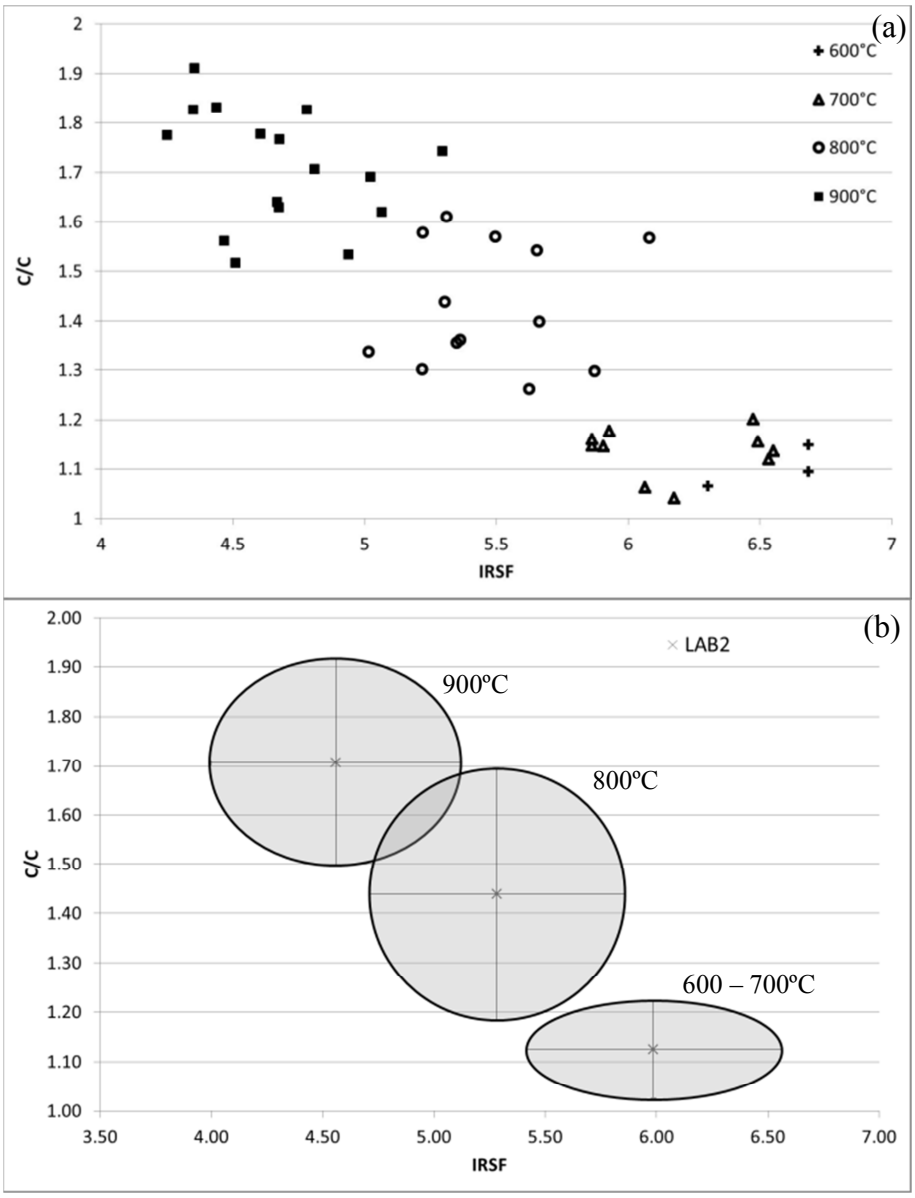

Figure 4.15 – C/C versus IRSF for calcined bone samples heated at different temperatures (a) for each sample and (b) for each temperature group (average values and 2SD circles)

5.2.1.7 Effects of pre-treatments

All the samples have also been treated for isotope analyses using sodium hypochlorite to remove any remaining organic matter and acetic acid to remove adsorbed and diagenetic carbonates. These samples do not contain any since they have never been in contact with soil after heating but the treatment was carried out nonetheless to see its impact on the structure and composition of heated bone apatite since all archaeological samples will be treated prior to isotope analyses.

As is to be expected, the pre-treatment had no effect on the amount of hydroxyl groups present (OH/P) and the samples containing cyanamide before treatment still contain cyanamide. The carbonate losses (A and B) are quite significant and extremely variable, and are higher in calcined bone than in charred bone (Table 4.10). The losses of both types of carbonates in calcined bone seem inversely correlated with temperature, with smaller losses observed in samples heated at 900°C (R^2 = 0.48 for API and 0.16 for BPI). Even though in calcined bone the decrease (in %) is higher in API than BPI during pre-treatment, the absolute decrease is higher in type B carbonates (average ΔBPI = 0.06; average ΔAPI = 0.03). This is confirmed by the increase in C/C ratios after pre-treatment.

There is an overall increase in crystallinity (Table 4.10). An increase in IRSF following acetic acid treatment has been observed in unburned bone and enamel, where it was interpreted as the product of recrystallization or *Ostwald ripening*, or as preferential removal of smaller, more reactive bioapatite crystallites (Lee-Thorp and van der Merwe 1991; Sponheimer & Lee-Thorp 1999). Mineral maturity (1030/1110) also increases but compared to the crystallinity indices where no variation is observed between charred and calcined bone, the increase in 1030/1110 is much higher in calcined bone than in charred bone. Finally, the OHSF and PSF increase during pre-treatment. There is no detectable variation in PPI.

Table 4.10 – Effect of pre-treatment on the infrared indices. Average values (±1sd) before and after pre-treatment are shown for the samples that were pre-treated. Difference between these indices before and after pre-treatment is indicated by Δ (positive values correspond to an increase while negative values correspond to a decrease in the calculated infrared indices; bold Δ highlights that the difference is significant – t-test *p*-values < 0.01)

		API			BPI			IRSF			C/C			OH/P		
		Before	After	Δ	Before	After	Δ	Before	After	Δ	Before	After	Δ	Before	After	Δ
LAB 2	Charred	0.13 ± 0.05	0.10 ± 0.06	-0.03	0.45 ± 0.18	0.35 ± 0.20	-0.10	4.30 ± 0.67	4.58 ± 0.66	0.28	1.07 ± 0.10	1.25 ± 0.21	**0.18**	0.40 ± 0.12	0.41 ± 0.13	0.01
	Calcined	0.06 ± 0.01	0.03 ± 0.02	**-0.03**	0.12 ± 0.04	0.06 ± 0.02	**-0.06**	5.22 ± 0.69	5.61 ± 0.48	**0.39**	1.44 ± 0.26	1.82 ± 0.31	**0.38**	0.67 ± 0.06	0.69 ± 0.07	0.02
	Calcined 600–700°C	0.05 ± 0.01	0.01 ± 0.01	**-0.04**	0.13 ± 0.03	0.06 ± 0.01	**-0.07**	6.02 ± 0.31	6.08 ± 0.34	0.06	1.13 ± 0.05	1.42 ± 0.07	**0.29**	0.71 ± 0.02	0.74 ± 0.03	0.03
	Calcined 800°C	0.05 ± 0.01	0.02 ± 0.01	**-0.03**	0.13 ± 0.05	0.06 ± 0.02	**-0.07**	5.28 ± 0.27	5.72 ± 0.20	**0.44**	1.43 ± 0.13	1.85 ± 0.14	**0.42**	0.66 ± 0.06	0.69 ± 0.06	0.03
	Calcined 900°C	0.06 ± 0.02	0.04 ± 0.02	**-0.02**	0.11 ± 0.03	0.07 ± 0.02	**-0.04**	4.53 ± 0.28	5.14 ± 0.26	**0.61**	1.71 ± 0.12	2.11 ± 0.11	**0.40**	0.64 ± 0.05	0.65 ± 0.07	0.01
	ALL	0.09 ± 0.05	0.06 ± 0.06	**-0.03**	0.26 ± 0.20	0.19 ± 0.19	-0.07	4.82 ± 0.82	5.17 ± 0.76	0.35	1.28 ± 0.28	1.57 ± 0.39	**0.29**	0.55 ± 0.16	0.57 ± 0.17	0.02
LAB 3	Pig rib	0.04 ± 0.01	0.03 ± 0.01	-0.01	0.05 ± 0.03	0.03 ± 0.03	-0.02	5.04 ± 0.52	5.02 ± 0.56	-0.02	1.57 ± 0.44	2.15 ± 0.90	0.58	0.60 ± 0.11	0.63 ± 0.11	0.03
	Seal bone	0.05 ± 0.01	0.03 ± 0.01	**-0.02**	0.35 ± 0.11	0.29 ± 0.07	-0.06	4.13 ± 0.33	4.24 ± 0.32	0.09	1.30 ± 0.11	1.44 ± 0.05	**0.14**	0.23 ± 0.03	0.24 ± 0.04	001
	ALL	0.04 ± 0.01	0.03 ± 0.01	**-0.01**	0.20 ± 0.17	0.16 ± 0.14	-0.04	4.58 ± 0.63	4.63 ± 0.60	0.05	1.43 ± 0.34	1.80 ± 0.72	0.37	0.41 ± 0.20	0.44 ± 0.22	0.03
OUT	ALL (calcined)	0.06 ± 0.01	0.02 ± 0.01	**-0.04**	0.17 ± 0.07	0.10 ± 0.06	**-0.07**	5.25 ± 0.29	5.27 ± 0.25	0.02	1.28 ± 0.10	1.71 ± 0.16	**0.43**	0.47 ± 0.09	0.49 ± 0.09	0.02
Archaeo -logical samples	Low	0.02 ± 0.01	0.01 ± 0.01	**-0.01**	0.20 ± 0.06	0.21 ± 0.07	0.01	5.15 ± 0.47	5.07 ± 0.56	-0.08	1.43 ± 0.06	1.46 ± 0.05	0.03	0.50 ± 0.05	0.51 ± 0.05	0.01
	High	0.03 ± 0.02	0.03 ± 0.01	0	0.26 ± 0.11	0.29 ± 0.11	0.03	4.71 ± 0.39	4.38 ± 0.26	**-0.33**	1.37 ± 0.09	1.42 ± 0.10	0.05	0.40 ± 0.06	0.43 ± 0.06	0.03
	ALL (calcined)	0.23 ± 0.02	0.02 ± 0.01	-0.01	0.24 ± 0.10	0.26 ± 0.10	0.02	4.86 ± 0.46	4.63 ± 0.51	-0.23	1.39 ± 0.08	1.43 ± 0.09	0.04	0.44 ± 0.07	0.45 ± 0.07	0.01

5.2.2 Laboratory heating experiments 3 (LAB 3)

This batch of experiments consisted of heating pig rib and seal long bone fragments after different treatments and with different additives but always at 800ºC and for 4 hours in a muffle furnace (Table 3.3). It is important to note that the seal bone was dry while the pig rib was still fresh. After heating all samples were calcined (white). The infrared spectra were recorded before and after pre-treatment with sodium hypochlorite and acetic acid which was carried out for isotope analyses.

5.2.2.1 Fat and organic removal treatments

The samples submitted to the different treatments used to remove fats and all other organic matter were analysed by FTIR before calcination (Figure 4.16a and b). It appears that in the untreated samples (A0) and samples treated for fat removal (B0), organic matter (i.e. collagen) is still present as is to be expected. When treated for organics removal (C0) or for fat and organic removal (D0) the band at 1250 cm^{-1} of Amide III in collagen disappears. Furthermore, the bands at 1550 and 1650 cm^{-1} (Amide II and I respectively) have lower absorbance once treated. Since these bands overlap with type A carbonates and structural water respectively (Table 4.1), it is to be expected that these do not disappear completely. Nevertheless, it is clear that the organic content is much lower after organic removal treatment. When using hydrazine hydrate as organic removal agent, a further indicator of the removal of organic matter from the pig rib and seal bone is a change in colour. The pig rib was slightly pink and the seal bone was beige, but after pre-treatment with hydrazine hydrate, all fragments were white, which is the colour of apatite.

(b)

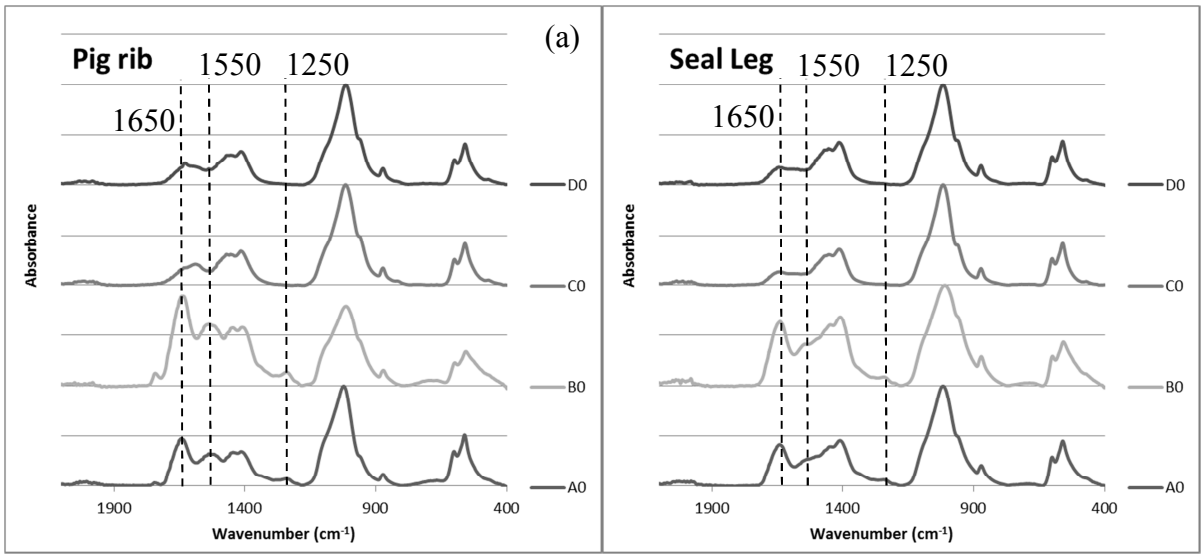

Figure 4.16 – Infrared spectra of the samples treated in different ways before calcination: A0 – untreated; B0 – fat removal; C0 – organic removal; D0 – fat + organic removal; (a) for the pig rig, and (b) for the seal bone

5.2.2.2 Compositional and structural changes

Once calcined the main difference between the pig rib and the seal bone samples is observed in the BPI which is much higher in the seal bone than in the pig rib. The API is more or less similar in both groups (Figure 4.17a). As for the BPI, the total amount of carbonates (CO_3/PO_4) is higher in seal bone than in pig rib. At the same time the hydroxyl group content is much higher in the pig rib than in the seal bone (Figure 4.17b).

Only one sample contains cyanamide (Seal – D3). Surprisingly, this sample was dry (not fleshed) and treated in order to remove all fats and organic matter so that the nitrogen contained in cyanamide ($–CN_2H$) can only come from the barley seeds with which it was heated or the atmosphere. Structurally, the crystallinity and mineral maturity are higher in the pig rib than in the seal bone.

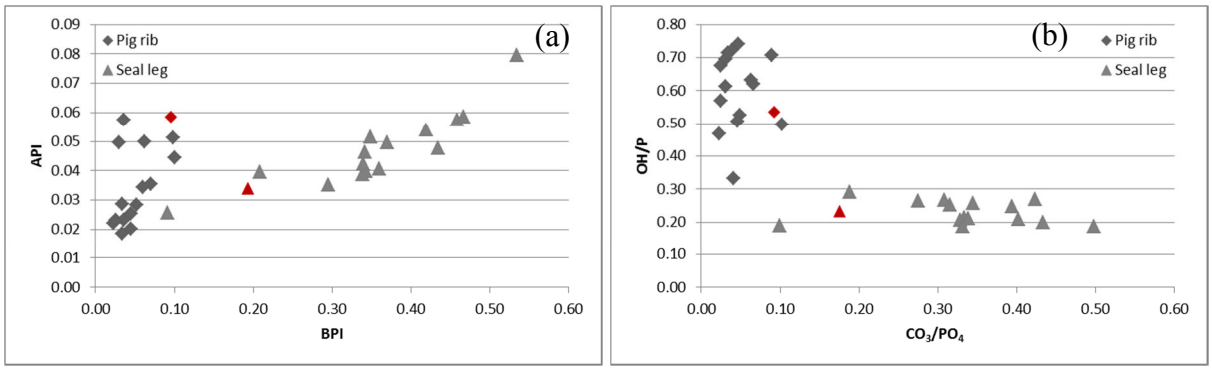

Figure 4.17 – (a) API versus BPI and (b) OH/P versus CO_3/PO_4 for the heated pig rib and seal bone fragments; the red symbols correspond to untreated samples heated without additives (A1)

5.2.2.3 Effect of pre-treatments

The pre-treatments with sodium hypochlorite and acetic acid induced a loss of carbonates of both types in the pig rib and the seal bone. The decrease after pre-treatment in API is lower in the pig rib than in the seal bone while the decrease in BPI is higher (Table 4.10). The changes in crystallinity (IRSF and 1060/1075) and mineral maturity (1030/1110) are minimal. However, while the PPI was not modified during pre-treatment in the cow tibia heated samples (LAB 2), here there is an increase.

5.3 Compositional and structural changes of modern burned bone

The infrared and compositional data of the animal joints burned under natural conditions (outdoor fires) is summarized in Appendix 6.4. All samples were still fresh (not dry) before burning expect for the dry pig scapula (P1 in Table 3.4). As noted for the laboratory experiments on the cow tibia, it seems that, when fully calcined, the duration of heating has little impact on the measured infrared indices. This was also observed by Zazzo et al. (2012) when they burned archaeological bone fragments on modern wood pyres. Therefore, even though the different burnings were carried out for different lengths of time, the results should not be influenced. All samples have been analysed by FTIR before and after pre-treatment for isotope analyses.

5.3.1 Compositional and structural changes

As observed for the laboratory experiments, the carbonate content (A and B – API, BPI, CO_3/PO_4) decreases, while of hydroxyl groups (OH/P), crystallinity (IRSF and 1060/1075) and mineral maturity (1030/1110) increase compared to unburned bone. One sample clearly shows the presence of cyanamide (L1_A) and it is most likely present in two others (P7 and Ch1). P7 is the fully fleshed pig scapula but the similarly fleshed pig trotter (P6) does not show the presence of any cyanamide. Four further samples could contain some cyanamide ($0.18 \leq CN/P < 0.25$).

5.3.2 Effect of pre-treatments

The changes observed here are similar to the changes observed in pre-treated heated bone (LAB 2). There is a decrease in carbonate content (both types) and no change in the hydroxyl group content (OH/P). The crystallinity does not change when measured with the IRSF (like for the LAB 2 calcined samples heated at 700°C) or the 1060/1075 but there is an increase in mineral maturity (1030/1110). As for the LAB 3 samples, there is also an increase in PPI (Table 4.10).

5.4 Composition and structure of archaeological calcined bone

A total of 110 archaeological cremated bone fragments from Ireland and the UK were analysed by infrared spectroscopy (Appendix 6.5). A subsample (56 samples) was also pre-treated for isotope analyses. Infrared spectra were recorded before and after pre-treatments.

5.4.1 Bone colour

Because of the changes that can occur due to post-burial alterations, all archaeological samples to which a colour code of 5 and above was assigned will be considered fully calcined. According to this classification, only eight samples out of 110 (seven from Knowth

and one from Parknabinnia) were not fully calcined. Hereafter, only calcined bone will be considered.

5.4.2 Composition and structure

Looking at the carbonate content of the archaeological calcined samples, they separate into two groups on the basis of the BPI. The first group presents BPI between 0.07 and 0.30 while the second group presents between 0.30 and 0.87. The second group not only has higher carbonate content but also lower IRSF. The first group comprises samples from both low and high-carbonate geological contexts but all the samples in the second group originate from high-carbonate geological contexts (Figure 4.18).

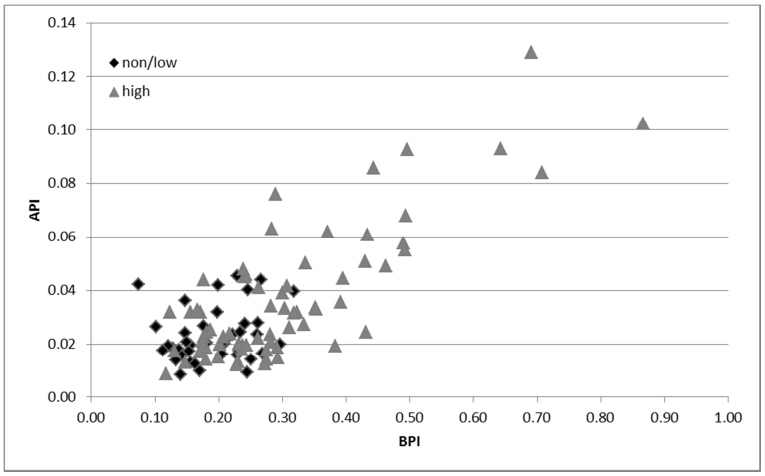

Figure 4.18 – API versus BPI for archaeological calcined bone from non/low carbonate geological contexts and from high carbonate geological contexts

Of the 110 archaeological samples 39% clearly show the presence of cyanamide ($CN/P \geq 0.25$) and an additional 26% could contain some cyanamide ($0.25 > CN/P \geq 0.18$). A comparison of the band intensity for cyanamide (CN/P) versus that of hydroxyl groups (OH/P) shows an inverse correlation between the two ($R^2 = 0.48$) that improves when only considering samples that clearly contain cyanamide ($R^2 = 0.57$) (Figure 4.19).

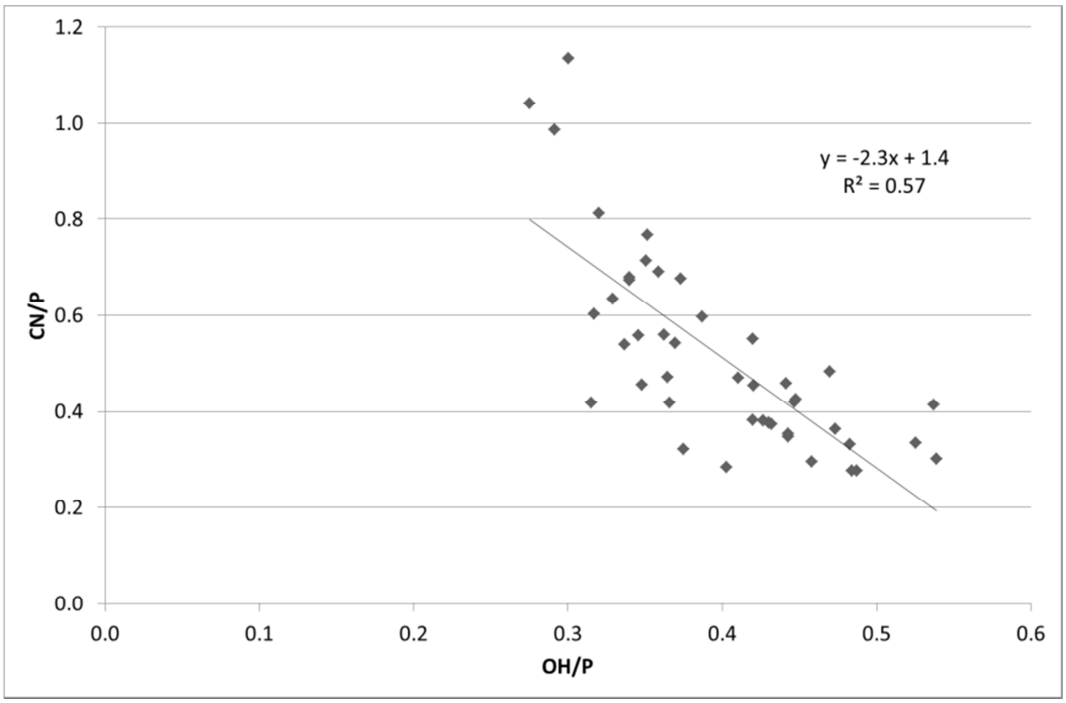

Figure 4.19 – CN/P versus OH/P for archaeological calcined bone fragments with CN/P ≥ 0.25

5.4.3 Effect of pre-treatments

After pre-treatment, there is an overall increase of B carbonates accompanied by a decrease in IRSF (Table 4.10). This is the opposite of what was observed above for modern heated and burned bone (LAB 2, LAB 3 and OUT), and previously for unburned bone and enamel (Lee-Thorp & van der Merwe 1991). There is no significant difference in the effects of pre-treatment on samples from low and high-carbonate geological contexts: the BPI remains similar or increases slightly regardless of geology. The changes in API are minimal. The PPI increases slightly and the mineral maturity (1030/1110) is modified in no particular way.

6 Discussion

6.1 Effects of pre-treatments

The impact of pre-treatments on modern heated bone compared to archaeological calcined specimens is unexpected (Table 4.10). The application of acetic acid is widely used to

remove exogenous carbonates that may be adsorbed or incorporated by calcined bone from the burial environment. This is true for archaeological calcined bone samples, but the modern bone fragments calcined in a furnace and in fires have never been buried and thus should not contain any exogenous carbonates. Following this rationale, it is expected, then, that acetic acid pre-treatment will remove exogenous carbonates from archaeological samples but will have a very limited impact on the modern samples heated in a laboratory furnace. However, when treated with acetic acid, the modern calcined samples show a significant decrease in carbonate content, accompanied by an increase in crystallinity. The archaeological calcined samples in contrast seem almost unaffected by acetic acid suggesting that they are less reactive than modern calcined specimens. A possible explanation is that modern burned bone contains some smaller, less well crystallized and more reactive crystallites that are removed by acetic acid, explaining the higher IRSF and lower carbonate content observed after pre-treatment. As observed in unburned bone, larger crystals tend to form over time making them less reactive (Lee-Thorp and van der Merwe 1991; Sponheimer & Lee-Thorp 1999; Trueman et al. 2004). If this also occurs in calcined bone after heating, the smaller, more reactive recrystallized crystallites will continue to recrystallize over time and become more stable which would explain why the carbonate losses and crystallinity changes after pre-treatment are minimal in archaeological samples. Following this argument, the less well recrystallized crystallites present in modern calcined bone would, over time, be incorporated into a more stable structure and so, these should not be removed. The use of acetic acid on archaeological samples, however, is still prudent to make sure that all external carbonates are removed. Infrared comparisons should be carried out on untreated modern samples and treated archaeological specimens.

A final observation from Table 4.10 is that carbonate losses (types A and B) after pre-treatment are lower in samples heated at 900°C compared to those heated at 700°C, while the

IRSF increases are higher. This is counter-intuitive as IRSF and carbonate content tend to be inversely correlated: greater carbonate substitution increases crystal distortion and leads to lower IRSF (LeGeros 1991). The reasons why this is not the case are not fully understood at this stage.

6.2 Comparison between different samples

6.2.1 LAB 3 compared to LAB 2

The API and BPI of the pig rib (LAB 3) fall within the ranges observed for LAB 2 but the BPI is much higher in the seal bone compared to the cow tibia (Figure 4.20).

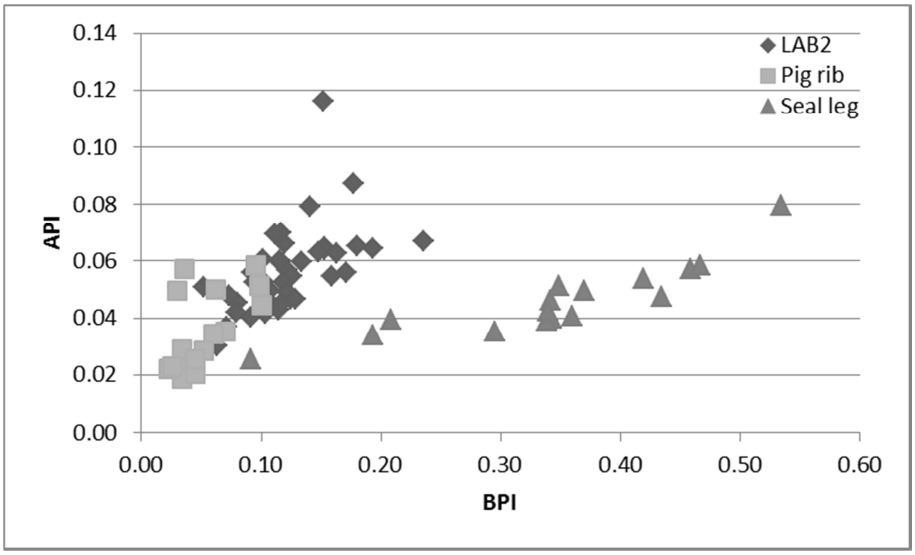

Figure 4.20 – API versus BPI for the heated pig rib and seal bone fragments compared to the cow tibia heated samples (LAB 2)

When comparing the C/C ratios and IRSF measured for the LAB 3 and LAB 2 samples (Figure 4.21) it is possible to see that the untreated pig rib and seal bone samples (A1 – in red on the graphs) that were burned at 800ºC almost fall within the corresponding temperature group of the cow tibia samples. However, when heated with additives or treated prior to heating, using the C/C ratio and the IRSF does not allow assessing the heating temperature as efficiently as it was possible for the LAB 2 experiments.

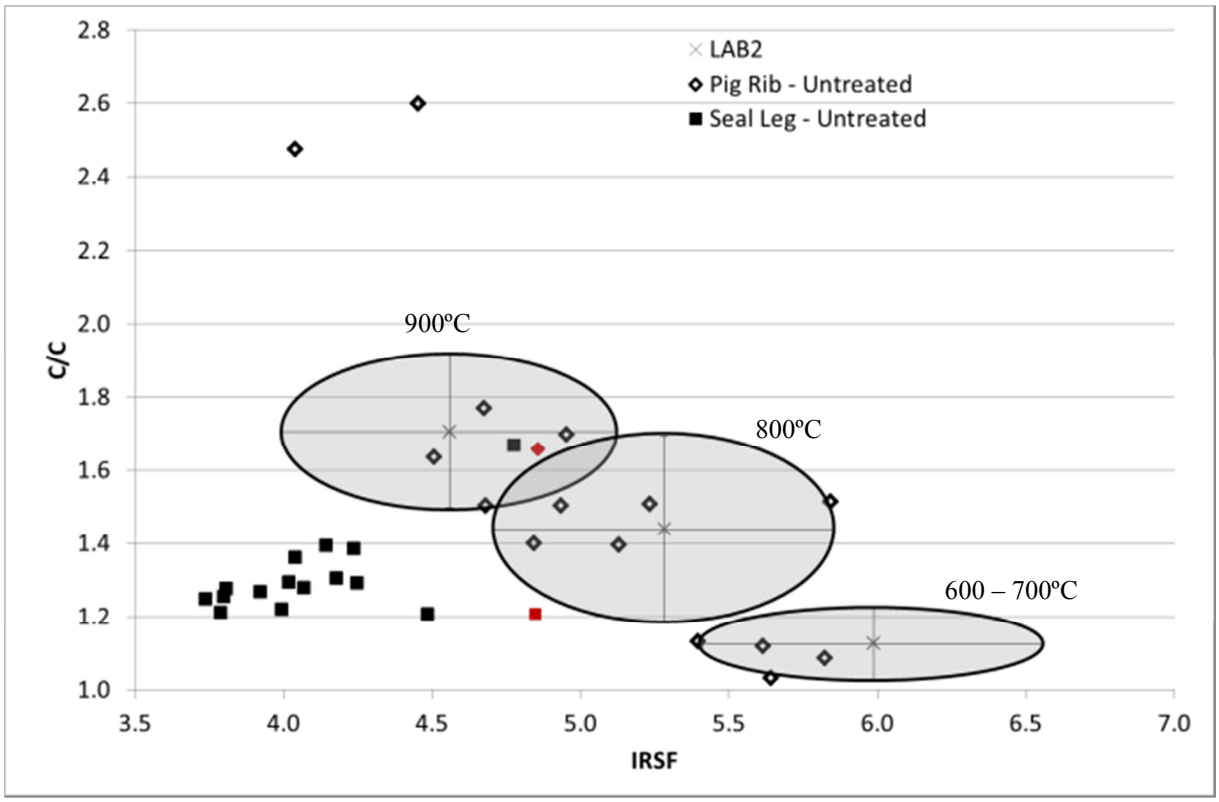

Figure 4.21 – C/C versus IRSF for the heated pig rib and seal bone compared to the cow tibia heated samples (LAB 2); the red dots correspond to untreated samples heated without additives (A1); the grey circles represent the average values for each temperature group (600–700, 800 and 900°C) observed in the heated cow tibia (LAB 2) with 2SD

From these results, it appears that the state of the bone prior to heating (dry or fresh) has an impact on the chemical composition of calcined bone apatite. It is possible that in dry bone, the crystallites are already more stable and therefore will loose and exchange less carbonates during calcination than fresh bone. This would explain the higher carbonate content observed in seal bone samples. The removal of organic matter appears to have an unpredictable impact on the chemical composition of calcined bone apatite.

6.2.2 Modern burned bone compared to modern laboratory heated bone

The carbonate content of the samples burned on outdoor pyres is very similar to that of LAB 2 and the pig rib (LAB 3), except for the dry pig scapula (P1) which has similar API and BPI to the dry seal bone (LAB 3) suggesting that the transformations occurring in bone apatite during heating are influenced by the state of the bone before heating (fresh versus dry).

When comparing the IRSF and C/C ratio measured on calcined bone fragments burned on outdoor fires with the laboratory experiments (LAB 2), it appears that the cow tibia and most pig bone fragments (leg, scapula and trotter), fall within the 800°C field (Figure 4.22), which is consistent with thermocouple indications of 600 to 900°C. However, other samples including the lamb and chicken bone fragments, fall outside the temperature fields observed in LAB 2. The temperature around the samples may have reached temperatures between 800 and 900°C but the experiments were not detailed enough to ascertain the range for 850°C. Notwithstanding these uncertainties, the results suggest that it should be possible to ascertain the temperature at which bone fragments were burned, or at least highlight that some samples were burned at higher temperatures than others.

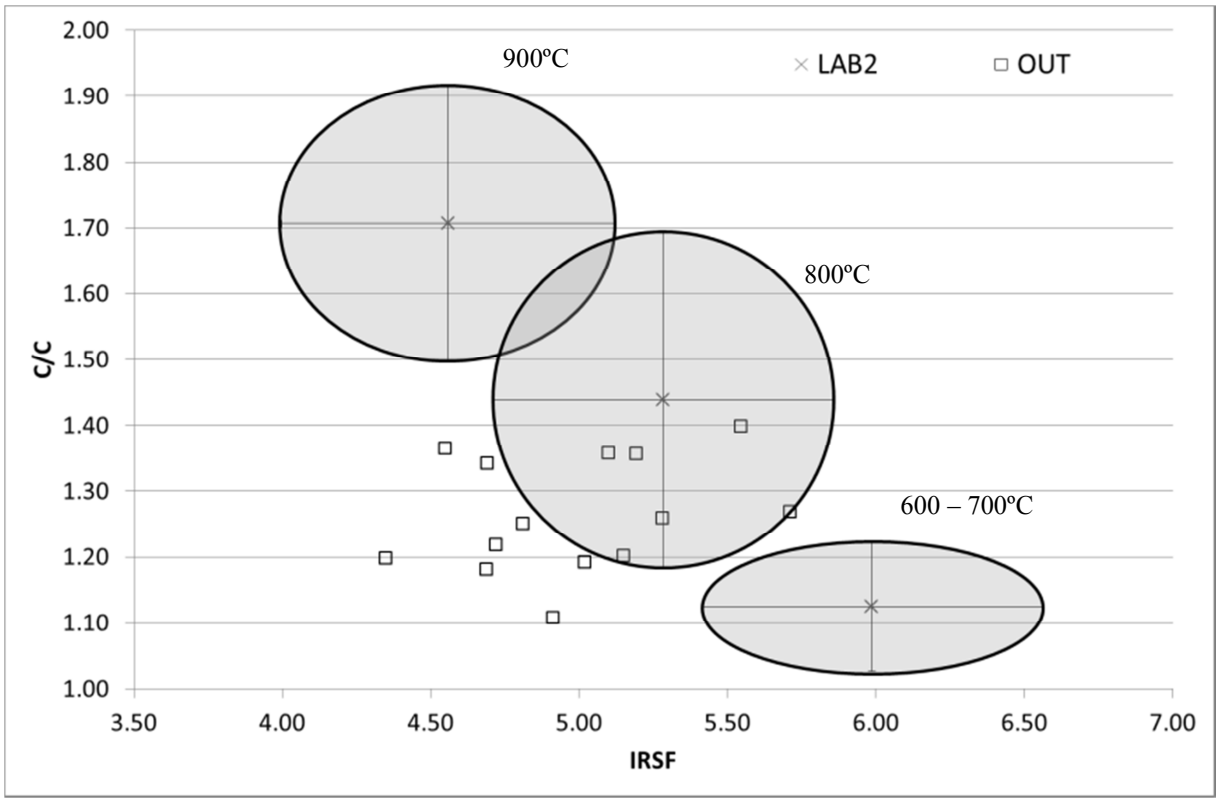

Figure 4.22 – C/C versus IRSF for samples burned on outdoor fires compared to the cow tibia heated samples (LAB 2); the grey circles represent the average values for each temperature group (600–700, 800 and 900°C) observed in the heated cow tibia (LAB 2) with 2SD

6.2.3 Archaeological compared to modern calcined bone

As discussed above, the infrared comparison of archaeological and modern calcined bone should be carried out on untreated modern samples but pre-treated archaeological specimens. The comparison shows that most archaeological samples have similar API and BPI to the modern samples that were dry before heating (Figure 4.23a). Looking at the cyanamide content, overall 39% of the archaeological samples contained cyanamide and a further 26% could contain some cyanamide. In contrasts, only 3 experimentally heated samples (3 %) and 3 samples of outdoor burnings (23 %) contained cyanamide (CN/P $\geq$ 0.25). When comparing the C/P 2 and the BPI for the archaeological calcined samples (Figure 4.23b), the values almost exclusively follow the 'upper' correlation seen in Figure 4.9, and the archaeological specimens overlap mainly with the seal bone samples (LAB 3). The calcined cow tibia, seal bone and pig rib samples, as well as those calcined outdoors, also follow the 'upper' correlation. This seems to confirm that the 'upper' correlation corresponds to calcined samples while the 'lower' one corresponds to charred samples. The C/P 2 however, does not seem to provide information about the temperature at which the samples were burned as it was observed for the heated cow tibia. Looking at the hydroxyl groups (OH/P) and type B carbonates (BPI), it appears that the archaeological samples are most similar to the modern samples heated on outdoor fires (Figure 4.23c). The dry seal bone has the lowest amount of hydroxyl groups.

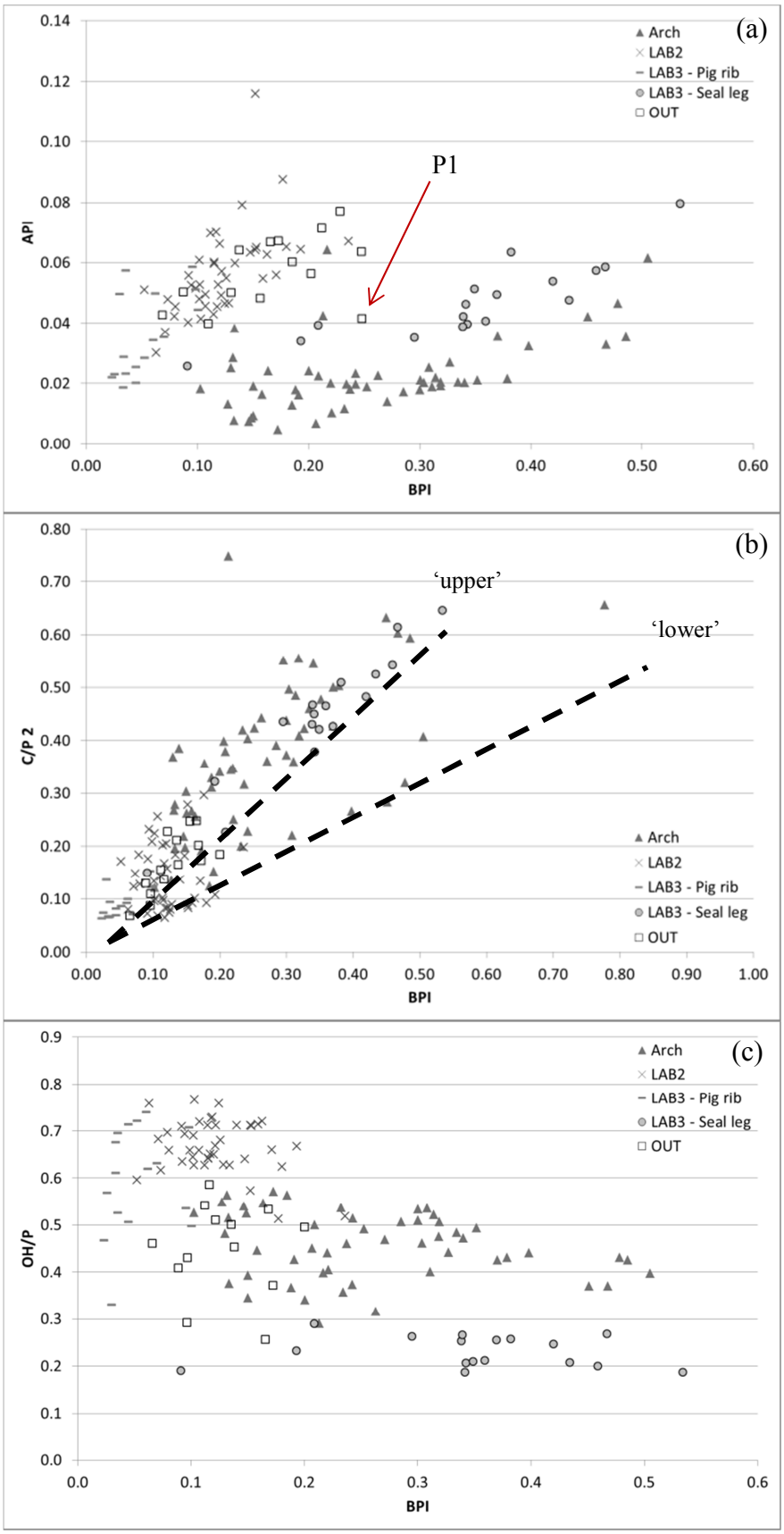

Figure 4.23 – (a) BPI versus API for untreated modern calcined samples, and pre-treated archaeological specimens; the dry pig scapula (P1) is highlighted; (b) C/P 2 versus BPI for untreated modern calcined samples, and pre-treated archaeological specimens; the upper and lower correlations are those observed in Figure 4.9; (c) OH/P versus BPI for untreated modern calcined samples, and pre-treated archaeological specimens

6.3 Useful infrared indices for the study of calcined bone

Fifteen potentially useful infrared indices were investigated here (Table 4.9) and it appears that, even though they do not provide exactly the same results, several indices do not provide additional information about the structure and composition of calcined bone. C/P 2 is able to discriminate unburned and charred samples when used together with the BPI ratio but this can be done visually and with the WAMPI. Furthermore, while in the heated cow tibia (LAB 2) C/P 2 seems to discriminate between samples heated at different temperatures, such discrimination does not seem to be possible in archaeological samples (Figure 4.23b). Finally, the presence of quartz has an impact on the C/P 2. The AB is also influenced by the presence of quartz and is less efficient than the C/C ratio in discriminating samples heated at different temperatures (Figure 4.11). The PPI, 1060/1075, 1030/1110, PSF and OHSF do not seem to provide additional information to the IRSF even though they may represent different characteristics of bone apatite. The IRSF can be measured on unburned and calcined bone, and it shows the highest sensitivity to temperature compared to the other indices. Therefore, it will be investigated here. Finally, while the CO_3/PO_4 ratio accounts for both types of carbonates, looking at each type individually using the API and BPI provides more detailed information about the composition of calcined bone apatite. The indices of interest for the study of calcined bone apatite are summarised in Table 4.11.

Table 4.11 – Useful infrared indices for the study of calcined bone apatite

Name	Measurement	Significance	Reference
BPI	A_{1415}/A_{605}	Amount of type B carbonates	1,2
API	A_{1540}/A_{605}	Amount of type A carbonates	2
IRSF	$(A_{605} + A_{565}) / A_{590}$	Crystallinity	3
C/C	A_{1450} / A_{1415}	Compares two carbonate bands : (A+B)/B	4
OH/P	A_{630} / A_{605}	Amount of hydroxyl groups	5
CN/P	A_{2010} / A_{605}	Amount of cyanamide	5
WAMPI	A_{1650}/A_{605}	Amount of water/amide	6

[1]LeGeros & LeGeros 1983; [2]Sponheimer & Lee-Thorp 1999; [3]Weiner & Bar-Yosef 1990; [4]Thompson et al. 2009; [5]Snoeck et al. 2014b; [6]Roche et al. 2010

6.4 Compositional changes of bone during and after calcination

Of the seven indices selected for the study of calcined bone, five are directly linked to the compositional changes that occur in bone apatite during heating: API, BPI, WAMPI, OH/P, and CN/P. These indices evaluate the amount of type A, B carbonates, organic matter, hydroxyl groups, and cyanamide respectively. It has already been observed that the carbonates (both A and B types) decrease and the organic content and structural water are completely removed, while the hydroxyl groups increase compared to unburned bone (e.g. Lebon et al. 2010; Thompson et al. 2013). Cyanamide is present in some, but not all, calcined samples (e.g. Zazzo et al. 2013). It remains to be discussed how these variations might be linked to each other. Only the calcined samples are considered here. In addition to white colour, a WAMPI below 0.05 was used to identify fully calcined samples. In total, 139 samples were considered to be fully calcined: 74 laboratory heated samples, 52 pre-treated archaeological cremated samples, and 13 outdoor burned samples.

6.4.1 Carbonates and hydroxyl groups

A striking observation is the difference in carbonate content between experimentally heated samples and archaeological remains: the former have much lower carbonate content of type B but show higher concentrations of type A carbonates than experimentally heated modern samples (Figure 4.23a). This difference could be a consequence of heating defleshed samples in laboratory conditions without fuel and where environmental factors such as humidity and wind have a lower impact, but in fact, modern samples burned with flesh and skin on outdoor pyres show a similar pattern. Nevertheless, the experimental pyres were small compared to those that would have been used for human cremations and it is possible that larger pyres would induce more reductive conditions around some parts of the bone that could limit the transfer of carbonates from the B site to the A site (as observed in heated enamel – Holcomb

& Young 1980). This would explain the variations seen in the carbonate content between archaeological and modern calcined samples. Another explanation is that small-scale post-burial alteration has occurred in the archaeological cremated bone. This would also be consistent with observations that, as noted above, the pre-treatments have different effects on modern and archaeological calcined bone. Interestingly, the carbonate content of archaeological calcined samples is similar to that of modern samples heated dry (seal bone LAB 3 and P1). It is unlikely, however, that the archaeological samples were burned dry.

Amongst the archaeological samples, it appears that those with high carbonate content (BPI > 0.30) originate from high-carbonate geological contexts. Possible explanations for this observation include intrinsic or taphonomic factors. For instance individuals living on high-carbonate geological contexts may reflect this in a higher bone apatite carbonate content, via their diet. However, blood bicarbonate levels are tightly controlled biochemically, so this seems unlikely. A taphonomic explanation includes two possibilities. One is that the cremated bone incorporated exogenous carbonates from the burial environment; in which case we would expect to observe typical calcitic C-O bands in the infrared spectra at 710 cm^{-1} (Hassan et al. 1977). This is not the case although small concentrations of calcite (< 5%) are difficult to detect using FTIR-ATR. Alternatively, external carbonates could be incorporated into the bone apatite structure itself after calcination. However, the pre-treatment on archaeological calcined bone did not seem to affect their carbonate content suggesting that little extraneous carbonate was present. External carbonates might, nevertheless, be incorporated structurally in bone apatite as a result of recrystallization that could be more difficult to remove during pre-treatment. Recent reliable radiocarbon results obtained on calcined bone however (e.g. Lanting et al. 2001; Zazzo & Saliège 2011) suggest that such soil/external contamination is unlikely. The higher acidity of low-carbonate geological contexts could be another explanation for this observation. In more acidic soils, the less well

crystallized crystallites that contain more carbonates could be dissolved preferentially, leaving only highly crystalline crystallites with very little carbonates in the archaeological records. All of the above makes it difficult to explain the observed link between the high carbonate concentrations (BPI > 0.30) in some archaeological samples and their high-carbonate geological contexts. Radiocarbon dating and stable isotope analyses ($\delta^{13}C$) could help highlight potential post-burial intake of soil carbonates.

Most samples heated in laboratory conditions (LAB 2 and LAB 3 pig rib) have higher hydroxyl group and lower carbonate contents than archaeological cremated specimens and modern samples burned on outdoor pyres. It is possible that the absence of large amounts of carbon dioxide in the combustion atmosphere in laboratory conditions favours the replacement of endogenous carbonates by hydroxyl groups from atmospheric water (or other potential sources). On outdoor pyres, the amount of carbon dioxide will be significantly higher than in a laboratory furnace because of the fuel, favouring the intake and replacement of carbonates instead of hydroxyl groups. The seal bone samples (LAB 3) have high carbonate content and low hydroxyl group content even though these were burned in a laboratory furnace but the seal bone was dry before heating. This could be the result of more crystalline crystallites in bone that had the time to dry naturally, which is also consistent with the insignificant loss of type B carbonates during pre-treatment (Table 4.10).

The fact that archaeological samples and samples burned on outdoor fires have similar hydroxyl group content (OH/P) but have higher content than samples burned dry and lower than samples heated fresh in laboratory conditions, suggest that the archaeological samples were indeed burned fresh and not dry. Being able to make such distinction would be very useful to differentiate samples that were burned shortly after death from those that could have been exhumed after having been buried for many years and then cremated dry (as seen in modern day Hong-Kong).

6.4.2 Cyanamide

The presence of cyanamide in cremated bone has been observed previously (e.g. Dowker & Elliott 1979; Vignoles et al. 1987; Habelitz et al. 2001; Zazzo et al. 2013) but its variable presence in cremated bone still requires a satisfactory explanation. It cannot be explained by the presence of fuel alone, nor can it be said that cremated bone lacking cyanamide has been burned in the absence of organic matter (e.g. flesh, skin). Some samples heated in laboratory experiments without any external fuel contained cyanamide, while others burned on outdoor pyres, still retaining flesh and skin, did not contain cyanamide. Furthermore, of the LAB 3 heating experiments, only one sample contains cyanamide (Seal bone – D3). Surprisingly, this sample was dry (not fleshed) and treated in order to remove all organic matter so that the nitrogen contained in cyanamide can only come from the barley seeds with which it was heated or from the atmosphere. This suggests that the process of production and incorporation of cyanamide is complex. Its presence in a high number of archaeological samples (39%) could suggest that larger pyres, creating more reducing conditions, favoured its incorporation into bone apatite.

Furthermore, cyanamide is present in a specific part of the structure. It appears as a single and very sharp band at 2010 cm^{-1}. The most likely positions would be in replacement of type A and/or B carbonates lost during the heating process. Interestingly, the hydroxyl group content is lower in samples containing significant amounts of cyanamide. This suggests that cyanamide partially replaces the hydroxyl groups (and type A carbonates). This had already been suggested by Habelitz et al. (2000). Considering only the archaeological calcined bone samples that contain cyanamide (CN/P ≥ 0.25) there is an inverse correlation between OH/P and CN/P ($R^2 = 0.57$ – Figure 4.20) with the following regression equation:

$$\frac{OH}{P} = -2.3\frac{CN}{P} + 1.4$$

In other words, one cyanamide replaces roughly two hydroxyl groups. Interestingly, the mass difference between hydroxyl groups (OH^- – 17g/mol) and cyanamide (CN_2H^- – 41g/mol) is approximately 2.4. These observations are consistent with the suggestion that, when present, cyanamide substitutes for hydroxyl groups within the bone apatite structure, or in other words, replaces type A carbonates.

Moreover, the amounts of type B carbonates, hydroxyl groups and cyanamide are linked to one another. Even though no relation between the amount of type B carbonates and cyanamide could be found, samples with higher type B carbonate content have lower amounts of hydroxyl groups, while samples with higher amounts of cyanamide also have lower amounts of hydroxyl groups. Since cyanamide and carbonates originate in large part from the combustion atmosphere, it seems that the final composition of bone apatite after heating depends mainly on the composition of this combustion atmosphere.

6.5 Structural changes of bone during and after calcination

It appears that the structural changes cannot be dissociated from compositional changes. Indeed, the huge loss of carbonates as well as the destruction of organic matter and loss of all structural water removes much of the distortion within the crystal structure that created strains in unburned bone. This decrease in distortions and strains that is observed in bone during heating is the reason why the crystallinity increases. The loss of carbonates and increase in hydroxyl groups make calcined bone apatite much more similar to synthetic hydroxyapatite that is much more crystalline due to its lower (or inexistent) amount of substitutions (e.g. carbonates).

A key observation in the experimentally heated samples is that the IRSF (indicator of crystallinity) increases up to 700°C and once calcined, decreases with increasing temperatures. This had already been observed by other scholars (e.g. Thompson et al. 2009;

Lebon et al. 2010) but no satisfactory explanation as to why this is the case has been forthcoming. A small increase in type B carbonates has been observed (Figure 4.12b) when comparing samples burned at 800 and 900°C that could explain this decrease in crystallinity. However, the reasons for the increase in type B carbonates are unclear.

Even if archaeological samples have lower IRSF than modern samples burned fresh, it is still much higher than unburned bone and even tooth enamel. The increase in crystallinity is responsible for the lower impact of post-burial alterations on the composition and structure of calcined bone. It had already been stated that heating above 550°C reduces the reactivity of the mineral phase and prevents compositional and structural characteristics from experiencing diagenetic modifications (Lebon et al. 2010; Quarta et al. 2013). The low impact of pre-treatment on archaeological calcined bone confirms this hypothesis.

6.6 Detection of heating temperature

The degree of calcination can easily be observed from the colour of the heated fragments and it is affected by both time and temperature. The infrared results further highlight that the carbonate content (A and B) decreases as bone turns from black to white, while the hydroxyl groups and crystallinity increase compared to unburned bone. Once the bone fragments are white and fully calcined, the duration of heating has little, if any, impact on the different infrared indices; however, temperature does. The C/C ratio (showing a modification of the proportion of type A and B carbonates) continues to increase with temperature, while the IRSF increases up to 700°C and then decreases again. Combining both indices, it appears possible to assess the temperature at which bone fragments were heated.

Even though their carbonate contents differ, the C/C ratios and IRSF of archaeological and modern samples are often similar. As previously discussed, this comparison is carried out on untreated modern samples and treated archaeological specimens. It is suggested that most archaeological samples were cremated around 800–900ºC (Figure

4.24). However some archaeological samples and some modern samples, specifically the lamb and chicken bone burned on outdoor pyres, fall outside of the pattern observed for the fully calcined bone fragments heated in laboratory conditions on the left of the 800°C field and below the 900°C field. These samples could have been burned between 800 and 900°C. The sample (BM2) at the right of the graph could have been burned between 700 and 800°C.

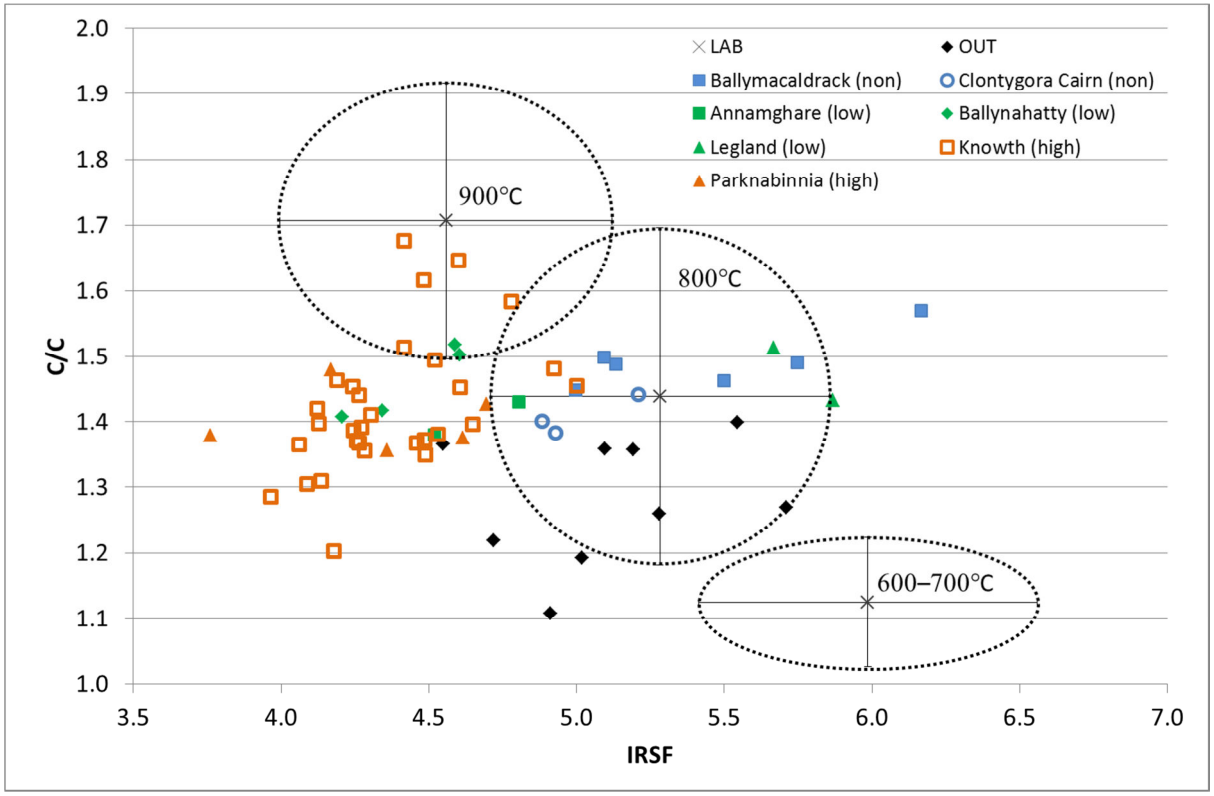

Figure 4.24 – C/C versus IRSF for untreated modern calcined samples, and pre-treated archaeological specimens; the grey circle represent the average values for each temperature group (600–700, 800 and 900°C) observed in the heated cow tibia (LAB 2) with 2SD; non, low and high refer to the non, low and high-carbonate geological contexts respectively

There is some patterning in the archaeological samples from different sites: the cremated bone fragments from Ballymackadrack (BM), Clontygora Cairn (C) and Legland (L) seem to have been burned at 800°C while some from Ballynahatty (BN) and Knowth (K) seem to have been burned at 900°C. The samples from Knowth (K), Parknabinnia (P) and Ballynahatty (BN) that fall outside the temperature fields defined by the heated cow tibia

samples (LAB 2), could have been burned between 800 and 900°C. Gathering experimental data for 750 and 850°C would be of particular interest.

When interpreting such data one has to consider that conditions on an outdoor fire are highly variable in time and space and that, due to the presence of flesh, skin, and above all, fats, the temperature attained can vary significantly locally and maintaining a wood fire with temperatures above 900°C would be rather difficult. Nevertheless, the fact that some samples have higher C/C ratios and lower IRSF than others suggests that these bones underwent different transformations. I suggest that this may be due to different cremation temperatures, but the dataset is small and it is not possible, at this stage, to completely exclude the influence of post-burial alterations.

6.7 Impact on the study of calcined bone

6.7.1 In archaeological contexts

The present study highlighted the difficulty of comparing results obtained on modern and archaeological calcined bone, as some post-heating modification seem to occur. Nevertheless, the infrared study of archaeological calcined bone can help assess differences in cremation practices between sites and between different contexts at the same site. By combining the C/C ratio and the IRSF it seems possible to tell if one bone has been burned at higher temperatures than another (though it may not possible, at this stage, to give the exact temperature since modern heated bone differs from archaeological bone). These differences in burning temperature could be the consequence of different burning conditions (temperature amount of fuel, size of the pyre, etc.). It also seems possible to discriminate between samples burned dry from those burned fresh. However this was only possible in modern bone, as most archaeological samples exhibit similar infrared spectra as the dry samples. There is however one significant difference between archaeological samples and modern specimens heated dry:

the latter have lower hydroxyl group content which could be used when studying archaeological samples to detect those that were burned dry. Finally, the presence of cyanamide in many archaeological samples (39%) could reflect more reducing conditions that could be found in larger pyres.

6.7.2 In forensic contexts

These results will also be useful for forensic scientists as it seems that it is possible to discriminate bone samples heated in different conditions – fresh or dry – and from different ages – modern and archaeological – by using the amount of type A and B carbonates left in the bone. Modern bone heated while still fresh will have generally higher carbonate content of type A and lower amount of type B compared to modern bone heated dry and archaeological burned bone. Furthermore, to discriminate modern from archaeological calcined bone fragments, forensic scientists could treat a fraction of the sample with acetic acid and measure its infrared spectra before and after pre-treatment. If the carbonate content decreases significantly, it is very likely that the sample is modern. This could provide a cost-effective screening method before deciding whether or not to obtain a radiocarbon date.

7 Conclusion

A large amount of data was gathered here but from the results, it is clear that only a small fraction can be used for the study of calcined bone. Of the many infrared indices proposed in the literature, only seven appear to provide useful and distinct information about the composition and structure of calcined bone. Furthermore, the carbon (%C) and carbonate content (pCO_2/g of sample) are strongly correlated to the BPI and do not seem to provide additional information. Nevertheless, the use of elementary analyses to measure the amount of nitrogen (% N) present in calcined bone confirmed that no detectable amounts of organic matter remained in bone after calcination.

Overall, during calcination, organic matter is destroyed, the carbonate content is reduced drastically, the structure becomes more ordered and there is an increase in hydroxyl groups within the structure of bone apatite. This is not new but here, as a result of the different experimental conditions and the study of archaeological samples, a number of new observations have been made:

(1) Temperature impacts on the composition and structure of bone apatite and more specifically on the calculated IRSF and C/C ratio, while time does not.

(2) The incorporation of exogenous carbonates is unlikely as shown by the limited impact of pre-treatment on the composition of archaeological cremated bone, however, isotope analyses are required to confirm it.

(3) Modern and archaeological samples react differently with acetic acid suggesting that their structure differs significantly, which is most likely the consequence of post-heating modifications during which smaller, less well crystallized crystallites become more stable over time. This highlights the fact that infrared comparisons between modern and archaeological calcined samples should be done on untreated modern samples and pre-treated archaeological specimens.

(4) The difference between modern samples heated dry and fresh indicates that the state of the bone prior to heating is important and that samples burned dry will have a different composition and structure than those burned fresh. In particular, very low OH/P ratios were calculated for samples heated dry. Here, however, no such archaeological sample was detected.

(5) The infrared results show that there is a competition between cyanamide, hydroxyl groups and carbonates. Low carbonate content favours the incorporation of cyanamide and hydroxyl groups while higher carbonate content limits these incorporations. The incorporation of cyanamide and hydroxyl groups seems to depend on the combustion

atmosphere. The conditions in which cyanamide is incorporated are still difficult to explain, but could be the consequence of more reducing conditions that could be reached in larger pyres. Furthermore, the hydroxyl group content is higher in samples burned without fuel (LAB 2 and pig rig LAB 3) than those burned on outdoor pyres and archaeological samples. The combustion atmosphere of samples burned outdoors contains much more carbon dioxide due to the burning of fuel, which explains a higher competition between carbonates and hydroxyl groups compared to laboratory conditions where the amount of carbon dioxide (even when additives were present) would be limited.

(6) While the laboratory experiments (LAB 2) confirmed the observation that the C/C ratio increases with temperature (Thompson et al. 2009), the results for samples burned outdoors and archaeological specimens showed that it is not that simple to assess the temperature at which bone fragments were burned. However, it is likely that samples having higher C/C ratios and lower IRSF were burned at higher temperatures than those with lower C/C ratios and higher IRSF. This, in turn, would allow observing variations in cremation practices within a same site and between different sites.

These results, while highlighting the need for further analyses, clearly show that infrared analyses of calcined bone provides useful information about its composition and structure, than can be used to discriminate samples from different origin and that underwent different transformations.

Chapter 5 – Influence of heating on carbon and oxygen isotopes in bone apatite carbonates

1 Introduction

In bone, carbon is present in both the carbonate fraction of bone apatite and the organic phase. Infrared analyses (see Chapter 4) have shown that when calcined, all organic matter is destroyed and the only carbon remaining in bone is contained within the carbonate fraction of bone apatite (with the possible exception of cyanamide). This carbonate content decreases significantly during heating but, in most samples, enough remains for radiocarbon dating and stable carbon isotope analysis. The infrared spectra and indices discussed in Chapter 4 also highlight that the final composition and structure of calcined bone is temperature-dependent: the C/C ratio related to the variation in type A and B carbonates, and the IRSF, linked to the crystallinity of the samples based in the relative positions of the phosphates in the structure of bone apatite, are both influenced by temperature. This suggests that the carbon and oxygen isotope composition of calcined bone could also be temperature-dependent. Furthermore, the infrared results suggest that after calcination, smaller, less crystalline crystallites are present in bone apatite. Over time, these become more stable and less reactive, as was observed in unburned bone (*Ostwald ripening*) (Lee-Thorp and van der Merwe 1991; Sponheimer & Lee-Thorp 1999; Pollard et al. 2007). The increased reactivity of the small, less well recrystallized crystallites may render them more prone to post-burial alteration. The observation that the archaeological calcined samples with the highest carbonate content (BPI > 0.30) were all retrieved from marine high-carbonate geological contexts (e.g. limestone, chalk) highlights the possibility that carbonates are incorporated into the structure of bone apatite from its burial environment. Pre-treatment of these samples with acetic acid, however, had almost no

effect on their carbonate content, which indicates that the carbonates were endogenous or permanently incorporated into bone apatite crystallites. It is difficult, however, to ascertain the origin of the carbon left in bone apatite after calcination using infrared analyses. Isotope analysis and radiocarbon dating of these samples present an opportunity to investigate the diagenetic exchanges (during and after calcination) and shed light on whether the difference observed between modern and archaeological heated bone are the result of post-burial alterations and/or the cremation processes themselves.

This chapter proposes models for the carbon and oxygen exchanges and losses during and after calcination. The experimental design used in this study to understand these exchanges and losses will be detailed. The chapter continues with the results that are then discussed and preliminary conclusions are offered.

2 Models for carbon and oxygen exchanges and losses

2.1 Carbon

During calcination, bone apatite loses and/or exchanges carbon with its surrounding environment as has been demonstrated by several experimental heating experiments (e.g. Hüls et al. 2010; Zazzo et al. 2012). The different sources of carbon to be considered are: endogenous bone apatite carbonates, atmospheric carbon dioxide, carbon from the combustion of organic matter and fuel. The carbon from the combustion of organic matter has to be separated into two fractions: (1) collagen in which the bone apatite is imbedded, and (2) flesh, fat, skin, and marrow which are present in and around the bone but not quite so intimately (Vaughan 1970; Wopenka & Pasteris 2005).

The losses occurring in bone during heating can be separated into 3 phases (Haas & Banewicz 1980; Van Strydonck et al. 2005): loss of water (non-structural) below 200°C, loss

of organic matter and structural water between 200 and 600°C and losses and exchanges of carbon from the carbonate fraction of bone apatite at higher temperatures. The processes of carbon losses and exchanges are complex and not yet fully understood. In addition to losses and exchanges, fractionation may also play a role in determining the isotope composition of calcined bone. For example, fractionation of about -4‰ at 500°C and -3‰ at 800°C between calcite and the surrounding carbon dioxide has been demonstrated by heating experiments (Scheele & Hoefs 1992). All the potential exchanges, losses and fractionations that have to be taken into account when studying the carbon isotope composition ($\delta^{13}C$ and $F^{14}C$) of heated bone are shown in Figure 5.1.

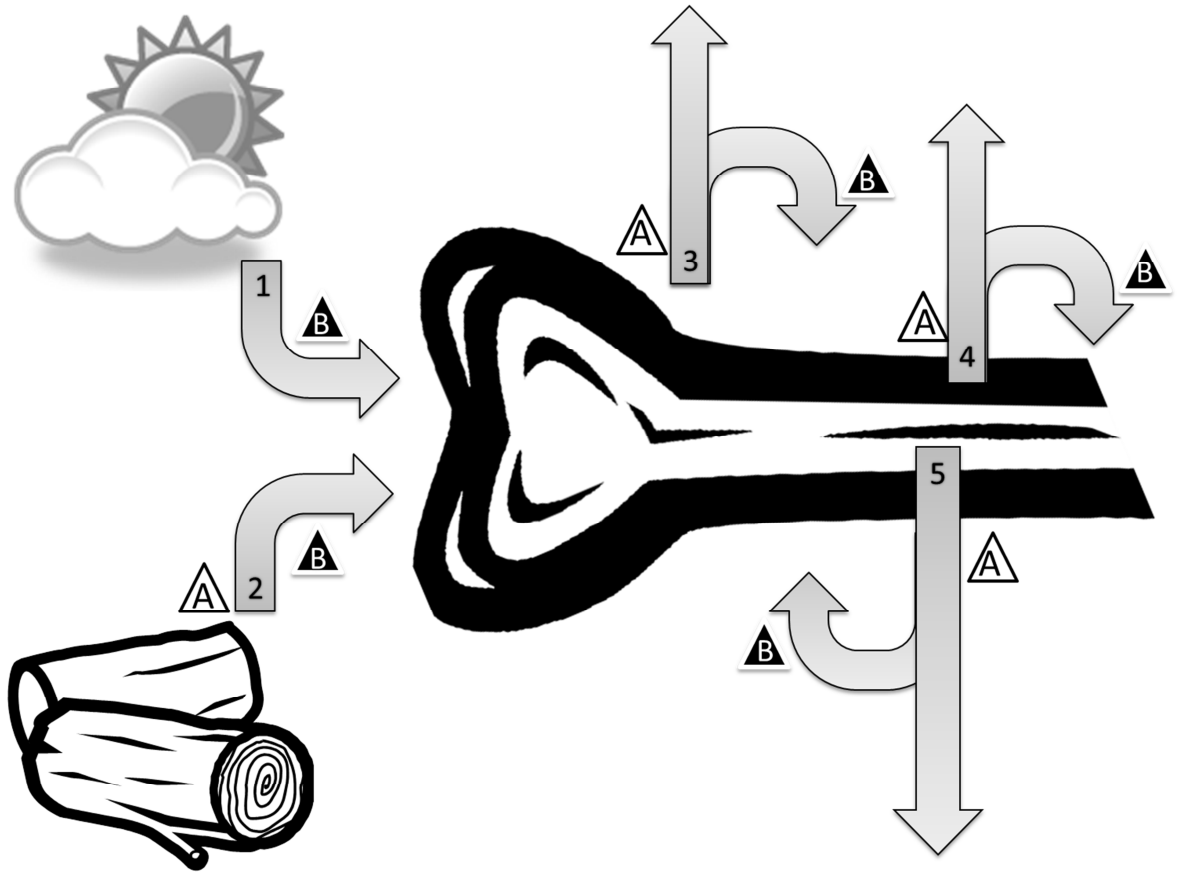

Figure 5.1 – Potential carbon exchanges, losses and fractionations that have to be taken into account when studying the carbon isotope composition of bone apatite during heating: 1 – atmospheric carbon dioxide; 2 – carbon dioxide released during the combustion of fuels; 3 – carbon dioxide released by the combustion of flesh, fat, skin and marrow; 4 – carbon dioxide released by the heating of bone apatite carbonates; 5 – carbon dioxide released by the combustion of collagen; A – potential fractionation between the carbon present in fuels, organic matter or bone apatite carbonates, and the carbon dioxide released into the combustion atmosphere; B – potential fractionation between the carbon dioxide from the combustion atmosphere around bone apatite and bone apatite carbonates; the arrows indicate the different carbonate/carbon dioxide flows

Considering all these carbon sources and possible fractionation mechanisms, the following equation can be written to explain the stable carbon isotope composition of bone apatite carbonates after calcination (before burial):

$$\delta^{13}C = \alpha(\delta^{13}C_1 + B_1) + \beta(\delta^{13}C_2 + A_2 + B_2) + \gamma(\delta^{13}C_3 + A_3 + B_3)$$
$$+ \varepsilon(\delta^{13}C_4 + A_4 + B_4) + \mu(\delta^{13}C_5 + A_5 + B_5)$$
$$\text{with } \alpha + \beta + \gamma + \varepsilon + \mu = 1$$

All parameters of this equation are detailed in the discussion (Table 5.1). Here it is assumed that two main pools of carbon are present during heating: the internal and external combustion atmospheres. The first consists of carbon released by the heating of bone apatite carbonates and by the burning of collagen. The second contains atmospheric carbon dioxide, carbon dioxide emitted by the fuel and carbon dioxide resulting from the burning of all organic sources except collagen (Figure 5.2). Once buried, calcined bone is susceptible to post-burial alterations that may involve the exchange of carbon with the soil.

2.2 Oxygen

Due to the fact that there are many sources of oxygen in the environment that could potentially exchange with bone apatite, the understanding of oxygen fractionation, exchanges and losses is even more complex than for carbon isotopes. When analysing oxygen isotopes, the following additional sources should be considered: atmospheric water and dioxygen, as well as body oxygen (apatite carbonates and phosphates, organic oxygen and structural water).

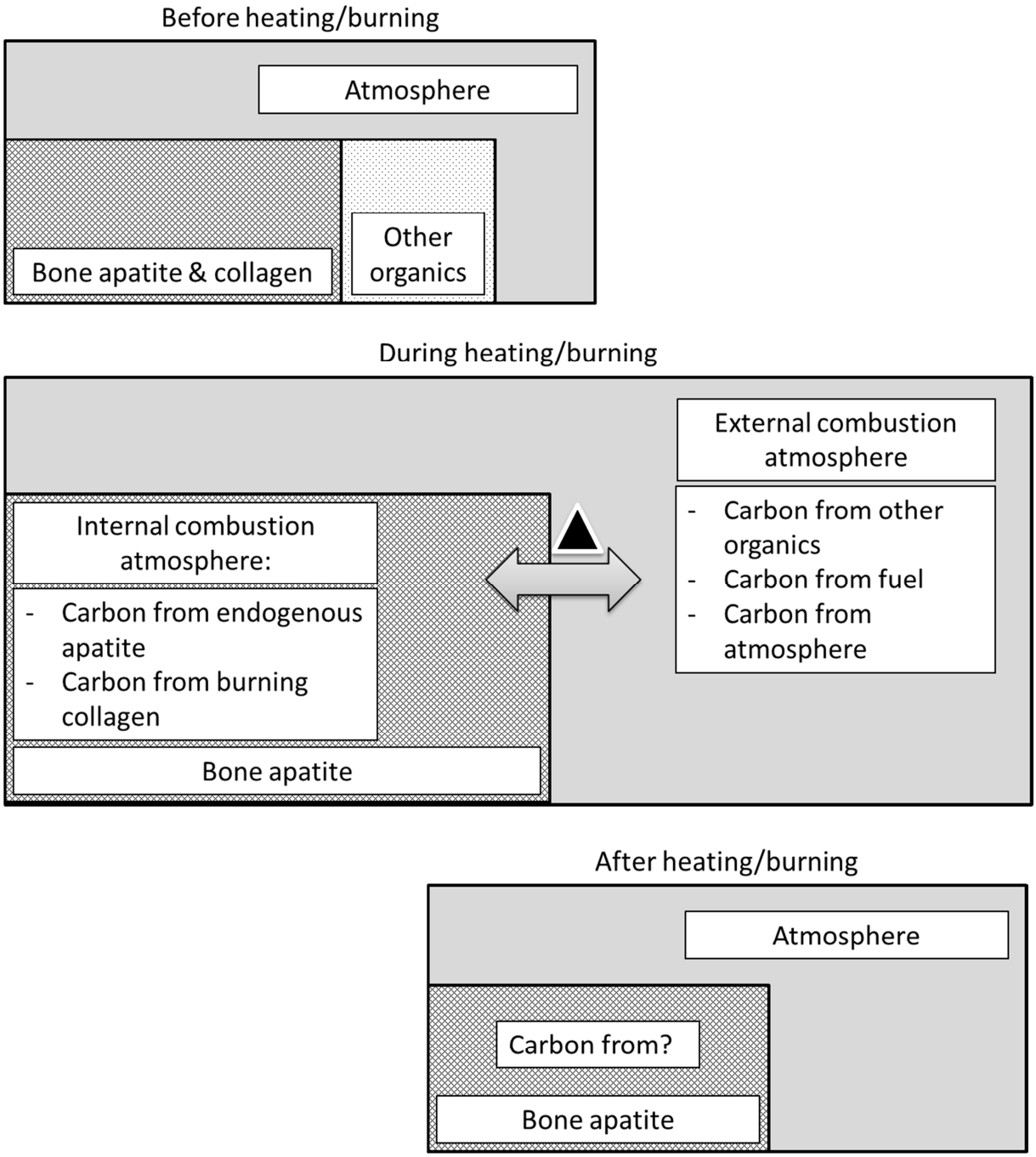

Figure 5.2 – The state of bone before, during and after heating detailing the internal and external combustion atmospheres and the sources of carbon available for exchange

3 Experimental design

The current experiments, carried out both in the laboratory and on natural outdoor fires, were mainly designed for understanding the carbon isotope composition of calcined bone apatite carbonates. Oxygen isotope exchanges are investigated in parallel but no specific experiment was developed here to study them. Carbon and oxygen isotopic measurements were made on all the samples and a few were also radiocarbon dated. The different laboratory heating experiments and outdoor cremations are detailed in Chapter 3. LAB 1 investigate the impact of oxygen availability and the presence of additives; in the LAB 2 experiments, the influence of fuel was avoided by heating the sample in a muffle furnace, and the impact of time and temperature was explored to detect potential carbon exchange between bone apatite and collagen (and small amounts of remaining flesh and marrow); in the LAB 3 experiments the influence of organic matter and more specifically the collagen was eliminated. While these experiments allowed for the controlled study of heating of bone, they are not fully representative of natural burning conditions. To reproduce as closely as possible the natural conditions under which bone may have been cremated, several outdoor burns were also carried out (see Chapter 3). Carbon and oxygen isotopic measurements were made on all the samples and a few were also radiocarbon dated.

In the last part of the isotopic study, the carbon and oxygen isotope composition of calcined bone from the archaeological sites of Ireland are presented. The samples from Knowth had previously been radiocarbon dated in an associated study (Schulting et al. forthcoming) allowing for the investigation of correlations between ^{13}C and ^{14}C in archaeological calcined bone.

All samples were pre-treated prior to isotope analysis with sodium hypochlorite (1% NaClO) and acetic acid (1M CH_3COOH). Further research, however, should include the isotopic comparison of untreated and treated samples.

4 Results

All $\delta^{13}C$ and $\delta^{18}O$ values are expressed in parts per mil (‰), measured on a Kiel IV carbonate device against the Vienna Pee Dee Belemnite (VPDB) as reference standard. The results will often be presented by comparing calcined to unburned values ($\Delta = \delta_{sample} - \delta_{unburned\ apatite}$). The isotope composition of unburned bone apatite and collagen of the modern samples were also measured (Appendix 6.7).

4.1 Experimental heating experiments

4.1.1 LAB 1

The results of the LAB 1 experiments (appendix 6.1) compare the carbon and oxygen isotope results obtained from bone fragments of the same lamb bone heated in different settings ('open' or 'closed') and with different additives (none, barley or millet seeds). The results (Figure 5.3) show that the variations in carbon isotope composition compared to unburned apatite values ($\Delta^{13}C$) depend mainly on the additives present with bone during heating. Even if some samples are still charred (L3, L6 and L8), the variations are clear: samples heated without additive (L1 to L4) have values going closer to collagen; those heated with barley (L7 and L8) show the largest variations in ^{13}C content and have values closest to barley seeds; similarly the samples heated together with millet seeds (L5 and L6) show positive $\Delta^{13}C$ values, going closer to millet seeds. The variations in oxygen ($\Delta^{18}O$) are less variable (between -10 and -13.5 ‰). All samples are significantly depleted in ^{18}O compared to unburned bone apatite. With the exception of L3 (still being charred and presenting higher concentration of carbonates than L6 and L8), the samples heated in 'closed' environments seem to have lower $\delta^{18}O$ values than those heated in and 'open' settings. The presence of additives doesn't seem, here, to impact on the oxygen isotope composition of the calcined samples.

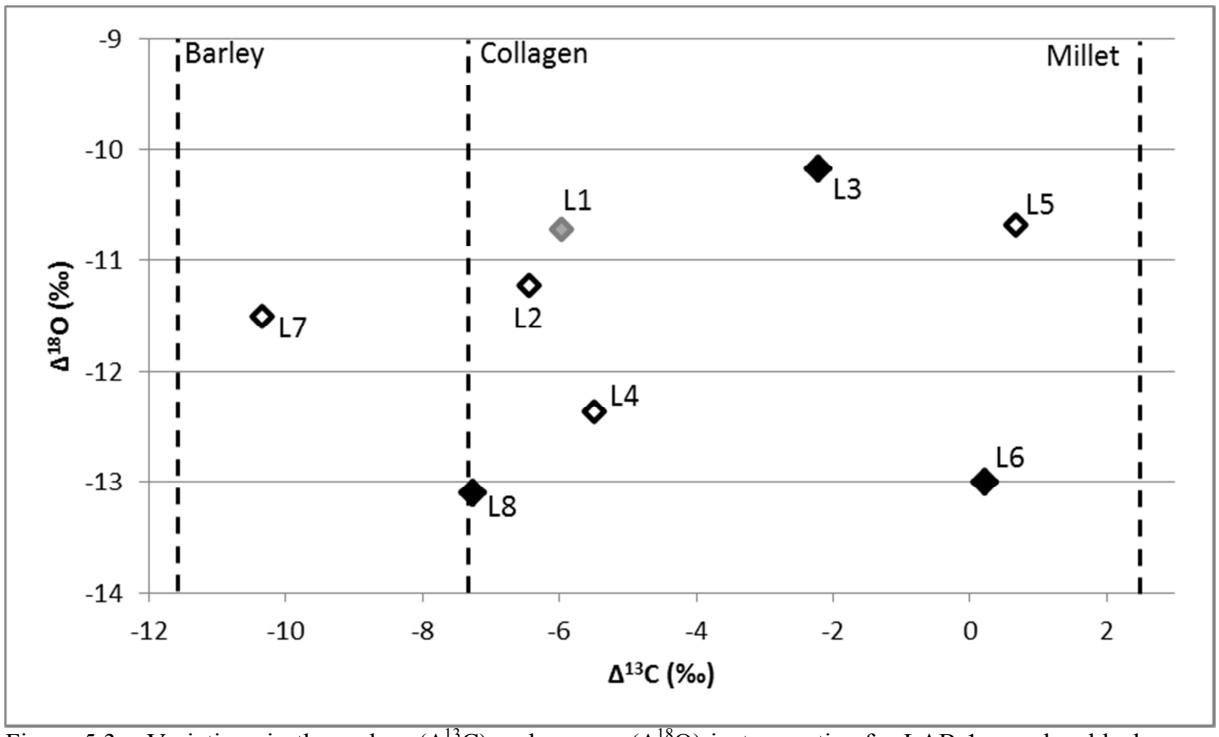

Figure 5.3 – Variations in the carbon ($\Delta^{13}C$) and oxygen ($\Delta^{18}O$) isotope ratios for LAB 1 samples; black, grey and white diamond correspond to charred, intermediate and calcined bone respectively; the sample codes (L1 to L8) refer to Table 3.2

From these results, it is clear that additives have an impact on the carbon isotope composition of calcined bone but not on its oxygen isotope ratio: even small amounts of an external carbon source (i.e. 5 g of seeds for c. 5–10 g of bone) exchanges with bone apatite carbonates and, apparently to a greater degree than collagen. The samples heated in a 'closed' setting are likely to have undergone some reducing conditions due to limited atmospheric dioxygen availability. Some of these samples are still black (L3, L6, L8) but other are white (L4) suggesting that full calcination is possible even when less atmospheric dioxygen is available. Furthermore, there seem to be little impact of these conditions on the oxygen isotope composition (less than 1‰ difference between 'open' (L2) and 'closed' (L4) settings).

4.1.2 LAB 2

The results for the LAB 2 heated bone fragments (Appendix 6.2) show a strong correlation between the carbon and oxygen isotope ratios ($R^2 = 0.73$ – Figure 5.4) independently of the degree of calcination (charred and calcined bone fragments together). All heated samples are depleted in both ^{13}C and ^{18}O compared to unburned bone, with calcined samples being more depleted than charred specimens. Two samples have $\delta^{13}C$ values more negative than collagen (though within measurement error).

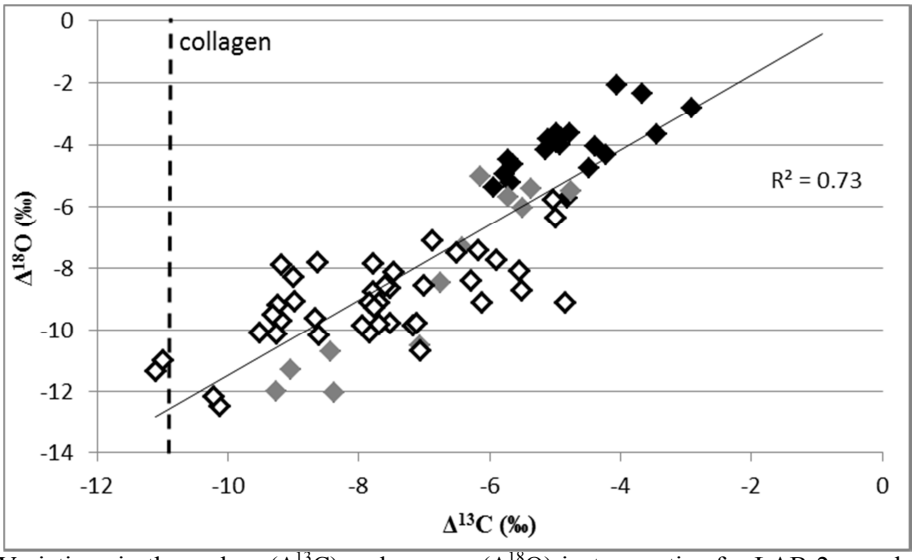

Figure 5.4 – Variations in the carbon ($\Delta^{13}C$) and oxygen ($\Delta^{18}O$) isotope ratios for LAB 2 samples; black, grey and white diamond correspond to charred (colour codes 3 and 3.5), intermediate (4, 4.5 and 5) and calcined (5.5 and 6) bone respectively (measurement error is smaller than the marker size)

Combining the results of all samples heated at the same temperature (for 30 minutes to 24 hours) it appears that both $\delta^{13}C$ and $\delta^{18}O$ values decrease with temperatures approaching 800°C and then increase again (Figure 5.5a). Similar observations were made by Harbeck et al. (2011 – Figure 5.5b) who heated two cow tibias up to 1000°C. Looking at the carbonate content (API and BPI) of the samples heated at 700, 800 and 900°C, only the samples heated at 900°C appear to have lower BPI than the others (Figure 4.12b, Chapter 4).

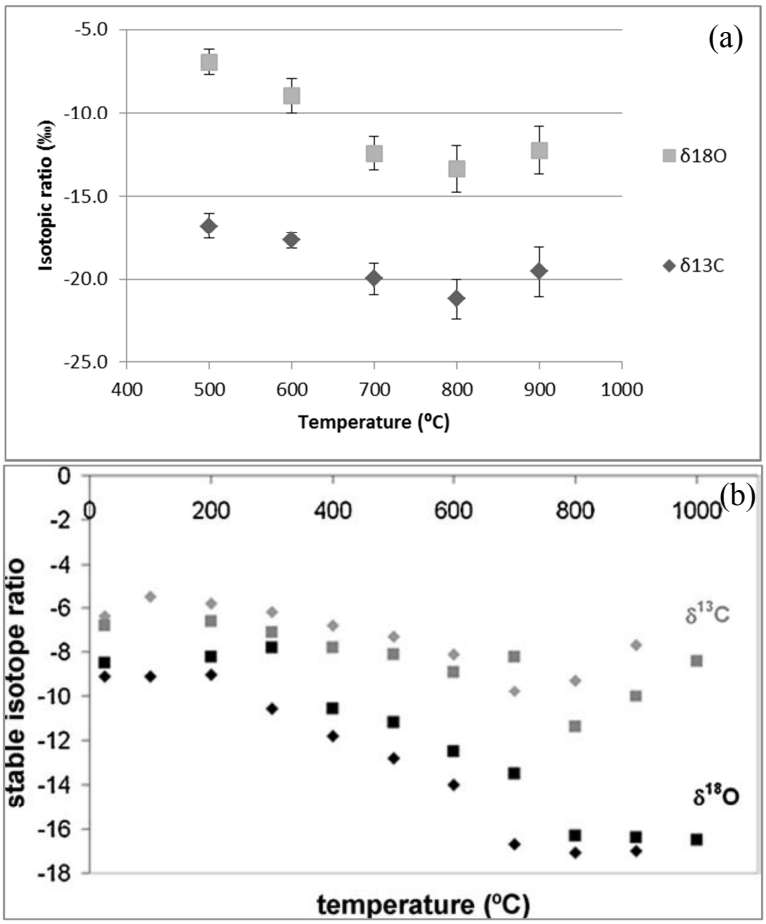

Figure 5.5 – Changes in carbon and oxygen isotopic ratios with temperature (a) for LAB2 and (b) from Harbeck et al. (2011)

The correlation observed between the carbon and oxygen isotope ratios of heated bone suggests that the exchanges and losses of carbon and oxygen occur in a similar way, most likely through the loss of carbon dioxide and exchanges with carbon dioxide from the combustion atmosphere only. Also, the observation that two samples are more depleted in ^{13}C than collagen suggest that some fractionation occurs between the carbon dioxide emitted by the combustion of collagen and bone apatite carbonate or that there is some exchange with fats and skin that have lower $\delta^{13}C$ values than collagen (Tieszen & Farge 1993). However, these are likely to burn away before bone apatite starts to exchange carbon with the combustion atmosphere. Furthermore, the fact that the samples heated at 800°C are more depleted in both ^{13}C and ^{18}O compared to those heated at 700 and 900°C may suggest, as observed for a calcite-CO_2 system (Scheele & Hoefs 1992) that the fractionation between

bone apatite carbonates and carbon dioxide present in the combustion atmosphere is dependent on the temperature. However, as observed in the calcite-CO_2 system, fractionation should decrease with temperature. The fact that the amount of carbonates (measured with the BPI and API) is very similar in calcined samples heated at different temperature suggests that the differences seen in isotope ratios are due to different exchanges happening or a combination of different exchanges and fractionations.

4.1.3 LAB 3

Several fresh pig rib samples did not contain enough carbonates after calcination and no reliable isotope ratio could be measured. For the samples providing reliable results (Appendix 6.3), those heated in the presence of barley seeds (green in Figure 5.6a) have lower $\delta^{13}C$ values than those heated together with cornflour (yellow). The treatment prior to heating does not seem to impact on the carbon isotope composition. For the oxygen isotope ratios, the only observation that can be made is that those heated with barley seeds or cornflour are enriched in ^{18}O if organic matter had been previously removed (green diamond and yellow dot).

For the dry seal bone samples (Figure 5.6b), there is clear patterning. Samples heated with barley seeds (green) have lower $\delta^{13}C$ values than the others that have similar $\delta^{13}C$ values to unburned bone apatite. The highest $\delta^{13}C$ values are observed in the samples burned with cornflour (yellow) but the $\delta^{13}C$ values are even higher than cornflour and unburned bone apatite. Two samples burned without additives also have $\delta^{13}C$ values higher than unburned bone apatite (black dot and diamond). These had their organic matter previously removed. In this case, the only sources of carbon available are carbon from the apatite carbonates and atmospheric carbon dioxide that in this case may need to be taken into account as no carbon dioxide is released from the combustion of fuel and/or organic matter ($\delta^{13}C_{CO2} \approx$ -8 ‰; $\delta^{18}O_{CO2} \approx$ 0 ‰). The patterning is even clearer for oxygen isotopes. The values are more enriched in ^{18}O in samples that were burned without barley seed or cornflour (c. 2‰ – black

and red). This was not observed in the pig rib samples. However, as seen in the pig rib samples, all samples heated after organic removal treatment (dots and diamonds) have higher $\delta^{18}O$ values (c. 1 ‰) compared to those heated without prior organic removal pre-treatment (squares and triangles). The results finally suggest that fats have very limited impact on the oxygen isotope ratio: very similar results are observed for sample heated without additives and with lard (black and red).

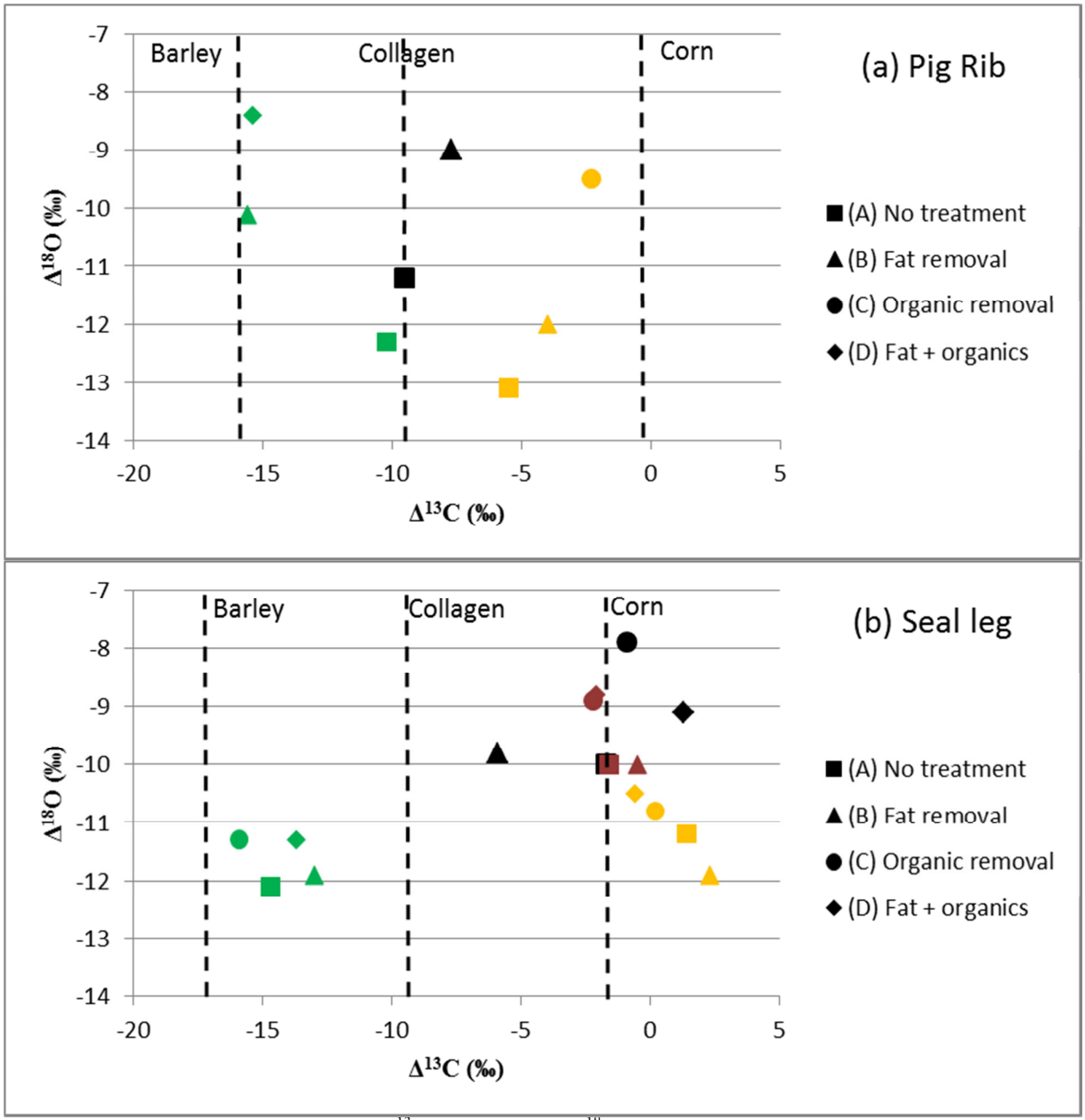

Figure 5.6 – Variations in the carbon ($\Delta^{13}C$) and oxygen ($\Delta^{18}O$) isotopic ratios for LAB 3 samples: (a) pig rib and (b) seal bone; black, red, green and yellow correspond to (1) no additives, (2) lard, (3) barley seeds and (4) cornflour respectively; carbon isotopic ratios for barley seeds, cornflour and collagen are highlighted

These results confirm the impact of additives on both carbon and oxygen isotope ratios. $\delta^{13}C$ values are close to the values of the additives used while $\delta^{18}O$ values are usually lower in samples heated with additives. Looking at the seal samples still containing organic matter burned without additives, they have lower $\delta^{13}C$ values (-11.3‰ and -15.5‰) than those burned without additives but after a chemical treatment to remove organic matter (-10.5‰ and -8.3‰). The samples without organic matter are enriched in ^{18}O compared to those still containing collagen and heated in the same conditions. Finally, the observation that some calcined seal samples have isotopes values higher than unburned bone strongly suggests that some isotope effect occurs between bone apatite carbonates and the carbon dioxide released by its heating, leaving heavier carbon isotopes in bone apatite. It could also be the consequence of the incorporation of atmospheric carbon dioxide but the fact that the highest values are obtained for samples heated in the presence of cornflour suggest otherwise.

4.2 Outdoor burnings

The carbon isotope ratios of the samples burned in natural conditions with different types of fuel (Appendix 6.4) clearly show the impact of fuels on the $\delta^{13}C$ values of calcined bone apatite carbonates. Indeed, the variation in carbon isotope composition ($\Delta^{13}C$) is positively correlated with the difference between the $\delta^{13}C$ values of unburned apatite and the fuel used ($R^2 = 0.57$ – Figure 5.7a). The sample L1_B burned with 'coal' 1 ($\delta^{13}C_{coal}$ = -24.3‰) seem to have exchanged all its carbon with carbon from the fuel. If the bone is left longer on the fire and millets seeds are poured onto the fire (L1_D), its $\delta^{13}C$ value increases going closer to isotope ratio of the millet seeds ($\delta^{13}C_{millet}$ = -12.9 ‰), highlighting once more the impact of fuels. The radiocarbon results (Appendix 6.4) confirm this and show that modern animal joints burned with different types of old fuels appear older when dated. There is a high variability in the dates with some samples still looking modern (post-1950) while other, burned with 400 years-old fuel (P6) appearing to be almost 400 years old. For the latter, it

seems that almost all its ^{14}C originates from the fuel. This is of particular interest since that sample still retained all flesh and skin prior to burning suggesting that the 'external' organic matter has very limited impact on the isotope composition of calcined bone apatite carbonates.

To calculate the percentage of carbon exchanges between bone apatite and fuel carbon, several equations were proposed (Snoeck et al. 2014a). The calculation based on the ^{14}C composition of bone ($F^{14}C$) showed a wide range of exchanges from 39 to 95%, similar to that observed in other studies: 48 to 91% (Zazzo et al. 2012) and 36 to 86% (Hüls et al. 2010). Calculations based on ^{13}C are more complex. While the ^{14}C composition of bone apatite and collagen are basically identical, their ^{13}C content is different. Two equations were proposed: the first equation (1) hypothesises that bone apatite only exchanges carbon with fuel while the second (2) assumes that all endogenous carbon is replaced by fuel or collagen carbon. When using these equations, however, the exchanges appeared to be above 100% in several cases. Only by considering a depletion of 2‰ between fuel carbon and carbon dioxide emitted by combustion of the fuel and/or between that carbon dioxide and bone apatite carbonates, is it possible to avoid exchanges higher than 100% (Snoeck et al. 2014a). Using the two adjusted equations 1* and 2* from Snoeck et al. (2014a), the percentage ^{13}C and ^{14}C exchanges were calculated for each sample (Figure 5.7b).

$$\%Carbon\ exchange\ with\ fuel = \frac{F^{14}C_{ap-burned} - 1.055}{F^{14}C_{fuel} - 1.055}$$

$$\%Carbon\ exchange\ with\ fuel\ 1^{*} = \frac{\delta^{13}C_{ap-burned} - \delta^{13}C_{ap-unburned}}{(\delta^{13}C_{fuel} - 2‰) - \delta^{13}C_{ap-unburned}}$$

$$\%Carbon\ exchange\ with\ fuel\ 2^{*} = \frac{\delta^{13}C_{ap-burned} - \delta^{13}C_{collagen}}{(\delta^{13}C_{fuel} - 2‰) - \delta^{13}C_{collagen}}$$

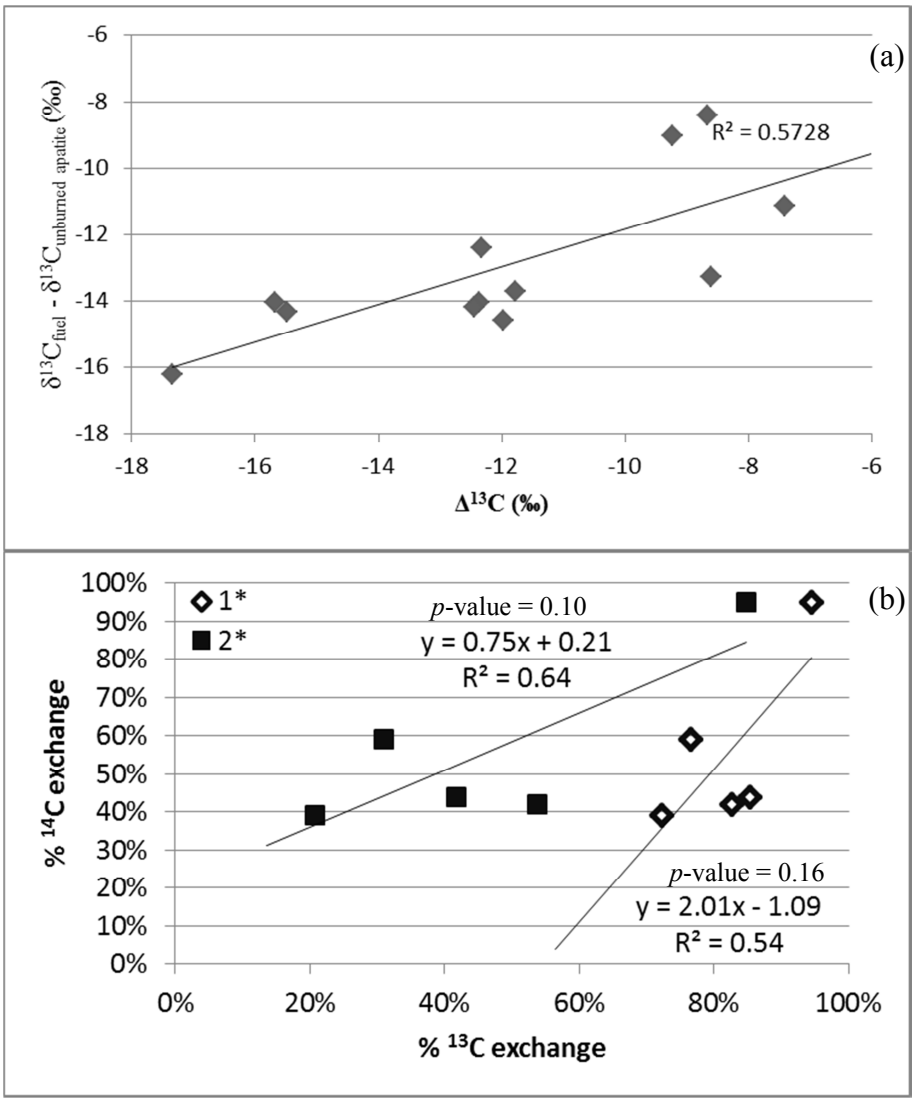

Figure 5.7 – (a) The difference in carbon isotopic ratios between fuels and unburned bone apatite versus the variation in the carbon isotopic ratios ($\Delta^{13}C$), and (b) calculations of carbon exchanges (in %) for ^{14}C and ^{13}C using both equations (1* and 2*)

It appears that neither equation explains fully the carbon exchanges with fuel (no 1:1 regression is observed in Figure 5.7b) suggesting that the carbon composition of calcined bone apatite carbonates is made of endogenous bone apatite carbon as well as carbon originating from the fuel and collagen. The variation in oxygen isotope ratio during burning ($\Delta^{18}O$) decreases when the % ^{13}C exchange with fuel increases (Figures 5.8a and b), but still remains generally lower that the $\delta^{18}O$ values of samples burned without fuel or additives.

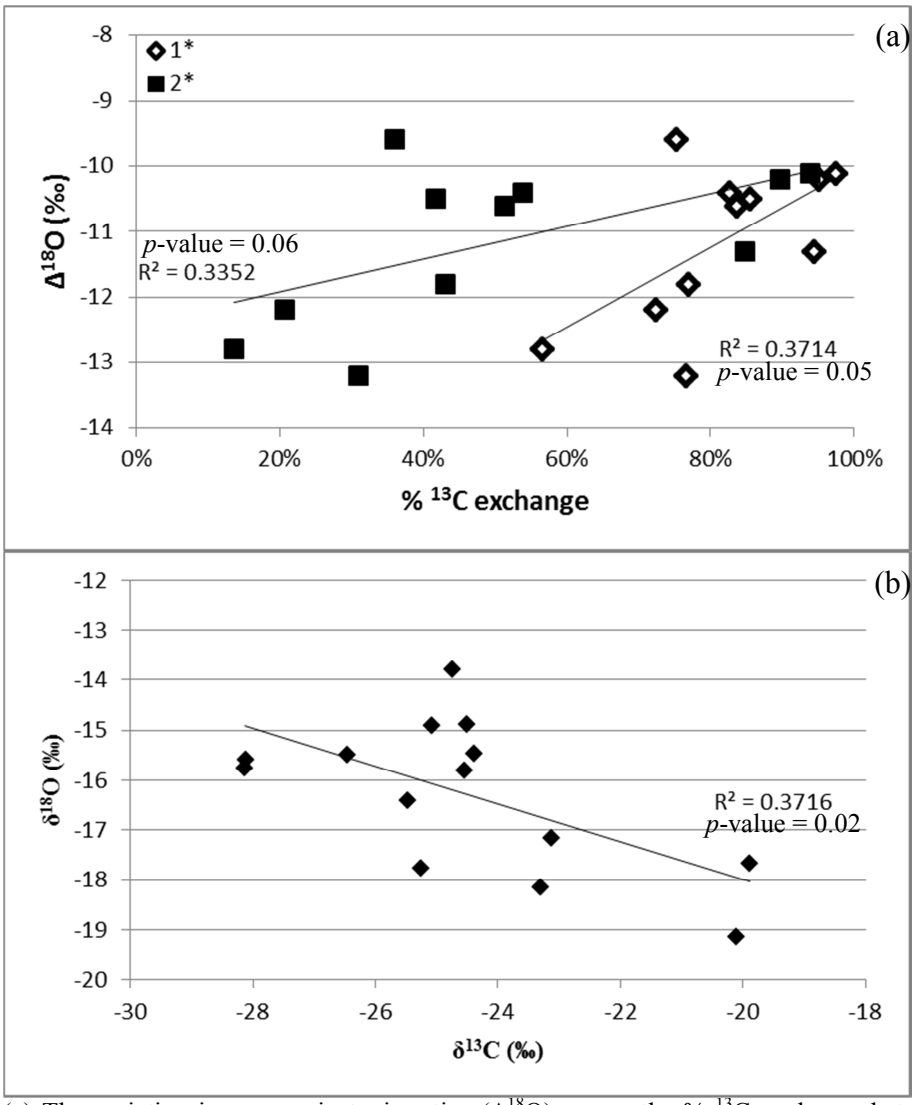

Figure 5.8 – (a) The variation in oxygen isotopic ratios ($\Delta^{18}O$) versus the % ^{13}C exchange between fuel and burned bone apatite for the samples burned on outdoor fires calculated with equations 1* and 2*; (b) $\delta^{18}O$ versus $\delta^{13}C$ values for the calcined samples burned on outdoor fires

4.3 Archaeological samples

4.3.1 Stable isotopic results

The stable isotope ratios of archaeological calcined samples (Appendix 6.5) show a wide variation in $\delta^{13}C$ and $\delta^{18}O$ values. All samples, dating from the Neolithic to the Middle Bronze Age, should have typical terrestrial C_3-plants based diet values prior to calcination as suggested by the isotopic measurements carried out on Irish unburned human bone samples from the same period (e.g. Schulting et al. 2012; forthcoming). In Knowth, for example, the

$\delta^{13}C$ values of the unburned human bone collagen (n = 14) range between -22.5 and -21.0‰, a very narrow range of 1.5‰ compared the range observed in calcined bone apatite samples (ca. 9‰ – Figure 5.9). The range in $\delta^{18}O$ values is also huge going from -12 to -22 ‰.

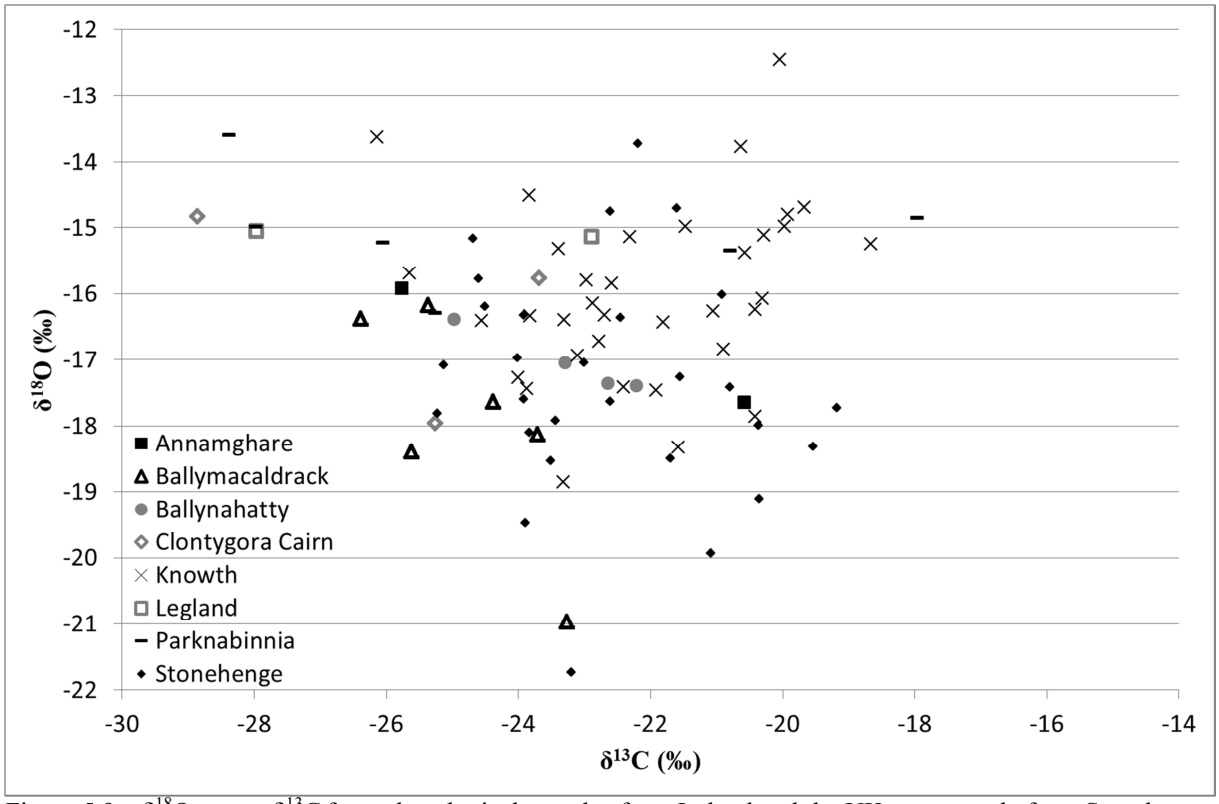

Figure 5.9 – $\delta^{18}O$ versus $\delta^{13}C$ for archaeological samples from Ireland and the UK; one sample from Stonehenge is not included in the graph as its isotope ratios were significantly different (St7 – $\delta^{13}C$ = -11.8‰ and $\delta^{18}O$ = -7.4‰)

4.3.2 Radiocarbon results

When comparing the $\delta^{13}C$ values of the archaeological calcined samples from Knowth to the radiocarbon dates (Figure 5.10) measured previously (Schulting et al. forthcoming), no pattern can be observed suggesting that the wood used for the cremation and the deceased were usually contemporary (i.e. the wood used for cremation had a similar age range as the body ± 20 years).

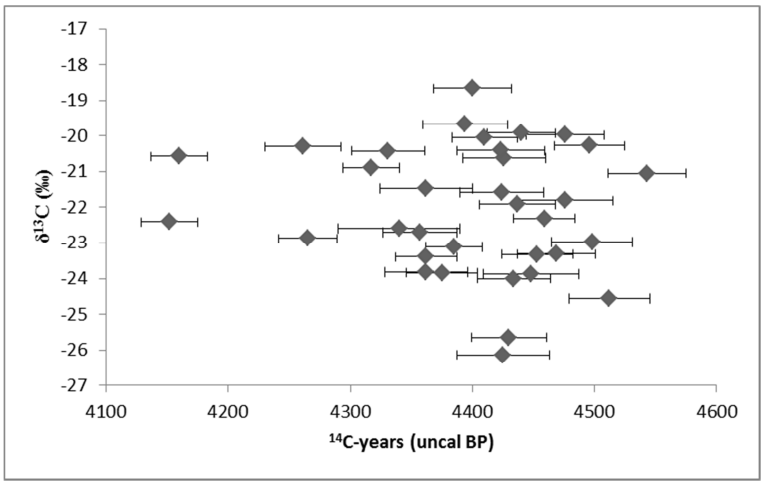

Figure 5.10 –$\delta^{13}C$ versus the radiocarbon dates (uncal BP) for the archaeological calcined bone fragments from Knowth (Schulting et al. forthcoming)

5 Discussion

For the purposes of this discussion, it is important to keep in mind the general equation proposed for the ^{13}C exchanges, losses and potential fractionations occurring in bone apatite during calcination (Figure 5.1):

$$\delta^{13}C = \alpha(\delta^{13}C_1 + B_1) + \beta(\delta^{13}C_2 + A_2 + B_2) + \gamma(\delta^{13}C_3 + A_3 + B_3)$$
$$+ \varepsilon(\delta^{13}C_4 + A_4 + B_4) + \mu(\delta^{13}C_5 + A_5 + B_5)$$
$$\text{with } \alpha + \beta + \gamma + \varepsilon + \mu = 1$$

5.1 Comparison between different samples

5.1.1 Modern heated and burned bone

The results of the laboratory heating experiments and outdoor burnings showed that:

(1) the presence of additives/fuel impacts on the carbon and oxygen isotope composition of calcined bone apatite. Samples burned with C3-additives/fuel are more depleted in ^{13}C and ^{18}O than those heated without (Figure 5.11);

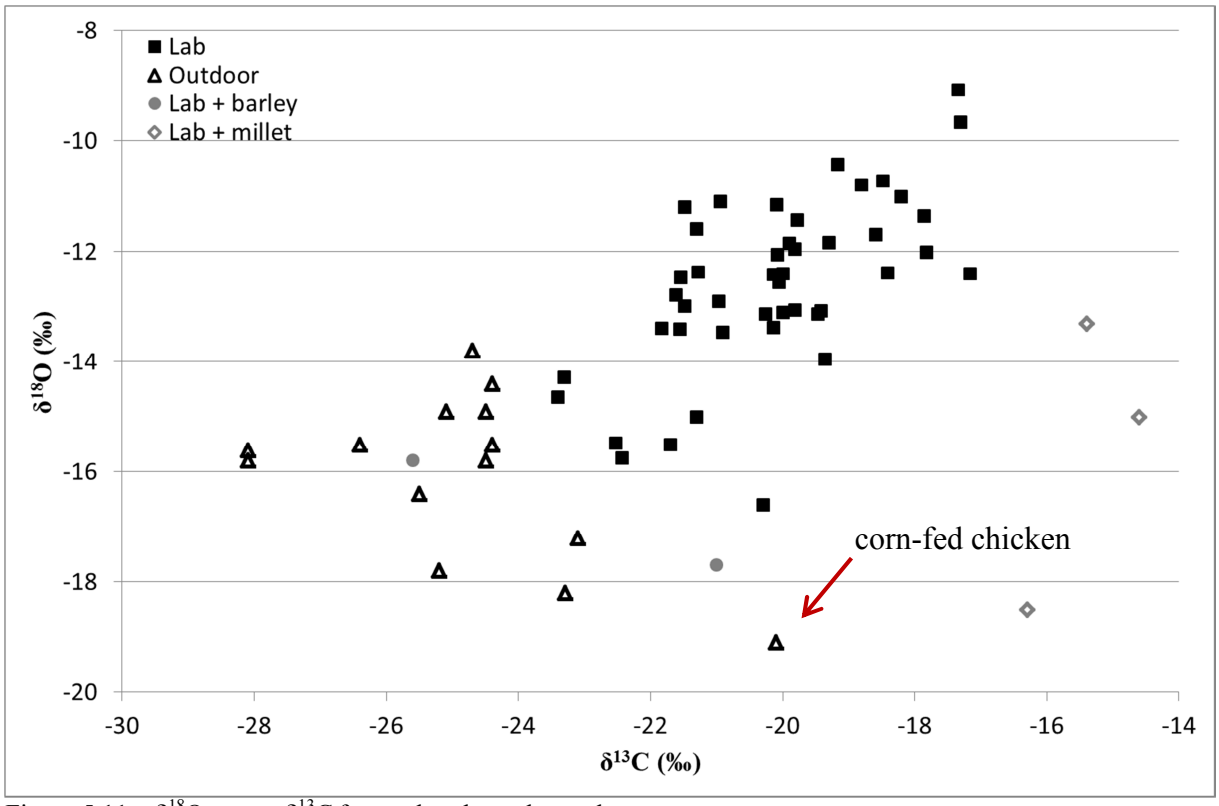

Figure 5.11 – $\delta^{18}O$ versus $\delta^{13}C$ for modern heated samples

(2) both $\delta^{13}C$ and $\delta^{18}O$ values of samples heated without additives decrease up to 800°C before increasing at higher temperature;

(3) the strong correlation ($R^2 = 0.73$) observed between the $\delta^{13}C$ and $\delta^{18}O$ values of heated bone suggests that the carbon and oxygen exchanges occur using similar pathways;

(4) an isotope effect leading to a fractionation of minimum 0.5 ‰ may occur between collagen and carbon dioxide released by the combustion of collagen and/or between that carbon dioxide and bone apatite carbonates ($A_5 + B_5 \leq -0.5$ ‰);

(5) a similar effect may occur between fuel carbon and bone apatite carbonates ($A_2 + B_2 \leq -2$ ‰);

(6) the loss of carbonates during heating of bone apatite is accompanied by an isotope effect leading to a potential fractionation of minimum 1 ‰ leaving more heavier isotopes in bone apatites ($A_4 \geq 1$ ‰);

(7) the exchanges with fuel are very variable;

(8) the variations in oxygen isotope composition ($\Delta^{18}O$) are lower when the carbon exchanges with fuel (% ^{13}C exchanges) are higher.

5.1.2 Archaeological and modern calcined bone

Most archaeological samples appear to have similar $\delta^{13}C$ and $\delta^{18}O$ values to samples burned with fuel suggesting that most of these were indeed burned on outdoor pyres (Figure 5.12). However, some archaeological samples seem to be more enriched in ^{13}C than others. Most of these appear to have cyanamide (t-test *p*-value = 0.001; no significant difference in $\delta^{18}O$ values) suggesting that (1) the presence of cyanamide limits the exchanges and incorporation of fuel carbon into the structure of bone apatite, (2) the lack of carbon dioxide in the combustion atmosphere favours the incorporation of cyanamide into bone apatite which is not possible when large amounts of carbon released by fuels are present, and/or (3) the carbon present in cyanamide is enriched in ^{13}C suggesting that it originates from collagen instead of fuel. A question remains as to whether the carbon present in cyanamide ($-CN_2H$) reacts with phosphoric acid liberating carbon that can then be included in the isotopic measurements. Previous research suggests that cyanamide reacts with phosphoric acid to create an amidinium phosphate (Steinman et al. 1964) but it is unclear if this product is stable and/or will liberate carbon. The release of carbon under the form of carbon dioxide is however unlikely as there is no oxygen present in cyanamide. This suggests that the presence of cyanamide limits the exchange of carbon with the combustion atmosphere or that cyanamide can only be incorporated when small concentrations of carbon dioxide are present in the combustion atmosphere. The latter could occur when bone is used as fuel or when bone is burned in reducing conditions (low concentrations of oxygen available for combustion). The lack of oxygen during combustion leads to incomplete oxidization of organic matter emitting CO and other components instead of CO_2 (González-Pérez et al. 2004). Such conditions are also used to produce charcoal. In any case, there seem to be a competition between

cyanamide and carbonates. No statistical different in $\delta^{13}C$ and $\delta^{18}O$ values between samples with high (BPI > 0.30) and low (BPI < 0.30) carbonate content was found (t-test *p*-values > 0.05).

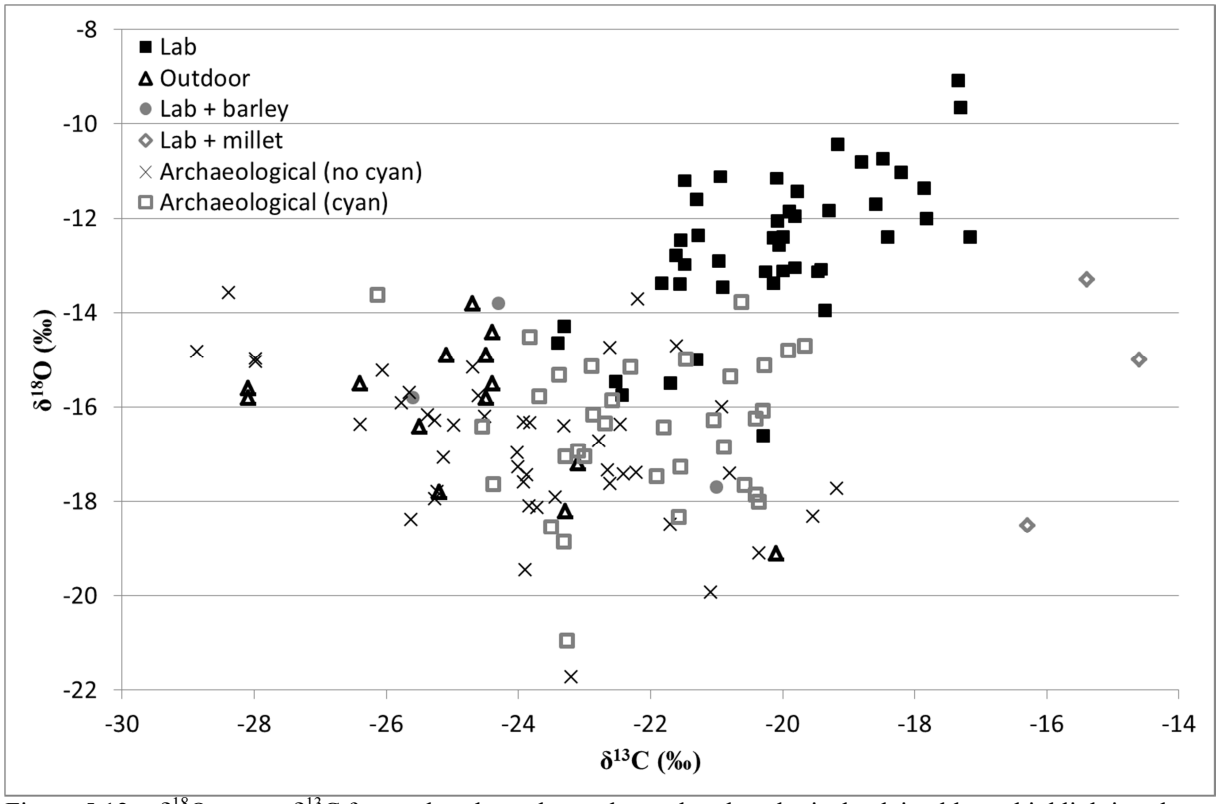

Figure 5.12 – $\delta^{18}O$ versus $\delta^{13}C$ for modern heated samples and archaeological calcined bone highlighting those having cyanamide (cyan – CN/P ≥ 0.25)

5.2 Isotopic changes during calcination

5.2.1 Carbon exchanges and losses

The difference in carbon isotope ratios between samples heated without additional fuel and those burned on outdoor fire clearly shows that the presence of fuels and additives has a significant impact on the isotope composition of calcined bone. There is still a question about the origin of the rest of the carbon present in bone apatite carbonates: endogenous bone apatite carbonates and/or collagen carbon. The carbon isotope results of the laboratory experiments carried out without additives and prior treatment are all comprised between the

$\delta^{13}C$ values of unburned apatite and collagen suggesting that some endogenous carbonates remain in bone apatite after calcination (with potential fractionation) but that there is a significant incorporation of collagen carbon into the carbonate fraction. This was confirmed by the simulations using the equations 1* and 2* (Figure5.7).

The lack of directional variation in the isotope ratios of the LAB 2 samples heated at the same temperature for different amounts of time suggests limited adsorption-desorption. However, some exchanges are still possible as demonstrated by the change in $\delta^{13}C$ seen in the lamb leg burned outdoors first without and then with millet seeds (L1_B and L1_D).

5.2.2 Oxygen exchanges and losses

The changes in oxygen isotopes are more difficult to understand. While it is clear that samples heated with fuel have generally lower $\delta^{18}O$ values than those heated without additives, the fact that samples that exchanged more ^{13}C with fuel are more enriched in ^{18}O than those exchanging less ^{13}C with fuel is surprising and, with the results of this research, the reasons why this is the case remain unclear. The strong correlation between the carbon and oxygen isotope values ($R^2 = 0.73$), however, suggests that the source(s) of carbon and oxygen are mostly the same, or at least that the carbonates present in bone apatite can only exchange with carbon dioxide and not dioxygen or water, suggesting that only the oxygen isotope composition of the combustion atmosphere carbon dioxide impacts on the $\delta^{18}O$ values of calcined bone apatite carbonates. The main source of oxygen in the carbon dioxide fraction of the combustion atmosphere is most likely atmospheric dioxygen since its presence is necessary for the combustion/oxidation of any organic matter (i.e. fuels, collagen).

5.2.3 Exchange models

Of all the terms present in the equation proposed for the calculation of the carbon isotope composition of calcined bone apatite carbonates, several are still unknown. For modern samples, only the various $\delta^{13}C$ values are known. In archaeological bone, the only available

data is the $\delta^{13}C$ value of the cremated sample. The various coefficients (α, β, etc.) and fractionation terms (A and B) need to be calculated or at least evaluated (Table 5.1).

$$\delta^{13}C = \alpha(\delta^{13}C_1 + B_1) + \beta(\delta^{13}C_2 + A_2 + B_2) + \gamma(\delta^{13}C_3 + A_3 + B_3)$$
$$+ \varepsilon(\delta^{13}C_4 + A_4 + B_4) + \mu(\delta^{13}C_5 + A_5 + B_5)$$
$$\text{with } \alpha + \beta + \gamma + \varepsilon + \mu = 1$$

Equations 1* and 2* are simplified versions of this equation but, as the results showed, these are too simplified, and do not fully explain the ^{13}C exchanges and losses occurring in bone apatite during calcination. Before trying to solve this global equation (Figure 5.1), there are a few assumptions that can be made:

(a) only 0.04% of the atmosphere is made of carbon dioxide and compared to the quantities of carbon dioxide that will be released by the combustion of fuels and organic matter, this is negligible (Snoeck et al. 2014a) ➔ α → 0;

(b) the carbon dioxide lost from the carbonate fraction of bone apatite during burning will be 'drowned' in the internal combustion atmosphere and is unlikely to 're-enter' bone apatite – unburned bone is made of 30% of collagen and only ca. 3% of carbonates ➔ $B_4 = 0$;

(c) an isotope effect leading to fractionation between carbon dioxide in the combustion atmospheres (internal and external) and bone apatite carbonates will discriminate against heavier isotopes as shown for calcite (Scheele & Hoefs 1992) ➔ $B_2 \leq 0$ and $B_5 \leq 0$;

(d) the contribution of the external organic matter (i.e. skin, flesh, marrow, etc.) can be considered minimal as these will have burned away before bone apatite reaches temperatures at which it starts to exchange carbon dioxide with the combustion atmosphere (> 500°C); additionally, compared to the amount of fuel carbon emitted into the external combustion atmosphere, the amount of carbon emitted by the combustion of the external

organic matter will be marginal as suggested by the radiocarbon results obtained for the fully fleshed pig trotter (P6) ➔ $\gamma \rightarrow 0$;

(e) the collagen, in which bone apatite is embedded will burn off and stay within the internal combustion atmosphere. Since it will burn off completely, no fractionation term has to be considered as all the carbon present in bone collagen will go into the internal combustion atmosphere ➔ $A_5 = 0$;

(f) when fuel burns off, different fractions will burn at different times with fractions made of lighter isotopes burning off first leaving the fraction with more heavy isotopes to burn off later when the bone is hot enough to exchange. This had been observed previously (Turney et al. 2006; Cousin et al. 2008; Hall et al. 2008) ➔ $A_2 \leq 0$;

(g) if an isotope effect leading to fractionation occurs in the carbonate fraction of bone apatite during heating, it is most likely that the lighter isotopes will leave preferentially. The results of the seal bone samples (LAB 3) support this hypothesis ➔ $A_4 \geq 0$;

(h) no negative exchanges are possible ➔ $\beta \geq 0$, $\varepsilon \geq 0$, $\mu \geq 0$;

(i) since temperature changes in time and space during outdoor experiments, all fractionation terms will be considered to be independent from temperature.

The equation can now be simplified to:

$$\delta^{13}C = \beta(\delta^{13}C_2 + A_2 + B_2) + \varepsilon(\delta^{13}C_4 + A_4) + \mu(\delta^{13}C_5 + B_5)$$

$$\text{with } \beta + \varepsilon + \mu = 1;\ A_2 \leq 0; A_4 \geq 0; B \leq 0$$

When considering what happens to the ^{14}C fraction of bone during calcination, another equation can be written:

$$F^{14}C = \beta(F^{14}C_2) + \varepsilon(F^{14}C_4) + \mu(F^{14}C_5)$$

$$\text{with } \beta + \varepsilon + \mu = 1$$

Fractionation terms (A and B) can be neglected. While fractionation has a significant impact on the $\delta^{13}C$ values, fractionation in ^{14}C has minimal impact on the measured radiocarbon dates and at this stage, minimal impact can be ignored (in future research aiming at refining this model, it may be necessary to take such fractionation into account). Furthermore, the radiocarbon age of collagen and bone apatite are identical ➔ $F^{14}C_4 = F^{14}C_5$. The contribution of fuel to the carbon isotope composition of calcined bone apatite (β) can be evaluated using the following equation:

$$\beta = \frac{F^{14}C - F^{14}C_4}{F^{14}C_2 - F^{14}C_4} \quad (1)$$

Assuming ^{13}C and ^{14}C exchanges between fuel and bone apatite carbonates are identical, it is possible to evaluate the proportion of original carbon remaining in bone apatite after calcination (ε) as a function of the potential fractionation occurring between fuel values and the carbon dioxide emitted by the burning of fuel (A_2), the fractionation occurring in bone apatite carbonates (A_4) and the fractionation occurring between the carbon dioxide present in the internal and external combustion atmospheres and the carbon that will enter the carbonate fraction of bone apatite (B_5 and B_2 respectively):

$$\varepsilon(A_2, A_4, B_2, B_5) = \frac{\delta^{13}C - \beta(\delta^{13}C_2 + A_2 + B_2) + (\beta - 1)(\delta^{13}C_5 + B_5)}{A_4 + \delta^{13}C_4 - \delta^{13}C_5 - B_5} \quad (2)$$

To calculate the different carbon contribution it is necessary to evaluation the different potential fractionation terms which is not possible with the data available here but it is possible to restrict the values of these parameters to possible ranges (Table 5.1).

Table 5.1 – Definitions of the various parameters and constraints

Parameters	Definition	Constraints
α	Contribution of atmospheric carbon dioxide	~ 0 %
B_1	Fractionation between atmospheric carbon dioxide and bone apatite carbonates	n/a
β	Contribution of fuel carbon	≥ 0 %
A_2	Fractionation between wood carbon and carbon dioxide emitted by the burning of fuel	≤ 0 ‰
B_2	Fractionation between carbon dioxide emitted by the burning of fuel and bone apatite carbonates	≤ 0 ‰
γ	Contribution flesh, skin and marrow carbon (‘external’ organic matter)	~ 0 %
A_3	Fractionation between organic carbon and carbon dioxide emitted by the burning of flesh, skin and marrow	n/a
B_3	Fractionation between carbon dioxide emitted by the burning of flesh, skin and marrow and bone apatite carbonates	n/a
ε	Contribution of endogenous bone apatite carbon	≥ 0 %
A_4	Fractionation between bone apatite carbonates and carbon dioxide emitted by the heating of bone apatite carbonates	≥ 0 ‰
B_4	Fractionation between carbon dioxide emitted by the heating of bone apatite carbonates and bone apatite carbonates	~ 0 ‰
μ	Contribution of collagen carbon (‘internal’ organic matter)	≥ 0 %
A_5	Fractionation between collagen carbon and carbon dioxide emitted by the burning of collagen	~ 0 ‰
B_5	Fractionation between carbon dioxide emitted by the burning of collagen and bone apatite carbonates	≤ 0 ‰

Looking at the oxygen fraction, and considering that the only possible exchanges occur between bone apatite carbonates and the carbon dioxide present in the combustion atmosphere and the same hypotheses (a), (b), (c), (d), (g), (h), and (i), as for carbon, it is possible to write the following equation:

$$\delta^{18}O = \beta(\delta^{18}O_2 + A_2^* + B_2^*) + \varepsilon(\delta^{18}O_4 + A_4^*) + \mu(\delta^{18}O_5 + B_5^*)$$

$$\text{with } \beta + \varepsilon + \mu = 1$$

However, the oxygen isotope ratios of fuels and collagen ($\delta^{18}O_2$ and $\delta^{18}O_5$ respectively) are unknown and the fractionation terms are most likely to be different for oxygen than for carbon (*), making it very difficult at this stage to evaluate the oxygen exchanges and losses. However, this sets the basic concepts for future research, and being able to monitor the variations in $\delta^{18}O$ values of the combustion atmosphere would greatly help refining this model.

5.3 Impact on the study of archaeological calcined bone

5.3.1 Diagenesis

The infrared results showed that some samples had higher carbonate contents than others (BPI > 0.30). It was suggested that this could be the consequence of the incorporation of exogenous carbonates from the soil as all samples with higher carbonate content originated from high-carbonate marine geological contexts (see Chapter 4). Such marine carbonates are usually significantly enriched in ^{13}C compared to calcined bone apatite ($\delta^{13}C \approx 0$ ‰) and small amounts should be easily detected. However, there is no statistical difference in neither $\delta^{13}C$ values nor $\delta^{18}O$ values between samples with high (BPI > 0.30) and low (BPI < 0.30) carbonate content suggesting that the large concentrations of carbonates are not diagenetic but have to be explained differently.

5.3.2 Radiocarbon dating

From the calculated amount of carbon coming from the combustion of fuels present in calcined bone apatite carbonates (39 to 95%), it appears that there is a very variable but significant intake of carbon from the fuel, the rest of the carbon present originating from the bone apatite itself or bone collagen. Bone apatite and collagen will have very similar if not identical radiocarbon ages ($F^{14}C$) and exchanges between bone apatite and collagen should not affect the radiocarbon dates. However, the exchanges with carbon from the fuel can have

a significant impact on the radiocarbon dates if the fuel and bone are not contemporaneous. Admittedly, in most cases, to burn bone, local contemporaneous wood would be used but if old wood is used, as done here, the dates can be significantly off, and the bone fragments will appear older than they actually are. Similarly, if bone fragments were to be burned dry centuries or millennia after the death of the individual, their age will be partially reset to the age of the fuel used to burn them (Zazzo et al. 2012).

5.3.3 Diets

With the results obtained here, it appears difficult to assess the diet of ancient populations from the carbon isotope composition of calcined bone remains. Indeed, the $\delta^{13}C$ value is much influenced by the $\delta^{13}C$ values of the fuels used and collagen and often there is only very limited amount of original bone apatite carbonates left.

5.3.4 Cremation practices

The various experiments carried out over the last decades together with those realised in this work, showed the complexity and variability of the carbon exchanges occurring in bone apatite during heating. However, it is clear that some information can still be extracted from the carbon and oxygen stable isotope ratios of calcined bone. Among other things, it appears possible to make the different between bone heated without the presence of any additional fuel from bone burned with fuel, the latter having lower $\delta^{13}C$ and $\delta^{18}O$ values (Figure 5.12). However, samples containing cyanamide generally have higher $\delta^{13}C$ values, sometimes even similar to samples heated without fuel. In this case, $\delta^{18}O$ values can be used to make the difference between samples heated without fuel and those presenting high amounts of cyanamide.

6 Conclusion

The carbon present in calcined bone apatite is made of a combination of endogenous, fuel and collagen carbon. The oxygen originates mostly from endogenous carbonates, fuel, collagen and atmospheric oxygen. The proportion in which each of these sources contributes to the composition of calcined bone apatite is extremely varied and, at present, impossible to evaluate in archaeological bone samples. Nevertheless, it appears possible to identify bones with different chemical compositions (e.g. presence of cyanamide) and samples heated in different conditions (e.g. with or without fuel). More specifically the following distinctions can be made: (1) modern samples heated with and without fuel/additives, the former being enriched in both ^{13}C and ^{18}O; (2) samples containing cyanamide have generally higher $\delta^{13}C$ values than those without cyanamide; and (3) samples heated with C_3 and C_4 fuels, the latter being enriched in ^{13}C. In addition to the possibility to discriminate between samples heated in different conditions, these results reinforce the hypothesis made in Chapter 4 that diagenesis is limited on archaeological calcined bone apatite and that, if fuel and bone are of contemporary age, radiocarbon dates will provide reliable results.

Chapter 6 – Heat influences on strontium isotopes and diagenesis

1 Introduction

This chapter concerns itself with the effects of heating on the strontium isotope composition of bone apatite and with the potential post-burial losses and exchanges of strontium between bone apatite and its burial environment. The principle aim is to assess the reliability of strontium isotope measurements carried out on archaeological cremated remains. The strontium isotope composition of calcined bone has been little studied. Here the topic is addressed by means of a model for strontium losses and exchanges during cremation and after burial, and an experimental study that compares the uptake of an artificially enriched strontium solution between enamel and cremated bone.

Previous studies (i.e. Harbeck et al. 2011; Harvig et al. 2014) hint at the potential for reliable $^{87}Sr/^{86}Sr$ measurements on calcined bone, but both leave unanswered questions: is there any exchange of strontium between calcined bone and its surrounding environment, either during the burning process itself (as has been demonstrated for carbon and oxygen – see Chapter 5), or during a subsequent exchange in the burial environment? This gap is addressed in this chapter.

2 Model for strontium isotopic exchanges and losses during and after calcination

No strontium isotopic fractionation should be expected during the heating of bone as the relative atomic mass difference between the two strontium isotopes (^{87}Sr and ^{86}Sr) is low and observable fractionation during biochemical transformations is implausible. Furthermore, the

melting point of strontium carbonate is around 1500ºC, much higher than the temperatures reached during cremation and so strontium is unlikely to volatilize from bone apatite either. However, it is more likely that there is an intake and/or exchange of strontium between bone apatite and its surrounding environment once buried. Nevertheless, because of the higher crystallinity of calcined bone apatite (see Chapter 4), it is hypothesised here that any such alteration will occur to a much lower extent than in unburned bone. Since enamel is considered to provide results reflecting the original strontium isotope composition because of its higher crystallinity and higher resistance to diagenetic changes, cremated bone apatite should also likewise provide reliable results.

Nevertheless, crystallinity is not the only factor that has to be taken into account; porosity also should be considered. Tooth enamel is compact and has a low porosity while both burned and unburned bone are much more porous. Many cavities are left unfilled after cremation due to the combustion and disappearance of collagen. This leads to a much higher contact surface between bone apatite and its surrounding environment, which could potentially increase the strontium intake and/or exchange (Hedges & Millard 1995). An exchange/intake model for strontium is detailed in Figure 6.1.

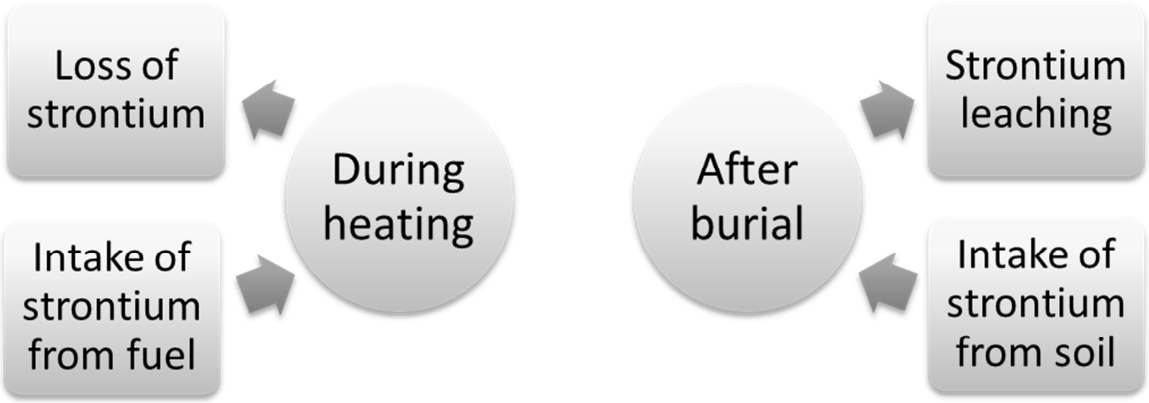

Figure 6.1 – Model for strontium losses and intakes during heating and after burial

3 Experimental design

To assess the reliability of the strontium isotope measurements obtained from calcined bone, a series of experiments were designed. Although it is recognised that the exchange of strontium in the fuel with bone during burning is remote, experiments were carried out as a check. One fragment of cow tibia was heated in a laboratory muffle furnace and another was burned on an open wood fire of known isotope composition. If the strontium isotope ratios of both samples are identical (within measurement error), it can be inferred that no exchange occurred between bone and wood during heating.

To study the potential exchange/intake of strontium from the surrounding depositional environment of buried calcined bone, several fragments of the same calcined cow tibia were immersed in a ^{87}Sr-enriched solution at room temperature for up to twelve months. The '^{87}Sr-spiked' solution used in the experiment is more enriched than any existing in the natural world by many orders of magnitude, and so it can be thought of as greatly speeding up the process of artificial contamination. In parallel, horse tooth enamel fragments were placed in the same solution. The samples were also monitored using infrared spectroscopy to observe any compositional or structural modifications due to the immersion of calcined bone in the ^{87}Sr-enriched solution. A new pre-treatment protocol aiming at removing strontium contamination from cremated bone using acetic acid and ultrasonication was developed.

Immersing pieces of calcined bone in an ^{87}Sr-enriched solution for a maximum of twelve months is not representative of real burial conditions lasting centuries or millennia. However, several field and experimental studies have found that uptake of strontium in unburned bone is rapid (e.g. Tuross et al. 1989). The use of enamel as a comparison follows the argument that if the behaviour of calcined bone in this 'artificial' environment is similar to tooth enamel, then calcined bone should be considered to be at least as reliable as tooth enamel for strontium isotope determinations.

4 Materials and methods

4.1 Samples

A modern horse tooth was selected for the immersion experiments. The dentine was mechanically removed using a micro-drill and enamel flakes were collected. The calcined bone fragments were obtained by burning a cow tibia on an outdoor wood fire. In both cases, fragments were collected for the immersion experiments without crushing. For the infrared measurements by Fourier Transform Infrared Spectroscopy in Attenuated Total Reflectance mode (FTIR-ATR), calcined bone powder from the same cow tibia heated in a muffle furnace was used. Aliquots of powder were also immersed in the enriched solution.

4.2 Enriched solution

An ^{87}Sr-enriched solution was made using strontium carbonate of certified composition (reference: MSR87C) obtained from Euriso-top (www.eurisotop.com). This carbonate contained mainly ^{87}Sr (89.7%) and only a small amount of ^{86}Sr (0.98%), with a strontium isotope ratio of 91.53061. A solution was made using milliQ water and 11 mg/L of this strontium carbonate, homogenized by ultrasonication. Several fragments of calcined bone and tooth enamel of c. 100 mg were placed into tubes and immersed in 10 mL of solution for 15 days, 1, 3, 6, 9 and 12 months.

The sample to solution ratio was chosen to ensure that the maximum variation in isotopic ratio would be around 30% between uncontaminated and immersed sample. The strontium concentration of the calcined bone used here is around 150 ppm, and in 100 mg of calcined bone there is approximately 0.015 mg of strontium. In 10 mL of solution there is 0.011 mg of strontium carbonate or c. 0.0065 mg of strontium. This facilitates the observation of the isotopic variations and avoids the complete overwriting of the original signal by the enriched solution.

4.3 Sample pre-treatments

The most common pre-treatments for isotopic analyses of enamel are the mechanical removal of the external layers of enamel following the idea that diagenesis should be restricted to the surface of the teeth in contact with soils (e.g. Evans et al. 2006), or successive acid leaching on crushed sample (e.g. Hoppe et al. 2003). Sillen et al. (1998), for example, used buffered 0.1M acetic acid on crushed samples and ultrasonication for 1 min and repeated this twenty times. Mechanical procedures are not possible on calcined bone as they cause the sample to disintegrate, while consecutive acid leaching on crushed calcined bone sample leads to its complete loss. Here, we based the pre-treatment protocol on the procedure using acetic acid. I use 1M acetic acid (as used for radiocarbon dating of calcined bone – Brock et al. 2010b) and ultrasonication on uncrushed samples but omitted the subsequent leaching steps.

After immersion, the tooth enamel and calcined bone samples were rinsed three times with milliQ water for 10 min in an ultrasonication bath. The samples were then divided into two 50 mg fractions. One fraction was treated with 1M acetic acid (1 mL per 10 mg of sample) for 3 min in an ultrasonic bath, followed by three rinses with milliQ water and 10 min ultrasonication. The other fragments did not undergo any further treatment. All samples were then dried in a freeze-dryer overnight. The limit of three minutes in the ultrasonication bath was chosen in order to limit sample loss observed when treating calcined bone fragments. Three sub-samples of enamel were also ultrasonicated for 30 minutes in acetic acid.

4.4 Strontium isotope composition and FTIR

The infrared equipment, the entire acid digestion process and subsequent Sr purification as well as the measurements on a Nu plasma MC-ICP-MS were carried out using NBS987 as standard as detailed in Chapter 3.

5 Results

5.1 Intake of strontium from the fuel

When the strontium isotope compositions measured for a cow tibia fraction calcined in a muffle furnace are compared to those obtained for a fraction of the same bone burned on a wood pyre of different isotope compositions (Table 6.1), no significant difference is observed. The results, while not conclusive since the experiment was carried out only on two samples, suggest that there is no detectable exchange of strontium with the fuel.

Table 6.1 – Strontium isotope ratio for calcined cow tibia heated in different conditions and the wood used for the outdoor fire

Sample	$^{87}Sr/^{86}Sr$ (± 2σ*)
Cow tibia heated in muffle furnace	0.710306 ± 11
	0.710323 ± 14
	0.710291 ± 16
	0.710303 ± 10
Cow tibia heated on outdoor wood pyre	0.710321 ± 8
	0.710394 ± 10
Wood used for outdoor fire	0.708519 ± 7

*2σ has been calculated following the equation: 2 x mean of the 60 ratio measurements x standard error

5.2 Exchanges and losses of strontium after burial

Isotope ratios were measured on the samples immersed in the ^{87}Sr-enriched solution before and after treatment with acetic acid and ultrasonication (Table 6.2). The percentage variations between uncontaminated and immersed samples (Table 6.3) are calculated as follows:

$$\Delta^{87}Sr/^{86}Sr\,(\%) = \frac{soaked - unsoaked}{enriched\ solution - unsoaked}$$

5.3 Simulation

In the experiment, the burial environment is replaced by a spiked solution with a $^{87}Sr/^{86}Sr$ value higher than 90. Most soils would be characterized by $^{87}Sr/^{86}Sr$ values between 0.70 and 0.75 (GEOROC). Considering the most extreme case of an individual having an original isotope ratio of 0.70 buried in a soil having a value of 0.75 and taking into account the isotopic changes measured experimentally (Table 6.3), the effect of strontium exchange between sample and soil have been simulated (Table 6.4) using the following equation:

$$Simulated\ ^{87}Sr/^{86}Sr = 0.70 + \%_{calculated\ (Table\ 6.3)} * (0.75 - 0.70)$$

The simulated variations in enamel, after a 3 minute treatment with acetic acid and ultrasonication, are still significant and shifts of up to 0.00672 are observed, while for treated calcined bone, the largest offset is 0.00103. This is more than six times less than seen in enamel and usually below the limit of interpretation generally accepted in archaeological contexts.

5.4 Infrared spectra

The spectra obtained for uncontaminated enamel and calcined bone (Figure 6.2a) show that the carbonate band is higher in enamel than in calcined bone. This to be expected as substituted carbonates are significantly reduced in heated bone, while hydroxyl groups increase (see Chapter 4). At the same time, crystallinity increases, as reflected in the infrared splitting factor (IRSF). The calculated IRSF is lower in enamel (3.30) than in calcined bone (5.45). The infrared spectra of the calcined samples exposed to the enriched strontium isotope solution (Figures 6.3b and c) indicate the appearance and increasing intensity with time of a band at c. 3690 cm^{-1}. No variations in IRSF and the OH band at 3580 cm^{-1} are observed.

Table 6.2 – Strontium isotope ratio for horse enamel and calcined cow bone immersed in the enriched solution

$^{87}Sr/^{86}Sr$ (± 2σ*)	Time (months)						
	0	**0.5**	**1**	**3**	**6**	**9**	**12**
Untreated enamel	0.70877 ± 1	7.25861 ± 102	11.86877 ± 128	12.25365 ± 127	18.11921 ± 366	14.42634 ± 230	16.48228 ± 649
Treated enamel (3 min)		5.75578 ± 52	9.10461 ± 80	6.18321 ± 46	12.92154 ± 192	10.73395 ± 86	13.88819 ± 342
Treated enamel (30 min)		5.56857 ± 23	4.03884 ± 23	3.66933 ± 13	n/a	n/a	n/a
Untreated calcined bone	0.71036 ± 1	6.12693 ± 31	7.38861 ± 50	5.71230 ± 25	8.15062 ± 71	5.38431 ± 29	8.69744 ± 252
Treated calcined bone		0.89179 ± 1	0.96404 ± 1	0.84011 ± 1	1.21357 ± 2	0.82947 ± 2	2.58847 ± 82

*2σ has been calculated following the equation: 2 x mean of the 60 ratio measurements x standard error

Table 6.3 – Percentage variations between uncontaminated and immersed samples for horse enamel and calcined cow bone

$\Delta^{87}Sr/^{86}Sr$ (%)	Months					
	0.5	**1**	**3**	**6**	**9**	**12**
Untreated enamel	7.2%	12.3%	12.7%	19.2%	15.1%	17.4%
Treated enamel (3 min)	5.6%	9.2%	6.0%	13.4%	11.0%	14.5%
Treated enamel (30 min)	5.4%	3.7%	3.3%	n/a	n/a	n/a
Untreated calcined bone	6.0%	7.4%	5.5%	8.2%	5.1%	8.8%
Treated calcined bone	0.2%	0.3%	0.1%	0.6%	0.1%	2.1%

Table 6.4 – Simulation of the strontium isotope ratio for enamel and calcined bone in 'natural' conditions considering an individual having an original isotopic ratio of 0.70 buried in a soil having a value of 0.75 and taking into account the isotopic changes measured experimentally (Table 6.3)

$^{87}Sr/^{86}Sr$	Months						
	0	**0.5**	**1**	**3**	**6**	**9**	**12**
Untreated enamel	0.70000	0.70361	0.70614	0.70636	0.70958	0.70755	0.70868
Treated enamel (3 min)		0.70278	0.70462	0.70301	0.70672	0.70552	0.70726
Untreated calcined bone		0.70298	0.70368	0.70275	0.70410	0.70257	0.70440
Treated calcined bone		0.70010	0.70014	0.70007	0.70028	0.70007	0.70103

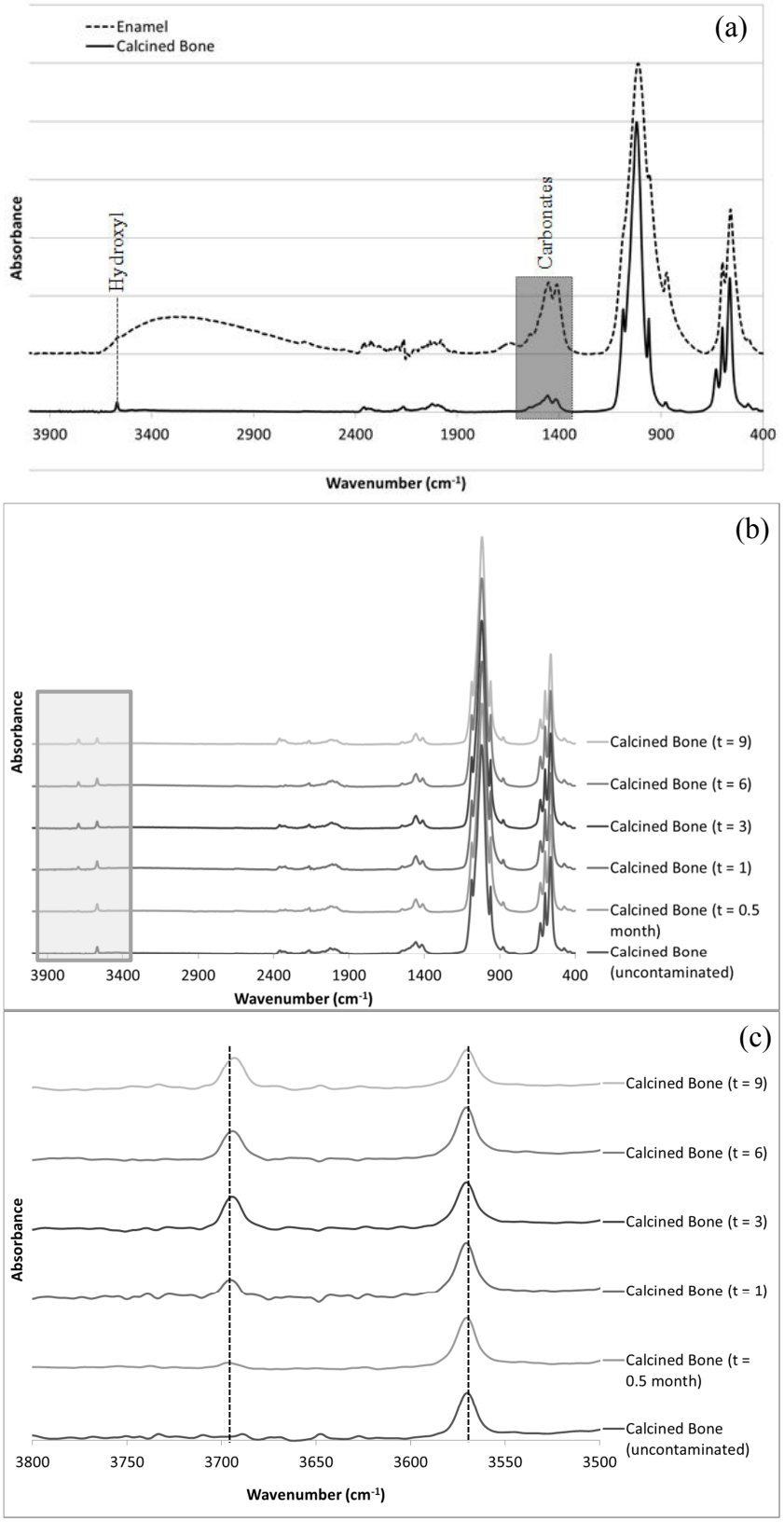

Figure 6.2 – (a) Infrared spectra of enamel and calcined bone highlighting the bands specific to hydroxyl groups and carbonates; (b) Infrared spectra of uncontaminated calcined bone and calcined bone immersed in strontium enriched solution for 0.5, 1, 3, 6 and 9 months; the grey shaded are highlights the appearance of a band at c. 3690 cm^{-1}; (c) Zoom on the infrared spectra of uncontaminated calcined bone and calcined bone immersed in strontium enriched solution for 0.5, 1, 3, 6 and 9 months; this shows the appearance of a band at c. 3690 cm^{-1} in calcined bone immersed in the enriched solution

6 Discussion

The changes in $^{87}Sr/^{86}Sr$ with immersion time as well as the differences between untreated and treated samples (Figure 6.3) show a rapid change in isotope composition during the first month of immersion, after which the increase is slower. The variation is higher in enamel (up to 19%) than in calcined bone (up to 8.2%). After treatment with acetic acid, the isotopic variation is very low in calcined bone (≤ 2.1%) but remains high in enamel (between 5 and 15%). When ultrasonicated for 30 minutes, the variation in tooth enamel falls to between 3 and 6%, still higher than in treated calcined bone.

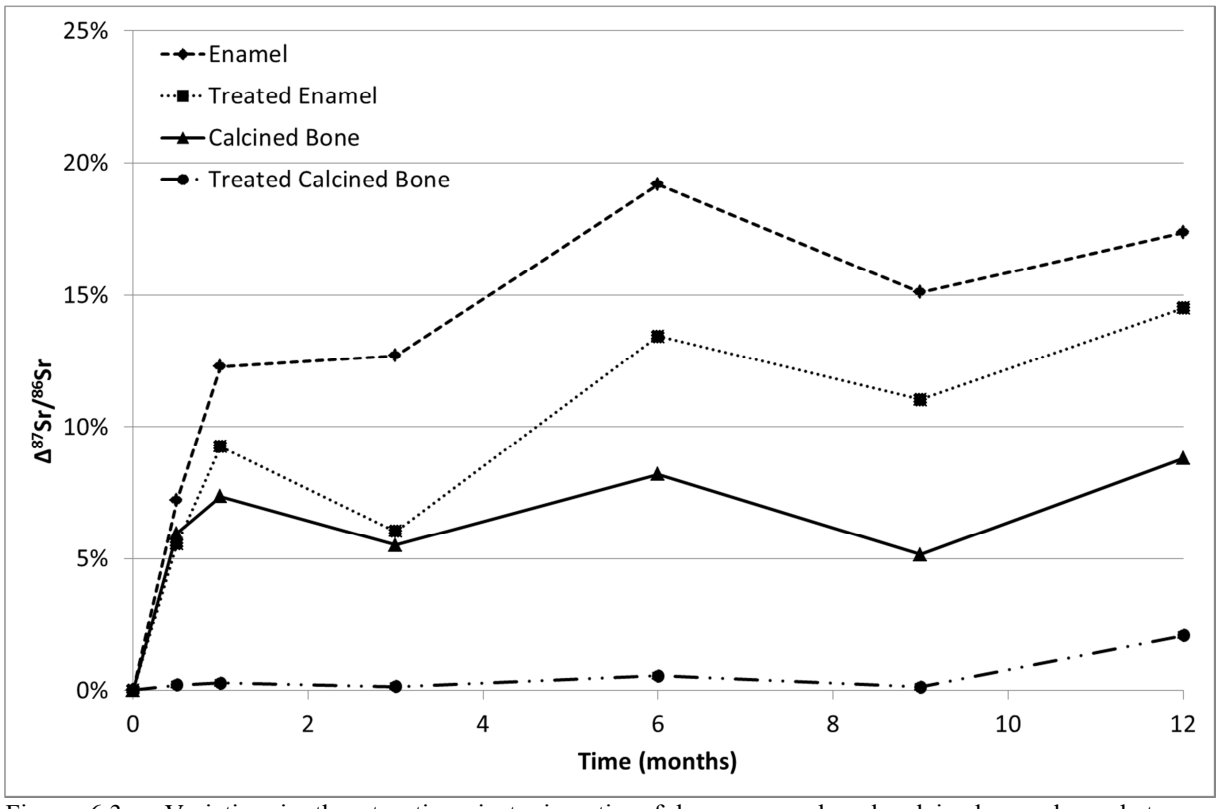

Figure 6.3 – Variation in the strontium isotopic ratio of horse enamel and calcined cow bone between uncontaminated and immersed in the enriched solution

The exogenous strontium could be either adsorbed onto the surface of the crystallites or incorporated into the crystallites themselves. The initial intake in the first month is so rapid that it suggests adsorption of strontium onto the crystallites at the surface of the bone

fragment followed (possibly) by slower adsorption/incorporation of strontium onto the crystallites present deeper into the bone fragment. The rapid adsorption at the surface of bone is similar to that describe in the medical experiments of Dahl et al. (2001). Since after pre-treatment with acetic acid and ultrasonication, the amount of exogenous strontium is minimal in calcined bone it is most likely to have been only adsorbed and not incorporated into the crystal structure. However, in the case of enamel, a significant amount of exogenous strontium remains after treatment with acetic acid suggesting that some exogenous strontium was incorporated into the crystal structure. This is not altogether surprising, given that the infrared spectra of calcined bone and enamel show that calcined bone has a much higher IRSF, suggesting higher crystallinity. This result suggests that crystallinity of the calcified tissue plays a more important role in post-burial alterations than porosity. Porosity may be important for initial passage of strontium ions into the interstices of calcined bone, but the data suggests that enhanced crystallinity prevents or greatly inhibits its incorporation into the crystal structure. The results suggest that, even in the extreme conditions in which our experiments were carried out, calcined bone is highly resistant to the enriched, exogenous strontium and that the impact of external strontium on the *in vivo* strontium isotope ratio is minimal once calcined bone fragments have been properly pre-treated.

The reasons for the appearance of a band at c. 3690 cm^{-1} in the infrared spectra of the samples immersed in the enriched solution are still unclear. It could be that this band is characteristic of hydroxyl groups in strontium-rich calcium apatites. However, that band was not observed in strontium-rich hydroxyapatite crystals (Li et al. 2007).

In summary, the results for the experiments demonstrate that there is no significant change in the $^{87}Sr/^{86}Sr$ composition of bone during heating. This result is consistent with previous research (Harbeck et al. 2011; Harvig et al. 2014). It also appears that calcined bone is resistant to post-burial exchanges and retains its original *in vivo* strontium isotope ratio.

Furthermore, it is clear that calcined bone is less affected than enamel by the presence of strontium in the burial environment, which is the consequence of calcined bone being more crystalline than enamel and so more resistant to strontium incorporation into its mineral structure. Furthermore, once treated with acetic acid and ultrasonication, the isotopic variation observed is minimal in calcined bone while still significant in enamel.

7 Archaeological implications

The ability to obtain $^{87}Sr/^{86}Sr$ ratios from calcined bone will enable the study of mobility of humans to times and places where cremation is the main funeral rite or where the soils are so acidic that only calcined bone survives, and also the provenance and habitats of animals found at sites where only burned bone survives. Forensic science can also benefit from these results since it is now possible to investigate provenance for individuals that were burned in accidental or intentional fires.

It is important to recognise that $^{87}Sr/^{86}Sr$ studies on calcined bone differ in an important respect from those on enamel. In the latter, the sequential development of the dentition and the lack of any subsequent changes in the chemical structure of the tooth crown enable a 'life history' approach. Thus, in humans, measurements of enamel on the first molar reflect place of residence during infancy, while the third molar records residency during later childhood and early adolescence (Ubelaker 1989). Bone, by contrast, undergoes remodelling once formed, though the rates at which this occurs once skeletal maturity has been attained are still unclear (Dempster 1999; Hedges et al. 2007; Robins & New 1997). Thus, $^{87}Sr/^{86}Sr$ measurements reflect a long-term average, probably those of the last decade or so of an individual's life. Where recovery of cremated material from distinct individuals is good, it should be possible to follow a similar life history approach by analysing the optic capsule of

the petrous bone, which forms in the first two years of life and, unlike the rest of the skeleton, does not appear to remodel subsequently (Jørkov et al. 2009; Harvig et al. 2014).

8 Conclusion

This study clearly demonstrates that calcined bone provides at least as reliable strontium isotope results as tooth enamel. This finding opens the door to the use of calcined bone fragments in mobility studies in both archaeological and forensic contexts. Furthermore, the results provide additional information about the process of adsorption/incorporation of strontium. While porosity allows strontium to penetrate within the sample and be adsorbed onto the surface of crystallites within the sample, it appears that the high crystallinity of these crystallites prevents the strontium from being incorporated into the crystallites themselves showing that crystallinity plays a major role in the susceptibility of a sample to undergo post-burial alterations while porosity does not.

Chapter 7 – Mapping the biologically available strontium isotopes in Ireland

1 Introduction

In order to study the mobility of ancient human and animal populations based in their strontium isotope ($^{87}Sr/^{86}Sr$) composition, it is first necessary to determine the distribution of strontium isotopes in the local landscapes. In particular it is necessary to evaluate the distribution of biologically available strontium isotopes, since mammalian strontium intake is primarily derived from the foodweb. As detailed in Chapter 2, the strontium present in biological system primarily derives from the underlying geology but also from other sources (e.g. precipitations, groundwater, etc.). It is therefore difficult to evaluate the biologically available strontium (BASr) using the strontium isotope data available for bedrocks. It has been shown that, with suitable caution, the BASr can be evaluated using modern plant samples (Evans et al. 2009; 2010; Hartman & Richards 2014). Indeed, plants represent a major source of biologically available strontium, and studies have shown that they both reflect and moderate the $^{87}Sr/^{86}Sr$ composition of the local bedrock geology (Sillen et al. 1998).

This chapter presents BASr maps for Ireland, where the archaeological sites studied in this thesis are located. It describes the experimental design developed to create the BASr maps, based in the first instance on the geology of Ireland, describes the sampling strategy and presents results as two different maps.

2 Irish Geology

The bedrock geology of Ireland is mainly composed of Palaeozoic rocks (251–542 Ma) with few Mesozoic outcrops (65–251 Ma) and a large tertiary volcanic basalt lava outcrop (c. 60

Ma) in the northeast of the Island (co. Antrim) (Holland & Sanders 2009). A detailed geological map combining the results of the Geological Survey of Ireland (GSI) and the Geological Survey of Northern Ireland (GSNI) reveals the presence of 83 different geological types across the island (Figure 7.1). The superficial geology is composed, among other things, of peat bogs and glacial till originating mostly from the last deglaciation around 12,000 BC. Most of Ireland was covered by an ice sheet during that period (GSI; Clark et al. 2012) but peat is mostly present in the western and central parts of the Island (Hammond 1978; Connolly et al. 2007).

3 Experimental design

The difference observed between the strontium isotope compositions of the biosphere and the underlying bedrock geology (e.g. Sillen et al. 1998) showed the importance of evaluating the biologically available strontium isotope composition around the studied archaeological sites to understand the variations observed in archaeological animal and human remains. The strontium isotope composition of the biosphere will be primarily influenced by the local bedrock geology; geological maps can therefore be used as a template to create boundaries between 'regions' that will have different biologically available strontium isotope compositions.

To create a map of the BASr for Ireland, I based my experimental design on the work done to create the BASr map for Britain (Evans et al. 2009; 2010). While sampling small mammal tooth enamel (modern or archaeological) is preferable, as they present a sampling of the local vegetation, it is not always possible (see Chapter 2) and here, only plant samples were collected to determine the BASr in Ireland.

3.1 Plant sampling strategy

Several considerations have to be kept in mind when sampling modern plants to establish the BASr of a particular area. It is important to avoid artificially fertilised fields as fertilisers and pesticides may contain strontium contamination. In river plain, sediments are likely to reflect a mixture from the different source areas, and close to the sea, there may be a sea spray effect. Additionally, plants only sample the strontium available for their own roots (i.e. micro habitat) and have different rooting depths which may impact on their strontium isotope composition depending, among other things, on the superficial geology (e.g. presence of peat bog). Furthermore, in regions with high topography, erosion should be taken into considerations.

In the frame of this work, most of these considerations were taken into account and, when possible, samples were taken as far away from fertilised fields (i.e. natural reserves, forests, etc.). To avoid sampling 'micro habitats', different plant samples were taken at each site and, when present, grass, shrub and tree samples were taken; where possible, leaves/branches from three different shrubs/trees were taken. The impact of the presence of peat bogs and sea spray effect on the strontium isotope composition of plants was also investigated. Nevertheless, even when trying to avoid contamination, it is not entirely possible, and possible outliers have to be detected.

3.2 Creation of BASr maps using ArcGIS

Two maps were then created using a Geographic Information System (ArcGIS 10.2 coupled with Geostatistical Analyst) with the help of John Pouncett (Spatial Technology officer of the School of Archaeology, University of Oxford). Areal interpolation (Krivoruchko et al. 2011) was based on the geological outcrops of the bedrock geological map (1:500.000 from GIS public data). The creation of the first map follows the steps of Evans et al. (2010) in which all $^{87}Sr/^{86}Sr$ values measured for a same geological formation (rock type) are averaged (multi-

part – one ‘polygon’ per rock type). For the second map, only the values obtained for a single geological outcrop are averaged. In other word, two outcrops having the same geology but being separated by another outcrop are considered to be independent entities (single-part – one ‘polygon’ per outcrop). The latter map avoids the simplification that the underlying bedrock geology is the only controlling factor of the BASr. Considering each outcrop individually allows factors such as variable rainfall and superficial geology to be taken into account. The selection of the classes (or ranges) is based on geometric intervals for single-part features.

3.3 Summary of the experimental design

The following steps will be followed to create the two different BASr maps for Ireland:

1. Sampling plant samples following the strategy detailed above, and measuring their $^{87}Sr/^{86}Sr$
2. Detect potential outliers
3. Compare the values obtained with those from Britain (Evans et al. 2010)
4. Detect the potential impact of the presence of peat bog and the sea spray effect
5. Create both BASr maps using ArcGIS as detailed above

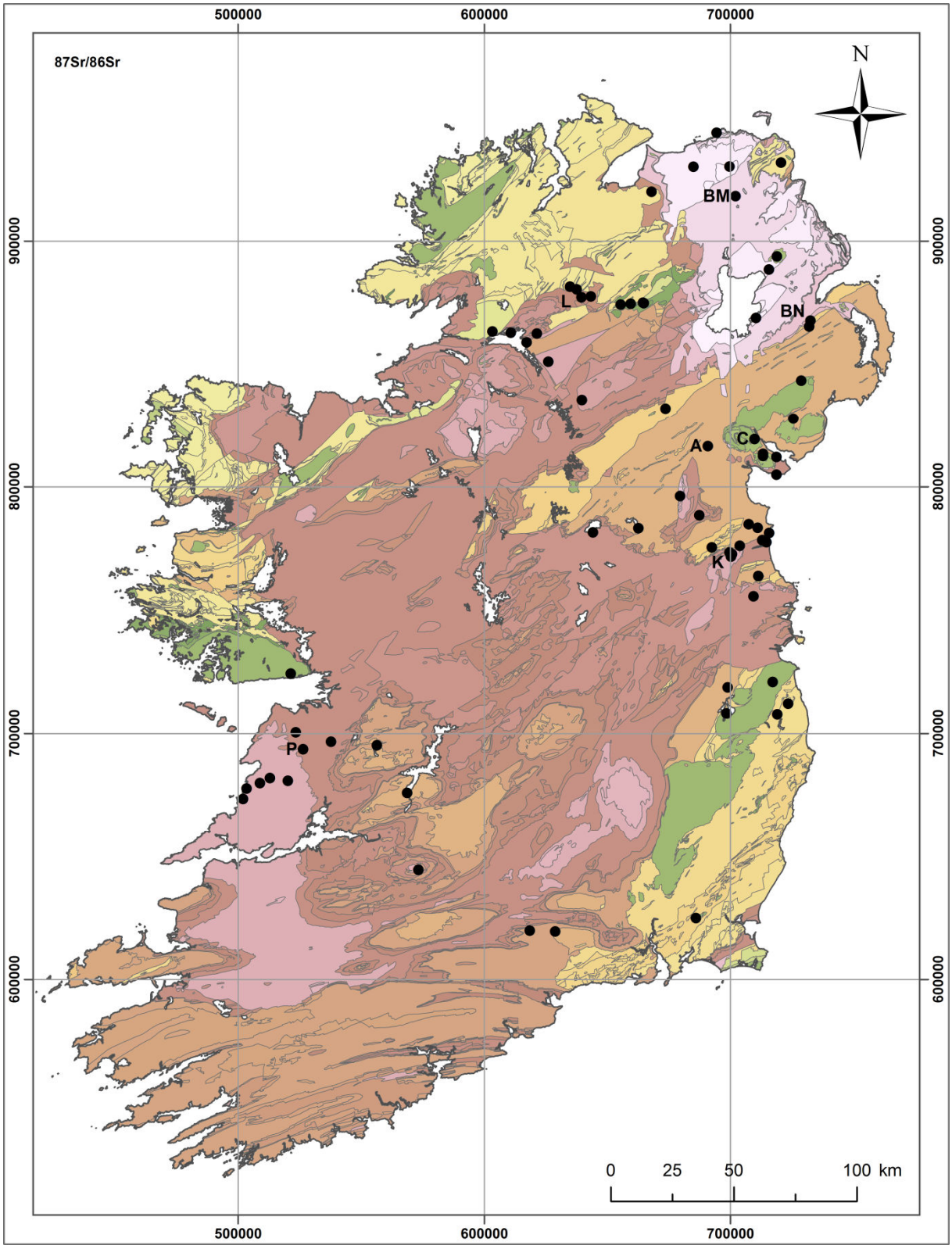

Figure 7.1 – (a) Bedrock geological map of Ireland (1:500.000 – GIS public data) highlighting the locations of the sites were plants samples were collected from; archaeological sites studied here are also included: A – Annaghmare; BM – Ballymacaldrack; BN – Ballynahatty; C – Clontygora; K – Knowth; L – Legland; P – Parknabinnia; (b) colour key

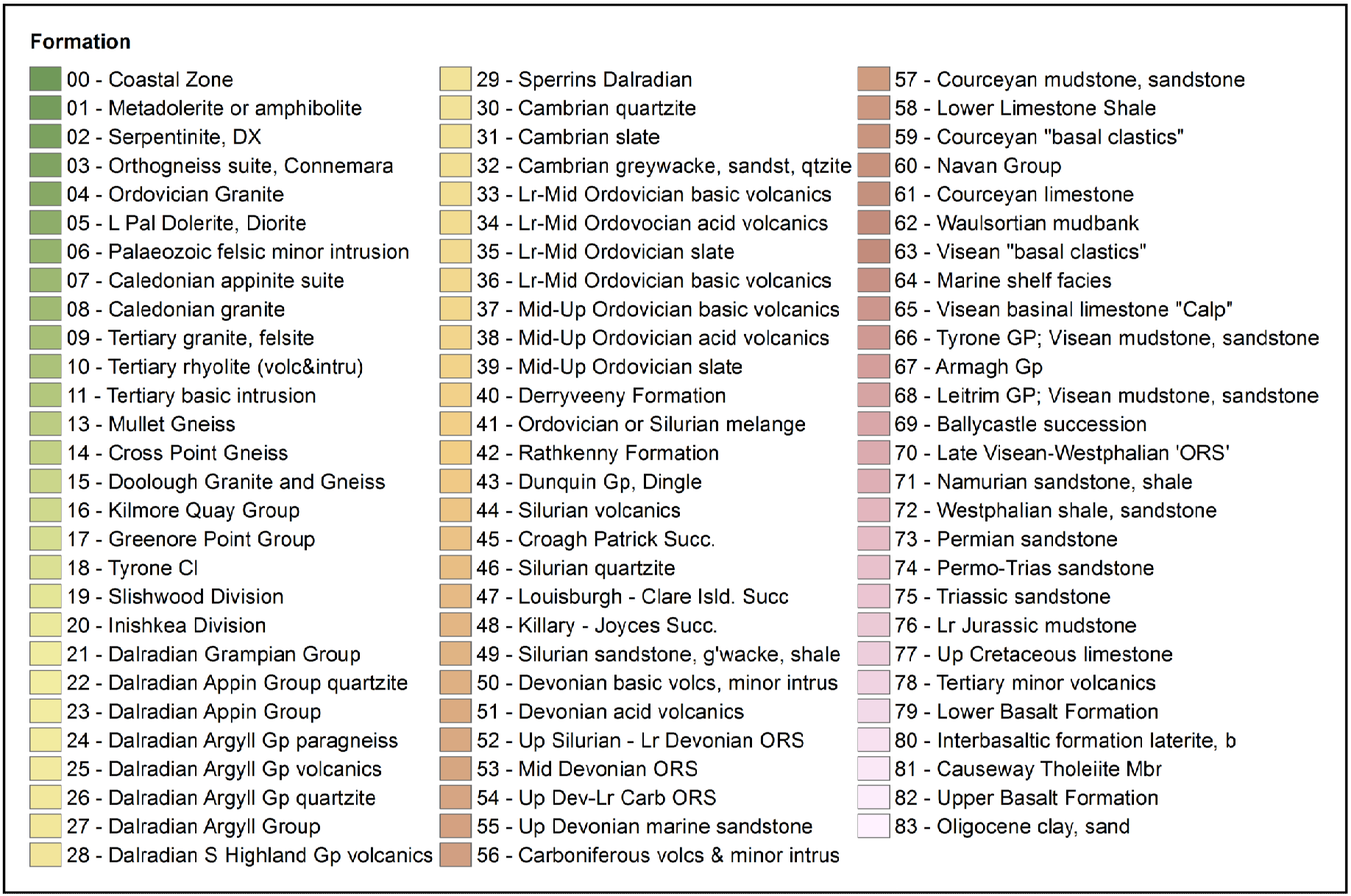
Formation
00 - Coastal Zone
01 - Metadolerite or amphibolite
02 - Serpentinite, DX
03 - Orthogneiss suite, Connemara
04 - Ordovician Granite
05 - L Pal Dolerite, Diorite
06 - Palaeozoic felsic minor intrusion
07 - Caledonian appinite suite
08 - Caledonian granite
09 - Tertiary granite, felsite
10 - Tertiary rhyolite (volc&intru)
11 - Tertiary basic intrusion
13 - Mullet Gneiss
14 - Cross Point Gneiss
15 - Doolough Granite and Gneiss
16 - Kilmore Quay Group
17 - Greenore Point Group
18 - Tyrone Cl
19 - Slishwood Division
20 - Inishkea Division
21 - Dalradian Grampian Group
22 - Dalradian Appin Group quartzite
23 - Dalradian Appin Group
24 - Dalradian Argyll Gp paragneiss
25 - Dalradian Argyll Gp volcanics
26 - Dalradian Argyll Gp quartzite
27 - Dalradian Argyll Group
28 - Dalradian S Highland Gp volcanics
29 - Sperrins Dalradian
30 - Cambrian quartzite
31 - Cambrian slate
32 - Cambrian greywacke, sandst, qtzite
33 - Lr-Mid Ordovician basic volcanics
34 - Lr-Mid Ordovocian acid volcanics
35 - Lr-Mid Ordovician slate
36 - Lr-Mid Ordovician basic volcanics
37 - Mid-Up Ordovician basic volcanics
38 - Mid-Up Ordovician acid volcanics
39 - Mid-Up Ordovician slate
40 - Derryveeny Formation
41 - Ordovician or Silurian melange
42 - Rathkenny Formation
43 - Dunquin Gp, Dingle
44 - Silurian volcanics
45 - Croagh Patrick Succ.
46 - Silurian quartzite
47 - Louisburgh - Clare Isld. Succ
48 - Killary - Joyces Succ.
49 - Silurian sandstone, g'wacke, shale
50 - Devonian basic volcs, minor intrus
51 - Devonian acid volcanics
52 - Up Silurian - Lr Devonian ORS
53 - Mid Devonian ORS
54 - Up Dev-Lr Carb ORS
55 - Up Devonian marine sandstone
56 - Carboniferous volcs & minor intrus
57 - Courceyan mudstone, sandstone
58 - Lower Limestone Shale
59 - Courceyan "basal clastics"
60 - Navan Group
61 - Courceyan limestone
62 - Waulsortian mudbank
63 - Visean "basal clastics"
64 - Marine shelf facies
65 - Visean basinal limestone "Calp"
66 - Tyrone GP; Visean mudstone, sandstone
67 - Armagh Gp
68 - Leitrim GP; Visean mudstone, sandstone
69 - Ballycastle succession
70 - Late Visean-Westphalian 'ORS'
71 - Namurian sandstone, shale
72 - Westphalian shale, sandstone
73 - Permian sandstone
74 - Permo-Trias sandstone
75 - Triassic sandstone
76 - Lr Jurassic mudstone
77 - Up Cretaceous limestone
78 - Tertiary minor volcanics
79 - Lower Basalt Formation
80 - Interbasaltic formation laterite, b
81 - Causeway Tholeiite Mbr
82 - Upper Basalt Formation
83 - Oligocene clay, sand

4 Plant samples

Modern plant samples were collected from about 70 sites (Figure 7.1) selected based on the underlying bedrock geology. Samples were taken from as many different geological contexts as possible focussing mostly on the regions around the archaeological sites studied in this work. GPS coordinated were recorded for each site (Appendix 6.9). Of the 83 geological formations present on the island of Ireland, 28 were sampled. These 28 geological types are amongst the most common around the archaeological sites studied in this work and in Ireland in general (e.g. Carboniferous limestone Formations 64 and 65 cover most of central Ireland – see Figure 7.1 and Table 7.2).

Before analyses, the plant samples were dried naturally and crushed in a coffee grinder. When samples were taken from three different shrubs/trees at a particular site, all three were crushed together in the coffee grinder. The samples were then ashed in a muffle furnace by step-heating from 200 to 650–700°C. The entire acid digestion process and subsequent strontium purification of the plant samples as well as the measurement of their isotope composition on a Nu Plasma MC-ICP-MS were carried out using NBS987 as standard as detailed in Chapter 3.

5 Results

The $^{87}Sr/^{86}Sr$ values of the plant samples (Appendix 6.9) were used to create a map of the biologically available strontium following the experimental design detailed above.

5.1 Outliers

If six or more $^{87}Sr/^{86}Sr$ values were available for a single outcrop, that outcrop was statistically analysed as an individual entity for the detection of outliers. If less than six values were measured, these were compared to those of each outcrops of the same rock type

(Formations 59 and 63 were considered as one single formation for the detection of outliers). Any samples being three standard deviations or more from the average value (calculated excluding the potential outlier) was considered as an outlier. Following that rationale, 11 of the 158 samples (ca. 7%) were considered as outliers (red values in Appendix 6.9).

5.2 Variation between different plant samples

For a single outcrop, after removal of outlier, the highest variation was found in granitic formations of the Mourne Mountains (Formation 9 – Table 7.1). This is no altogether surprising as granites (whole rocks) usually exhibit a wide range of $^{87}Sr/^{86}Sr$ values which was shown for the Mourne Mountains (Meighan et al. 1988). Very low variations are found in limestone formations (Formations 64 and 65). When comparing average values obtained for different outcrops of the same formation type, difference also appear confirming that the underlying bedrock geology is not the sole factor impacting on the BASr values.

Table 7.1 – Selection of $^{87}Sr/^{86}Sr$ values for plant samples of particular outcrops and calculated averages

Sites (per outcrop)	**$^{87}Sr/^{86}Sr$ values**	**Average**
Formation 9 –Tertiary (Palaeogene) granite, felsite and granophyre (23–65 Ma)		
I94	0.7126 0.7140 0.7164	0.7143
I95	0.7111 0.7195	0.7153
A18 (C)	0.7103 0.7130	0.7117
Formation 64 – Carboniferous marine shelf facies; Limestone & calcareous shale (299–359 Ma)		
A12	0.7082 0.7083	0.7082
I51, I97, I98 (P)	0.7083 0.7084 0.7085 0.7087 0.7088 0.7090	0.7086
I22	0.7095 0.7097	0.7096
Formation 65 – Carboniferous Visean basinal limestone; Marine basinal facies (Tobercolleen and Lucan Formations); Dark-grey argillaceous and cherty limestone & shale (299–359 Ma)		
I26	0.7092 0.7096	0.7094
I28, I37	0.7082 0.7083 0.7089	0.7085

The results presented in Table 7.1 for granitic and limestone formations show that, even though, higher variation is observed in the values measured on plants samples from the

granitic formations, all the samples from granitic formation have higher values than those from the limestone formations. This highlights the possibility that values measured in human and animal remains may exhibit different strontium isotope composition based on the origin of their food, and that mobility studies in Ireland based on strontium isotopes should be possible. Table 7.2 contains more data regarding the differences between different outcrops and different geological formations.

Comparing the values obtained for different plant types (grass, shrub and trees) from the same site, no tendency could be observed. Variations seem linked to the geological formations and not to plant type with high variations observed in granitic formations and almost no variation in limestone formations.

5.3 Comparison of the results with those from the UK

The range of measured values observed in plants samples (excluding outliers) from Ireland (0.7065–0.7195) is similar to the range observed for the UK (0.7070–0.7222). When comparing the $^{87}Sr/^{86}Sr$ values of outcrops of similar types from Ireland and the UK (Table 7.1), some are very similar (differences below 0.0002 –formations 33, 40, 59 and 75), while others are less so (differences between 0.0016 and 0.0018 – formations 39, 54 and 68). No differences, however, exceed 0.0020 suggesting no major inconsistencies.

Table 7.2 – Average BASr values for outcrops and rock types from which plant samples were collected (based on the data from Appendix 6.9); the values are compared to the values obtained for similar rock types in the UK

Site(s) (n)	Outcrop measured values (± 1SD)	Rock type measured values (± 1SD)	Rock type measured values (± 1SD) for UK*
Formation 5 – Lower Palaeozoic gabbro, dolerite and diorite (416–542 Ma)			
A3(1), A3(2-bog) (3)	0.7097 ± 0.0002		n/a
Formation 8 – Caledonian (Silurian - Devonian) granite and granodiorite (359–444 Ma)			
I93 (1)	0.7118	0.7106 ± 0.0009	n/a
I38, I46 (3)	0.7106 ± 0.0013		
I54 (2)	0.7097 ± 0.0001[a]		

Table 7.2 (*continued*)

Site(s) (n)	Outcrop measured values (± 1SD)	Rock type measured values (± 1SD)	Rock type measured values (± 1SD) for UK*
Formation 9 –Tertiary (Palaeogene) granite, felsite and granophyre (23–65 Ma)			
I94 (3)	0.7143 ± 0.0019	0.7138 ± 0.0019	n/a
I95 (2)	0.7153 ± 0.0059[a]		
A18 – C (2)	0.7117 ± 0.0019[a]		
Formation 10 – Tertiary (Palaeogene) rhyolite (23–65 Ma)			
I06 (2)	0.7082 ± 0.0005[a]		n/a
Formation 11 – Tertiary (Palaeogene) basic intrusion, dolerite and gabbro (23–65 Ma)			
I15 (2)	0.7082 ± 0.0001[a]		n/a
Formation 19 – Slishwood Division (Neoproterozoic); Quartzo-feldspathic paragneiss (>542 Ma)			
A10 (2)	0.7097 ± 0.0005[a]		n/a
Formation 27 – Dalradian Argyll group; Psammitic and pelitic schist, marble, amphibolite, diamictite (>542 Ma)			
A08 – L (2)	0.7133 ± 0.0014[a]	0.7121 ± 0.0018[a]	0.7117 ± 0.0015 (12p)
A09 (2)	0.7108 ± 0.0011[a]		
Formation 29 – Sperrins Dalradian Southern Highland Group; Pelitic & psammitic schist, phyllite & marble (>542 Ma)			
I88 (3)	0.7134 ± 0.0008	0.7110 ± 0.0035[a]	0.7117 ± 0.0015 (12p)
I89 (2)	0.7085 ± 0.0002[a]		
Formation 32 – Cambrian marine greywacke, shale, sandstone and quartzite (488–542 Ma)			
I40 (2)	0.7102 ± 0.0020[a]		0.7115 ± 0.0002[a] (2w)
Formation 33 – Lower-Mid Ordovician basic volcanic basalt (444–488 Ma)			
A04, A05 (2)	0.7105 ± 0.0012[a]		0.7105 ± 0.0008 (11p)
Formation 35 – Lower-Mid Ordovician slate (444–488 Ma)			
I43 (2)	0.7093 ± 0.0008[a]		0.7105 ± 0.0008 (11p)
Formation 39 – Mid-Upper Ordovician slate (444–488 Ma)			
I82 (3)	0.7121 ± 0.0009		0.7105 ± 0.0008 (11p)
Formation 40 –Mid-Upper Ordovician Derryveeny formation; Marine to fluvial; Greywacke, shale, sandstone & conglomerate (444–488 Ma)			
A01 – BN (3)	0.7087 ± 0.0006	0.7106 ± 0.0026[a]	0.7105 ± 0.0008 (11p)
A16 (2)	0.7125 ± 0.0004[a]		
Formation 42 – Ordovician - Silurian Rathkenny formation; "Moffat shale" facies; Shale and greywacke (416–488 Ma)			
I24 (1)	0.7108		n/a

Table 7.2 (*continued*)

Site(s) (n)	Outcrop measured values (± 1SD)	Rock type measured values (± 1SD)	Rock type measured values (± 1SD) for UK*
Formation 49 – Silurian deep marine turbidite sequence; mudstone, sandstone, greywacke, shale and conglomerate (416–444 Ma)			
A02, A17 – A, I19, I27, I91, I92 (11)	0.7109 ± 0.0005	0.7104 ± 0.0008	0.7117 ± 0.0014 (10p)
I35 (2)	0.7093 ± 0.0001[a]		
I87 (2)	0.7088 ± 0.0001[a]		
I48 (2)	0.7108 ± 0.0001[a]		
I80 (2)	0.7110 ± 0.0003[a]		
Formation 52 – Upper Silurian – lower Devonian continental redbed facies; Sandstone, siltstone & mudstone (359–444 Ma)			
A13 (2)	0.7097 ± 0.0010[a]		0.7104 ± 0.0012 (12p)
Formation 54 – Upper Devonian – Lower Carboniferous continental redbed facies; Sandstone, conglomerate & siltstone (299–416 Ma)			
I50 (1)	0.7123	0.7120 ± 0.0003[a]	0.7104 ± 0.0012 (12p)
I79 (3)	0.7118 ± 0.0026		
Formation 56 – Carboniferous volcanic and minor intrusions; Basalt, trachyte, syenite & tuff			
I73 (2)	0.7077 ± 0.0001[a]		n/a
Formation 59 – Carboniferous shallow marine & coastal plain (basal clastics); Sandstone, mudstone and conglomerate (299–359 Ma)			
A06 (2)	0.7103 ± 0.0009[a]		0.7104 ± 0.0012 (12p)
Formation 63 – Carboniferous shallow marine & coastal plain (Basal Clastics); Sandstone, mudstone & conglomerate (299–359 Ma)			
A07 (2)	0.7096		0.7104 ± 0.0012 (12p)
Formation 64 – Carboniferous marine shelf facies; Limestone & calcareous shale (299–359 Ma)			
A12 (2)	0.7082 ± 0.0001[a]	0.7089 ± 0.0005	0.7092 ± 0.0002 (11p)
I51, I97, I98 – P (6)	0.7086 ± 0.0002		
I22 (2)	0.7096 ± 0.0001[a]		
Formation 65 – Carboniferous Visean basinal limestone; Marine basinal facies (Tobercolleen and Lucan Formations); Dark-grey argillaceous and cherty limestone & shale (299–359 Ma)			
I26 (2)	0.7094 ± 0.0002[a]	0.7089 ± 0.0006	0.7092 ± 0.0002 (11p)
I28, I37 (3)	0.7085 ± 0.0004		
Formation 66 – Carboniferous Tyrone GP; Visean mudstone, sandstone and evaporite; Marginal marine (Mullaghmore, Downpatrick & Clogher Valley Formations) (299–359 Ma)			
A11 (2)	0.7094 ± 0.0010[a]		0.7104 ± 0.0012 (12p)
Formation 68 – Carboniferous Leitrim GP; Visean mudstone, sandstone and evaporite; Marginal marine (Meenymore Formation) (299–359 Ma)			
A15 (2)	0.7086 ± 0.0005[a]		0.7104 ± 0.0012 (12p)
Formation 70 – Carboniferous (Late Visean-Westphalian) continental redbed; Sandstone, conglomerate & mudstone (299–359 Ma)			
A14 (2)	0.7107 ± 0.0022[a]		0.7104 ± 0.0012 (12p)

Table 7.2 (*continued*)

Site(s) (n)	Outcrop measured values (± 1SD)	Rock type measured values (± 1SD)	Rock type measured values (± 1SD) for UK*
Formation 71 – Carboniferous Namurian sandstone, shale; Fluvio-deltaic & basinal marine (Turbiditic); Shale, sandstone, siltstone & coal (299–359 Ma)			
I96, Knowth (K), Newgrange (6)	0.7089 ± 0.0002	0.7098 ± 0.0009	0.7104 ± 0.0012 (12p)
I61, I62, I63, I64 (11)	0.7104 ± 0.0007		
Formation 75 – Triassic sandstone and mudstone with evaporite; Continental redbed facies, lagoonal & shallow marine (200–251 Ma)			
I31 (2)	0.7095 ± 0.0007[a]		0.7096 ± 0.0004 (1p, 1d, 3s)
Formation 79 – Palaeocene Lower Basalt Formation; Olivine basalt lava (56–65 Ma)			
I01 – BM (2)	0.7069 ± 0.0004[a]		0.7079 ± 0.0011 (5p)
Formation 82 – Palaeocene Upper Basalt Formation; Olivine basalt lava (56–65 Ma)			
I03 (3)	0.7099 ± 0.0007	0.7084 ± 0.0020[a]	0.7079 ± 0.0011 (5p)
I05 (2)	0.7070 ± 0.0005[a]		
Formation 83 – Oligocene Lacustrine; Clay, sand & lignite (23–34 Ma)			
I02 (2)	0.7074 ± 0.0005[a]	0.7078 ± 0.0005[a]	0.7093 ± 0.0006 (6d)
I04 (2)	0.7082 ± 0.0001[a]		

*From Evans et al. (2010) – the values are taken for the most similar UK formation; the values are calculated on plant values (p) only if more than three plant values were available, soil (s), water (w) and dentine (d) values were used if not enough plant data was available; the bedrock ages are based on the geochronometric scale from Holland & Sanders (2009); [a]standard deviation calculation on 2 measurements only

5.4 Presence of peat bog

In the A03 site, peat bogs were clearly visible. Two samples (grass and shrub) were taken away from the bog and an additional one (grass) was taken from the bog. The values are identical for all three samples (0.7095 and 07098 away from the bog and 0.7098 from the bog). This suggests that bog has a limited impact on the strontium isotope composition of plants or that its isotope composition is similar to that of the local bedrock.

5.5 Sea spray effect

As an island, the strontium isotope ratios of plants from coastal zones could well be affected by a sea spray effect (Whipkey et al. 2000; Frei et al. 2009). Two series of samples were taken on the same geological formations but at different distances from the coast: the first

series from the west coast of Ireland, on Carboniferous sandstone (I61 to I65 – Formation 71), and the second from the east coast, on Silurian mudstone (I19, I20, I91, I92 – Formation 49). The aim was to see if there is a significant isotope effect of sea spray on plants in Ireland, and if that is the case, how far inland the effect can be detected.

The strontium isotope ratios (Figure 7.2) show that plant samples taken very close to the sea (< 50 m) have ratios between 0.7092 and 0.7094, very close to the value of modern sea water (0.7092 – Hess et al. 1986). Samples that were taken further away from the coast exhibit higher isotope ratios. The lower values of the samples taken at 17 km from the west coast (I61) require further investigation. This could be due to different superficial geology but are unlikely to be linked to a sea spray effect as these samples were the furthest away from the sea, and intervening values were higher.

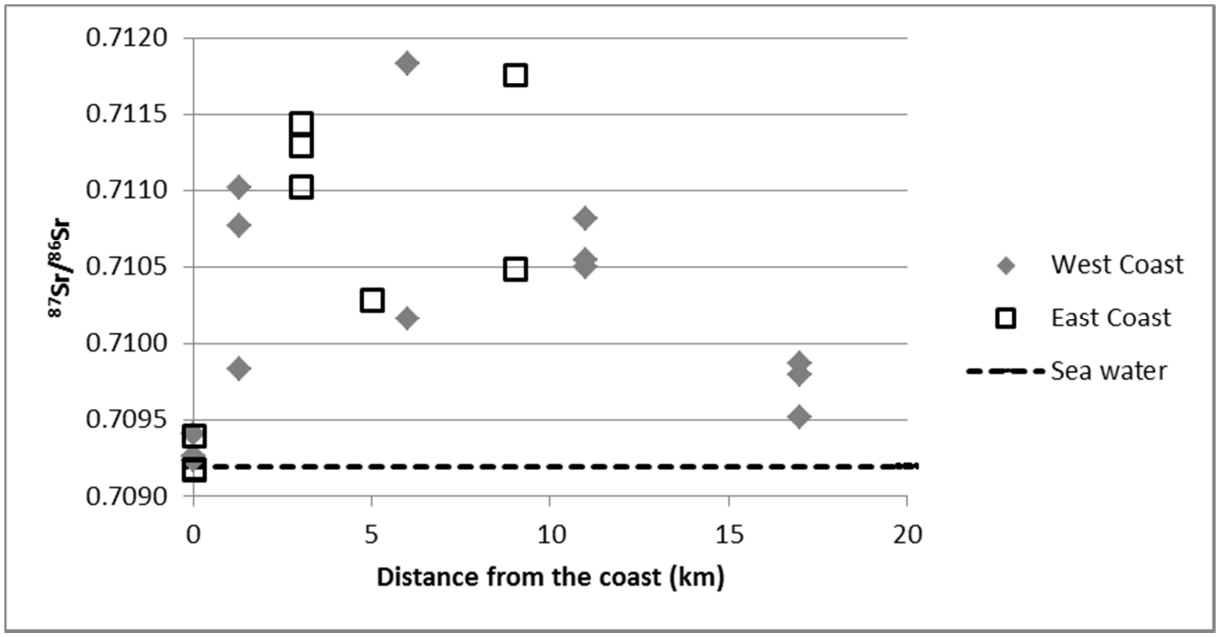

Figure 7.2 – Strontium isotope ratios of plant samples taken on the west and east coast of Ireland compared to the strontium isotopic ratio of sea water

The results of other samples taken from site close to the coast confirm that the sea spray effect impacts on the isotope ratio of plant samples in direct proximity of the coast (< 50 m). Indeed, samples from sites I17 and I21 have average values of 0.7094 while samples

taken from other sites on the same geological rock type (Formation 64) have an average value of 0.7089. I17 was taken from a beach while I21 was taken 50 m from the estuary of the Boyne River 800 m from the coast. The sea spray effect coming in as far as 800 m is most likely due to the estuary. Two sites (I16 and I85) located close to the coast have however distinctly different values than 0.7092. The first site (I16) is located on a beach and the average value is 0.7103 which could be due to the presence of the Mourne Mountains right next to it which granitic geology presents higher strontium isotope ratios (plant samples have values around 0.7150). The second (I85) is located at the Giant's Causeway in Northern Ireland and has a value of 0.7079. While the samples from I17 and I21 were taken directly on the beach (at sea level), the samples from I85 were taken from higher above.

The results show that sea spray effect is limited to the immediate vicinity of the coast (< 500 m) but that it can go further inland in the case of an estuary. For the purpose of the creation of the map, it will be assumed here that all sites within 250 m from the coast are affected by the sea spray effect and up to 1 km from the estuary of the Boyne River. Following that rationale, the $^{87}Sr/^{86}Sr$ values of I16, I17, I20, I21, I65 and I85 were reset at sea value of 0.7092. In future work, however, and as highlighted by Evans et al. (2009), and the values obtained for I16 and I85, topography should be taken into account.

5.6 Maps

Taking the previous results into account, two maps were created following the experimental design. The first one (multi-part – Figure 7.3) considers each rock type as a single entity; the second (single-part – Figure 7.4) looks at each outcrop individually.

5.6.1 Multi-part

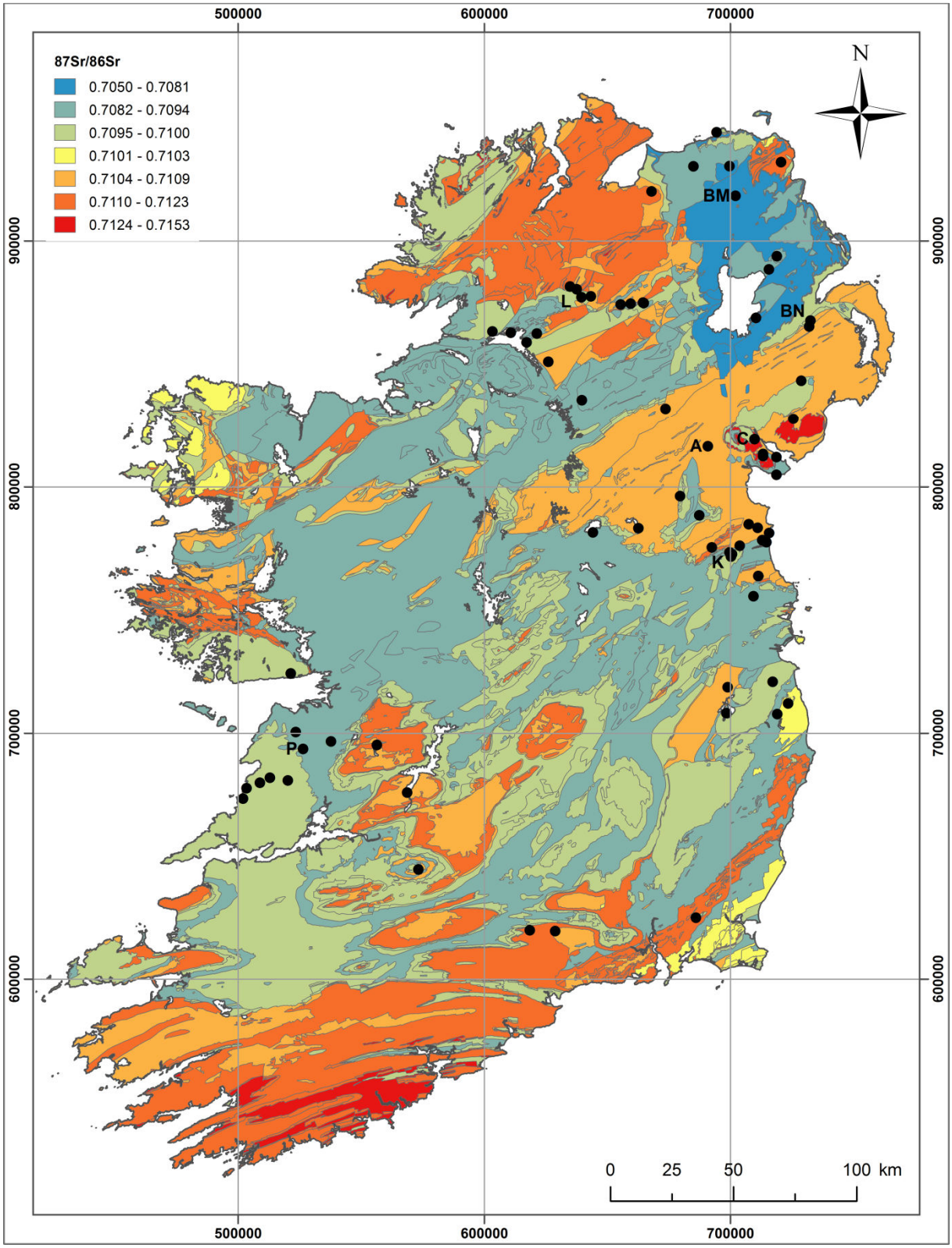

Figure 7.3 – BASr map for Ireland (multi-part)

5.6.2 Single-part

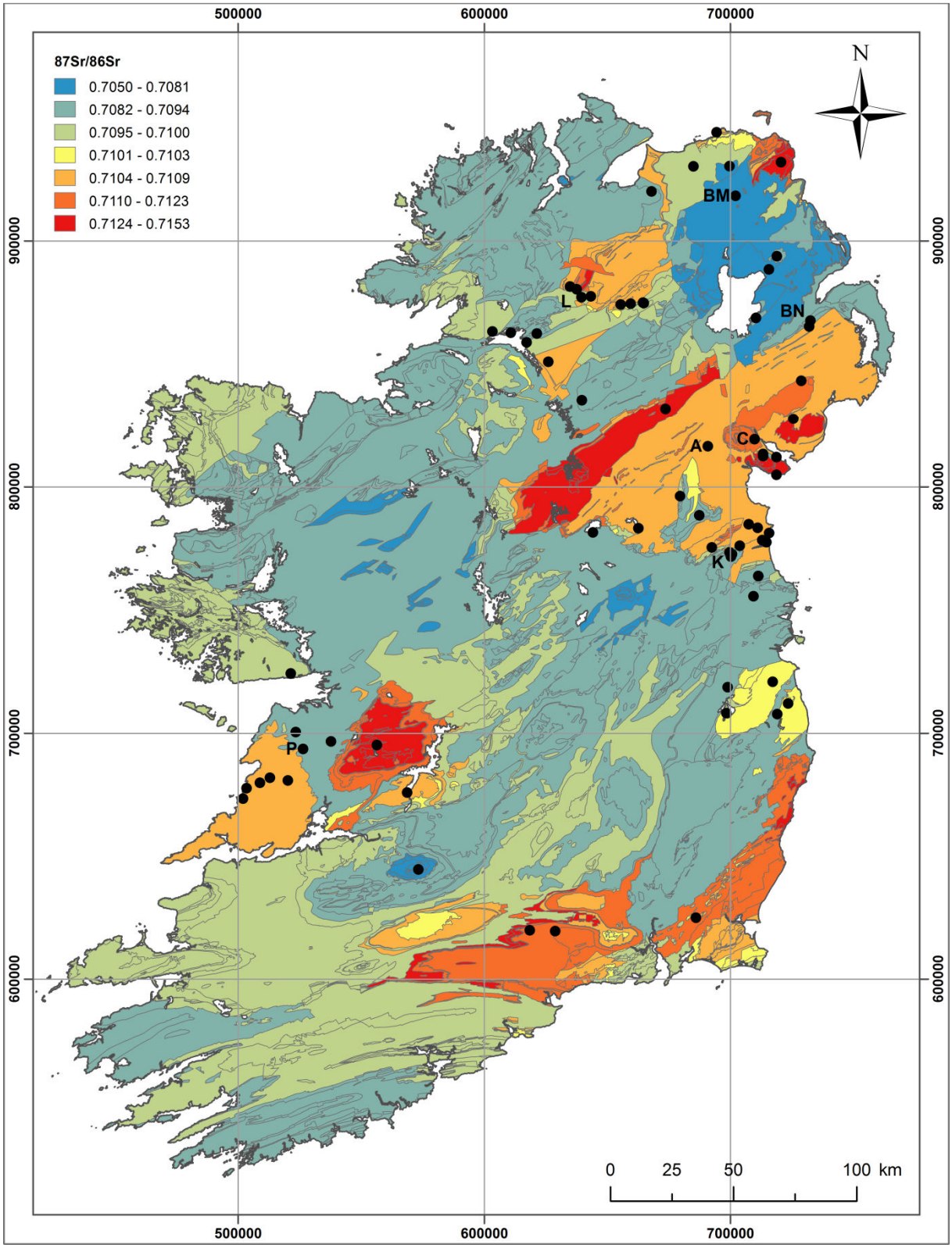

Figure 7.4 – BASr map for Ireland (single-part)

6 Discussion and Conclusion

The first map (multi-part) allows for a better prediction of the BASr values of outcrops that were not sampled based on their rock type. On the downside, it averages all the values obtained for a same rock type assuming that only bedrock geology impacts on the BASr, ignoring potential contributions from rainwater, groundwater, superficial geology, etc. By considering each outcrop individually, the second map (single-part) allows such contributions to be taken into account. However, this method ignores the rock type and only considers outcrop boundaries. This implies that only outcrops from which plant samples were collected will provide reliable results. Considering all of the above, it is clear that neither maps are ideal but the first one (multi-part) is the best to predict the overall BASr of the Island while the second (single-part) should be preferentially used if most (all if possible) outcrops of the studied region have been sampled.

In order to use these maps based on modern plants in archaeological contexts, it would be useful to know whether any major changes have occurred over time. In this work, the Irish Neolithic and Bronze Age are the periods of interest. Since the Neolithic, sea levels have not changed much (Carter 1982; Carter et al. 1989) suggesting no drastic change in coastal lines. The finding that the sea spray effect reaches up to 250 meters inland made for modern Ireland, should be valid for Neolithic times. While it is not possible to ascertain that the Neolithic landscape would be similar to that of today, and that results obtained from modern plants correspond exactly to the past, pollen records suggest that most deforestation occurred in the Early Neolithic (Lamb and Thompson 2005; Plunkett et al. 2008). Here, it will be assumed that the results are valid at least as far as the Neolithic and Bronze Age periods are concerned.

Chapter 8 – Applied study: Irish Neolithic and Bronze Age

1 Introduction

Seven archaeological sites (Figure 7.1) were investigated using the results obtained in the previous chapters. In addition to the passage tombs of Knowth, six other sites dating from the Neolithic to the Middle Bronze Age feature in this case study: four Neolithic court tombs (Annaghmare, Co. Armagh, Clontygora, Co. Armagh, Legland, Co. Tyrone and Parknabinnia, Co. Clare), a megalithic circular chamber close to the Ballynahatty timber circle and the Giant's Ring henge monument, Co. Down, and Middle Bronze Age urns found near the Neolithic court tomb of Ballymacaldrack, Co. Antrim. Cremated bone fragments from each site were analysed (Table 8.1). In addition, for three of the sites (BN, K & P), several tooth enamel fragments were also analysed. Carbon, oxygen and strontium isotope ratios were measured for each sample and infrared analyses were carried out after pre-treatment with sodium hypochlorite and acetic acid (as highlighted in Chapter 4).

Table 8.1 – Archaeological sites with geological formation (see Table 7.2), age and number of unburned tooth and cremated bone samples

Code	Site	Geological formation	Age	n cremated bone	n enamel
A	Annaghmare	49	Neo	2	/
BM	Ballymacaldrack	79	MBA	3	/
BN	Ballynahatty	40	Neo	4	3
C	Clontygora	9	Neo	3	/
K	Knowth	71	Neo	35	8
L	Legland	27	Neo	2	/
P	Parknabinnia	64	Neo	4	4

I begin this chapter by a brief overview of the sites including archaeological and geological information. Structural and isotopic results are then discussed for each site and

inter/intra-site comparisons are made. For each site, a local BASr map is created based on the single-part BASr map (Figure 7.4). Average BASr values are calculated for 5, 10 and 20 km catchment areas using ArcGIS with the help of John Pouncett. The impact of these results on the study of mobility and cremation processes in Neolithic and Bronze Age Ireland is discussed.

2 Archaeological and geological background

In this section, a brief archaeological background of each site is given describing the monument from which human remains were sampled. If available, information about the landscape and the geological formations around the sites are detailed. The formation numbers given here correspond to those of Chapter 7 (Figure 7.1 and Table 7.2). The location of the archaeological sites can be found in Figure 7.1.

2.1 Annaghmare (Co. Armagh)

The Neolithic court tomb of Annaghmare is composed of three chambers, the last two of which were undisturbed. The chambers contained both unburned and cremated bone fragments together with pottery and flint. There are two additional lateral chamber but they do not appear to have been used for burial (Waterman 1965). It appears that the tomb was ritually sealed when it was no longer of use (Waterman 1965; Jones 2007). The site is located ca. 7 km west from the granitic Mourne Mountains (Formations 8 and 9) on a Silurian mudstone formation (49) that remains unchanged in a 5 km radius around the site (GSNI).

A first radiocarbon date was obtained for this site on charcoal found behind the blocking of the forecourt (UB-241– Smith et al. 1970) with a second on a child mandible from chamber 2 (UB-6741– Schulting et al. 2012). Here, two calcined bone fragments – a long bone piece from chamber 3 (A1) and a cranial fragment from chamber 4 (A2) – are analysed. The latter is also radiocarbon dated. There seem to be some confusion over the

numbering of the chambers in the surviving documentation as no chamber 4 appears in the excavation report; this is being further investigated, but at least the samples are clearly labelled as deriving from this site.

Table 8.2 – Radiocarbon dates obtained for a piece of charcoal (Smith et al. 1970) and an unburned child mandible (Schulting et al. 2012) from Annaghmare (IntCal 09)

Sample	Lab code	^{14}C	calBC (95%)
Charcoal	UB-241	4310 ± 70	3317 – 2678
Child mandible	UB-6741	4556 ± 35	3486 – 3104

2.2 Ballymacaldrack (Co. Antrim)

Ballymacaldrack is better known for its Neolithic court tomb, also called Dooey's Cairn, in which cremated human remains were found (Collins 1976). It was not possible, however, to find that material but cremated human remains from various broken urns discovered in a quarry, not far from the site, are available (Tomb & Davies 1938; 1941). These are not contemporary with the Neolithic court tomb and date instead to the Middle Bronze Age (based on the pottery style – Brindley 2007). The geology around the site is a lower basalt formation (79) with upper basalt (82) and some clay (83) outcrops at ca. 9 km north of the site. To the south and west, the lower basalt formation (79) remains unchanged for about 20 km (GSNI).

Two calcined bone fragments from urns 3, 4 and 5 were selected. The urns are believed to contain the remains of single individuals (Tomb & Davies 1938). All samples are from long bones except BM1a which is a cranial fragment. The urns themselves were discovered close to the basalt bedrock, under about one meter of glacial clay (Tomb & Davies 1941).

2.3 Ballynahatty (Co. Down)

Several Neolithic monuments can be found at Ballynahatty (Co. Down). The best known is the Giant's Ring henge, consisting of a circular rampart (or ring-bank) of about 180 meters of diameter with a megalithic monument in the middle. It is one of the largest field monuments in Co. Down (Collins 1957). The site is close to the sea (ca. 10 km) and only 500 meters from the River Lagan, making it easily accessible by sea and land (Hartwell 2002). Pollen records from the area highlight that during the Mesolithic, the region around Ballynahatty was mainly woodland but during the Mesolithic–Neolithic transition and the Early Neolithic, some deforestation occurred and a mixed agricultural economy was established. The records show that the landscape remained open throughout the Neolithic period, during which the megalithic tombs were constructed, and the Bronze Age (Plunkett et al. 2008). The site itself is on a narrow band of Mid-Upper Ordovician formation (40) with the sea 10 km to the east, volcanic basalt formations (79 and 82) about 5 km to the north and Silurian mudstone (49) less than 2 km to the south (GSNI).

From the different monuments of that area, the one of interest for this thesis is the megalithic circular chamber excavated in 1855, about 300 meters north-west of the Giant's Ring (MacAdam 1855; Hartwell 1991). The circular chamber, separated into six compartments (A to F – Figure 8.1), was apparently used for different funeral practices: in A and B several urns were found containing burned human bone; D contained human burned bone on which were resting up to five unburned skulls; several parcels of calcined bone lying on the floor separated by stones were found in chambers E and F suggesting these were from different individuals (MacAdam 1855; Hartwell 1991). The combination of inhumation and cremation suggests a certain number of interments on different occasions during the Neolithic (Hartwell 1991). Ten samples from the circular chamber (one animal bone, six unburned

bone and three cremated bone) were radiocarbon dated of which six successfully gave a date (Table 8.2 – Schulting et al. 2012).

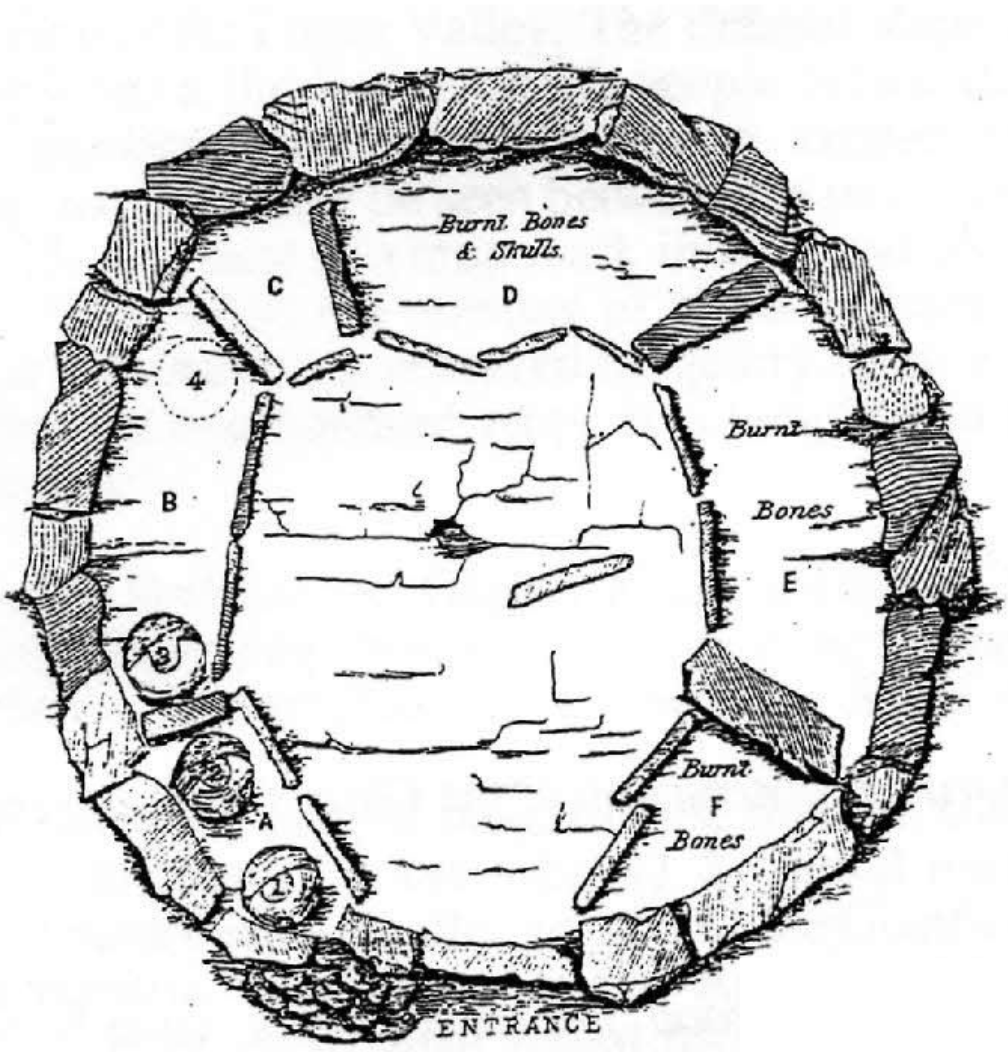

Figure 8.1 – Plan for Ballynahatty megalithic circular chamber 1855 (McAdam 1855)

A total of seven samples are studied here: three unburned tooth enamel and four calcined bone fragments (two long bone and two cranial fragments). The teeth came from three different mandibles (one of which was radiocarbon dated: AX34.2) and the calcined bone fragments came from four different groups of calcined bone found in compartments E and F, suggesting that seven different individuals are represented here.

Table 8.3 – Radiocarbon dates obtained for unburned and calcined human bone from the megalithic circular tomb from Ballynahatty excavated in 1855 (Schulting et al. 2012 – IntCal 09)

Sample	Lab code	^{14}C	calBC (95%)
AX34.2 human mandible	UB-6723	4165 ± 36	2882 – 2629
A.64 human maxilla M1	UB-7059	4465 ± 38	3343 – 3020
AX34.6 human mandible LM2	UB-7194	4587 ± 34	3501 – 3116
AX34.8 cremated human cranium Grp.1	UB-7247a	4452 ± 33	3337 – 2943
	UB-7247b	4440 ± 33	3331 – 2929
AX34.10 cremated human cranium Grp.3	UB-7248	4507 ± 36	3355 – 3095
AX34.11 human mandible RM1	UB-7521	4584 ± 37	3501 – 3106

2.4 Clontygora (Co. Armagh)

The large court tomb at Clontygora is on the granitic plateau south-east of Newry. The site is about 2.5 km from Carlingford Lough opening directly on the Irish Sea. The bedrock is made of Tertiary granite (Formation 9) with Silurian mudstone (49) around it and other granite formations (8 and 9) within 20 km. The tomb is composed of three chambers as most court tombs and is one of the most impressive monuments of this type. Unfortunately, while the first chamber was almost intact, the two others have almost disappeared. Human calcined bone fragments were recovered as well as charcoal from Chambers I and II. While most court tombs were closed after use, it seems that Clontygora Large Cairn was not (Davies & Paterson 1937). The three calcined long bone fragments analysed here originate form an undisturbed layer in Chamber 1, one of which was also radiocarbon dated.

2.5 Knowth (Co. Meath)

The Boyne Valley in Co. Meath presents the highest density of passage tombs in Western Europe, including the three major mounds of Knowth, Newgrange and Dowth. The main mound at Knowth is the largest megalithic passage tomb of the Middle Neolithic period (c. 3200–2900 cal. BC) and is situated along the river Boyne (Eogan 1973). Directly around it are 20 smaller mounds (Figure 8.2). The stones used to build these passage tombs originate from different places: sandstones or large greywacke is thought to have come from areas 3 to

5 km north-east of Knowth; quartz came from the granitic mass of the Wicklow Mountains to the south; the rounded granite and granodiorite appears to originate from Dundalk Bay further north. All these materials were used together with local resources: black shale, stone from the alluvial deposits, sod and earth (Cooney 2000, 137). A recent discovery has shown the presence of County Tyrone rock amongst the Newry granodiorite cobble associated with white quartz fragments outside the Knowth passage tombs. These are almost certainly from the beach at Dunany Point (Meighan 2011). In the direct vicinity of Knowth, a large variety of agricultural land was available with a combination of pasture and arable land (Cooney 2000, 49). Knowth is located on Carboniferous sandstone (Formation 71), about 10–15 km from the Boyne river estuary. Silurian mudstone (49) can be found north of the site, Carboniferous limestone (65) in the south and an Ordovician-Silurian outcrop (42) less than 10 km to the south-west (GSNI).

Both unburned and cremated bone fragments were discovered in the megalithic passage tombs of Knowth. One hypothesis to account for this dual burial practice is that those living close to the site were initially inhumed while those living further away were cremated as it would have been easier to carry an urn containing calcined bone fragments and ashes than an entire corpse. This hypothesis relies on the previous observation that the stones used to build the megalithic passage tomb from Knowth originate from different places (Cooney 2000; Meighan 2011). Furthermore, the lack of evidence of burning near the site and the fragmented remains suggests that cremation took place elsewhere and that the bone fragments were introduced in the chamber only later (Schulting et al. forthcoming). Nevertheless, the unburned bone fragments were also very fragmented and could originate from individuals that were not initially buried at Knowth.

A recent radiocarbon dating program (Schulting et al. forthcoming) analysed 18 human unburned and 40 cremated bone fragments from eight different mounds at Knowth,

including the main mound (Knowth 1). The results highlight a main phase of use of the tombs for the deposition of human remains between 3200–2900 BC and showed that both funerary practices were contemporary. The study also included the stable isotopic analyses of the unburned bone revealing a terrestrial C_3-based diet.

Here, 30 of the radiocarbon dated cremated bone fragments are analysed by infrared and isotopic analyses (mostly cranial and long bone fragments). In addition eight unburned tooth enamel fragments are also investigated (Table 8.3).

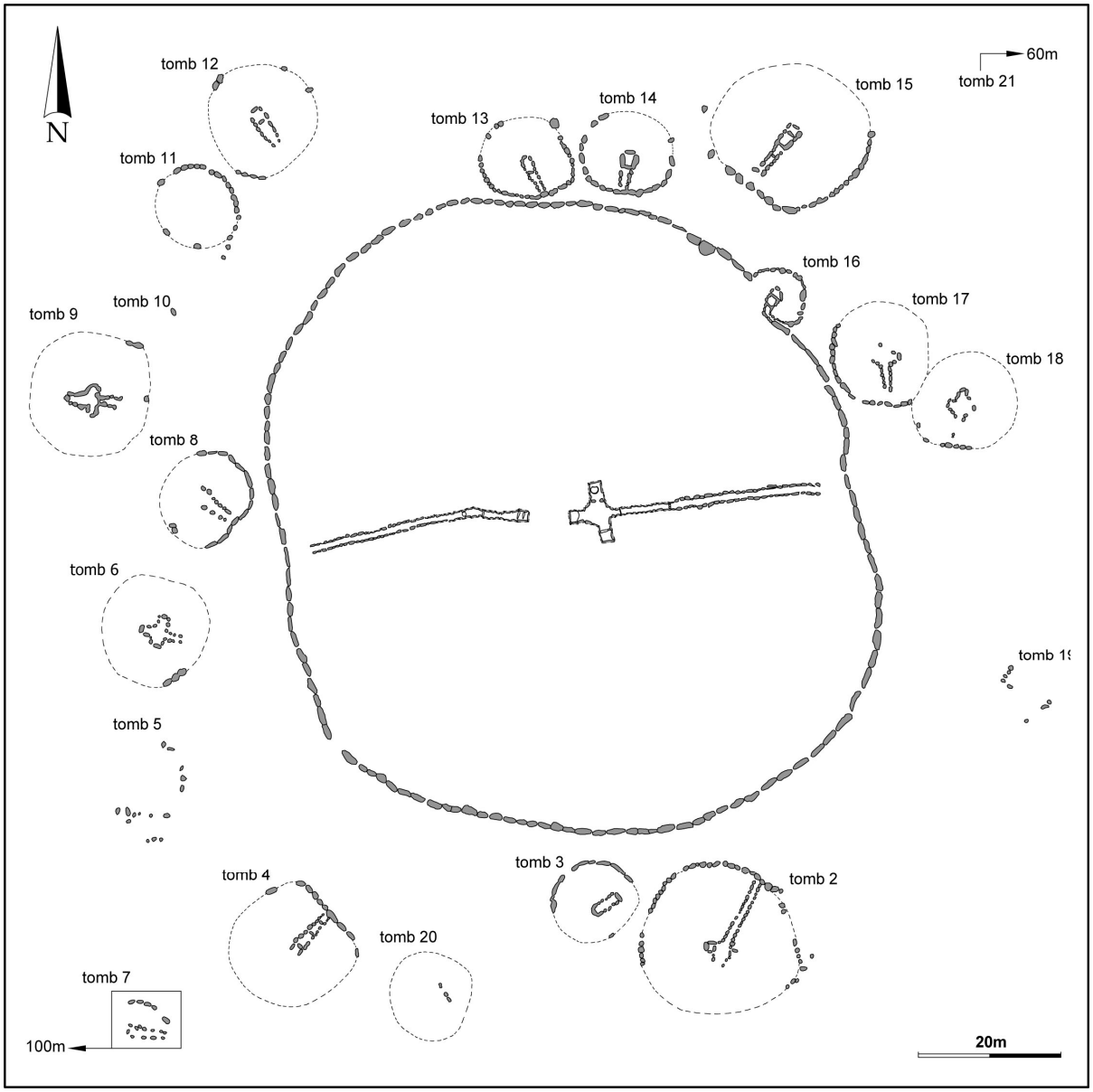

Figure 8.2 – Plan of the Knowth passage tomb cemetery (Schutling et al. forthcoming)

Table 8.4 – Samples from Knowth including context and radiocarbon dates (Schulting et al. forthcoming – IntCal 09)

Tomb	#	Context	Context 2	Find no.	Lab code	^{14}C	calBC (95%)
Cremated bone samples							
1BE, Eastern passage tomb	K30	LHR	deposit 1	E70:163a	UBA-12673	4362 ± 38	3090 – 2901
	K31	end recess	on flagstone	E70:186	UBA-12675	4448 ± 39	3337 – 2931
	K34	RHR	deposit 1	E70:50146b	UBA-12678	4379 ± 25	3089 – 2913
	K3				OxA-21887	4476 ± 32	3340 – 3028
	K4	RHR	deposit 2	E70:422a	OxA-21888	4498 ± 33	3353 – 3091
	K5	RHR	deposit 3	E70:218a	OxA-22024	4424 ± 34	3326 – 2921
	K35	RHR	deposit 4	E70:50148a	UBA-12679	4459 ± 25	3332 – 3023
	K6	RHR	deposit 5	E70:425	OxA-21991	4426 ± 34	3327 – 2922
	K35	RHR	deposit 6	E70:424	UBA-12680	4410 ± 27	3263 – 2921
	K32	RHR	deposit B	E70:50142	UBA-12676	4476 ± 39	3346 – 3026
	K1	RHR	deposit C	E70:50143	OxA-21941	4543 ± 32	3366 – 3103
	K33	RHR	cremation 4	E70:50144d	UBA-12677	4416 ± 24	3263 – 2924
	K2				OxA-21886	4469 ± 32	3330 – 3025
1CW, Western passage tomb extension	K7	K98CR5	orthostat 5	E70:50159a	OxA-21992	4261 ± 31	2920 – 2762
	K37	K98CR5	orthostat 5	E70:50159b	UBA-12681	4160 ± 23	2877 – 2636
	K8	K98CR3	orthostat 29	E70:50158	OxA-21993	4423 ± 36	3327 – 2920
tomb 2	K9	RHR	n/a	E70:50166	OxA-22025	4437 ± 31	3329 – 2929
tomb 6	K10	RHR	n/a	E70:104a	OxA-22026	4375 ± 29	3089 – 2910
	K38	RHR	n/a	E70:104b	UBA-12682	4385 ± 23	3089 – 2917
tomb 9	K11	end recess	deposit 1	E70:50171	OxA-22027	4357 ± 30	3083 – 2903
tomb 15	K13	chamber	segment 3 primary	E70:598	OxA-21874	4453 ± 29	3336 – 3014
	K14	chamber	segment 3 secondary	E70:599	OxA-21942	4430 ±31	3327 – 2926
	K12	chamber	segment 4	E70:595a	OxA-21889	4394 ± 35	3263 – 2910
	K39	"Beaker"	above floor	E70:3771	UBA-12683	4265 ± 24	2912 – 2877
tomb 16	K15	chamber	primary	E70:637	OxA-21875	4440 ± 28	3283 – 2935
	K40	chamber	secondary	E70:639a	UBA-12684	4362 ± 25	3081 – 2908
	K16				OxA-21890	4416 ± 33	3322 – 2918
	K17	chamber	tertiary	E70:641	OxA-21891	4400 ± 32	3077 – 2914
	K41	passage	primary	E70:644	UBA-12685	4317 ± 23	3011 – 2890
	K42	passage	secondary	E70:645	UBA-12686	4362 ± 34	3089 – 2902
tomb 17	K43	chamber	socket 11	E70:728	UBA-12687	4425 ± 38	3328 – 2921
	K44	n/a	in upper fill	E70:726	UBA-12688	4152 ± 23	2874 – 2634
tomb 18	K18	LHR	under basin	E70:747	OxA-22028	4434 ± 30	3328 – 2928

Table 8.4 – (*continued*)

Tomb	#	Context	Context 2	Find no.	Lab code	^{14}C	calBC (95%)
Unburned enamel samples							
1BE, Eastern passage tomb	KT1	LHR	compartment 1	K70:167	n/a		
	KT2	LHR	compartment 2	K70:168-1			
	KT3	LHR	compartment 2	K70:168-2			
	KT4	LHR	compartment 2	K70:168-3			
tomb 2	KT5	centre of chamber	n/a	K70:117			
	KT6	RHR	n/a	K70:120			
tomb 14	KT7	chamber	n/a	K70:50188			
tomb 15	KT8	chamber	segment 4	K70:595			

2.6 Legland (Co. Tyrone)

The Neolithic court tomb of Legland presents similarities with the 'Large Cairn' at Clontygora, but it only contains two chambers and the forecourt seems to have been incorporated in the cairn. Human cremated bone fragments were found in the forecourt and Chamber 1 together with pyre material, charcoal and burned red earth. Furthermore, some parts of Chamber 1 were blackened as if burned, suggesting on-site cremation. Such finds were not present in chamber 2 suggesting different uses for the chambers (Davies 1939). The geology around the site is quite varied with a mixture of Neoproterozoic outcrops (Formations 19, 27 and 29) and Carboniferous sandstones (59, 63 and 70). The site itself is on a Dalradian (Neoproterozoic) formation (27). Attempts to date the site were done by radiocarbon dating two unburned animal bone fragments but they were much younger than the Neolithic use of the site (AD 1529–1955) (Schutling et al. 2012). Here, two calcined bone fragments (one cranial and one long bone) were studied, one of which was also radiocarbon dated.

2.7 Parknabinnia (Co. Clare)

The Neolithic court tomb of Parknabinnia (Cl 153 – Figure 8.3) is located on Roughan Hill, south-east of the Burren. Comprised of two chambers, it is atypical in that it has a narrower

forecourt than most court tombs and a short heel-shaped cairn rather than a long, trapezoidal cairn (Jones & Walsh 1996). The tomb is located in the north-west of County Clare on the west coast of Ireland. It is one of several Neolithic monuments in the south-east Burren, an area that seems to have been a particular focus for Neolithic farmers as suggested by the important field systems found on Roughan Hill (Jones 1998; 2003; Cooney 2000). Pollen studies have shown that the present open landscape of the Burren developed over the course of the Holocene and that much of the character of the landscape today is the result of farming practices in the past. Before the Neolithic, pine and hazel dominated but deforestation began in the earlier 4th millennium BC by Neolithic farmers (Lamb and Thompson 2005). It has been suggested that court tombs could have been built for the local community, while portal tombs, such as Poulnabrone (ca. 8 km North of Parknabinnia), could be used by 'outsiders' (Jones 2007). In any case, the high density of tombs and ancient field walls, as well as the pollen records showing deforestation of the Burren uplands suggests intensive land use for agricultural purposes. Parknabinnia is situated on carboniferous limestone (Formation 64), with carboniferous shale and sandstone (Formation 71) less than 5 km to the west. Other, older Silurian and Upper-Devonian formations (49 and 54) can be found to the east and south-east.

Human skeletal remains (both inhumed and cremated) from Parknabinnia were recovered from both chambers together with animal bone, lithic artefacts, potsherds, and bone artefacts. The skeletal remains were highly fragmented, but at least twenty individuals are represented (Beckett 2005; Beckett & Robb 2006). Several radiocarbon dates were made on unburned human bone from both chambers (Table 8.4 – Schulting et al. 2012) suggesting an early use that continued for several centuries.

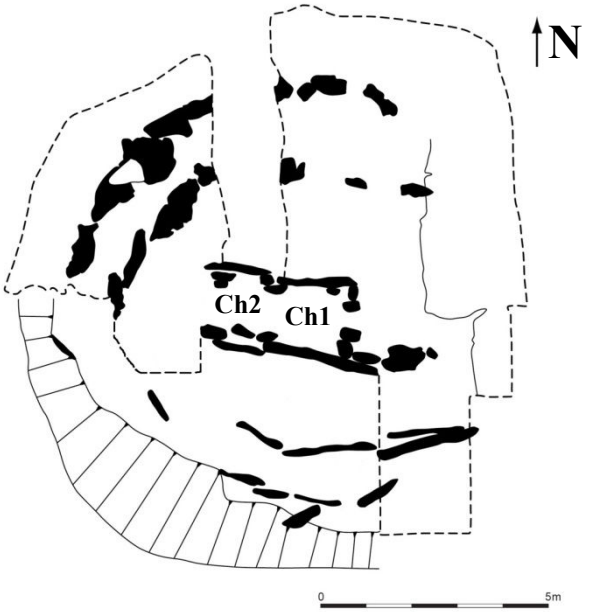

Figure 8.3 – Plan for Parknabinnia court tomb (Cl 153); drawn by Libby Mulqueeny (Schulting et al.2012)

Table 8.5 – Radiocarbon dates obtained for unburned human bone from Parknabinnia Court tomb with the overall range for each chambers (cal BC 95%) (Schulting et al. 2012 – IntCal 09)

Sample	Lab code	Date (BP)	calBC (95%)
Human bone from Chamber 1 (3635–2621 cal BC)	GU-10577	4705 ± 60	3635 – 3368
	GU-10570	4645 ± 55	3632 – 3168
	GU-10573	4640 ± 75	3635 – 3107
	GU-10581	4550 ± 60	3499 – 3030
	GU-10576	4535 ± 60	3496 – 3025
	GU-10574	4455 ± 60	3346 – 2930
	GU-10579	4315 ± 55	3097 – 2764
	GU-10571	4235 ± 55	3006 – 2628
	GU-10575	4195 ± 55	2905 – 2621
Human bone from Chamber 2 (3693–2930 cal BC)	GU-10578	4785 ± 60	3693 – 3376
	GU-10580	4725 ± 60	3638 – 3372
	GU-10572	4455 ± 60	3346 – 2930

Here, eight samples were studied: four tooth enamel and four calcined skull fragments. Five came from chamber 1 and three from chamber 2 (Table 8.5). Three sub-samples of a calcined bone fragment (P3) were analysed to observe the variation within one sample.

Table 8.6 – Samples from Parknabinnia including context

	Chamber	Context	Find no.	Element
P1	1	443	986.01	skull fragment
P2		443	1018.01	skull fragment
P3		582	1959.02	skull fragments
PT1		582	1908.11	upper M2
PT2		565	1728.04	lower M1/2
P4	2	533	1433.01	skull fragment
PT3		584	1952.01	incisor
PT4		586	2099.01	lower M1/2

3 Results

The results of the infrared and isotopic analyses carried out on archaeological samples (Appendix 6.5 & 6.6) are described in this section. Local maps based on the single-part BASr map (Figure 7.4) are created for each site, and the average BASr values for 5, 10 and 20 km catchment areas are calculated (Table 8.6).

Table 8.7 – BASr for the outcrop on which each site lies ('local BASr') and the average BASr values calculated for 5, 10 and 20 km catchment areas (whole area); the values between brackets represent the number of different geological formations involved in the calculation of the average BASr

	Local BASr	**1SD**	**5km BASr**	**10km BASr**	**20km BASr**
Annaghmare	0.7109	0.0005	0.7106 (2)	0.7107 (7)	0.7108 (15)
Ballymacaldrack	0.7069	0.0004	0.7069 (3)	0.7070 (8)	0.7080 (15)
Ballynahatty	0.7087	0.0006	0.7093 (5)	0.7093 (10)	0.7091 (16)
Clontygora	0.7117	0.0019	0.7113 (5)	0.7116 (7)	0.7114 (9)
Knowth	0.7089	0.0002	0.7094 (8)	0.7100 (17)	0.7098 (19)
Legland	0.7133	0.0014	0.7110 (6)	0.7104 (8)	0.7099 (17)
Parknabinnia	0.7086	0.0002	0.7089 (2)	0.7091 (2)	0.7095 (8)

The overall results show a wide variation in the strontium isotope composition of the tooth enamel and calcined bone samples (Figure 8.6a), ranging from 0.7066 to 0.7136. This variation is within that seen in sampled modern plants across Ireland (0.7065 to 0.7195, n = 158, excluding 11 outliers). As observed in Chapter 5, there is a correlation between the intensity of the cyanamide band at 2010 cm^{-1} (CN/P) observed in calcined bone and the $\delta^{13}C$ values of these specimens (Figure 8.6b). Chapter 4 highlighted that, when comparing the

archaeological infrared data with the experimental data (LAB 2), it appeared that some archaeological samples followed the pattern while many others fell outside the temperature fields (Figure 8.6c). Finally, when comparing the $\delta^{13}C$ and $\delta^{18}O$ values of all calcined bone of the seven sites, the correlation observed in modern bone samples burned on outdoor fires (Figure 5.8b) is not visible (Figure 8.6d).

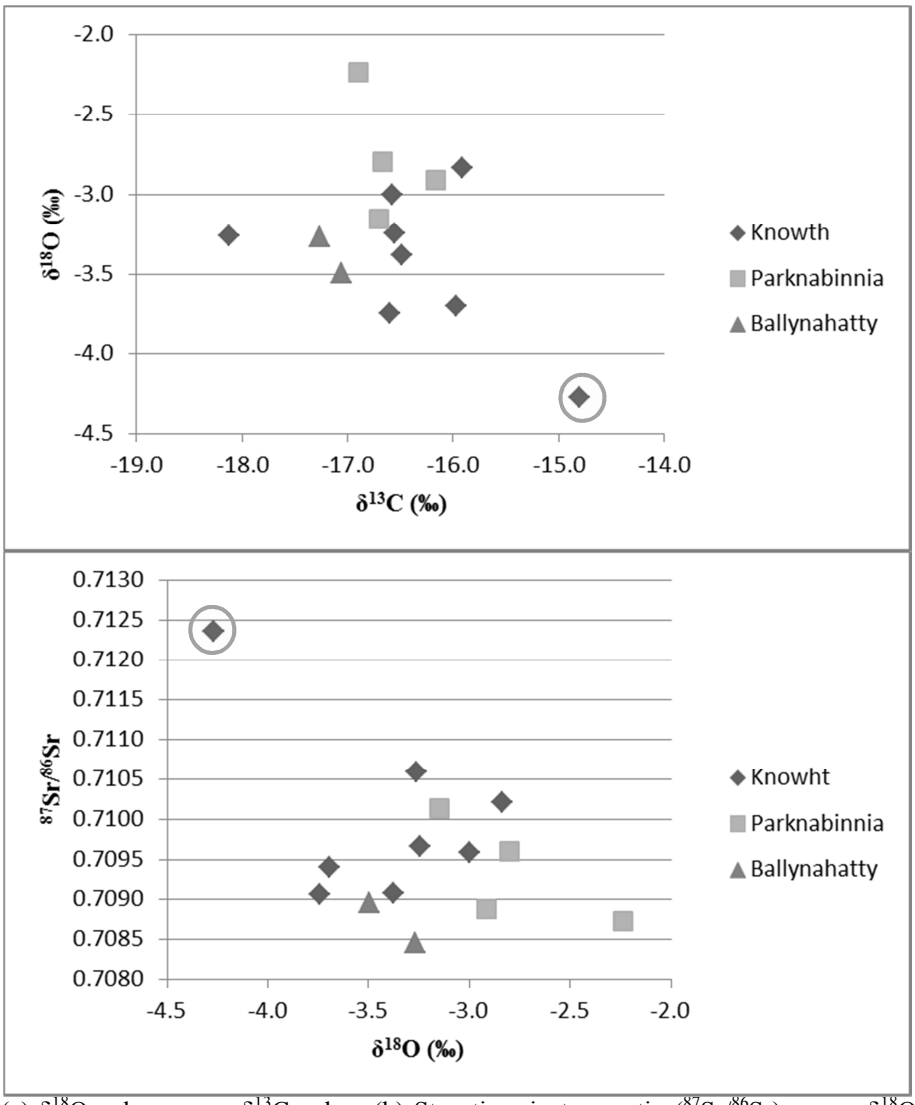

Figure 8.4 – (a) $\delta^{18}O$ value versus $\delta^{13}C$ value; (b) Strontium isotope ratio ($^{87}Sr/^{86}Sr$) versus $\delta^{18}O$ value for all tooth enamel samples from Knowth, Parknabinnia and Ballynahatty; the outlier from Knowth is highlighted

The tooth enamel samples have $\delta^{13}C_{ap}$ values around -16/-17‰, similar to those observed for tooth enamel of Irish lambs eating a controlled C_3-plant based diet (Zazzo et al. 2010). Furthermore, the results show generally higher $\delta^{18}O_c$ values in enamel at Parknabinnia

than at Knowth and Ballynahatty (Figure 8.4a). The first site is on the west coast while the two other sites are on the east coast where rainfall is depleted in ^{18}O (up to 2‰) compared to the west (Darling & Talbot 2003). Except for one sample from Knowth, the strontium isotope ratios of the enamel samples are between 0.7084 and 0.7107 (Figure 8.4b). The sample with the highest $^{87}Sr/^{86}Sr$ value (0.7125) is also the most depleted in ^{18}O and most enriched in ^{13}C.

3.1 Radiocarbon dating

The radiocarbon dating results (Table 8.7) show that two of the three samples are from the Early Neolithic period (A2 and L1) while the third one (C2) dates to the early part of the Early Bronze Age, about one millennium younger.

Table 8.8 – Radiocarbon results for archaeological calcined samples from Ireland (IntCal 13)

Site	Lab code*	Date (uncal BP)	cal BC (95%)
Annaghmare (A2)	OxA-X-2579-44	4572 ± 28	3494–3116
	OxA-30188	4532 ± 36	3364–3101
Clontygora (C2)	OxA-X-2579-47	3706 ± 27	2199–2026
Legland (L1)	OxA-X-2579-46	4515 ± 28	3353–3105

*Samples dated at ORAU are routinely issued with OxA- laboratory numbers. Those issued with OxA-X-numbers are research measurements with non-standard or experimental methods (see Appendix 3).

3.2 Annamghare (Co. Armagh)

Only two samples were analysed from Annaghmare. The first (A1) has a higher $^{87}Sr/^{86}Sr$ value (ca. 0.0015), is depleted in ^{13}C (ca. 5 ‰) and enriched in ^{18}O (ca. 2 ‰) compared to the other (A2). The latter also contains cyanamide and its infrared indices (C/C ratio and IRSF) indicate that it could have been burned at 800°C (Figure 8.7). The average BASr values calculated for the catchment areas are similar to the $^{87}Sr/^{86}Sr$ value of A1 (Figure 8.8). BASr values similar to the $^{87}Sr/^{86}Sr$ value of A2 (0.7090) can only be found in coastal regions located about 20 km away from the site, or on the Carboniferous limestone outcrops (formation 65) 50 km or more to the south.

3.3 Ballymacaldrack (Co. Antrim)

The strontium isotope results from Ballymacaldrack show very little variation between the samples (max 0.0008). For each pair of samples, the variation is even lower (max 0.0002), and is entirely consistent with the oestological report indicating that the remains in each urn represent a single individual (Tomb and Davies 1938; 1941). The results are consistent with the local BASr as well as the BASr calculated for 5, 10 km catchment areas, which are similar as the geology does not change for some distance around the site, but not with the 20 km catchment (Figure 8.10). The infrared results (C/C ratio and IRSF) suggest that the bodies from which the samples derive were burned in similar ways around 800°C except for one specimen (BM1b) that falls slightly to the right of the 800°C field defined by laboratory experiments (LAB 2). While the strontium results are very similar for each pair, the $\delta^{13}C$ and $\delta^{18}O$ values and cyanamide content are different. The most marked difference is between the two samples from Urn 3 (BM1a and BM1b). The first one is a cranial bone fragment while the second is a piece of long bone. Looking at all six samples together, there is a correlation between the cyanamide content (CN/P) and the $\delta^{13}C$ values and an inverse correlation between the $\delta^{13}C$ and $\delta^{18}O$ values (Figure 8.9). This will be discussed in the final sections of this chapter.

3.4 Ballynahatty (Co. Down)

As observed for the samples from Ballymacaldrack, there is a strong correlation between the cyanamide content of the calcined samples from Ballynahatty and their $\delta^{13}C$ values. Furthermore, there is an almost perfect inverse correlation between the $\delta^{13}C$ and $\delta^{18}O$ values. Comparing the strontium isotope results obtained for tooth enamel and calcined bone, it appears that the enamel samples exhibit lower ratios (0.7085–0.7090) than calcined bone (0.7094–0.7104) (t-test *p*-value = 0.005). Enamel samples have values consistent with the

local BASr and the average BASr values calculated for 5, 10 and 20 km catchments (Figure 8.12). Calcined bone samples have values approaching those of the outcrop 2 km south of the site (Formation 49 – 0.7109 ± 0.0005). Of the four calcined bone samples, three (BN1, BN3 and BN4) have very similar values (0.7103–0.7104) while BN2 has a slightly lower value (0.7094). The infrared results (C/C ratio and IRSF) suggest at least two of the samples (BN1 and BN2) were burned at higher temperature (close to 900°C) than those from Ballymacaldrack (Figure 8.11).

3.5 Clontygora (Co. Armagh)

The three calcined bone samples from Clontygora have similar strontium isotope ratios (0.7091–0.7093), but these are completely different to the BASr value of the granite outcrop on which the site lies, and the BASr averages calculated for different catchment areas (0.7113–0.7117).They have, however, values very similar to the sea water value of 0.7092 (Figure 8.14). The bone fragments appear to have been burned around 800°C as suggested by their infrared indices (C/C ratio and IRSF). Only one of the samples shows the presence of cyanamide, and, even though they are not as good as for the previous sites (e.g. Ballynahatty), it is still possible to observe a correlation between CN/P and $\delta^{13}C$ values and the inverse correlation between the $\delta^{13}C$ and $\delta^{18}O$ values of the calcined bone samples (Figure 8.13).

3.6 Knowth (Co. Meath)

A total of 26 calcined bone fragments (charred samples were excluded) and eight unburned enamel samples from Knowth were analysed. The results will not be presented for each sample individually as done for the other sites, but instead these will be split into three groups. ‘Bone 1’ includes the calcined bone with no or lower cyanamide content (CN/P < 0.50), than those in the second group, ‘Bone 2’ (CN/P > 0.50). The last group (‘Teeth’)

presents the tooth enamel results. The limit of CN/P > 0.50 was chosen as the highest CN/P observed at all other site is 0.48 (except for the not fully calcined bone P4 from Parknabinnia). Knowth is indeed the only site presenting samples with such high CN/P and is also the site with the highest proportion of samples with CN/P ≥ 0.25 (77% compared to 39% average).

Most of the samples have $^{87}Sr/^{86}Sr$ values falling within the range of BASr values calculated for the 5, 10 and 20 km catchment areas (0.7094–07100 – Figure 8.16). A few samples (two unburned tooth and five calcined bone fragments) have values between 0.7100 and 0.7110 going towards the BASr values of the formation 2 km to the north and that extends up to the Mourne Mountains (49 – 0.7109 ± 0.0005). One enamel sample has a value of 0.7125. Such BASr values can be found in the Mourne Mountains (Formations 8 and 9) ca. 50 km in the north.

Looking at tombs from which the analysed enamel and calcined bone fragments originate (Figure 8.5a), the three samples with highest strontium isotope ratio (> 0.7105) are from tombs 2, 14 and 15. The two tombs with the highest number of samples analysed are the eastern passage of the main mound (tomb 1BE) and tomb 16. The samples found in tomb 1BE show a similar range of $^{87}Sr/^{86}Sr$ values compared to tomb 16. Furthermore, comparing the results obtained for the samples of the difference recesses of tomb 1BE (RHR, LHR and ER – right-hand recess, left-hand recess and end recess respectively) no difference can be observed (for RHR and LHR, t-test *p*-value = 0.43) even though four of the five samples of the LHR are unburned tooth enamel fragments while all those from the RHR are calcined bone pieces (Figure 8.5b). No variation was observed with the age (radiocarbon dates) of the samples.

Once again there is a correlation between the $\delta^{13}C$ values and the CN/P for the calcined bone fragments. The inverse correlation between $\delta^{13}C$ and $\delta^{18}O$ values observed in most

archaeological site and in modern samples burned outdoors exists in the group of bone samples that have lower CN/P ('Bone 1') but not in the other ('Bone 2'). Finally, the C/C ratio and IRSF indicate that some samples fall within the 800°C and 900°C fields but most of them fall outside these fields (Figure 8.15).

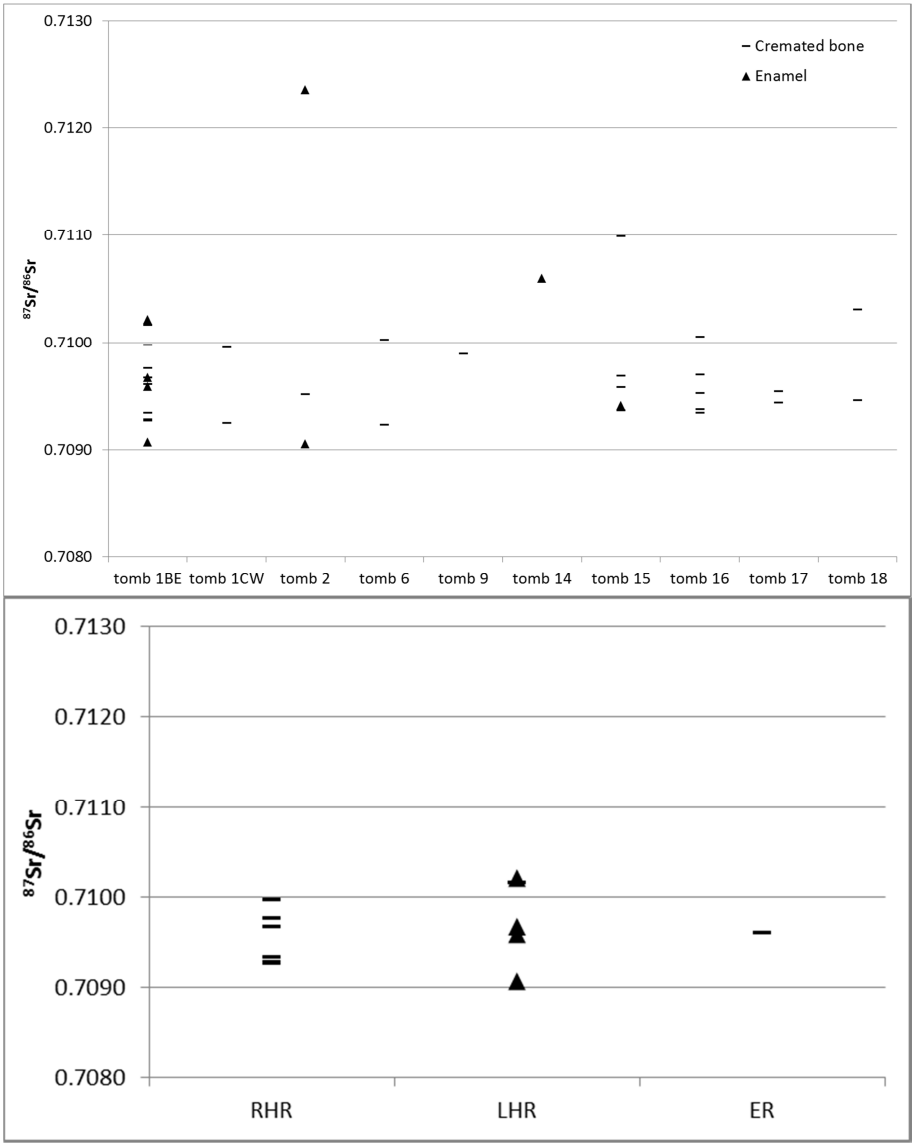

Figure 8.5 – Strontium isotope results for the unburned enamel and calcined bone samples from (a) the different tombs at Knowth and (b) for the Eastern passage of the main mound (1BE) separated depending on their context (RHR, LHR and ER – right-hand recess, left-hand recess and end recess respectively)

3.7 Legland (Co. Tyrone)

The two samples from Legland have very distinct strontium isotope ratios (0.7099 and 0.7136). The first sample has a ratio similar to the average BASr calculated for the 20 km catchment area (Figure 8.18), while the second has a ratio corresponding to the BASr value measured for the outcrop on which the site is (Formation 27 – 0.7133 ± 0.0014). The infrared data suggests both samples were heated around 800°C. L1, which has the lowest strontium isotope ratio, contains cyanamide and is depleted in ^{13}C. No variation in $\delta^{18}O$ is observed (Figure 8.17).

3.8 Parknabinnia (Co. Clare)

The results obtained for the three sub-samples (P3a, P3b and P3c) of the same calcined bone show a small variation in $^{87}Sr/^{86}Sr$ values (0.0004) but a much higher variability in the $\delta^{13}C$ and $\delta^{18}O$ values: ca. 3 ‰ and 1.5 ‰ respectively. The infrared results are very similar for each sub-sample.

Of the eight samples analysed from Parknabinnia, only two enamel fragments from chamber 2 (T3 and T4) have $^{87}Sr/^{86}Sr$ values in range with the local BASr and the average BASr values calculated for 5, 10 and 20 km catchment areas (Figure 8.20). The two other enamel samples, as well as two cremated bone fragments (all from Chamber 1), have strontium isotope ratios between the BASr value of outcrop on which the site lies (Formation 64 – 0.7086 ± 0.0002) and the adjacent outcrop BASr value (Formation 71 – 0.7104 ± 0.0007). Two final samples have values above 0.7110 that can be found on the Slieve Aughty uplands in the east and south-east (Formations 49 and 54). Once again there is a correlation between the CN/P and the $\delta^{13}C$ values of the calcined bone samples and an inverse correlation between the $\delta^{13}C$ and $\delta^{18}O$ values (P4 being still charred (colour code 4.5) is not included for the calculation of this correlation). All samples fall outside the temperature fields but are still close to the 800°C and 900°C fields (Figure 8.19).

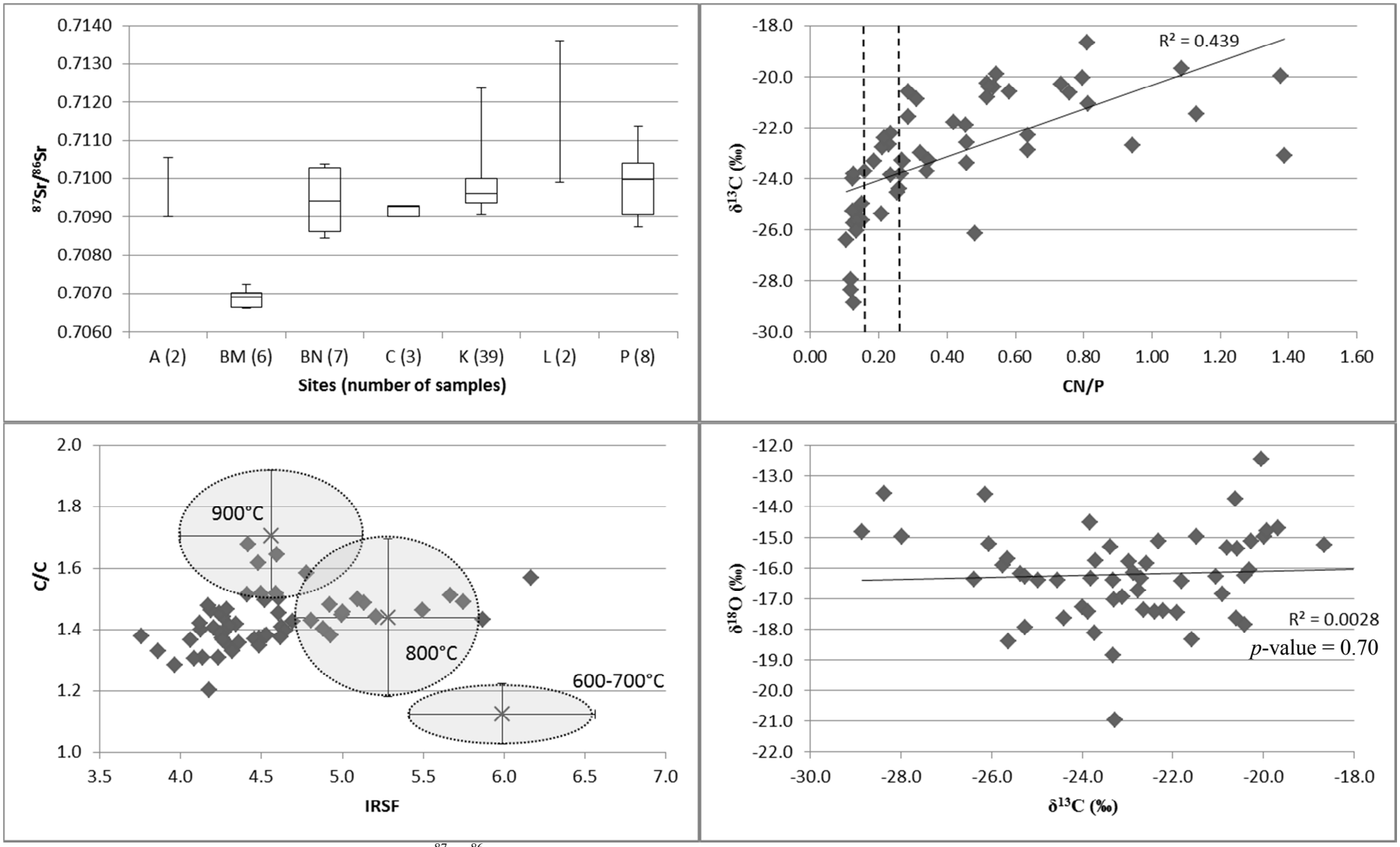

Figure 8.6 – (a) Boxplot for strontium isotope ratios ($^{87}Sr/^{86}Sr$) for each site calculated for all samples (tooth enamel and calcined bone); if only two samples, both values are shown; (b) $\delta^{13}C$ value versus CN/P ratio; (c) C/C ratio versus IRSF; (d) $\delta^{18}O$ value versus $\delta^{13}C$ value for all calcined bone fragments

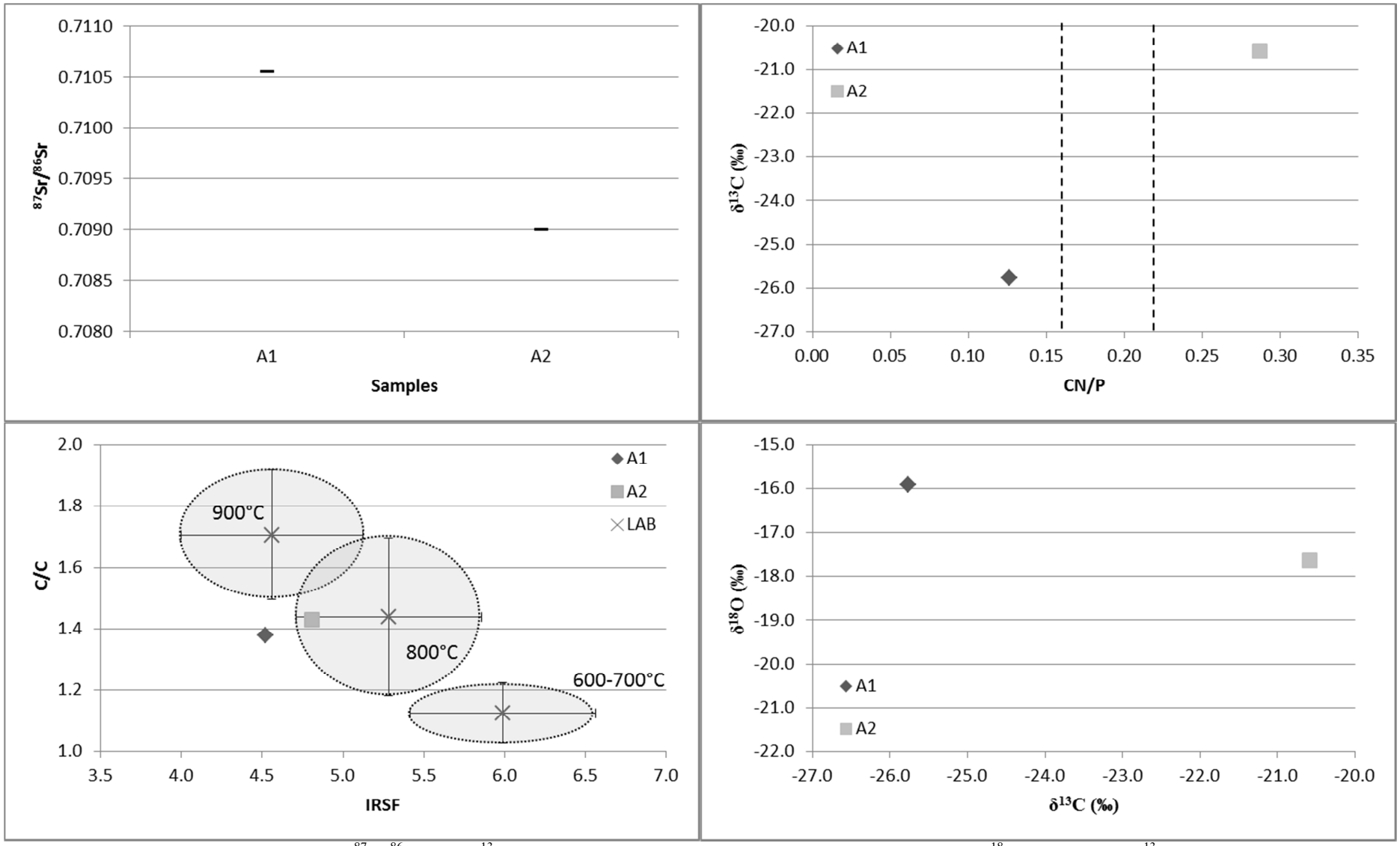

Figure 8.7 – (a) Strontium isotope ratios ($^{87}Sr/^{86}Sr$); (b) $\delta^{13}C$ value versus CN/P ratio; (c) C/C ratio versus IRSF; (d) $\delta^{18}O$ value versus $\delta^{13}C$ value for all calcined bone fragments from Annaghmare

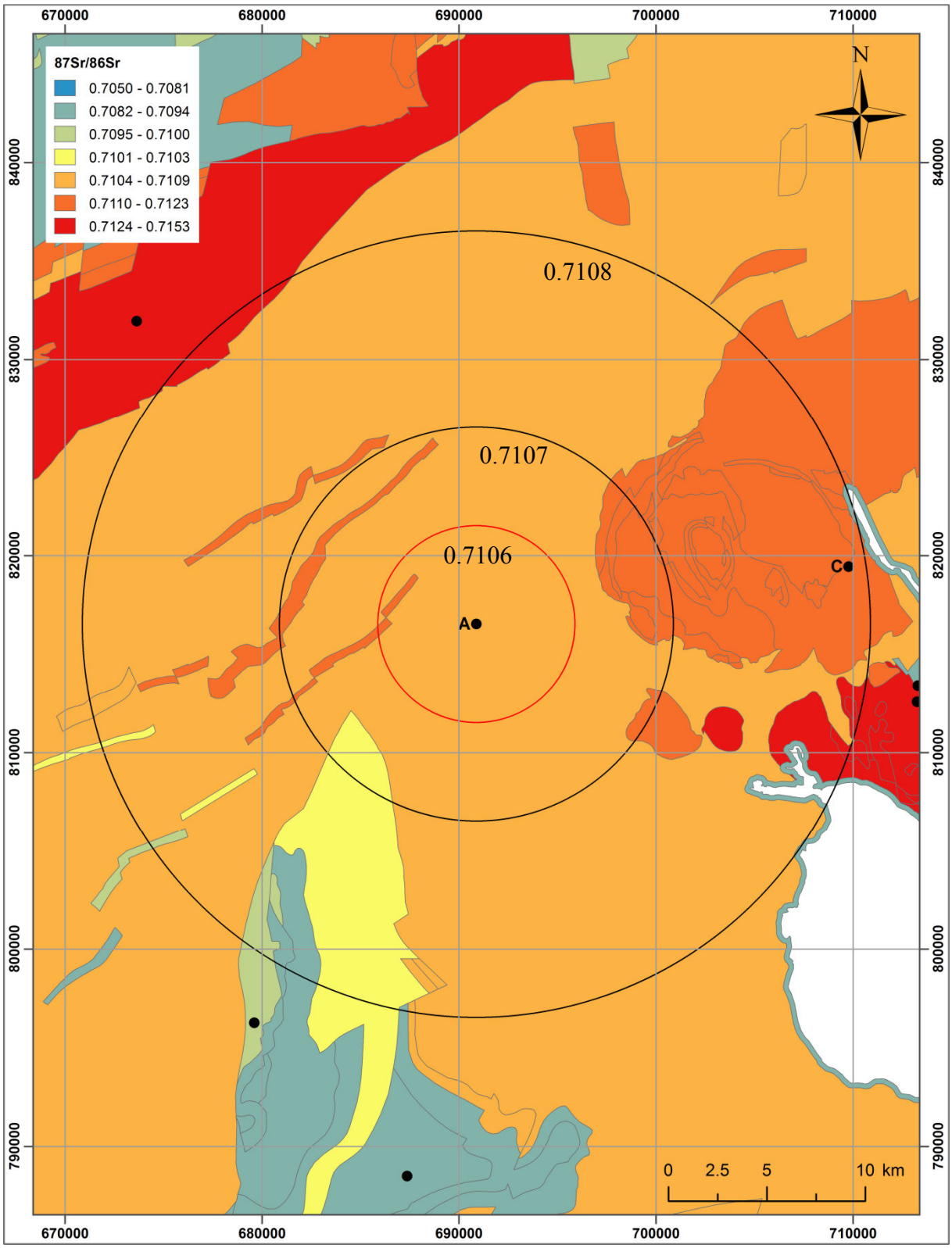

Figure 8.8 – 5, 10 and 20 km catchment areas around the site of Annaghmare based on the single-part BASr map; average BASr values for each catchment area are indicated

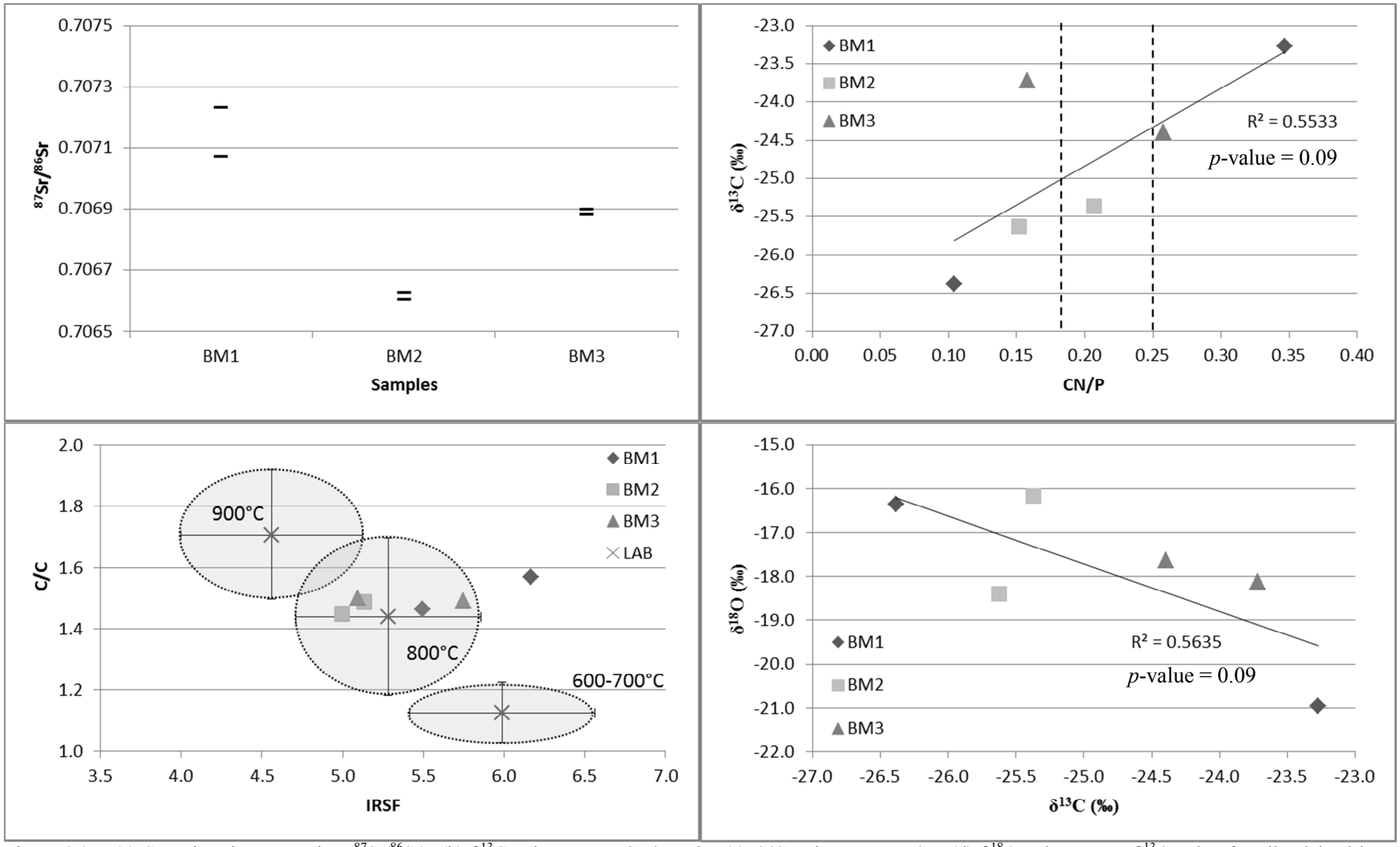

Figure 8.9 – (a) Strontium isotope ratios ($^{87}Sr/^{86}Sr$); (b) $\delta^{13}C$ value versus CN/P ratio; (c) C/C ratio versus IRSF; (d) $\delta^{18}O$ value versus $\delta^{13}C$ value for all calcined bone fragments from Ballymacaldrack

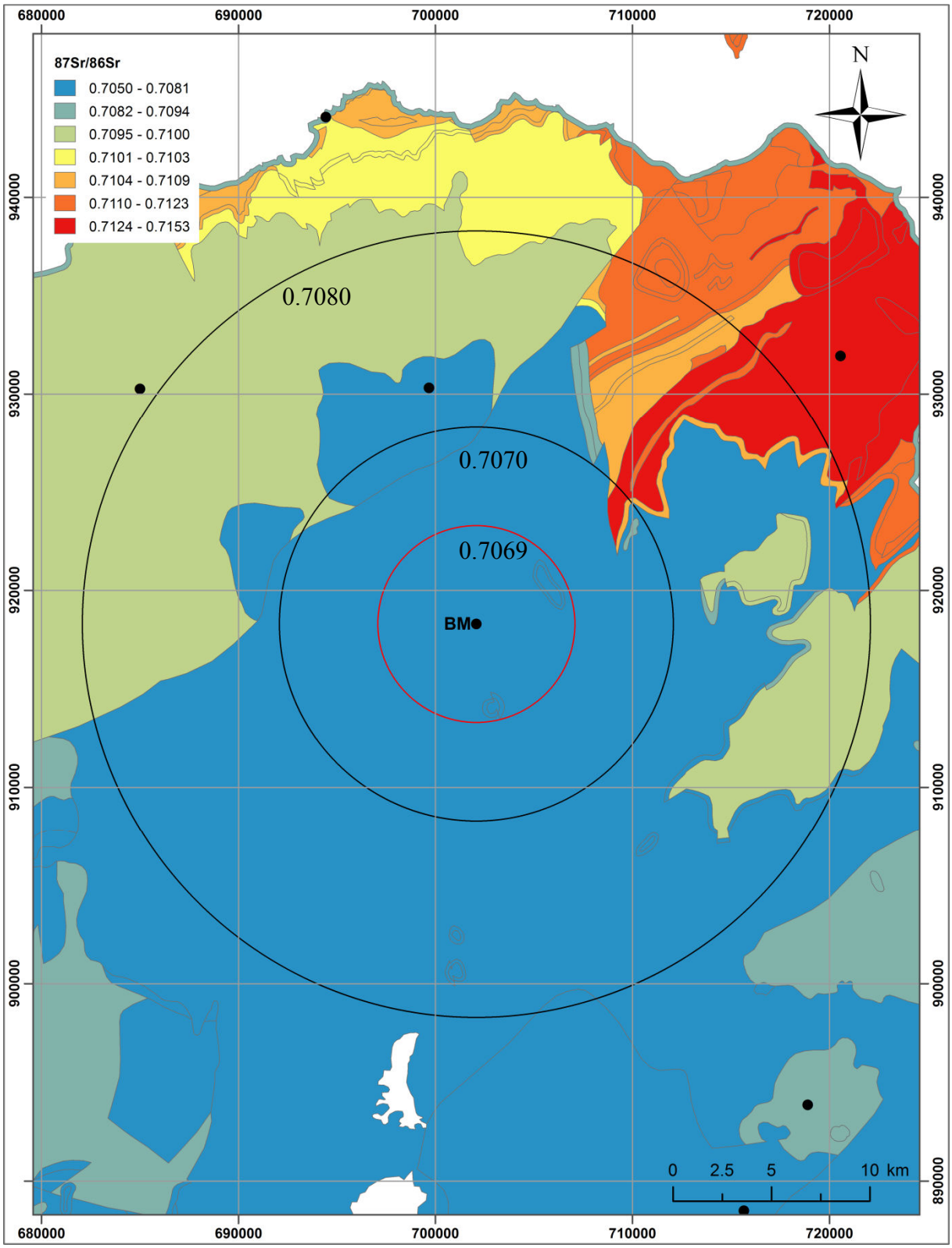

Figure 8.10 – 5, 10 and 20 km catchment areas around the site of Ballymacaldrack based on the single-part BASr map; average BASr values for each catchment area are indicated

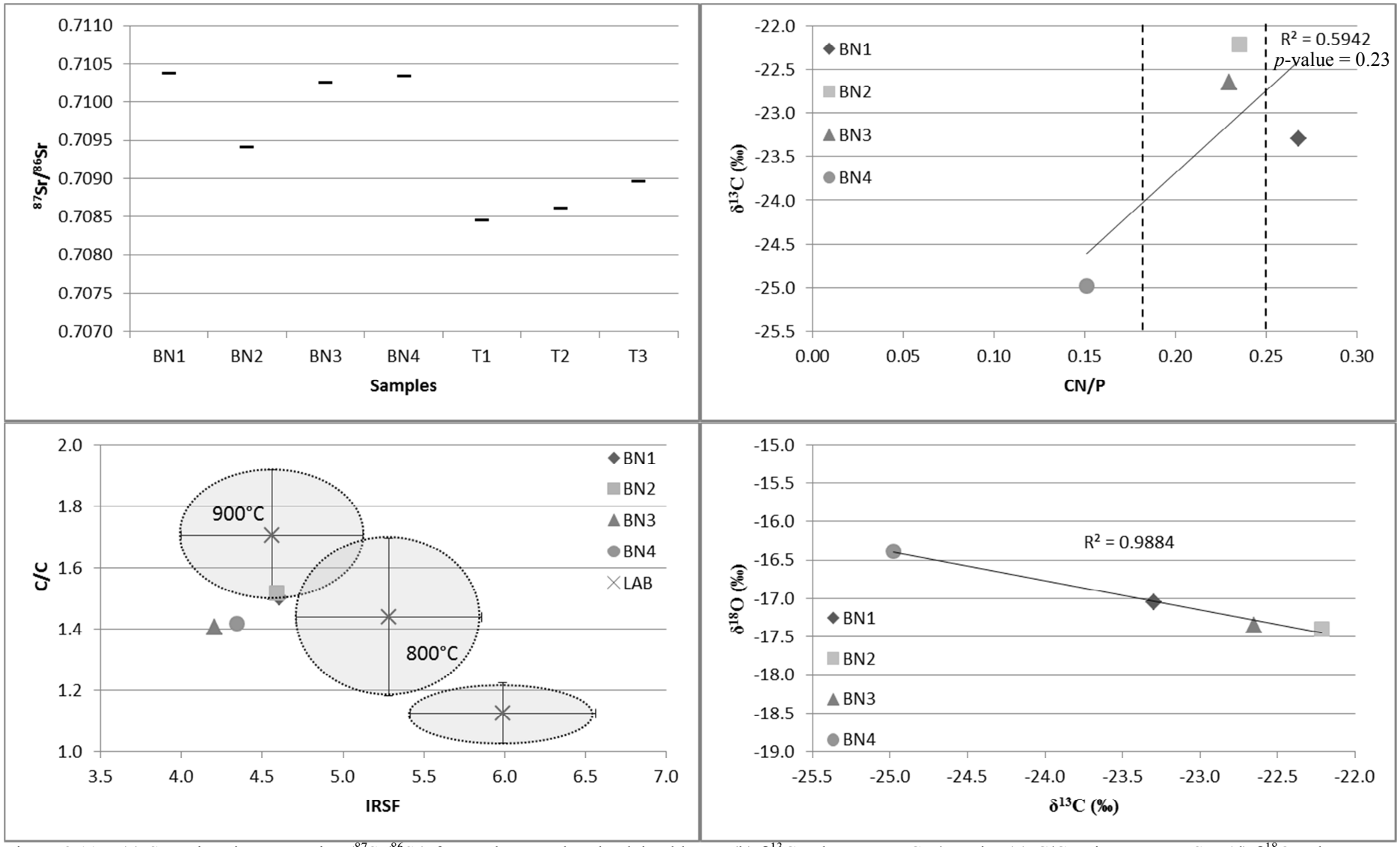

Figure 8.11 – (a) Strontium isotope ratios ($^{87}Sr/^{86}Sr$) for tooth enamel and calcined bone; (b) $\delta^{13}C$ value versus CN/P ratio; (c) C/C ratio versus IRSF; (d) $\delta^{18}O$ value versus $\delta^{13}C$ value for all calcined bone fragments from Ballynahatty

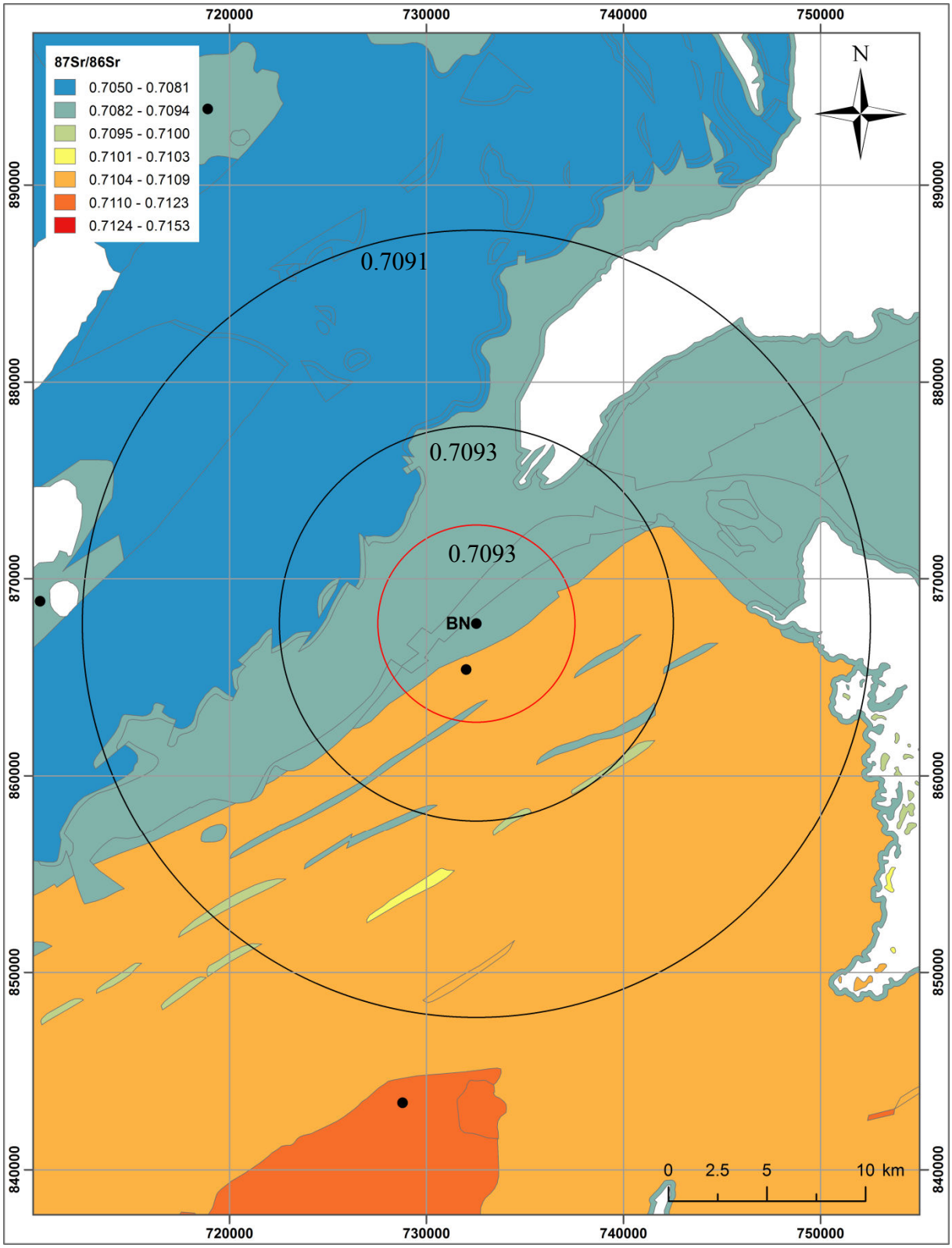

Figure 8.12 – 5, 10 and 20 km catchment areas around the site of Ballynahatty based on the single-part BASr map; average BASr values for each catchment area are indicated

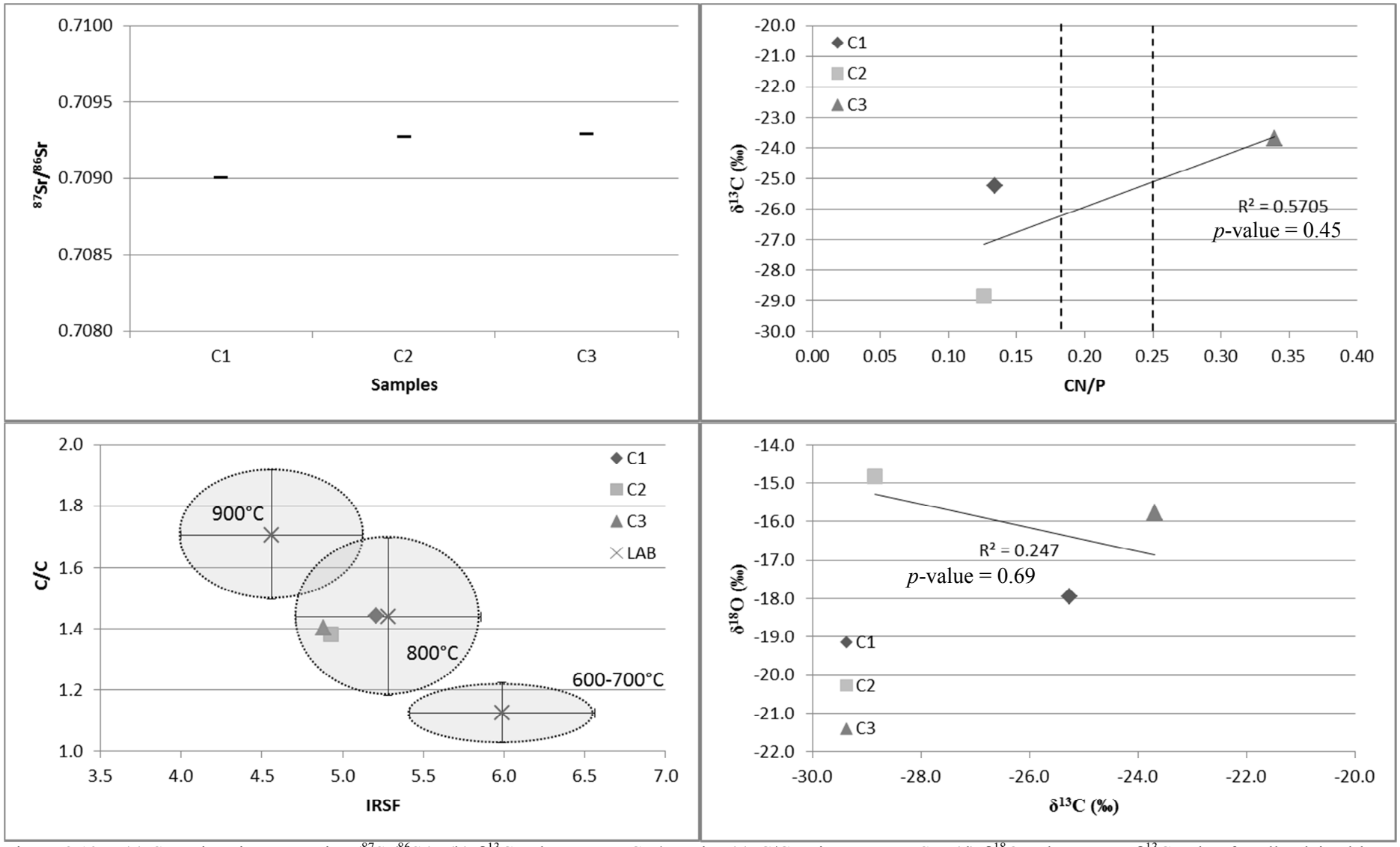

Figure 8.13 – (a) Strontium isotope ratios ($^{87}Sr/^{86}Sr$); (b) $\delta^{13}C$ value versus CN/P ratio; (c) C/C ratio versus IRSF; (d) $\delta^{18}O$ value versus $\delta^{13}C$ value for all calcined bone fragments from Clontygora

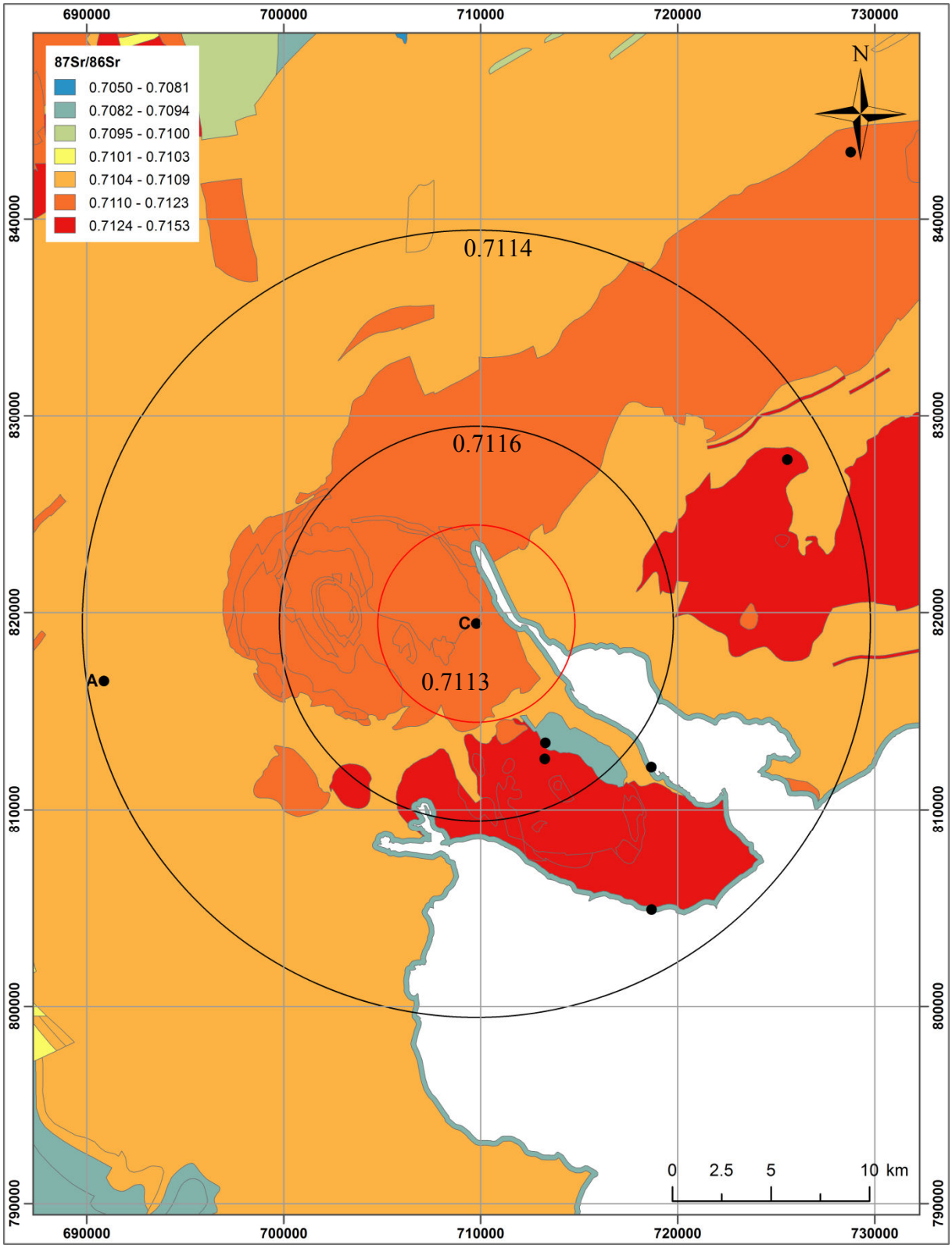

Figure 8.14 – 5, 10 and 20 km catchment areas around the site of Clontygora based on the single-part BASr map; average BASr values for each catchment area are indicated

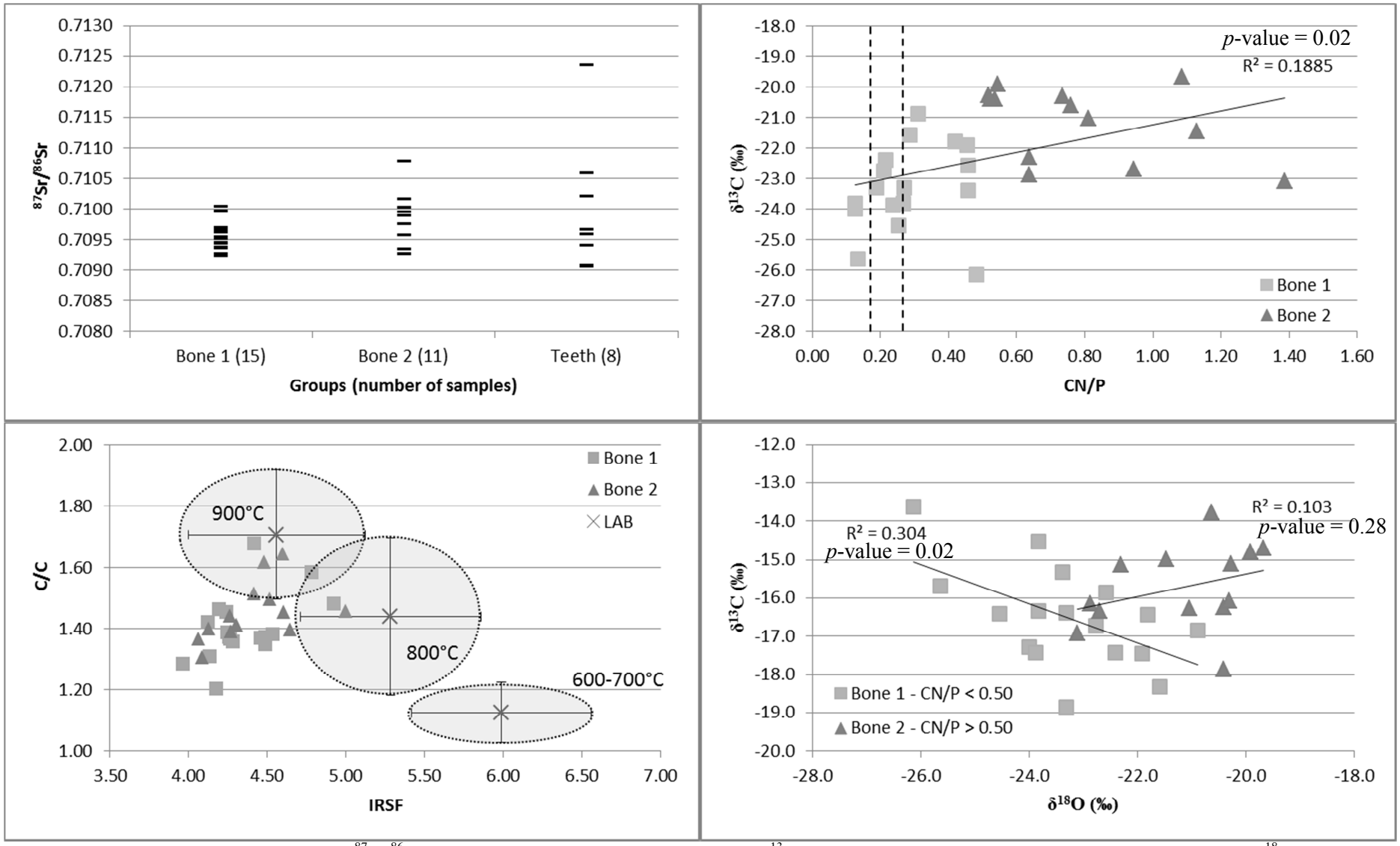

Figure 8.15 – (a) Strontium isotope ratios ($^{87}Sr/^{86}Sr$) for tooth enamel and calcined bone; (b) $\delta^{13}C$ value versus CN/P ratio; (c) C/C ratio versus IRSF; (d) $\delta^{18}O$ value versus $\delta^{13}C$ value for all calcined bone fragments from Knowth

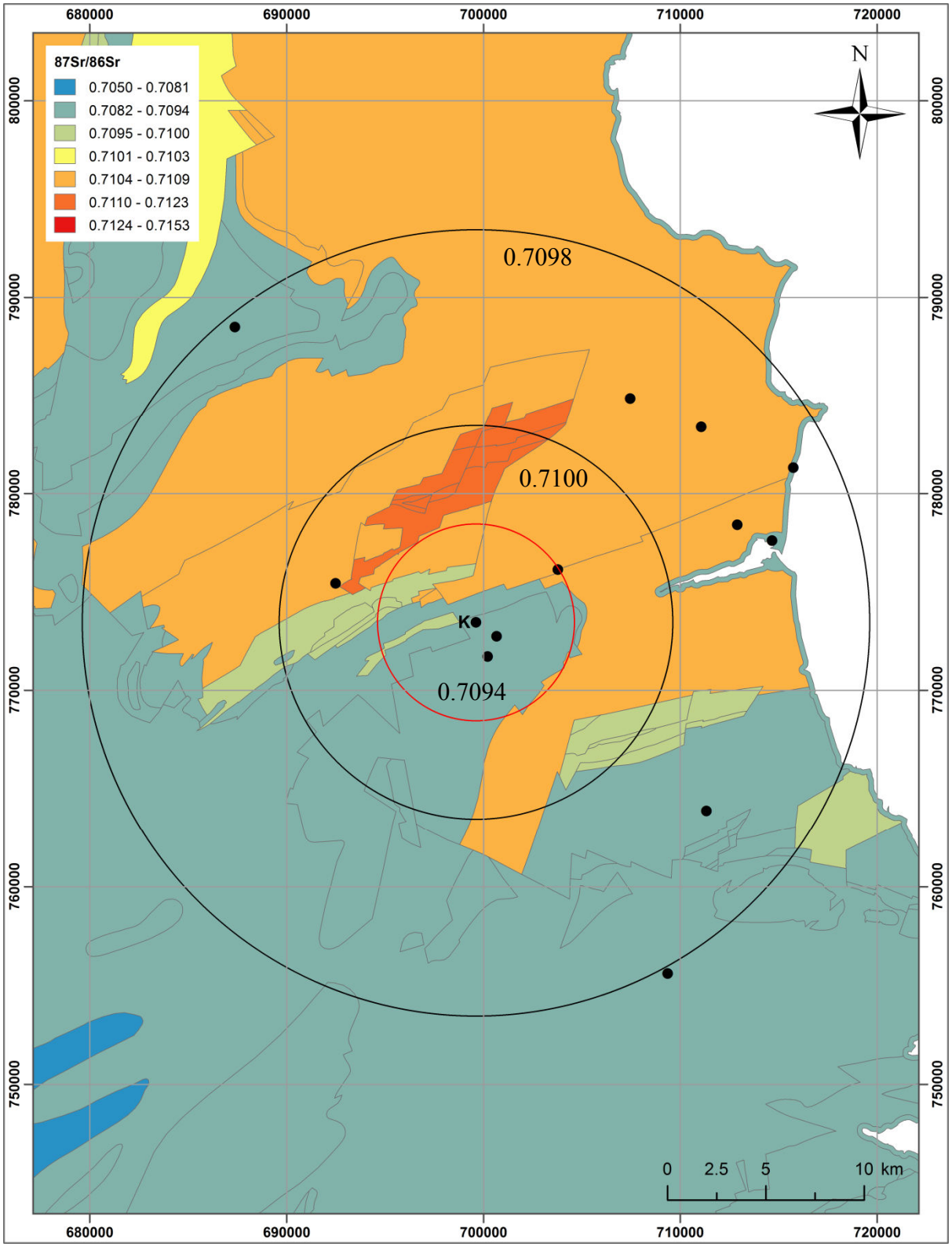

Figure 8.16 – 5, 10 and 20 km catchment areas around the site of Knowth based on the single-part BASr map; average BASr values for each catchment area are indicated

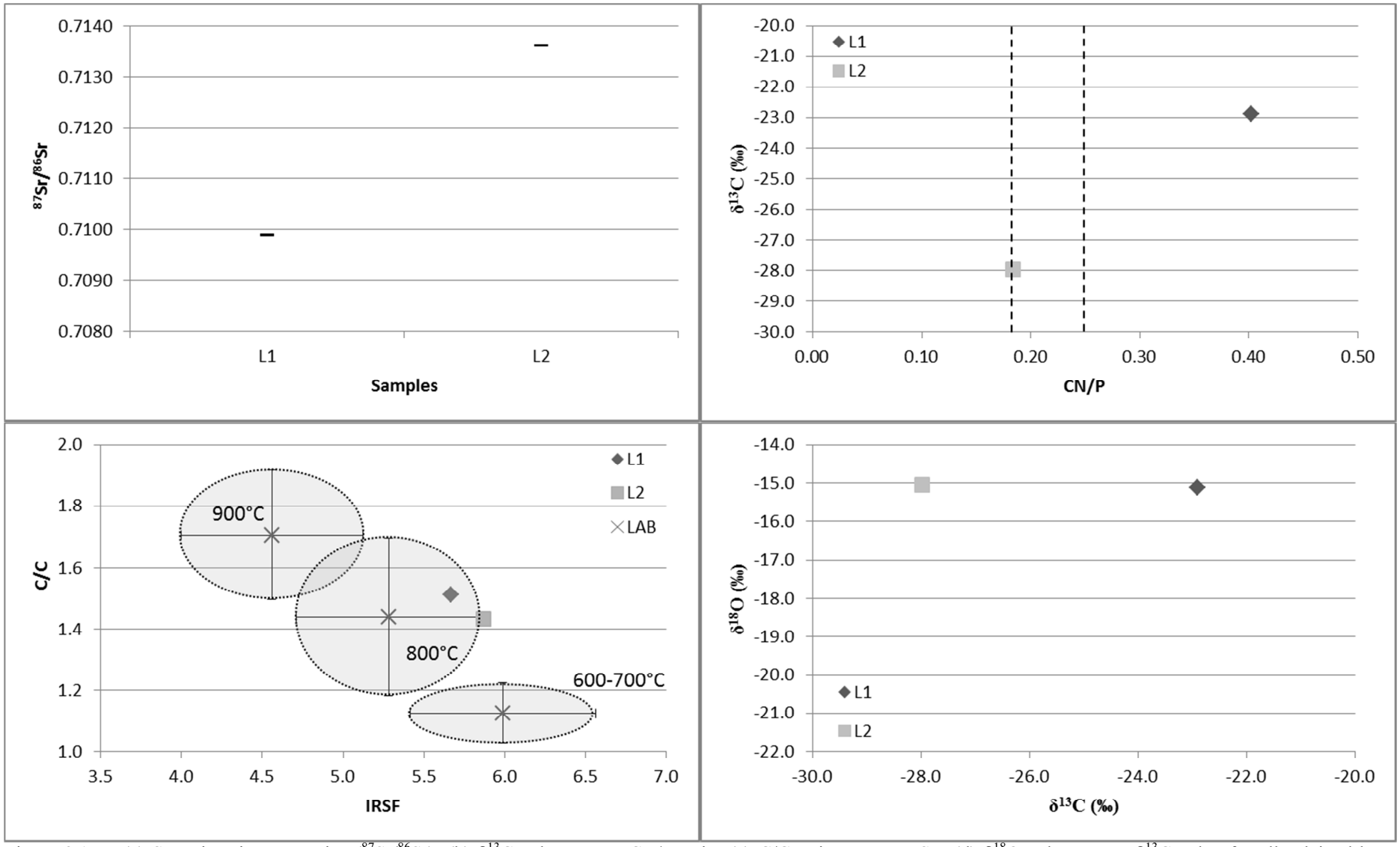

Figure 8.17 – (a) Strontium isotope ratios ($^{87}Sr/^{86}Sr$); (b) $\delta^{13}C$ value versus CN/P ratio; (c) C/C ratio versus IRSF; (d) $\delta^{18}O$ value versus $\delta^{13}C$ value for all calcined bone fragments from Legland

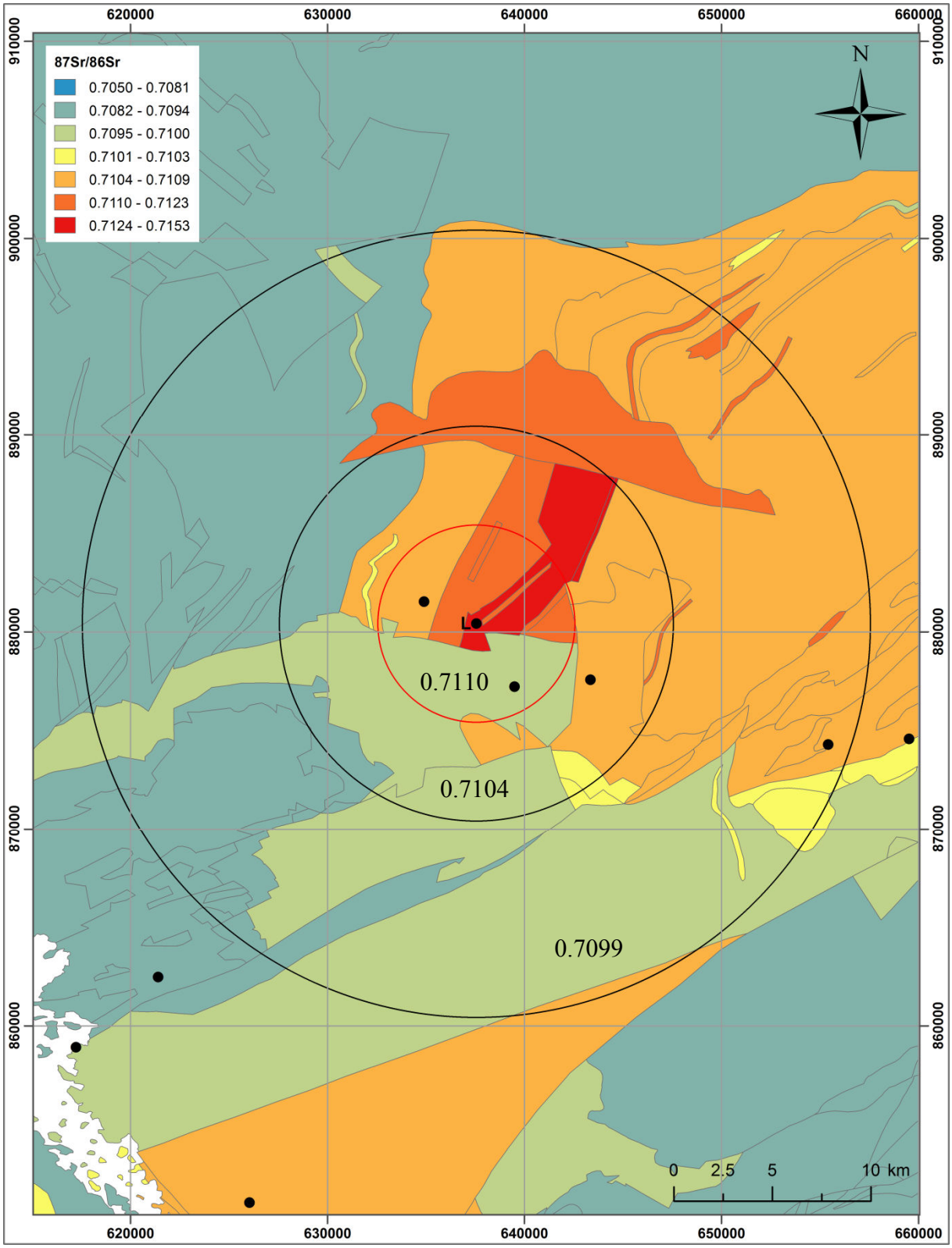

Figure 8.18 – 5, 10 and 20 km catchment areas around the site of Legland based on the single-part BASr map; average BASr values for each catchment area are indicated

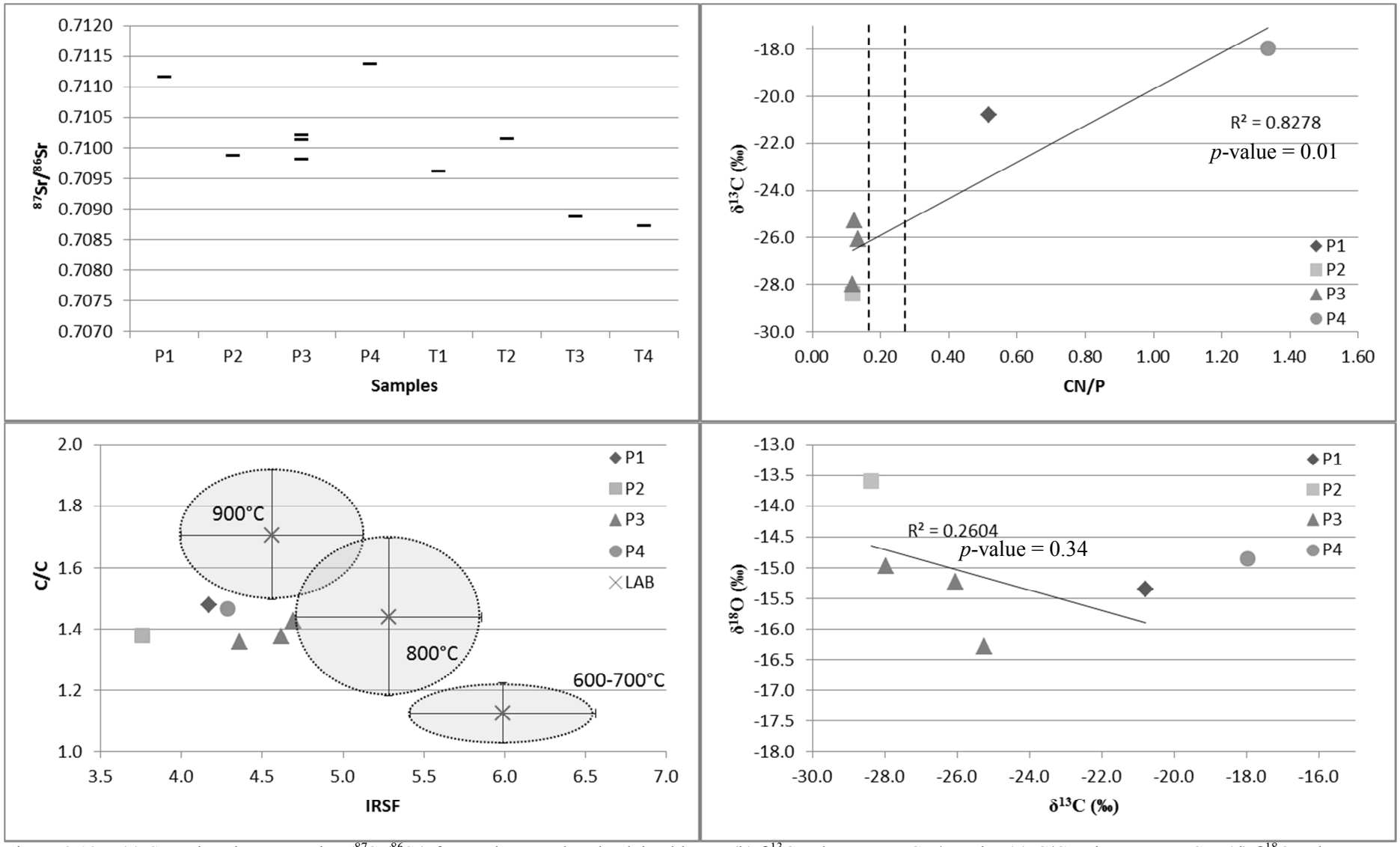

Figure 8.19 – (a) Strontium isotope ratios ($^{87}Sr/^{86}Sr$) for tooth enamel and calcined bone; (b) $\delta^{13}C$ value versus CN/P ratio; (c) C/C ratio versus IRSF; (d) $\delta^{18}O$ value versus $\delta^{13}C$ value for all calcined bone fragments from Parknabinnia

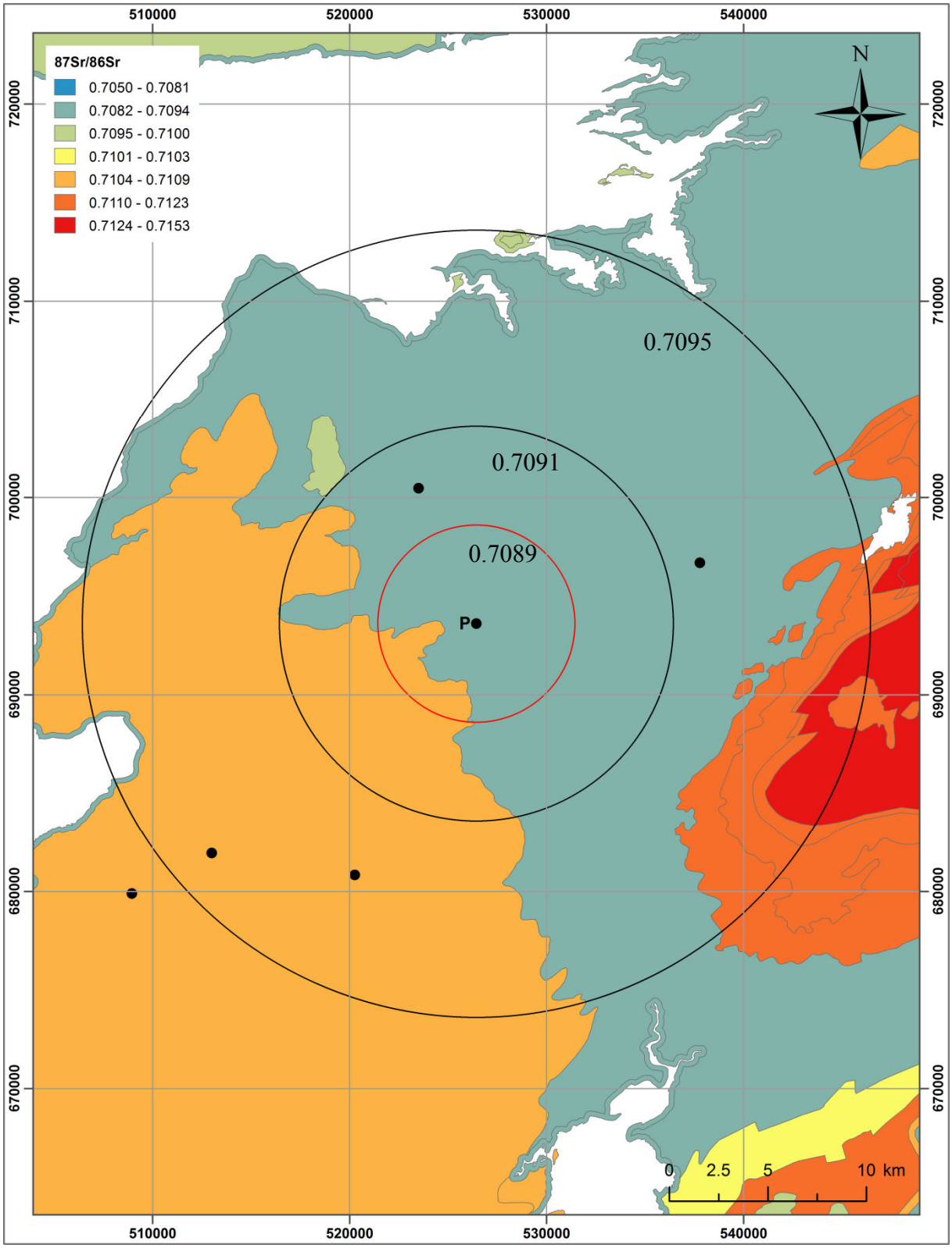

Figure 8.20 – 5, 10 and 20 km catchment areas around the site of Parknabinnia based on the single-part BASr map; average BASr values for each catchment area are indicated

4 Discussion

4.1 Definition of non-locals

As comprehensively detailed by Montgomery (2010), the mere fact that an individual has a strontium isotope ratio similar to BASr value of the local outcrop where his remains were found does not mean the individual actually originates from that site. Indeed, he could have lived somewhere else but eaten food growing on that outcrop, lived on the same outcrop but not close to the site (e.g. the geology around Ballymacladrack remains similar for more than 20 km to the south), or originated from another outcrop with similar BASr values (as seen in Ireland, there are many outcrops with similar BASr values – see Chapter 7). Furthermore, it is possible that an individual ate food from two different outcrops with distinct BASr values that when combined produce an apparent $^{87}Sr/^{86}Sr$ value similar to the BASr value of the place where he was buried, etc. Finally, as highlighted by the analyses of three sub-samples of the same calcined bone fragments (P3), there is some variability in the strontium isotope ratio of cremated individuals and variations lower than 0.0004 in $^{87}Sr/^{86}Sr$ values of calcined bone should not be interpreted. This variability may be due to bone turnover as, contrarily to tooth enamel that will keep its strontium isotope ratio permanently once formed, the strontium isotope composition of bone will change over time. Consequently, the measured values are an average of all the food and drinks consumed by that individual over the last decade or more of his life.

When defining 'local' individuals, it is crucial to keep these caveats in mind. Nevertheless, here, I make the assumption that most individuals having a strontium isotope ratio in range with the regional BASr values are likely to be 'locals'. In this work, an individual will be defined as a non-local if both following conditions are validated: (1) the sample has a strontium isotope ratio two standard deviations or more away from the average

BASr value measured for the outcrop where its remains were excavated, and (2) its $^{87}Sr/^{86}Sr$ value is not between the BASr value of the local outcrop and that of the BASr calculated for the 5, 10 and 20 km catchment areas. Following that rationale, it is possible to define '5, 10 and 20 km non-locals' (Table 8.8). The number of non-locals evaluated for each site reveals that the number of non-locals is extremely variable going from 0% (Ballymacaldrack) to 75% (Parknabinnia). The highest variability observed in the number of non-locals looking at the different catchment areas is in Knowth, where 65% of the individuals are defined as non-locals for the 5 km catchment area but only 21 % for the 10 km catchment area.

Table 8.9 – Number of non-locals for 5, 10 and 20 km catchment areas

	5km	**10km**	**20km**
Annaghmare	1/1	1/1	1/1
Ballymacaldrack	6/0	6/0	6/0
Ballynahatty	4/3	4/3	4/3
Clontygora	3/0	3/0	3/0
Knowth	12/22	27/7	24/10
Legland	1/1	1/1	2/0
Parknabinnia	2/6	2/6	2/6
TOTAL	**29/33 (53 %)**	**44/18 (29 %)**	**42/20 (32 %)**

This method is one possible way to define non-locals but each site should still be seen as an individual entity. Indeed, in the case of Clontygora, all three samples appear to be 'locals' because of the very high variability of the $^{87}Sr/^{86}Sr$ values measured in plant samples for the local outcrop. However, it is unlikely that plants growing on Tertiary granitic formations will have values as low as 0.7093 suggesting that the three individuals from Clontygora are actually non-locals. Furthermore, for Legland, the geology is so varied around the site that the individual defined as non-local for the 5 and 10 km catchment areas could very well originate from less than 10 km from the site.

4.2 Northern Counties

The number of samples for each Northern site is very limited (between two and seven) and it is difficult to discuss the behaviour of Neolithic and Bronze Age humans in that region with such low numbers. Nevertheless, the results highlight interesting differences between the various sites. Looking at the two Neolithic court tombs of Annaghmare and Clontygora that are only 20 km away from each other, both site are on outcrops with high strontium isotope ratios and average BASr values above 0.7105. Yet, only one sample from Annaghmare has a $^{87}Sr/^{86}Sr$ value consistent with the BASr value of the local outcrop. All others (one from Annaghmare and three from Clontygora) have values between 0.7090 and 0.7093, bracketing the sea water value of 0.7092. However, the use of marine resources has been shown to be minimal during the Irish and British Neolithic (Richards et al. 2003; Schulting et al. 2012; forthcoming; Schulting 2013; Ditchfield 2014) and the sea spray effect is limited to coastal regions. This suggests that these four individuals must originate from different regions such as the basalt formations of Co. Antrim more than 50 km to the north, or, more likely, from southern regions where limestone is the main rock type (about 50 km to the south, south-west). Nevertheless, to confirm this, measuring strontium concentration on these samples could allow detecting intake of marine resources such as algae and salt (Montgomery 2010).

The radiocarbon date obtained for Annaghmare (3494–3116 cal BC) falls within the range seen in the previous radiocarbon dates obtained for the site. The date for Clontygora (2199–2026 cal BC) appears much younger. It is likely that the bone dated for Clontygora is not contemporary with its construction, but corresponds to a re-use of the monument during the Early Bronze Age. Indeed, while the court tomb at Annaghmare seems to have been ritually sealed during the Neolithic when it was no longer of use, it was not the case at Clontygora.

While the two previous sites clearly showed the presence of non-locals, at Ballymacaldrack, no non-locals were found. Indeed, all $^{87}Sr/^{86}Sr$ values obtained from calcined bone fragments are in range with the local BASr value, though the geology remains the same for about 10 km to the north and more than 20 km to the south. In this case, any individual relying on food grown on the basalt outcrop will appear to be local. The situation at Ballynahatty and Legland is more complex. Both sites lie on small geological outcrops with much variation in the surrounding area. At Legland it seems that the individual with lower strontium isotope ratio mainly consumed food originating from south of the site where the BASr values are lower, while the second ate dominantly food from north of the site. At Ballynahatty, there is an interesting difference between the enamel and calcined bone samples. The enamel samples have values similar to the local BASr values and that of outcrops located in the north, while cremated bone fragments exhibit values more consistent with the BASr values of the outcrop present 2 km south of the site which remains similar for about 70 km to the south, south-west. The archaeology suggests that different funerary rites are represented in the circular chamber and it appears that the different rites were reserved to different subsets of individuals with those from the north being inhumed while those from the south being cremated. Looking at cremation practices, it seems that at most sites, bodies were burned at 800°C but at Ballynahatty, it is possible that some were burned at higher temperatures (900°C).

4.3 Knowth

The first striking result obtained for the calcined bone from the various passage tombs of Knowth is the large number of samples containing cyanamide (ca. 77%) and the high CN/P (> 0.50) seen in more than half of the samples containing cyanamide. Such high CN/P values are not observed in the other sites or any of the heated modern bone. This could suggest different cremation practices compared to other sites. Knowth, and the Boyne Valley in

general, was an important centre of activity. It is possible that the pyres used to cremate the deceased were much bigger than at other sites, limiting oxygen availability (making difficult the complete combustion of organic matter and fuel into CO_2), favouring the incorporation of cyanamide into the structure of bone apatite. These hypothetical larger pyres would also reach higher temperatures. This is suggested by the observation that several samples from Knowth fall within the 900°C field.

Turning to the $^{87}Sr/^{86}Sr$ values obtained for unburned enamel and calcined bone, most samples have values between the local BASr signal and the calculated average BASr values for 10 and 20 km catchment areas suggesting that those buried at Knowth (both unburned and cremated) used fields in the vicinity of the tombs for pastures and crops combining northern and southern regions (as suggested by Cooney 2000). A few samples show values consistent with the geological formation (49) to the north which remains unchanged up to the Mourne Mountains. None, however, have values corresponding to the very wide Carboniferous limestone outcrops (65) to the south and west of Knowth going as far as the Wicklow Mountains (ca. 50 km to the south). Finally, one enamel sample has a value comparable to the Mourne Mountains granite BASr. This sample also has the highest $\delta^{13}C$ and lowest $\delta^{18}O$ values of all analysed enamel samples (Figure 8.4a) reinforcing its non-local attribution.

Considering all of the above, it appears that those interred at Knowth originated mainly from the direct surroundings of the site (79% of locals for 10 km catchment area) with a few individuals from the north up to the Mourne Mountains, but there is however no evidence for individuals originating from the south and the Wicklow Mountains. There is definitely no difference between unburned and inhumed individuals refuting the hypothesis according to which cremated individuals came from further away (from similar regions as the stones used to build the tombs) as it would be easier to carry an urn/bowl containing calcined bone fragments than an entire corpse. Instead, it seems that both unburned and cremated

individuals were brought to the tombs (as suggested by the highly fragments remains found) from the vicinity of the site and as far as the Mourne Mountains. The results for each tomb/recess do not highlight a preferential tomb for non-locals. Finally, the radiocarbon dated obtained for the non-locals calcined bone fragments suggest a continuous movement of individuals between the site and the surrounding regions.

One suggestion that could be made regarding the two individuals showing the highest strontium isotope ratios (0.7110 and 0.7125) is that they both came from the Mourne Mountains (or another region with high BASr values). Indeed, the first sample (0.7110) is a calcined bone fragment while the second (0.7125) is a piece of tooth enamel. The tooth enamel shows the origin of the food consumed during childhood/early adolescence while the calcined bone fragments has a $^{87}Sr/^{86}Sr$ value averaging the food consumed over the last 10-15 years. It is therefore possible that these individuals lived in one place (e.g. the Mounre Mountains) during their childhood but moved towards Knowth during their lifetime. This would lead to an $^{87}Sr/^{86}Sr$ value in calcined bone between 0.7125 and the BASr value of the local outcrop.

An interesting observation can be made for the four sites located within 50 km of to the Mounre Montains (Annaghmare, Ballynahatty, Clontygora, and Knowth – Figure 8.21). Many samples from Knowth and the cremated individuals from Ballynahatty seem to consume food originating from the Silurian mudstone formation (north of Knowth and South of Ballynahatty – large orange outcrop on Figure 8.21) while an individual (out of two) from Annaghmare and all those from Clontygora that are actually on the Silurian mudstone formation, or very close to it, have $^{87}Sr/^{86}Sr$ values completely inconsistent with its BASr value. These have instead, values more consistent with the limestone formation values to the south-west or the basalt formations to the north (though the latter probably exhibit too low BASr values). This observation lets us wonder why those not buried directly on the Silurian

mudstone outcrop consumed food from that outcrop while those buried on the outcrop would not use the available local resources.

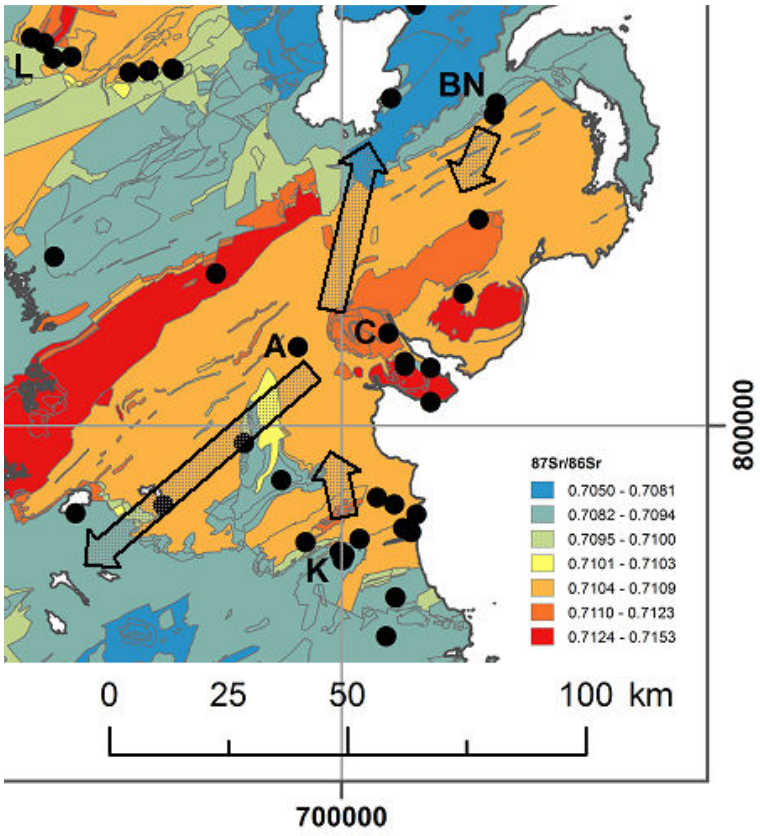

Figure 8.21 – Zoom on the BASr map (single-part) around the Mourne Mountains highlighting possible mobility patterns during the Neolithic and Bronze Age

Looking at other sites in the vicinity of the Boyne Valley, a particular case study that comes to mind is the isotopic study of the Early Bronze Age 'Tara Boy' found at the Tara Hill about 15 km south-west of Knowth (Sheridan et al. 2013). Its strontium isotope ratio of 0.7112 measured on tooth enamel is indeed inconsistent with the BASr values of the Carboniferous limestone where he was buried (Formation 65 – 0.7085 ± 0.0004). It has a similar value to one of the calcined bone fragments (0.7110) which has been suggested to originate from the Silurian mudstone formation (49 – 0.7109 ± 0.0005) north of the site (or even the Mourne Mountains – see previous paragraphs). Nevertheless, while this narrows down the possibilities within Ireland, as already highlighted by Sheridan et al. (2013), it

cannot be excluded that this individual originated from somewhere else, as suggested by the exotic grave goods he was buried with. Interestingly, at Knowth, no individuals showed strontium isotope ratios below 0.7090 that would have been consistent with the Carboniferous limestone formation (65) which could maybe suggest that farming was limited in that region. Analysing more human remains from Tara Hill (both unburned and cremated) would improve the understanding of dynamics, funeral rites and farming practices in the Boyne Valley region during the Neolithic and Bronze Age.

4.4 Parknabinnia

The strontium isotopic results for Parknabinnia highlight three different groups: one (P1 and P4 – chambers 1 and 2 respectively) with ratios higher than 0.7112; a second (P2, P3, T1 and T2 – chamber 1) with intermediate ratios from 0.7096 to 0.7102; and a final group (T3 and T4 – chamber 2) with lower ratios between 0.7086 and 0.7087, corresponding to the local BASr value (Figure 8.22).

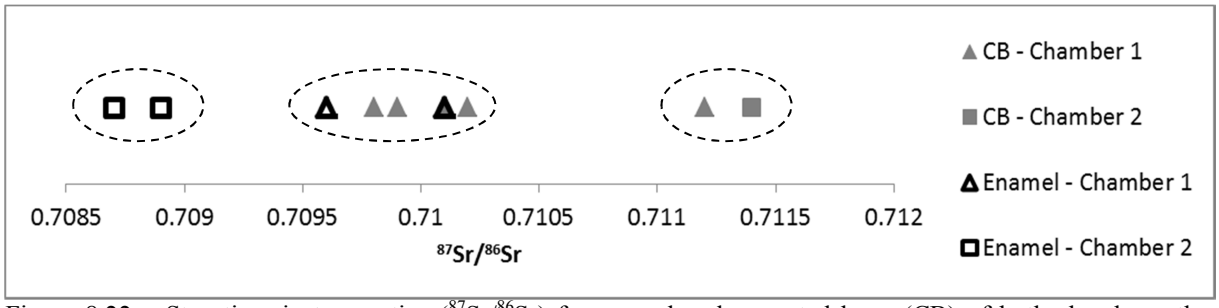

Figure 8.22 – Strontium isotope ratios ($^{87}Sr/^{86}Sr$) for enamel and cremated bone (CB) of both chambers; the three groups are highlighted

From the infrared data, P1 and P4 differ compared to P2 and P3: they contain cyanamide and have slightly higher C/C ratios. P1 and P4 also have the lowest carbon isotopes and highest strontium values. The fact that P1 and P4 are separated from P2 and P3 in so many different ways indicates that P1 and P4 originate from different areas. Additionally, it is possible that P1 and P4 were burned on different pyres. Indeed, while the

correlation between the $\delta^{13}C$ and $\delta^{18}O$ values of the calcined bone fragments (P1, P2 and P3) is not as good as observed for other sites (e.g. Ballynahatty), when looking only at P2 and P3, the correlation becomes much better (Figure 8.23). Furthermore, since they contain cyanamide P1 and P4 could have been burned on larger pyres but further investigation is required. Indeed, while at Knowth, is it likely that the presence of cyanamide highlights the use of larger pyres, at Ballymacaldrack, two samples from the same individual (BM1a and BM1b) have very different CN/P.

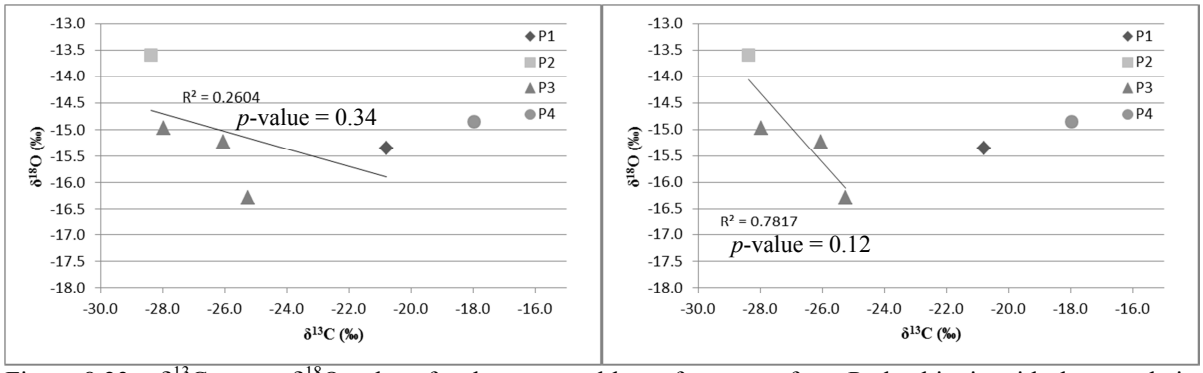

Figure 8.23 – $\delta^{13}C$ versus $\delta^{18}O$ values for the cremated bone fragments from Parknabinnia with the correlation calculated (a) for P1, P2 and P3, and (b) for P2 and P3 only

While P2 and P3 were excavated from chamber 1, P4 came from chamber 2 but P1 also came from chamber 1. Furthermore, P1 and P2 came from the same context (443) suggesting that people buried at the same time in Parknabinnia came from different places. Comparing the $^{87}Sr/^{86}Sr$ values to the surrounding BASr values, the enamel fragments from chamber 1 appear to be locals; the samples from chamber 2 except P1 seem to originate from the Carboniferous sandstone regions to the west. The calcined bone samples with values higher than 0.7112 (P1 and P4) most likely originate from the east or south-east regions 15 km from the site.

Tooth enamel fragments were also analysed for the portal tomb of Poulnabrone, Co, Clare (Kador 2010; Ditchfield 2014) situated on the same geology (Site I97, Formation 64). The results show that all but one sample (17 enamel fragments in total) have values between

0.7082 and 0.7092 consistent with the local BASr value (07086 ± 0.0002), suggesting most of them were local. The non-local has a value of 0.7102, similar to that of the samples from Chamber 1 at Parknabinnia, suggesting that this individual too came from western regions (located ca. 3.5 km from Poulnabrone and ca. 2.5 km from Parknabinnia). These results, however, do not support the hypothesis that portal tombs were for outsiders while court tombs were used by locals (Jones 2007); on the contrary. Since no average BASr values are available for catchment areas around Poulnabrone, it will be assumed that non-locals must have $^{87}Sr/^{86}Sr$ values more than three standard deviations (instead of two) away from the average BASr calculated for the outcrop on which both sites are (Formation 64). Following this rationale, only one (maybe two) individual(s) (out of 17) could be considered as a non-local in the Portal tomb of Poulnabrone, while six of the eight samples analysed at Parknabinnia appear to be non-locals (Figure 8.24).

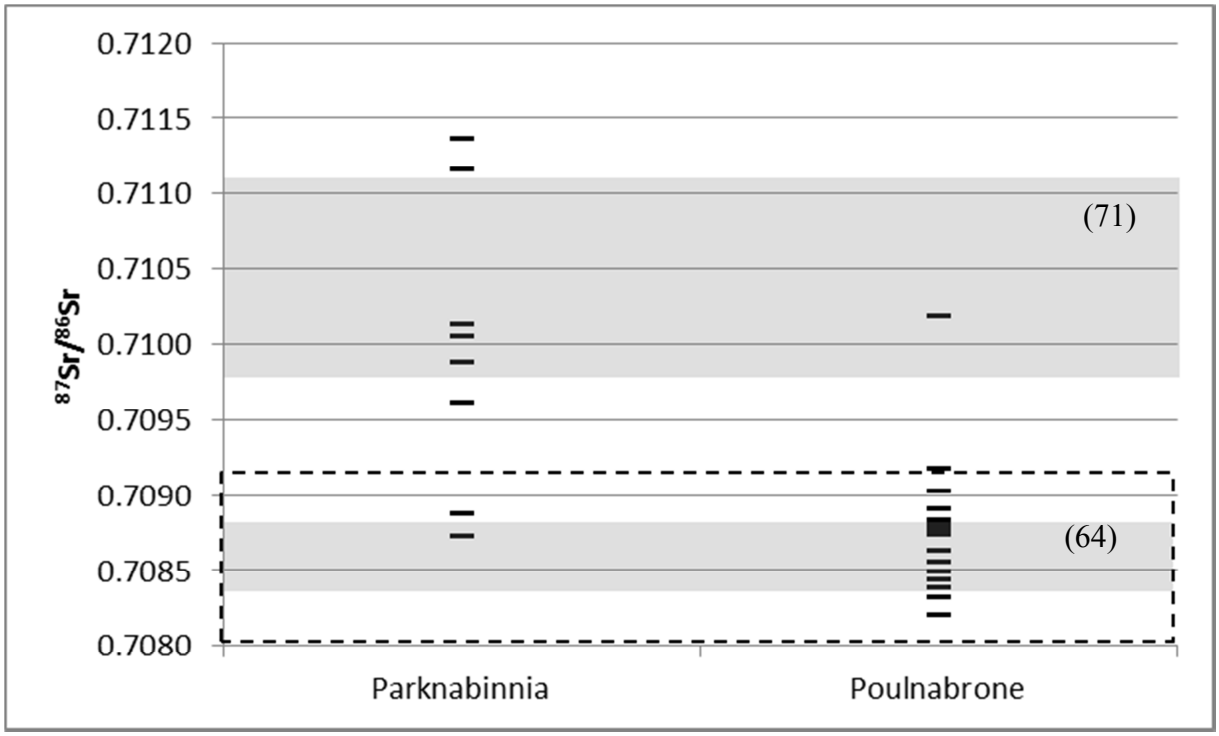

Figure 8.24 – Strontium isotope results for the unburned enamel and calcined bone samples from Parknabinnia and unburned enamel samples from Poulnabrone (Kadro 2010; Ditchfield 2014); the grey shaded areas correspond to the average BASr values calculated for the Carboniferous limestone outcrop (Formation 64) on which both sites lie and the Carboniferous sandstone (Formation 71) lying west of the sites (± 1SD); the dotted rectangle corresponds to the average BASr value ± 3SD of formation 64 used to detect non-locals

4.5 Archaeological implications

4.5.1 Mobility

The results of this chapter show the possibility of studying human mobility during the last decade or more of their lives using strontium isotope ratios of calcined bone fragments. Up till now, most strontium isotope studies used unburned tooth enamel fragments comparing the place where individuals ate during their childhood and the place where they were buried. Such studies of Early Neolithic people in Europe revealed a patrilocal kinship where more females where defined as non-locals than males. Amongst the males, less variability in their $^{87}Sr/^{86}Sr$ values was observed for those buried with stone adzes (Bickle et al. 2011; Bentley et al. 2012; Bentley 2013). Such interpretations are very difficult when studying Irish Neolithic calcined human remains. First it is difficult to sex calcined remains (none of the samples from Knowth could be sexed), and secondly, due to the extreme fragmentation of the samples (such as at Knowth) it is very difficult to associate artefacts with specific individuals.

Nevertheless, many other questions can be answered by using calcined bone fragments. For example, many Neolithic monuments in Ireland contain a combination of unburned and cremated bone and the reasons for this dual burial practice are unclear. The results obtained for Ballynahatty, for example, highlight that cremated bone fragments had higher strontium isotope ratios than the unburned pieces suggesting different funeral rites for different groups of individuals. At Knowth this is not the case but at Parknabinnia, it seems to be the case. The two individuals with the most extreme strontium isotope ratios were cremated while only unburned remains appeared to be local. Taking this into account, it appears that some individuals from Ballynahatty and Parknabinnia either moved in the last decade or so of their life or their cremated remains were brought to the site. This level of interpretation was not possible with tooth enamel where it was only possible to tell if the buried individual ate locally or not during childhood and early adolescence.

4.5.2 Cremation practices

The interpretation of cremation practices based on infrared and isotopic results is not straightforward. Indeed, two bone samples originating from a single cremated individual can exhibit different isotopic, compositional and structural characteristics (e.g. BM1a and BM1b from Ballymacaldrack). This highlights the extreme variability in conditions (temperature, oxygen availability, carbon exchange rates) around the body during heating. Nevertheless, the good inverse correlation observed between the $\delta^{13}C$ and $\delta^{18}O$ values ($R^2 > 0.55$) for the calcined bone fragments of Ballynahatty and Ballymacaldrack may suggest similar cremation practices for the individuals buries at that site. The less good correlation observed at Knowth and Parknabinnia ($R^2 < 0.31$) may highlight more variable cremation practices. Furthermore, a high number of samples having high CN/P (> 0.50) at a particular site (e.g. Knowth) could suggest the use of larger pyres for cremation.

5 Conclusion

The results of this chapter highlight the type of information that can be obtained from calcined bone fragments in archaeological contexts. It is possible to extract information about their place of origin and the way in which they were cremated. In this particular Irish Neolithic and Bronze Age case study, it appears that several individuals moved from one place to another during their lifetime (or once deceased as calcined bone fragments). These results represent a first attempt to study the mobility during Neolithic and Bronze Age Ireland using cremated archaeological remains and strontium isotopes. More work, however, is required before fully understanding mobility and funerary practices in Ireland during these periods.

Chapter 9 – Discussions and conclusions

1 Introduction

This chapter summarises the main outcomes of this work and proposes future research that could be carried out based on its results. General conclusions close this final chapter.

2 Themes

2.1 Diagenesis

Diagenesis of calcined bone has to be considered in two phases: first, all modifications taking place during heating (heating alterations), and then, those occurring once the calcined bone fragments have been deposited in an urn, soil, etc. (post-burial alterations). The heating alterations are comprehensively detailed in Chapters 4, 5 and 6, and, while not providing a complete understanding of the structural, composition and isotopic changes occurring in bone apatite, the results of this thesis are a new step towards that end.

An important structural change taking place during heating is an increase in crystallinity. This increase renders bone apatite more stable and less reactive making it far less susceptible to post-burial alterations than unburned bone. Nevertheless, the comparison of the infrared results obtained from modern and archaeological calcined samples showed that modern calcined bone was more reactive to acetic acid than archaeological specimens. It seems that after heating, the structure of calcined bone still changes (most likely shortly after heating), and the smaller, less well recrystallized crystallites, thus more reactive, become more stable over time, as seen in unburned bone (Ostwald ripening – e.g. Lee-Thorp and van der Merwe 1991). Nevertheless, these changes do not seem to affect the isotope composition ($\delta^{13}C$, $\delta^{18}O$ and $^{87}Sr/^{86}Sr$) of calcined bone. Indeed, artificial strontium contamination

experiments showed that, after an appropriate pre-treatment, almost all the strontium contamination could be removed. They also demonstrate that the susceptibility of a sample to undergo post-burial alterations is much more influenced by its crystallinity than its porosity. Furthermore, the $\delta^{13}C$ and $\delta^{18}O$ values of archaeological bone mostly fall within the range of values observed for modern samples burned in natural conditions.

These observations, together with the comparable radiocarbon dates obtained from paired calcined bone and charcoal from the same context (Lanting et al. 2001), strongly suggest that once calcined, the carbon, oxygen and strontium isotope compositions of bone apatite remain unchanged. Bearing in mind the possible problems linked to the exchanges occurring during heating (e.g. exchange of carbon with fuel older than the body), it is possible to obtain reliable radiocarbon dates, gather information about the mobility of individuals that were cremated and, to some extent, reconstruct ancient cremation practices.

2.2 Radiocarbon dating

Most isotope studies carried out on calcined bone over the last decade have focussed on radiocarbon dating. Here, the results confirm that exchanges with fuel carbon can lead to shifts in the radiocarbon age of the sample but, admittedly, in most cases, the fuel would be contemporary with the body and no effect on the radiocarbon dates would be observed. Nevertheless, analysing two or more calcined bone fragments from a single individual could help detecting the use of 'old' fuel, since the uptake of fuel carbon appears to be highly variable. Indeed, the results obtained for two samples from a single urn (BM1) at Ballymacaldrack ($\delta^{13}C$ values and CN/P – Figure 8.9b) indicate that different bone fragments from the same individual burned in the same fire may exhibit very different properties. This suggests that the fragments have undergone different transformations and exchanges with fuel. The first fragment does not present any cyanamide and has a lower $\delta^{13}C$ value implying that it has exchanged more with the fuel than the other fragment. It also has the highest $\delta^{18}O$

value of all the samples from Ballymacaldrack which again points to higher carbon exchange with the fuel (although the reasons why higher $\delta^{18}O$ values correspond to higher carbon exchange with the fuel are yet unclear). This is of particular interest for radiocarbon dating as, if two samples identified as originating from the same individual present different carbon and oxygen isotope ratios and cyanamide content (fast and easy to obtain), it would be possible to test if the individual was burned with 'old' fuel. If both samples provide statistically identical radiocarbon dates, it is more than likely that the body and the fuel were contemporary. However, if this is not the case and the sample containing cyanamide appears younger than the other (as it exchanged less carbon with the fuel), then the fuel is likely to have been older than the body. Following this rationale, even though samples containing cyanamide can sometimes be more difficult to graphitize (Zazzo et al. 2013), it appears that samples with higher $\delta^{13}C$ values and high amounts of cyanamide should be preferentially selected for radiocarbon dating.

2.3 Mobility

Calcined bone, thanks to its higher crystallinity compared to unburned bone and tooth enamel, is far less susceptible to post-burial alterations. In addition, no detectable changes in $^{87}Sr/^{86}Sr$ values during heating were observed. Furthermore, the artificial contamination experiments carried out here showed that, even though some exogenous strontium can be adsorbed onto the crystallites of calcined bone apatite, most of these are removed when pre-treated with acetic acid and ultrasonication. This demonstrates the potential of using strontium isotope ratios of calcined bone to study the mobility of cremated human (and faunal) remains.

2.4 Cremation practices

The infrared spectra combined with the carbon and oxygen isotope compositions of calcined bone apatite emphasised the possibility to discriminate bone fragments heated in different conditions. First, modern heated dry bone exhibits different structure and composition than heated fresh bone. Though no archaeological sample could be identified as having been burned dry in this work, this highlights the possibility of detecting individuals whose remains were cremated or accidentally burned when already in a skeletonised state. Furthermore, the presence of cyanamide in calcined bone apatite could reflect more reducing conditions in the pyres (less oxygen availability) which could be found in larger pyres. In archaeological sites where cyanamide is detected in the majority of the calcined samples (e.g. Knowth), it is likely that larger pyres were used as opposed to sites where only a few samples contain cyanamide. In addition, the laboratory experiments (LAB 2) demonstrated that samples heated at different temperatures exhibit different structural properties and have different C/C ratios and IRSF. While it was difficult in archaeological samples and modern samples burned on outdoor pyres to assess the exact temperature at which they were burned, it appears possible to identify samples that were burned at higher temperatures than others. Finally, the $\delta^{13}C$ and $\delta^{18}O$ values of calcined bone allow the discrimination of samples heated with and without fuel, the latter being enriched in ^{13}C and ^{18}O unlike the former.

3 Future research

3.1 Biologically available strontium in Ireland

The maps of the biologically available strontium (BASr) created for Ireland are a first attempt to characterize the island. There are however several improvements to the isoscapes that could be made. Such improvements require an in-depth understanding of ArcGIS which

proved too time-consuming to achieve within the timeframe of this work. Including topography and rainfall information could improve the maps. Furthermore, it should be possible in the single-part map (considering each geological outcrop as an individual entity) to predict the BASr value of the outcrops that were not sampled with a heightened accuracy by modelling their value based on BASr of the nearest outcrops of the same geological type.

Looking at the local maps, the key information missing here is the standard deviation for the different averages calculated. Obtaining such data is not straightforward and requires further research together with ArcGIS and statisticians. Last but not least, different local maps could be created taking into account the different strontium concentrations of the different food types (crops are strontium-rich while animal flesh is strontium-poor) and whence these could originate (Montgomery 2010).

3.2 Structural and isotopic study of cremated bone

3.2.1 Presence of cyanamide

In this work, I suggested that the presence of cyanamide could be linked to more reducing conditions during heating. This had been previously hypothesised (Zazzo et al. 2013) but the results of the present study are not altogether sufficient to actively confirm such hypothesis. More experimental work should be carried out such as comparing the results of bone heated on small and large pyres, as well as samples burned on the same pyre but at different heights (e.g. one sample placed at the bottom of the pyre where reducing conditions are more likely to occur and another on top of the pyre where oxygen availability is higher).

3.2.2 Carbon and oxygen isotopes of the carbonate fraction

The $\delta^{13}C$ and $\delta^{18}O$ values of calcined bone measured in this work improved the current understanding of the isotopic exchanges occurring during heating. However, while providing additional information, there are still grey areas. For example, the inverse correlation between

the $\delta^{13}C$ and $\delta^{18}O$ values of bone apatite carbonates observed in the modern samples heated outdoors and in the archaeological samples of several sites can be used to assess the amount of carbon intake from the fuel. It is, however, unclear why the $\delta^{18}O$ values increase when the proportion of carbon present in calcined bone apatite originating from the fuel increases. Furthermore, fractionation between carbon of the carbonates present in bone apatite and the carbon dioxide lost during heating could be demonstrated but not quantified. The potential isotopic fractionation between the carbon dioxide present in the combustion atmosphere (originating from the combustion of fuel and bone organic matter) and the carbonates incorporating that carbon dioxide could be neither confirmed nor discounted. These issues call for more research and heating experiments.

3.2.3 Oxygen isotopes of the phosphate fraction

The study of the phosphate fraction of bone apatite went beyond the scope of this work. Future research, however, should investigate the possibility of extracting useful isotopic information from this fraction, particularly as the P-O bonds of phosphates are much stronger than the C-O bonds of carbonates. Furthermore, phosphates are much more stable within the structure of bone apatite than carbonates. It is likely that the oxygen from the phosphates of bone apatite is less affected during heating than those from the carbonates. It would therefore be possible to extract the original oxygen isotope value from the phosphate fraction of calcined bone.

3.2.4 Strontium concentrations of calcined bone apatite

This work focussed on the strontium isotope composition of calcined bone apatite but gave very little attention to the strontium concentration. Strontium concentration has been shown to highlight, among other things, the intake of marine resources (strontium-rich) or potential landscape management: for example, a particular population could grow their crops on a strontium-rich geological outcrop and let their livestock graze on a strontium-poor area with a

different BASr value. Such practice would be reflected in their strontium concentration and isotope composition (Montgomery et al. 2007; Montgomery 2010). Combining the results obtained here with strontium concentration determination could help assess, for example, if the three cremated individuals from Clontygora ($^{87}Sr/^{86}Sr$ between 0.7090 and 0.7093) had a partially marine-based diet ($^{87}Sr/^{86}Sr$ of 0.7092).

3.2.5 Reconstructing the life-history of cremated individuals

Unlike tooth enamel that provides information about the place of residence during infancy/early adolescence, the $^{87}Sr/^{86}Sr$ value of calcined bone reflects an average of the places of residence where an adult individual lived during the last decade or more of his/her life. It may be possible, however, to obtain a signal reflecting residence during infancy by measuring the optic capsule of the petrous bone which forms in the first two years of life and, unlike the rest of the skeleton, does not appear to remodel subsequently (Jeffrey & Spoor 2004; Jørkov et al. 2009; Harvig et al. 2014). It should also be possible to address childhood mobility by analysing dentine which does survive the cremation process.

3.3 Archaeological applications

This work's applied study focussed on Neolithic and Bronze Age sites in Ireland, but there are many other sites in Ireland and elsewhere where burned bone remains have been recovered. Cremation was already practiced in Ireland in the Mesolithic period. Of the few human remains surviving from Mesolithic Ireland, the cremated remains found about ten years ago at Castleconnell are of great significance. These were directly radiocarbon dated to around 7400–7000 cal. BC (Collins & Coyne 2003; Collins & Coyne 2006). As human remains from this period are rare in Ireland, extracting useful information from them could shed some new light on the customs of the inhabitants of Mesolithic Ireland.

From the Mesolithic to the Bronze Age, cremation was widespread and cremated remains have been excavated from Bronze Age Denmark (Olsen et al. 2011) and Mesolithic Sweden, for example at Skateholm (Persson & Persson 1988). Allowing for the infrared and isotopic studies of cremated remains in Scandinavia would fill in some gaps in the archaeological records of that region since, because of the high acidity of the soil, unburned bone is destroyed (Nielsen-Marsh et al. 2007) and calcined bone is all that survives.

Further archaeological cremated remains can be found as far apart as Aboriginal Australia and the Caribbean. Undisturbed cremation burials were excavated in Tayata (southern Oaxaca, Mexico). These appear to be from the eleventh century BC and are the earliest evidence of this burial practice in Central America. Cremation is known to have been used at a later date only for the elite such as Mixtec kings and Aztec emperors (Duncan et al. 2008). It is likely that these peoples' diet relied partly on maize (C_4). Gathering $\delta^{13}C$ values from their bone apatite carbonates would help improve the understanding of the variation in $\delta^{13}C$ values during the heating of bone apatite.

In addition to cremated human remains, many archaeological sites yield large quantities of burned animal remains. In habitat and/or artisanal zones, animal bones could have been burned on domestic fire to reduce waste or used as fuel (e.g. Théry-Parisot 2002; Cain 2005; Morin 2010) when no wood was available, as would have been the case in arctic steppe conditions during the Palaeolithic. In sanctuaries, temples and religious sites more generally, animal offerings were frequent and, in many cases, burned on ritual fires (e.g. Hamilakis & Konsolaki 2004) with sometimes additional libations. In cemeteries, animal remains are often found together with human cremated remains (e.g. Eogan & Cleary forthcoming) perhaps burned together as offerings for the departed and/or the divinities.

A particular site that would benefit from the results of this work is the Abri Pataud in the Dordogne region, France, which has been heavily studied over the last few decades (e.g.

Nespoulet et al. 2008). Many calcined animal bone samples dating from the Aurignacian and Gravettian layers were recently dated (Zazzo et al. 2013); however, the question of the use of these bones as waste or fuel remains unanswered. Applying the results of this work to these samples should make it possible to discriminate samples burned with and without fuel. Another site that could benefit from these results is located in Akrotiri, Cyprus. This site is the oldest human occupied site of Cyprus from the 12th millennium BC where calcined bone fragments of dwarf hippopotamus were found. The archaeology suggests that these bones could have been the leftovers of a Palaeolithic feast during which remaining waste was burned (Simmons 1988; Simmons 1999). However, this hypothesis has been heavily debated (Ammerman & Noller, 2005; Simmons & Mandel 2007). Indeed, it is possible that the bones were burned accidentally several centuries or millennia later. By gathering structural and isotopic information from these burned bone fragments it could be possible to determine if the bones were burned defleshed, shortly after the feast, or dry, at a much later stage, shedding a much needed and clearer light to the current debate.

4 Conclusions

As detailed in the introduction chapter, the present research tried to address three main questions. Namely, (1) what isotopic, chemical and structural changes occur in bone apatite during and after heating? (2) Which isotopes and infrared indices can provide reliable information about archaeological calcined bone, and what information can be obtained from them? (3) How can the information gathered from calcined bone increase the current knowledge about past populations?

A brief answer to the first question is that there are considerable changes during heating but there are limited modifications to the composition and structure of bone apatite after calcination. During calcination, the structure and composition of bone apatite are

modified. There is a significant loss of carbonates, incorporation of hydroxyl groups and sometimes cyanamide. Furthermore there is an increase in crystallinity. Isotopically, no modification in the $^{87}Sr/^{86}Sr$ values of bone is observed during calcination but there is a significant change in $\delta^{13}C$ and $\delta^{18}O$ values of bone apatite carbonates due to losses and exchanges between bone apatite and other sources of carbon and oxygen present in the combustion atmosphere.

The second question stems from the previous one. Indeed, since no detectable changes were observed in the $^{87}Sr/^{86}Sr$ during and after heating, strontium isotope ratios can be used for mobility studies. Carbon and oxygen isotopes of bone apatite carbonates are more complex as their composition changes during heated. Therefore, while not informing on diet and hydrology, they provide information on the way in which the bone was heated. Finally, of the various infrared indices investigated here, only seven appear to be of use for the study of calcined bone and three are of particular interest for the study of archaeological calcined bone: IRSF, C/C ratio and CN/P. Of these, the first two are correlated to the temperature reached during heating while the final one seems to provide information about the size of the pyres.

Finally, using the various isotopes and infrared indices selected above, it is possible to investigate the mobility and funerary practices of past populations. For example, in Neolithic Ireland, it appears that different subsets of the population (based in their $^{87}Sr/^{86}Sr$ values) were buried differently at some sites (e.g. Ballynahatty and Parknabinnia): some were cremated while others were inhumed. These results open the possibility to deepen the current knowledge on past populations where cremation was practiced as mobility studies using calcined bone can now be widely applied archaeologically.

Bibliography

Ambrose S.H. & Krigbaum J. 2003. Bone chemistry and bioarchaeology. *Journal of Anthropological Archaeology*, 22:193–199.

Ammerman A.J. & Noller. J.S. 2005. New light on Aetokremnos. *World Archaeology*, 37(4):533–543

Beasley M.M., Bartelink E.J., Taylor L. & Miller R.M. 2014. Comparison of the transmission FTIR, ATR, and DRIFT spectra: implications for assessment of bone bioapatite diagenesis. *Journal of Archaeological Science*, 46:16–22

Beckett J.F. & Robb J. 2006. Neolithic burial taphonomy, ritual, and interpretation in Britain and Ireland: a review. *Social archaeology of funerary remains*, 57–80

Beckett J.F. 2005. Selective burial in Irish megalithic tombs; burial practice, age, sex, and representation in the Neolithic. In: *Proceedings of the Fifth Annual Conference of the British Association for Biological Anthropology and Osteoarchaeology*, 31–39

Bentley R.A. 2006. Kinship and mobility during the prehistoric spread of farming: Isotope evidence from the skeletons. *General Anthropology*, 13(1):1 & 7–10.

Bentley R.A. 2013. Mobility and the diversity of early Neolithic lives: Isotopic evidence from skeletons. *Journal of Anthropological Archaeology.* 32: 303-312

Bentley R.A., Bickle P., Fibiger L., Nowell G.M., Dale C.W., Hedges R.E.M, Hamilton J., Wahl J., Francken M., Grupe G., Lenneis E., Teschler-Nicola M., Arbogast R.-M., Hofmann D. & Whittle A. 2012. Community differentiation and kinship among Europe's first farmers. *Proceedings of the National Academy of Sciences*, 129(24):9326–9330

Bentley R.A., Price T.D. & Stephan E. 2004. Determining the "local" $^{87}Sr/^{86}Sr$ range for archaeological skeletons: A case study from Neolithic Europe. *Journal of Archaeological Science*, 31:365–375.

Bentley R.A., Price T.D., Luning J., Gronenborn D., Wahl J. & Fullagar P.D. 2002. Prehistoric migration in Europe: Strontium isotope analysis of Early Neolithic skeletons. *Current Anthropology*, 43(5):799–803.

Berna F., Goldberg P., Horwitz L.K., Brink J., Holt S., Bamford M. & Chazan M. 2012. Microstratigraphy evidence of in situ fire in the Acheulean Strata of Wonderwerk Cave, Northern Cape Province, South Africa. *Proceedings of the National Academy of Sciences*, 109(20):E1215–E1220

Bickle P., Hofmann D., Bentley R.A., Hedges R.E.M., Hamilton J., Laiginhas F., Nowell G.M., Pearson D.G., Grupe G. & Whittle A.W.R., 2011. Community heterogeneity in the Linearbandkeramik. *Antiquity*, 330:1243–1258

Biltz R.M. & Pellegrino E.D. 1983. The composition of rectrystallised bone mineral. *Journal of Dental Research*, 62(12):1190–1195

Bosch Reig F., Gimeno Adelantado J.V. & Moya Moreno J.V. (2002). FTIR quantitative analysis of calcium carbonate (calcite) and silica (quartz) mixtures using the constant ratio method. Application to geological samples. *Talanta*, 58:811–821

Brindley A.L. 2007. *The dating of food vessels and urns in Ireland*. Department of Archaeology, National University of Ireland.

Brock F., Higham T. & Bronk Ramsey C. 2007. Radiocarbon dating bone samples recovered from gravel sites. English Heritage Research Department Report Series 30/2007. English Heritage, London. http://ads.ahds.ac.uk/catalogue/ archive/bigravels_eh_2007/

Brock F., Higham T. & Bronk Ramsey C. 2010a. Pre-screening techniques for identification of samples suitable for radiocarbon dating of poorly preserved bones. *Journal of Archaeological Science*, 37:855-865

Brock F., Higham T., Ditchfield P. & Bronk Ramsey C. 2010b. Current pre-treatment methods for AMS radiocarbon dating at the Oxford Radiocarbon Accelerator Unit (ORAU). *Radiocarbon*, 52(1):103–12

Budd P., Montgomery J., Barreiro B. & Thomas G.C. 2000. Differential diagenesis of strontium in archaeological human dental tissues. *Applied Geochemistry*. 15(5):687–694

Burton J.H., Price T.D. & Middelton W.D. 1999. Correlation of bone Ba/Ca and Sr/Ca due to biological purification of calcium. *Journal of Archaeological Science*, 26:609–616

Cain C.R. 2005. Using burned animal bone to look at Middle Stone Age occupation and behaviour. *Journal of Archaeological Science*, 32:873–884

Carter R.W.G. 1982. Sea-level changes in Northern Ireland. *Proceedings of the Geologists' Association*, 93(1):7–23

Carter R.W.G., Forbes D.L., Jennings S.C., Orford J.D., Shaw J. & Taylor R.B. 1989. Barrier and lagoon coast evolution under differing relative sea-level regimes: examples from Ireland and Nova Scotia. *Marine Geology*, 88(3):221–242

Clark P.U., Shakun J.D., Baker P.A., Bartlein P.J., Brewer S., Brook E., Carlson A.E. & Williams J.W. 2012. Global climate evolution during the last deglaciation. *Proceedings of the National Academy of Sciences*, 109(19):E1134–E1142

Collins A.E.P. 1957. Excavations at the Giant's Ring, Ballynahatty. *Ulster Journal of Archaeology*, 44–50

Collins A.E.P. 1976. Dooey's Cairn, Ballymacaldrack, County Antrim. *Ulster Journal of Archaeology*, 1–7

Collins T. & Coyne F. 2003. Fire and water... Early Mesolithic cremations at Castleconnell, Co. Limerick. *Archaeology Ireland*, 17(2):24–27

Collins T. & Coyne F. 2006. As Old as we Felt... *Archaeology Ireland*, 20(4):21

Connolly J., Holden N.M. & Ward S.M. 2007. Mapping peatlands in Ireland using a rule-based methodology and digital data. *Soil Science Society of America Journal*, 71(2):492–499

Cooney G. 2000. *Landscape of Neolithic Ireland*. London: Routledge.

Copeland S.R., Sponheimer M., de Ruiter D.J., Lee-Thorp J.A., Codron D., le Roux P.J., Grimes V. & Richards, M. P. 2011. Strontium isotope evidence for landscape use by early hominins. *Nature*, 474(7349):76–78

Copeland S.R., Sponheimer M., Lee-Thorp J. A., de Ruiter D.J., leRoux P J., Grimes V., Codron D., Berger L.R. & Richards, M. P. 2010. Using strontium isotopes to study site accumulation processes. *Journal of taphonomy*, 8(2):115–127

Cousin J., Chen W., Fourmentin M., Fertein E., Boucher D., Cazier F., Nouali H., Dewaele D., Douay M. & Rothman L.S. 2008. Laser spectroscopic monitoring of gas emission and measurements of the $^{13}C/^{12}C$ isotope ratio in CO_2 from a wood-based combustion. *Journal of Quantitative Spectroscopy and Radiative Transfer*, 109(1):151–167

Dahl S.G., Allain P., Marie P.J., Mauras Y., Boivin G., Ammann P., Tsouderos Y., Delmas P.D& Christiansen, C. (2001). Incorporation and distribution of strontium in bone. *Bone*, 28(4):446–453

Darling W.G. & Talbot J.C. 2003. The O & H stable isotopic composition of fresh waters in the British Isles: 1, Rainfall. *Hydrology and earth System Sciences*, 7(2):163–181

Davies O. & Paterson T.G.F. 1937. Excavation at Clontygora large cairn, Co. Armagh. *Proceedings of the Belfast Natural History and Philosophical Society*, 1(2):20–42

Davies O. 1939. Excavations at Legland horned cairn. *Proceedings of the Belfast Natural History and Philosophical Society 1* (2nd series)(5):16–24

Dempster D.W. 1999. New concepts in bone remodeling. In: Seibel M.J., Robins S.P. & Bilezikian J.P. (eds.), *Dynamics of Bone and Cartilage Metabolism*:261-273. San Diego: Academic Press.

Ditchfield P. 2014. Stable isotope analysis. In: Lynch A. (ed.), *Poulnabrone, Co. Clare. Excavation of an Early Neolithic Portal Tomb*:86–92. Dublin: Department of Arts, Heritage and the Gaeltacht, Archaeological Monograph Series.

Dowker S.E.P. & Elliott J.C. 1979. Infrared adsorption bands from NCO^- and NCN^{2-} in heated carbonate-containing apatites prepared in the presence of NH_4^+ ions. *Calcified Tissues International*, 29:177–178

Duncan W.N., Balkansky A.K., Crawford K., Lapham H.A. & Meissner N.J. 2008. Human Cremation in Mexico 3,000 Years Ago. *Proceedings of the National Academy of Sciences*, 105(14):5315–5320

Duvernay F., Chiavassa T., Borget F. & Aycard J.P. 2005. Carbodiimide production from cyanamide by UV irradiation and thermal reaction on amorphous water ice. *The Journal of Physical Chemistry A*, 109(4):603–608

Elias M. 1980. The feasibility of dental strontium analysis for diet-assessment of human populations. *American Journal of Physical Anthropology*, 53:1–4

Eogan G. & Cleary K. (eds.). forthcoming. *Excavations at Knowth 6: The Archaeology of the Large Passage Tomb at Knowth, Co. Meath*. Dublin: Royal Irish Academy.

Eogan G. 1973. Review: A Decade of Excavations at Knowth, Co. Meath. *Irish University Review*, 3(1):66–79

Evans J.A., Chenery C.A. & Fitzpatrick A.P. 2006. Bronze age childhood migration of individuals near Stonehenge, revealed by strontium and oxygen isotope tooth enamel analysis. *Archaeometry*, 48(2):309–321

Evans J.A., Montgomery J. & Wildman G. 2009. Isotopes domain mapping of $^{87}Sr/^{86}Sr$ biosphere variation on the Isle of Skye, Scotland. *Journal of the Geological Society, London*, 166:617–631

Evans J.A., Montgomery J., Wildman G. & Boulton N. 2010. Spatial variations in biosphere $^{87}Sr/^{86}Sr$ in Britain. *Journal of Geological Society, London*, 167:1–4

Farlay D., Panczer G., Rey C., Delmas P. & Boivin G. 2010. Mineral maturity and crystallinity index are distinct characteristics of bone mineral. *Journal of Bone and Mineral Metabolism*, 28(4):433–445

Faure G. & Powell T. 1972. *Strontium Isotope Geology*. Springer, New York

Featherstone J.D.B., Pearson S. & LeGeros R.Z. 1984. An infrared method for quantification of carbonate in carbonated apatites. *Caries Research*, 18:63–66

Frei K.M. & Price T.D. 2012. Strontium isotopes and human mobility in prehistoric Denmark. *Archaeological and anthropological sciences*, 4(2):103–114

Garvie-Lok S.J., Varney T.L. & Katzenberg M.A. 2004. Preparation of bone carbonate for stable isotope analysis: the effects of treatment time and acid concentration. *Journal of Archaeological Science*, 31:763–776

González-Díaz P.F. & Santos M. 1977. On the hydroxyl ions in apatites. *Journal of Solid State Chemistry*, 22:193–199

González-Pérez J.A., González-Vila F.J., Almendros G. & Knicker H. 2004. The effect of fire on soil organic matter—a review. *Environment international*, 30(6):855–870

Haas H. & Banewicz J. 1980. Radiocarbon dating of bone apatite using thermal release of CO_2. *Radiocarbon*, 22(2):537–544

Habelitz S., Pascuala L. & Duran A. 2001. Transformation of tricalcium phosphate into apatite by ammonia treatment. *Journal of Materials Science*, 36:4131–4135

Hall H.V. & Schultz S.L. 2008. *U.S. Patent Application 12/214,688*

Hamilakis Y. & Konsolaki E. 2004. Pigs for the gods: Burnt animal sacrifices as embodied rituals at a Mycenaean sanctuary. *Oxford Journal of Archaeology*, 23(2):135–151

Hammond R.F. 1981. *The peatlands of Ireland*. An Foras Tuńtais.

Harbeck M., Schleuder R., Schneider J., Wiechmann I., Schmahl W.W. & Grupe G. 2011. Research potential and limitations of trace analyses of cremated remains. *Forensic Science International*, 240:191–200

Hartman G. & Richards M. 2014. Mapping and defining sources of variability in bioavailable strontium isotope ratios in the Eastern Mediterranean. *Geochimica et Cosmochimica Acta*, 126:250–264

Hartwell B. 1991. Ballynahatty: A Prehistoric ceremonial centre. *Archaeology Ireland*, 12–15

Hartwell B. 2002. A Neolithic ceremonial timber complex at Ballynahatty, Co Down. *Antiquity*, 76:526-532

Harvig L., Frei K.M., Price T.D. & Lynnerup N. 2014. Strontium isotope signals in cremated petrous portions as indicator for childhood origin. *PloS ONE*, 9(7):e101603

Hassan A.A., Termine J.D. & Vance Haynes C.J. 1977. Mineralogical studies on bone apatite and their implications for radiocarbon dating. *Radiocarbon*, 19(3):364–374

Hedges R.E.M. & Millard A.R. 1995. Bones and groundwater: towards the modelling of diagenetic processes. *Journal of Archaeological Science*, 22(2):155–164

Hedges R.E.M., Clement J.G., Thomas C.D.L. & O'Connell T.C. 2007. Collagen turnover in

the adult femoral mid-shaft: modeled from anthropogenic radiocarbon tracer measurements. *American Journal of Physical Anthropology*, 133(2):808–816

Hess J., Bender M.L. & Schilling J.G. 1986. Evolution of the ratio of strontium-87 to strontium-86 in seawater from Cretaceous to present. *Science*, 231(4741):979–984

Holcomb D.W. & Young R.A. 1980. Thermal decomposition of human tooth enamel. *Calcified Tissue International*, 31(1):198–201

Holland C.H. & Sanders I. 2009. *The geology of Ireland*. Dunedin Academic

Hoppe K.A., Koch P.L. & Furutani T.T. 2003. Assessing the preservation of biogenic strontium in fossil bones and tooth enamel. *International Journal of* Osteoarchaeology. 13:20–28

Hu Y., Ambrose S.H. & Wang C. 2006. Stable isotopic analysis of human bones from Jiahu Site, Henan, China: Implications for the transition to agriculture. *Journal of Archaeological Science*, 33:1319–1330

Hüls C.M., Erlenkeuser H., Nadeau M.-J., Grootes P.M. & Andersen N. 2010. Experimental Study on the Origin of Cremated Bone Apatite Carbon. *Radiocarbon*, 52(2–3):587–599

Jeffery N. & Spoor F. 2004. Prenatal growth and development of the modern human labyrinth. *Journal of Anatomy*, 204(2):71–92

Jones C. & Walsh P. 1996. Recent discoveries on Roughan Hill, County Clare. *Journal of the Royal Society of Antiquaries of Ireland*, 126:86–107

Jones C. 1998. The discovery and dating of the prehistoric landscape of Roughan Hill in Co. Clare. *Journal of Irish Archaeology*, 9:27–43

Jones C. 2003. Neolithic beginnings of Roughan Hill and the Burren. In: Armit I., Murphy E., Nelis E. & Simpson D. (eds.), *Neolithic Settlement in Ireland and Western Britain*:188–194. Oxford: Oxbow Books.

Jones C. 2008. *Temples of Stone: Exploring the Megalithic Tombs of Ireland*. Collins Press

Jørkov M.L.S., Heinemeier J. & Lynnerup N. 2009. The petrous bone – A new sampling site for identifying early dietary patterns in stable isotopic studies. *American Journal of Physical*

Anthropology, 139:199-209

Kador T. 2010. Searching for Neolithic migrants at the introduction of agriculture to Ireland. Heritage Council Research Grants 2010 Final Project Report.

King C.L., Tayles N. & Gordon K.C. 2011. Re-examining the chemical evaluation of diagenesis in human bone apatite. *Journal of Archaeological Science*, 38:2222–2230

Koch P.L., Tuross N. & Fogel M.L. 1997. The effects of sample treatment and diagenesis on the isotopic integrity of carbonate in biogenic hydroxylapatite. *Journal of Archaeological Science*, 24:417–429

Krivoruchko K., Gribov A. & Krause E. 2011. Multivariate areal interpolation for continuous and count data. *Procedia Environmental Sciences*, 3:14–19

Krueger H.W. 1991. Exchange of carbon with biological apatite. *Journal of Archaeological Science*, 18:355–361

Kusaka S., Ando A., Nakano T., Yumoto T., Ishimaru E., Yoneda M., Fujio H. & Katayama K. 2009. A strontium isotope analysis on the relationship between ritual tooth ablation and migration among the Jomon people in Japan. *Journal of Archaeological Science*, 36:2289–2297

Kusaka S., Nakano T., Yumoto T. & Nakatsukasa M. 2011. Strontium isotope evidence of migration and diet in relation to ritual tooth ablation: A case study form the Inariyama Jomon site, Japan. *Journal of Archaeological Science*, 38:166–174

Kyle J.H. 1986. Effects of post-burial contamination on the concentration of major and minor elements in human bones and teeth – The implications for Palaeodietary research. *Journal of Archaeological Science*, 13:403–416

Laffoon J.E., Davies G.R., Hoogland M.L.P. & Hofman C.L. 2012. Spatial variation of biologically available strontium isotopes ($^{87}Sr/^{86}Sr$) in an archipelagic setting: A case study from the Caribbean. *Journal of Archaeological Science*, 39:2371–2384

Lamb H. & Thompson A. 2005. Unusual mid-Holocene abundance of Ulmus in western Ireland-human impact in the absence of a pathogen? *The Holocene*, 15(3):447–452

Lanting J.N. & Brindley A.L. 1998. Dating Cremated Bone: The Dawn of a New Era. *The Journal of Irish Archaeology*, IX:1–7

Lanting J.N. & Brindley A.L. 2000. An Exciting New Development: Calcined Bones Can Be 14C-Dated. *The European Archaeologist*, 13:7–8

Lanting J.N., Aerts-Bijma A.T. & van der Plicht J. 2001. Dating of cremated bones. *Radiocarbon*, 43(2A):249–254

Lebon M., Reiche I., Bahain J.-J., Chadefaux C., Moigne A.-M., Frohlich F., Sémah F., Schwarcz H.P. & Falguères C. 2010. New parameters for the characterization of diagenetic alterations and heat-induced changes of fossil bone mineral using Fourier transform infrared spectrometry. *Journal of Archaeological Science*, 37:2265–2276

Lee-Thorp J.A. & Sponheimer M. 2003. Three case studies used to reassess the reliability of fossil bone and enamel isotope signals for paleodietary studies. *Journal of Anthropological Archaeology*, 22:208–216

Lee-Thorp J.A. & van der Merwe N.J. 1991. Aspects of the chemistry of modern and fossil biological apatites. *Journal of Archaeological Science*, 18:343–354

Lee-Thorp J.A. 2002. Two decades of progress towards understanding fossilization processes and isotopic signals in calcified tissue minerals. *Archaeometry*, 44(3):435–446

Lee-Thorp J.A. 2008. On isotopes and old bones. *Archaeometry*, 50(6):925–950

LeGeros R.Z. & LeGeros J.P. 1983. Carbonate analyses of synthetic, mineral and biological apatites. *Journal of Dental Research*, 82:259

LeGeros R.Z. 1981. Apatites in biological systems. *Progress in crystal growth and characterization*, 4(1):1–45.

LeGeros R.Z. 1991. *Calcium phosphates in oral biology and medicine*. Karger, Paris.

LeGeros R.Z. 2008. Calcium phosphate-based osteoinductive materials. *Chemical reviews*, 108(11):4742–4753

LeGeros R.Z., Balmain N. & Bonel G. 1986. Structure and composition of the mineral phase of periosteal bone. *Journal of Chemical Research (Synopses)*, 1:8–9

LeGeros R.Z., Trautz O.R., Klein E. & LeGeros J. P. 1969. Two types of carbonate substitution in the apatite structure. *Cellular and Molecular Life Science*, 25(1):5–7

Leventouri T. 2006. Synthetic and biological hydroxyapatites: Crystal structure questions. *Biomaterials*, 27: 3339–3342

Li Z.Y., Lam W.M., Yang C., Xu B., Ni G.X., Abbah S.A., Cheung K.M.C., Luk K.D.K. & Lu W.W. 2007. Chemical composition, crystal size and lattice structural changes after incorporation of strontium into biomimetic apatite. *Biomaterials*, 28(7):1452–1460

MacAdam J. 1855. Discovery of an ancient sepulchral chamber. *Ulster Journal of Archaeology 3*, (Series 1):358–365

Meighan I.G. 2011. The sourcing of Irish Bronze Age gold. *Archaeology Ireland*, 25(4):31–32

Meighan I.G., McCormick A.G., Gibson D., Gamble J.A. & Graham I.J. 1988. Rb-Sr isotopic determinations and the timing of Tertiary central complex magmatism in NE Ireland. *Geological Society, London, Special Publications*, 39(1):349–360

Míková J. & Denková P. 2007. Modified chromatographic separation scheme for Sr and Nd isotope analysis in geological silicate samples. *Journal of Geosciences*, 52: 221–226.

Mkukuma L.D., Skakle J.M., Gibson I.R., Imrie C., Aspden R.M. & Hukins D.W. 2004. Effect of the proportion of organic material in bone on thermal decomposition of bone mineral: an investigation of a variety of bones from different species using thermogravimetric analysis coupled to mass spectrometry, high-temperature X-ray diffraction, and Fourier transform infrared spectroscopy. *Calcified Tissue International*, 75:321–328

Montgomery J. 2010. Passports from the past: Investigating human dispersals using strontium isotope analysis of tooth enamel. *Annals of human biology*, 37(3):325–346

Montgomery J., Evans J.A. & Cooper R.E. 2007. Resolving archaeological populations with Sr-isotope mixing models. *Applied Geochemistry*, 22(7):1502–1514

Morin E. 2010. Taphonomic implications of the use of bone as fuel. In: Thery-Parisot I., Chabal L. & Costamagno S. (eds.), The taphonomy of burned organic residues and

combustion features in archaeological contexts. Proceedings of the round table, Valbonne, May 27–29 2008. *P@lethnology*. 2:209–217

Munro L.E., Longstaffe F.J. & White C.D. 2007. Burning and boiling of modern deer bone: Effects on crystallinity and oxygen isotope composition of bioapatite phosphate. *Palaeogeography, Palaeoclimatology, Palaeoecology*, 249:90–102

Munro L.E., Longstaffe F.J. & White C.D. 2008. Effect of heating on the carbon and oxygen-isotope compositions of structural carbonate in bioapatite from modern deer bone. *Palaeogeography, Palaeoclimatology, Palaeoecology*, 266:142–150

Naysmith P., Scott E.M., Cook G.T., Heinemeier J., van der Plicht J., Van Strydonck M., Bronk Ramsey C., Grootes P.M. & Freeman S.P.H.T. 2007. A cremated bone intercomparison study. *Radiocarbon*, 49(2):403–8

Nelson B.K., DeNiro M.J., Schoeninger M.J., De Paolo D.J. & Hare P.E. 1986. Effects of diagenesis on strontium, carbon, nitrogen and oxygen concentration and isotopic composition of bone. *Geochimica et Cosmochimica Acta*, 50(9):1941–1949

Nespoulet R., Chiotti L., Henry-Gambier D., Agsous S., Lenoble A., Morala A., Guillermin P., Vercoutere C., Grimaud-Herve D., Marquer L., Patou-Mathis M., Pottier C., Vannoorenberghe A. & Verez M. 2008. L'Occupation humaine de l'abri Pataud (Les Eyzies-de-Tayac, Dordogne) il y a 22 000 ans: problématique et résultats préliminaires des fouilles du niveau 2. In : J. Jaubert, J.-G. Bordes, I. Ortega (Eds.), *Les Sociétés Paléolithiques dans un Grand Sud-Ouest: Nouveaux Gisements, Nouveaux Résultats, Nouvelles Méthodes*:325–334. Actes des Journées de la Société Préhistorique Française, 24 et 25 novembre 2006, Mémoire de la SPF XLVII, Talence

Nicholson R.A. 1993. A morphological investigation of burnt animal bone and an evaluation of its utility in archaeology. *Journal of Archaeological Science*, 20(4):411–428

Nielsen-Marsh C.M., Smith C.I., Jans M.M.E., Nord A., Kars H. & Collins M.J. 2007. Bone diagenesis in the European Holocene II: taphonomic and environmental considerations. *Journal of Archaeological Science*, 34(9):1523–1531

O'Connell T.C., Hedges R.E.M., Healey M.A. & Simpson A.H.R.W. 2001. Isotopic comparison of hair, nail and bone: modern analyses. *Journal of Archaeological Science*, 28(11):1247–1255

Olsen J., Heinemeier J., Bennike P., Krause C., Hornstrup K.M. & Thrane H. 2008. Characterisation and blind testing of radiocarbon dating of cremated bone. *Journal of Archaeological Science*, 35:791–800

Olsen J., Heinemeier J., Hornstrup K.M., Bennike P. & Thrane H. 2012. 'Old wood' effect in radiocarbon dating of prehistoric cremated bones? *Journal of Archaeological Science*, 40(1):30–34

Olsen J., Hornstrup K.M., Heinemeier J., Bennike P. & Thrane H. 2011. Chronology of the Danish Bronze Age based on 14C dating of cremated bone remains. *Radiocarbon*, 53(2):261–275

Paschalis E.P. 2009. Fourier Transform Infrared analysis in bone. *Osteoporosis Internatonal*, 20:1043–1047

Paschalis E.P., Betts F., DiCarlo E., Mendelsohn R. & Boskey A.L. 1997. FTIR microspectroscopic analysis of normal human cortical and trabecular bone. *Calcified tissue international*, 61(6):480–486

Paschalis E.P., DiCarlo E., Betts F., Sherman P., Mendelsohn R. & Boskey A. L. 1996. FTIR microspectroscopic analysis of human osteonal bone. *Calcified tissue international*, 59(6):480–487

Paschalis E.P., Mendelsohn R. & Boskey A.L. 2011. Infrared assessment of bone quality. *Clinical Orthopaedics and Related Research*, 469:2170–2178

Pasteris J.D., Wopenka B., Freeman J.J., Rogers K., Valsami-Jones E., van der Houwen J. A. & Silva M.J. 2004. Lack of OH in nanocrystalline apatite as a function of degree of atomic order: Implications for bone and biomaterials. *Biomaterials*, 25: 229–238

Pellegrini M. & Snoeck C. In prep. Bioapatite carbonate pre-treatments for isotopic measurements.

Person A., Bocherens H., Mariotti A. & Renard M. 1996. Diagenetic evolution and experimental heating of bone phosphate. *Palaeogeography, Palaeoclimatology, Palaeoecology*, 126:135–149

Persson O. & Persson E. 1988. Anthropological report concerning the interred Mesolithic populations from Skateholm Project, Southern Sweden. Excavation Seasons 1983-1984. In: Larsson L. (ed.), *The Skateholm Project. I. Man and Environment*:89–105. Almqvist and Wiksell International, Stockholm: Acta Regiae Societatis Humaniorum Litterarum Ludensis LXXIX

Pestle W.J., Crowley B.E. & Weirauch M.T. 2014. Quantifying inter-laboratory variability in stable isotope analysis of ancient skeletal remains. *PloS one*, 9(7):e102844

Plunkett G., Carroll F., Hartwell B., Whitehouse N.J. & Reimer P.J. 2008. Vegetation history at the multi-period prehistoric complex at Ballynahatty, Co. Down, Northern Ireland. *Journal of Archaeological Science*, 35(1):181–190

Podlesak D.W., Torregrossa A.M., Ehleringer J.R., Dearing M.D., Passey B.H. & Cerling T.E. 2008. Turnover of oxygen and hydrogen isotopes in the body water, CO_2, hair, and enamel of a small mammal. *Geochimica et Cosmochimica Acta*, 72(1):19–35

Pollard A.M., Batt C.M., Stern B. & Young S.M.M. 2007. *Analytical chemistry in archaeology*. Cambridge University Press.

Porder S., Paytan A. & Hadly E.A. 2003. Mapping the origin of faunal assemblages using strontium isotopes. *Paleobiology*, 29(2):197–204

Posner A.S., Blumenthal N.C. & Betts F. 1984. Chemistry and structure of precipitated hydroxyapatites. In: Nriagu J.O. & Moore P.H. (eds.), *Phosphate minerals*:330–350. Springer Berlin Heidelberg.

Praprotnik M. & Janežič D. 2005. Molecular dynamics integration and molecular vibrational theory. II. Simulation of nonlinear molecules. *The Journal of chemical physics*, 122(17):174102

Price T.D., Burton J.H. & Bentley R.A. 2002. The characterization of biologically available strontium isotope ratios for the study of prehistoric migration. *Archaeometry*, 44(1):117–135

Pucéat E., Reynard B. & Lécuyer C. 2004. Can crystallinity be used to determine the degree of chemical alteration of biogenic apatites? *Chemical Geology*, 205(1):83–97

Quarta G., Calcagnile L., D'Elia M., Maruccio L., Gaballo V. & Caramia A. 2013. A combined PIXE-PIGE approach for the assessment of the diagenetic state of cremated bones submitted to AMS radiocarbon dating. *Nuclear Instruments and Methods in Physics Research B*, 294:221–225

Rajendran J. 2011. XANES and FTIR Study on Dried and Calcined Bone. Unpublished Master Dissertation: The University of Texas at Arlington.

Reimer P.J., Bard E., Bayliss A., Beck J.W., Blackwell P.G., Ramsey C.B., Buck C.E., Cheng H., Edwards L., Friedrich M., Grootes P.M., Guilderson T.P., Haflidason H., Hajdas I., Hatté C., Heaton T.J., Hoffmann D.L., Hogg A.G., Hughen K.A., Kaiser K.F., Kromer B., Manning S.W., Niu M., Reimer R.W., Richards D.A., Scott E.M., Southon J.R., Staff R.A., Turney C.S.M. & van der Plicht J. 2013. IntCal13 and Marine13 radiocarbon age calibration curves 0–50,000 years cal BP. *Radiocarbon*, 55(4):1869–1887

Rey C., Collins B., Goehl T., Dickson I.R. & Glimcher M.J. 1989. The carbonate environment in bone mineral: A resolution-enhanced Fourier Transform Infrared Spectroscopy study. *Calcified Tissues International*, 45:157–164

Rey C., Miquel J.L., Facchini L., Legrand A.P. & Glimcher M.J. 1995. Hydroxyl groups in bone mineral. *Bone*, 16(5):583–586

Richards M.P., Schulting R.J. & Hedges R.E.M., 2003. Sharp shift in diet at onset of Neolithic. *Nature*, 425:366

Robins S.P. & New S.A. 1997. Markers of bone turnover in relation to bone health. *Proceedings of the Nutrition Society*, 56(3): 903-914

Roche D., Ségalen L., Balan E. & Delattre S. 2010. Preservation assessment of Miocene-Pliocene tooth enamel from Tugen Hills (Kenyan Rift Valley) through FTIR, chemical and stable-isotope analyses. *Journal of Archaeological Science*, 37:1690–1699

Rodriguez-Navarro C., Ruiz-Agudo E., Luque A., Rodriguez-Navarro A.B. & Ortega-Huertas M. 2009. Thermal decomposition of calcite: Mechanisms of formation and textural evolution of CaO nanocrystals. *American Mineralogist*, 94(4):578–593

Scheele N. & Hoefs J. 1992. Carbon isotope fractionation between calcite, graphite and CO_2: an experimental study. *Contributions to Mineralogy and Petrology*, 112(1):35–45

Schoeninger M.P. & DeNiro M.J. 1982. Carbon isotopic ratios of apatite from fossil bone cannot be used to reconstruct diets of animals. *Nature*, 297:577–578

Schulting R.J. & Richards M. 2002. The wet, the wild, and the domesticated: the Mesolithic-Neolithic transition on the west coast of Scotland. *European Journal of Archaeology*, 5(2):147–189

Schulting R.J. 2011. Mesolithic-Neolithic transitions: An isotopic tour through Europe. In: Pinhasi R. & Stock J.T. (eds.), *Human Bioarchaeology of the Transition to Agriculture*:17–41. New York: Wiley-Liss

Schulting R.J. 2013. On the northwestern fringes: Earlier Neolithic subsistence in Britain and Ireland as seen through faunal remains and stable isotopes. In: Colledge S., Conolly J., Dobney K., Manning K. & Shennan S. (eds.), *The Origins and Spread of Stock-Keeping in the Near East and Europe*:313–338. Walnut Creek, California: Left Coast Press.

Schulting R.J., Bronk Ramsey C., Reimer P.J., Eogan G., Cleary K., Cooney G. & Sheridan A. forthcoming. Dating the human remains from Knowth. In: Eogan G. & Cleary K. (eds.), *Excavations at Knowth 6: The Archaeology of the Large Passage Tomb at Knowth, Co. Meath*. Dublin: Royal Irish Academy.

Schulting R.J., Murphy E., Jones C. & Warren G. 2012. New dates from the north and a proposed chronology for Irish court tombs. *Proceedings of the Royal Irish Academy, Section C*, 112(1):1–60

Sealy J.C. van der Merwe, N. J., Sillen, A., Kruger, F. J., & Krueger, H. W. 1991. $^{87}Sr/^{86}Sr$ as a dietary indicator in modern and archaeological bone. *Journal of Archaeological Science*, 18:399–416

Sheridan J.A., Montgomery J., Pellegrini M. & Cahill Wilson J. 2013. Tara Boy: local hero or international man of mystery? In: O'Sullivan M., Scarre C. & Doyle M. (eds.), *Tara - from the past to the future. Towards a new research agenda*:207–232. Wordwell, Dublin

Shipman P., Foster G., & Schoeninger M. 1984. Burnt bones and teeth: an experimental study of color, morphology, crystal structure and shrinkage. *Journal of Archaeological Science*, 11(4):307–325

Sillen A. & Hoering T. 1993. Chemical characterization of burnt bones from Swartkrans. In: Brain C.K. (ed.), *Swartkrans: A Cave's Chronicle of Early Man*:243–249. Pretoria: Transvaal Museum Monograph 8

Sillen A. & LeGeros R.Z. 1991. Solubility profiles of synthetic apatites and of modern and fossil bones. *Journal of Archaeological Science*, 18(3):385–397

Sillen A. & Parkington J. 1996. Diagenesis of bones from Eland's Bay Cave. *Journal of Archaeological Science*, 23:535–542

Sillen A. & Sealy J.C. 1995. Diagenesis of strontium in fossil bone: A reconsideration of Nelson et al. (1986). *Journal of Archaeological Science*, 22:313–320

Sillen A. 1986. Biogenic and diagenetic Sr/Ca in Plio-Pleistocene fossils of the Omo Shungura formation. *Paleobiology*, 12(3):311–323

Sillen A. 1989. Diagenesis of the inorganic phase of cortical bone. In: Price T.D. (ed.), *The chemistry of prehistoric human bone*:211–229. Cambridge University Press, Cambridge

Sillen A., Hall G., Richardson S. & Armstrong R. 1998. $^{87}Sr/^{86}Sr$ ratios in modern and fossil food-webs of the Sterkfontein Valley: implications for early hominid habitat preferences. *Geochimica et Cosmochimica Acta*, 62:2463–2473

Simmons AH. & Mandel R. 2007. Not such a new light: a response to Ammerman and Noller. *World Archaeology*. 39(4):475–482

Simmons AH. 1988. Extinct pygmy hippopotamus and early man in Cyprus. *Nature*. 333 (6173):554–57

Simmons AH. 1999. *Faunal Extinctions in an Island Society: Pygmy Hippopotamus Hunters of the Akrotiri Peninsula, Cyprus* . Plenum/Kluwer, New York.

Skinner H.C. 2005. Mineralogy of bone. In O. Selinus (ed.), *Essentials of medical geology: Impacts of the natural environment on public health*:667–678. London: Elsevier

Smith A.G., Pearson G.W. & Pilcher J. 1970. Belfast radiocarbon dates II. *Radiocarbon*, 12(1):291–297

Snoeck C. 2011. Cremated bone, radiocarbon dating and bioarchaeology. Unpublished MSc Dissertation: The University of Oxford.

Snoeck C., Brock F. & Schulting R.J. 2014a. Carbon exchanges between bone apatite and fuels during cremation: Impact on radiocarbon dates. *Radiocarbon*, 56(2):591–602

Snoeck C., Lee-Thorp J.A. & Schutling R.J. 2014b. From bone to ash: Compositional and structural studies of burned bone. *Palaeogeography, Palaeoclimatology, Palaeoecology*.

Snoeck C., Lee-Thorp J.A., Schulting R.J., de Jong J., Debouge W. & Mattielli N. 2015. Calcined bone provides a reliable substrate for strontium isotope ratios as shown by an enrichment experiment. *Rapid Communication in Mass Spectrometry*, 29:107–114

Sønju Clasen A.B. & Ruyter I.E. 1997. Quantitative determination of type A and type B carbonate in human deciduous and permanent enamel by means of Fourier Transform Infrared spectrometry. *Advances in Dental Research*, 11(4):523–527

Sponheimer M. & Lee-Thorp J.A. 1999. Alteration of enamel carbonate environments during fossilization. *Journal of Archaeological Science*, 26:143–150

Steinman G., Lemmon R.M. & Calvin M. 1964. Cyanamide: a possible key compound in chemical evolution. *Proceedings of the National Academy of Sciences*, 52(1):27–30

Stiner M.C., Kuhn S.L., Weiner S. & Bar-Yosef O. 1995. Differential burning, recrystallization, and fragmentation of archaeological bone. *Journal of Archaeological Science*, 22:223–237

Suetsugu Y., Shimoya I. & Tanaka J. 1998. Configuration of carbonate ions in apatite structure determined by polarized infrared spectroscopy. *Journal of the American Ceramic Society*, 81(3):746–748

Surovell T.A. & Stiner M.C. 2001. Standardizing infra-red measures of bone mineral crystallinity: An experimental approach. *Journal of Archaeological Science*, 28:633–642

Tauber H. 1981. ^{13}C evidence for dietary habits of prehistoric man in Denmark. *Nature*, 292:332–333

Termine J.D. & Posner A.S. 1966. Infrared analysis of rat bone: age dependency of amorphous and crystalline mineral fractions. *Science*, 153(3743):1523–1525

Termine J.D., Eanes E.D., Greenfield D.J., Nylen M.U. & Harper R.A. 1973. Hydrazine-deproteinated bone mineral. *Calcified tissue research*, 12(1):73–90

Théry-Parisot I. 2002. Fuel Management (Bone and Wood) During the Lower Aurignacian in the Pataud Rock Shelter (Lower Palaeolithic, Les Eyzies de Tayac, Dordogne, France). Contribution of Experimentation. *Journal of Archaeological Science*, 29:1415–1421

Thompson T.J.U., Gauthier M. & Islam M. 2009. The application of a new method of Fourier Transform Infrared Spectroscopy to the analysis of burned bone. *Journal of Archaeological Science*, 36:910–914

Thompson T.J.U., Islam M. & Bonniere M. 2013. A new statistical approach for determining the crystallinity of heat-altered bone mineral from FTIR spectra. *Journal of Archaeological Science*, 40:416–422

Thompson T.J.U., Islam M., Piduru K. & Marcel A. 2011. An investigation into the internal and external variables acting on crystallinity index using Fourier Transfrom Infrared spectroscopy on unaltered and burned bone. *Palaeogeography, Palaeoclimatology, Palaeoecology*, 299:168–174

Tieszen L.L. & Farge T. 1993. Effect of diet quality on the isotopic composition of respiratory CO_2, bone collagen, bioapatite and soft tissues. In: Lambert J.B. (ed.), *Prehistoric Human Bone: Archaeology et the Molecular Level*:121–155. Berlin: Springer-Verlag

Tomb J.J. & Davies O. 1938. Urns from Ballymacaldrack. *Ulster Journal of Archaeology*, 1(3):219–221

Tomb J.J. & Davies O. 1941. Further urns from Ballymacaldrack. *Ulster Journal of Archaeology*, 4(3):63

Trueman C.N., Behrensmeyer A.K. Tuross N. & Weiner S. 2004. Mineralogical and compositional changes in bones exposed on soil surfaces in Amboseli National Park, Kenya: Diagenetic mechanisms and the role of sediment pore fluids. *Journal of Archaeological Science*, 31:721–739

Trueman C.N., Privat K. & Field J. 2008. Why do crystallinity values fail to predict the extent of diagenetic alteration of bone mineral? *Palaeogeography, Palaeoclimatology, Palaeoecology*, 266:160–167

Turney C.S.M., Wheeler D. & Chivas A.R. 2006. Carbon isotope fractionation in wood during carbonization. *Geochimica et Cosmochimica Acta*, 70(4):960–964

Tuross N., Behrensmeyer A.K. & Eanes E.D. 1989. Strontium increases and crystallinity changes in taphonomic and archaeological bone. *Journal of Archaeological Science*, 16(6):661–672

Ubelaker DH. 1989. The Estimation of Age at Death from Immature Human Bone. In: Iscan M.Y. (ed.), *Age Markers in the Human Skeleton*:55–70. Springfield, Illinois: C.C. Thomas

Van Strydonck M, Boudin M. & De Mulder G. 2010. The carbon origin of structural carbonate in bone apatite of cremated bones. *Radiocarbon*. 52(2–3):578–586

Van Strydonck M., Boudin M. & De Mulder G. 2009. ^{14}C dating of cremated bone: The issue of sample contamination. *Radiocarbon*, 51:553–568

Van Strydonck M., Boudin M., Hoefkens M. & De Mulder G. 2005. ^{14}C-dating of cremated bones, why does it work? *Lunula*, 13:3–10

Van Strydonck M., Decq L., Brande T.V., Boudin M., Ramis D., Borms H. & De Mulder G. 2013. The protohistoric ‘quicklime burials’ from the Balearic Islands: cremation or inhumation. *International Journal of Osteoarchaeology*.

Vaughan J.M. 1970. *The physiology of bone*. Oxford: Clarendon Press.

Vignoles M., Bonel G. & Young R.A. 1987. Occurence of nitrogenous species in precipitated B-type carbonated hydroxyapatites. *Calcified Tissues International*, 40:64–70

Vogel J.C. & van der Merwe N.J. 1977. Isotopic evidence for early maize cultivation in New York State. *American Antiquity*, 42(2):238–242

Wang Y. & Cerling T.E. 1994. A model of fossil tooth and bone diagenesis: Implications for palaeodiet reconstruction from stable isotopes. *Palaeogeography, Palaeoclimatology, Palaeoecology*, 107:281–289

Waterman D.M. 1965. The court cairn at Annaghmare, Co. Armagh. *Ulster Journal of Archaeology*, 28:3–46

Weiner S. & Bar-Yosef O. 1990. States of Preservation of Bones from Prehistoric Sites in the Near East: A Survey. *Journal of Archaeological Science*, 17:187–196

Weis D., Kieffer B., Maerschalk C., Barling J., de Jong J., Williams G.A., Hanano D., Pretorius W., Mattielli N., Scoates J.S., Goolaerts G., Friedman R.M. & Mahoney J.B. 2006. High-precision isotopic characterization of USGS reference materials by TIMS and MC-ICP-MS. *Geochemistry, Geophysics, Geosystems*, 7(8).

Whipkey C.E., Capo R.C., Chadwick O.A. & Stewart B.W. 2000. The importance of sea spray to the cation budget of a coastal Hawaiian soil: a strontium isotope approach. *Chemical Geology,* 168(1):37–48

Wopenka B. & Pasteris J.D. 2005. A mineralogical perspective on the apatite in bone. *Materials Science and Engineering C*, 25:131–143

Wright L.E. & Schwarcz H.P. 1996. Infrared and isotopic evidence for diagenesis of bone apatite at Dos Pilas, Guatemala: Palaeodietary implications. *Journal of Archaeological Science*, 23:933–944

Yoder C.H., Pasteris J.D., Worcester K.N. & Schermerhorn D.V. 2012. Structural water in carbonated hydroxylapatite and fluorapatite: Confirmation by solid state 2H NMR. *Calcified tissue international*, 90(1):60–67

Zazzo A. & Saliège J.-F. 2011. Radiocarbon Dating of Biological Apatites: A Review. *Palaeogeography, Palaeoclimatology, Palaeoecology*, 310:52–61

Zazzo A., Balasse M. & Patterson W.P. 2006. The reconstruction of mammal individual history: refining high-resolution isotope record in bovine tooth dentine. *Journal of Archaeological Science*, 33(8):1177–1187

Zazzo A., Balasse M., Passey B.H., Moloney A.P., Monahan F.J. & Schmidt O. 2010. The isotope record of short-and long-term dietary changes in sheep tooth enamel: implications for quantitative reconstruction of paleodiets. *Geochimica et Cosmochimica Acta*, 74(12):3571–3586

Zazzo A., Lebon M., Chiotti L., Comby C., Delqué-Količ E., Nespoulet R. & Reiche I. 2013. Can we use calcined bone for ^{14}C dating the Paleolithic? *Radiocarbon*, 55(2–3) :1409–1421

Zazzo A., Saliège J.-F., Lebon M., Lepetz S. & Moreau C. 2012. Radiocarbon dating of calcined bones: insights from combustion experiments under natural conditions. *Radiocarbon*, 54(3–4) :1–12

Zazzo A., Saliège J.-F., Person A. & Boucher H. 2009. Radiocarbon dating of calcined bones: Where does the carbon come from? *Radiocarbon*, 51(2):601–611

Websites

Bone Biology and Mechanics Lab – IUPUI: Indiana University-Purdue University at Indianapolis, accessed 05.09.2014, http://www.iupui.edu/~bbml/boneintro.shtml

GEOROC – Geochemistry of Rocks of the Oceans and Continents, accessed 08.07.2014, http://georoc.mpch-mainz.gwdg.de/georoc/

GSI – Geological Survey of Ireland, accessed 08.09.2014, http://www.gsi.ie/

GSNI – Geological Survey of Northern Ireland, accessed 08.09.2018, http://www.bgs.ac.uk/gsni/

Appendices

1 Impact of contamination on infrared indices

1.1 Quartz

One of the potential contaminants that can be found in archaeological calcined bone fragments is quartz. Pure quartz (Q) was analysed as well as an archaeological bone sample (B) that did not contain any detectable amount of quartz. A mixture (B&Q) of these two samples was then prepared, homogenised (c. 60% bone – 40% quartz in weight), and was characterised through infrared spectroscopy (Figure A.1).

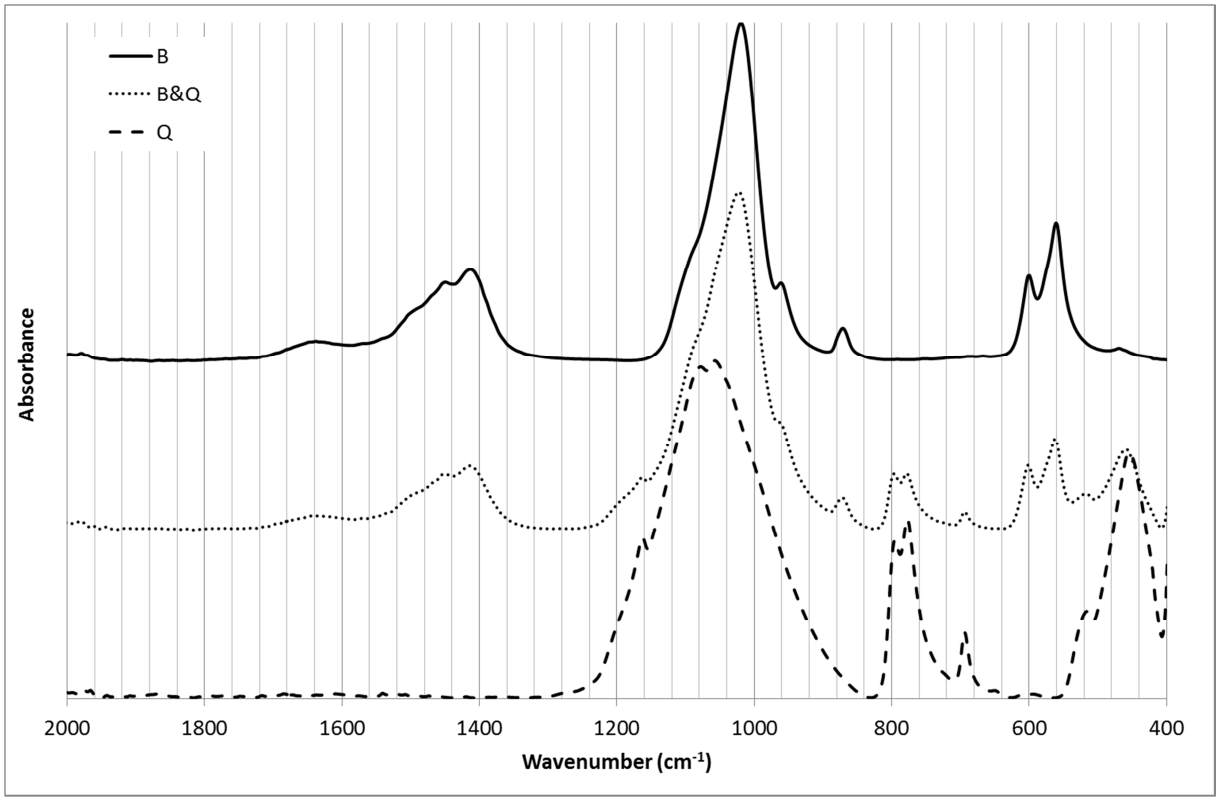

Figure A.1 – FTIR spectra of an unburned archaeological bone (B), quartz (Q), and a mixture of unburned bone and quartz (B&Q)

From the calculation of the various carbonate to phosphate ratios in the samples with and without quartz (Table A.1), it appears that C/P 2 and C/P 1_a are the most affected by the

presence of quartz. For C/P 1_b, this can be expected since the major absorbance wavelength of quartz is 1090 cm^{-1}, a band which overlaps significantly with the main phosphate band at 1035 cm^{-1} used to measure the C/P 1_b leading to an underestimation of the amount of carbonates present in bone. The C/P 2 is also affected by the presence of quartz because of the very broad band at 1090 cm^{-1} which overlaps partially with the carbonate band at 870 cm^{-1} leading this time to an overestimation of the amount of carbonates.

Table A.1 – Carbonate to phosphate ratios in archaeological bone (B) and archaeological bone mixed with quartz (B&Q); the mean and range are calculated for each triplicate

	B		**B&Q**		**Variation (%)**
	Mean	*Range*	*Mean*	*Range*	
C/P 1 or BPI	1.07	1.05–1.10	0.99	0.97–1.01	-7%
C/P 1_b	0.27	0.26–0.28	0.19	0.18–0.20	-30%
C/P 2	0.39	0.37–0.40	0.50	0.47–0.51	28%
API	0.92	0.90–0.95	0.86	0.84–0.88	-7%
CO_3/PO_4	0.76	0.74–0.79	0.77	0.75–0.79	1%

From the FTIR spectra, the BPI, API and CO_3/PO_4 should not be affected by the presence of quartz since no quartz band are present in the 1600–1400 and 650–550 cm^{-1} ranges; however, there is a shift in BPI and API values while the ranges of CO_3/PO_4 values are almost identical in both cases. Nevertheless, it is unlikely that archaeological bone samples would contain as much as 40% of quartz. The API and BPI will therefore still be measured to evaluate the amount of type A and B carbonates respectively.

The presence of quartz does not only affect the carbonate to phosphate ratios but also any other index using the main phosphate band at 1035 cm^{-1} or any band between 1300 and 650 cm^{-1}. Indeed, if quartz is present, using the band at 1035 cm^{-1} instead of the phosphate bands at 605 or 565 cm^{-1} will lead to an underestimation of, for example, the carbonate content.

1.2 Soil carbonates

Another type of common contaminants that can be observed in archaeological calcined bone fragments is soil carbonates. They can be adsorbed by bone from its environment after burial, in which case, a band around 710 cm^{-1} (Figure A.2) typical of calcite or aragonite can be observed. The presence of soil carbonates in the sample is a problem: it affects all carbonate bands (870, 1415 & 1450 cm^{-1}) and it is difficult to discriminate between bone apatite carbonate and soil carbonates and the concentration of bone apatite carbonates will be overestimated. If carbonates are incorporated into the structure and not adsorbed as calcite or aragonite, it will not be possible to detect them using FTIR as the 710 cm^{-1} will not be present.

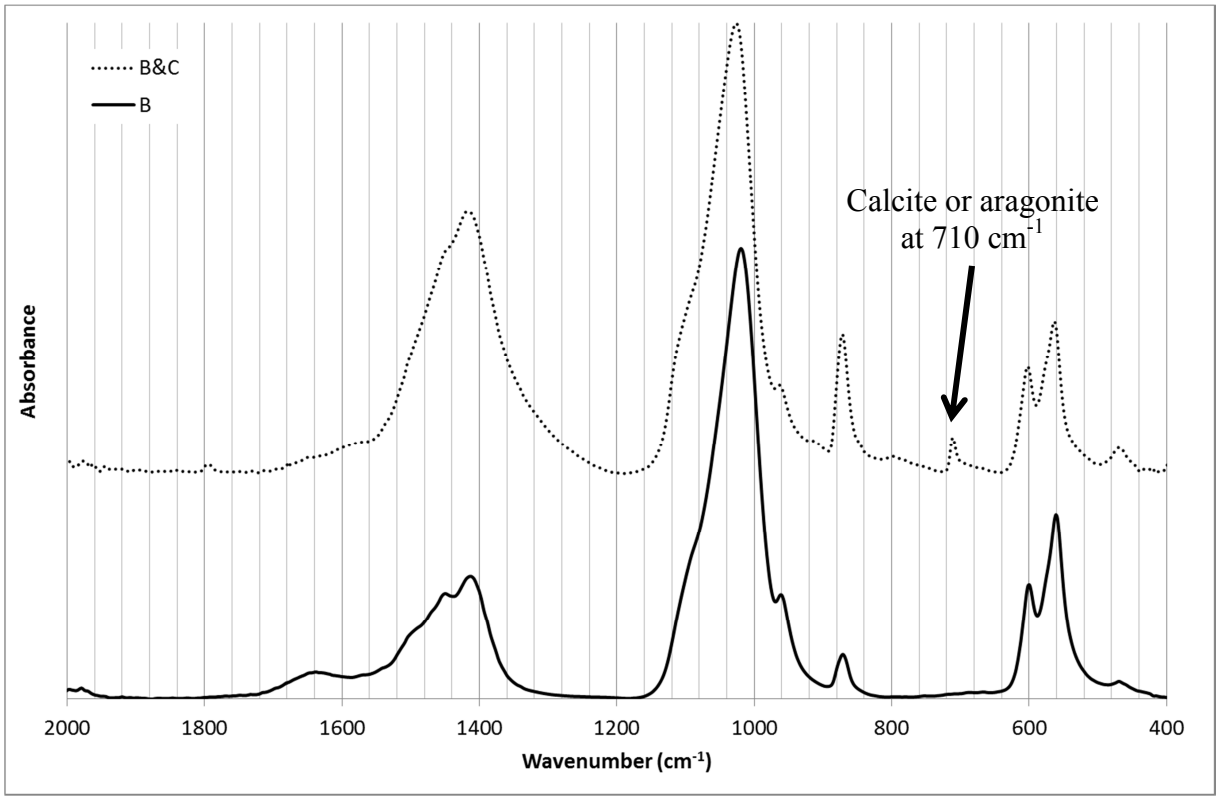

Figure A.2 – FTIR spectra of an archaeological bone that contains no or very little soil carbonate (B), and an archaeological bone containing significant amounts of soil carbonate (B&C)

2 Band area versus band intensity indices

All the infrared indices detailed in Chapter 4 are calculated using the maximum absorbance intensity of the bands or absorbance intensity at a fixed wavenumber but some authors also used band areas (e.g. Termine & Posner 1966; Lebon et al. 2010). To test the relation between indices measured using band intensity and band area, several indices were calculated replacing band intensity by band area (Figure A.3 and Tables A.2 and A.3).

Table A.2 – Area ranges and corresponding bands

	Area range (cm^{-1})	**Corresponding band (cm^{-1})**	**Functional Group(s)**
A1	500–590	565	Phosphates (PO_4^{3-})
A2	590–620	605	Phosphates (PO_4^{3-})
A3	620–660	630	Apatitic hydroxyl groups (OH^-)
A4	900–1200	1035	Phosphates (PO_4^{3-})
A5	1380–1440	1415	Type B carbonates (CO_3^{2-})
A6	1440–1520	1450	Type A + B carbonates (CO_3^{2-})
A7	1520–1600	1540	Amide II + Type A carbonates (CO_3^{2-})

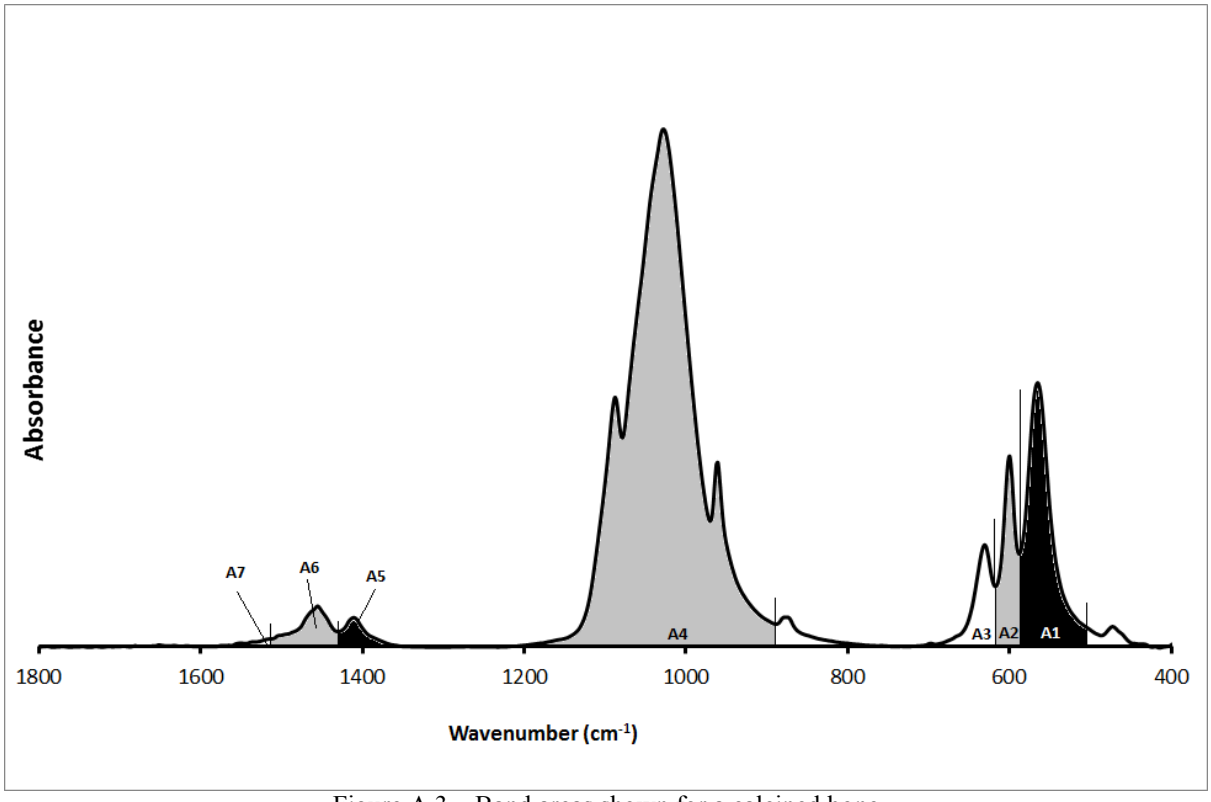

Figure A.3 – Band areas shown for a calcined bone

From the R^2 values calculated for a linear regression (Table A.3) it appears that most indices calculated with band areas provide the same information as their equivalent measured using band intensity ($R^2 \geq 0.96$). Two area ratios reach slightly lower values: A6/A5 and A3/A2. The correlation between A3/A2 and OH/P goes up to $R^2 = 0.96$ when looking only at calcined bone for which this index was specifically developed since no hydroxyl groups are visible in the infrared spectra of unburned bone. However, for the A6/A5, the correlation remains the same. Nevertheless, the correlation is high enough that this ratio will not be further analysed, and only indices calculated using band intensities will be investigated.

Table A.3 – Area ratios and corresponding indices; R^2 values calculated for linear correlation

Area ratio	**Corresponding index**	**Significance**	**R^2**
A5/A2	C/P 1 or BPI – A_{1415}/A_{605}	Amount of type B carbonates	0.99
A5/A4	C/P 1_a – A_{1415}/A_{1035}		0.96
(A5+A6)/(A1+A2)	CO_3/PO_4 – $(A_{1415} + A_{1450}) / (A_{605} + A_{565})$	Amount of type A + B carbonates	0.96
A7/A2	API – A_{1540}/A_{605}	Amount of type A carbonates	0.98
A6/A5	C/C – A_{1450}/A_{1415}	Compares two carbonate bands: (A+B)/B	0.88
A3/A2	OH/P – A_{630}/A_{605}	Amount of hydroxyl groups	0.90

3 Pre-treatment for radiocarbon dating of calcined bone

The currently used pre-treatment protocol at the Oxford Radiocarbon Accelerator Unit (ORAU) for radiocarbon dating of calcined bone involves several bleaches with 1.5% sodium chlorite ($NaClO_2$) at pH3 followed by several rinses with milli-Q water and leaching with 1M acetic acid (Brock et al. 2010b). Sodium chlorite is used to remove organic matter from bone apatite. However, once calcined, no organic matter remain in the sample and such pre-treatment is possibly superfluous. Furthermore, the use of $NaClO_2$ instead of NaClO – commonly used to pre-treat enamel and bone apatite for stable isotopic analyses (e.g. Koch et al. 1997) – may not be the most efficient as its oxidising power is much lower than that of NaClO. Indeed, the use of $NaClO_2$ on several modern unburned bone samples showed that almost no organic matter was removed, while none remained after pre-treatment with NaClO as shown by the infrared spectra and the measurement of the amount of nitrogen in the samples (%N) which can be used as a proxy for the amount of proteins present (Figure A.4). However, the use of NaClO induces the incorporation of atmospheric carbon dioxide that will have a significant impact on the radiocarbon dates (Zazzo et al. 2006; Pellegrini & Snoeck in prep). The subsequent pre-treatment with acetic acid, however, removes these adsorbed atmospheric carbon contributions. Nevertheless, each step in the pre-treatment could affect the radiocarbon dates and limiting pre-treatment to what is necessary could improve the radiocarbon dates obtained. Another argument in favour of limiting the pre-treatment to acetic acid is that phosphoric acid should not react with potential organic matter still present in calcined bone apatite. Furthermore, shorter pre-treatments allow saving time and money and limiting the amount of sample loss.

To test for the impact of $NaClO_2$ pre-treatment on the radiocarbon dates obtained on calcined bone fragments, two samples were pre-treated following both the ‘new’, simpler pre-treatment and the traditional one (Brock et al. 2010b). The ‘new’ pre-treatment is limited to

several leaching steps with 1M acetic acid. The dates obtained are statistically identical (X^2 test with OxCal v4.8 using R_combine function) with both pre-treatments (Table A.4) suggesting that $NaClO_2$ pre-treatment is unnecessary.

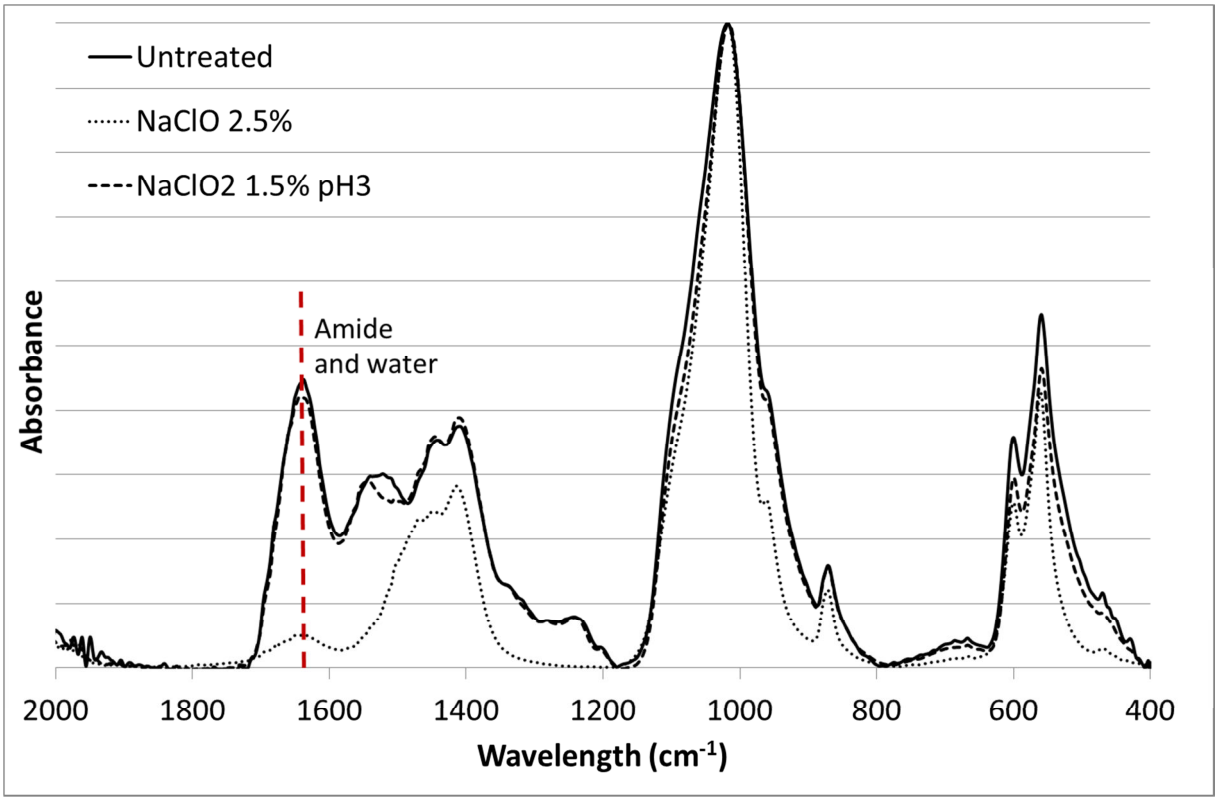

Figure A.4 – Infrared spectra of modern bone untreated, pre-treated with 2.5% NaClO and 1.5% $NaClO_2$ at pH3; the band at 1650 cm^{-1} corresponding to amide (organic matter) and water is highlighted: minimal variation is observed between untreated (%N = 4.8) and pre-treated with $NaClO_2$ (%N = 5.1), while the band at 1650 cm^{-1} is much smaller after the use of NaClO (due to the presence of water as no organic matter remains in that sample – %N < 0.01)

Table A.4 – Radiocarbon and stable isotope results for archaeological samples (IntCal 13)

Site	Pre-treatment	OxA*	BP	$\delta^{13}C$	X^2 test
Annaghmare	'new'	X-2579-44	4572 ± 28	-20.4	df=1, T=0.8 (5% 3.8)
	traditional	30188	4532 ± 36	-20.5	
Ness of Gruting	'new'	X-2579-41	3964 ± 31	-27.6	df=1, T=3.6 (5% 3.8)
	traditional	X-2579-42	4043 ± 28	-27.6	

*Samples dated at ORAU are routinely issued with OxA- laboratory numbers. Those issued with OxA-X-numbers are research measurements with non-standard or experimental methods (see Brock et al 2010b).

To confirm the limited impact of the presence of organic matter on the isotope composition of the carbon dioxide released during phosphoric acid treatment, several aliquots

of IAEA-C01 carbonate ($\delta^{13}C$ = 2.5 ‰) were contaminated with 10 and 50% of collagen of know carbon isotope composition ($\delta^{13}C_{coll}$ = –22.1 ‰). These were then all reacted with phosphoric acid without any prior pre-treatment. The carbon dioxide emitted by the reaction was trapped cryogenically. The isotopes were then measured and the $\delta^{13}C$ values show limited variation of the isotope ratio (Table A.5).

Table A.5 – Stable carbon isotope ratio for marble samples contaminated with collagen

Organics content (%wt.)	**$\delta^{13}C$**	**%intake of collagen**
0%	2.44	/
0%	2.43	/
10%	2.28	0.7
10%	2.10	1.4
50%	2.31	0.5
50%	2.22	0.9

The results presented here highlight the fact that a simple pre-treatment of several washes with 1M acetic acid over 24 hours is sufficient prior to radiocarbon dating of calcined bone and that no pre-treatment with $NaClO_2$ is required.

4 Isotopic memory effect

4.1 LAB 1

The results obtained by common acid bath (Snoeck 2011) and using a carbonate device for LAB 1 (Table A.6) are compared to one another and strong linear correlations can be found between the $\delta^{13}C$ and $\delta^{18}O$ measured using both methods ($R^2 > 0.96$) if two samples (L1 and L2) are not taken into account. There is, however, an average offset of about 2 ‰ in carbon and 1.2 ‰ in oxygen. When L1 and L2 are taken into account, the correlations drop to 0.40 and 0.80 for $\delta^{13}C$ and $\delta^{18}O$ respectively. L1 and L2 were the two first samples to be measured in the common acid bath after the in-house standard (NOCZ: $\delta^{13}C$ = 2.1‰; $\delta^{18}O$ = 1.9‰) and are much more enriched in ^{13}C when measured with a common acid bath compared to the carbonate device.

Table A.6 – Results for the LAB 1 experiment

	Time (h)	Heating environment	Colour code	pCO_2/g	Carbonate device		Common acid bath	
					$\delta^{13}C$	$\delta^{18}O$	$\delta^{13}C$	$\delta^{18}O$
L0	0	unburned	0	2.31	-15.3	-4.3	-13.9	-3.3
L1	0.5	open	5	0.35	-21.3	-15.0	-10.4	-8.8
L2	1	open	6	0.28	-21.7	-15.5	-14.7	-12.0
L3	2	closed	4	0.68	-17.5	-14.5	-16.9	-14.6
L4	4	closed	6	0.26	-20.8	-16.7	-17.7	-14.4
L5	4	open + millet	6	0.23	-14.6	-15.0	-12.9	-13.3
L6	4	closed + millet	4	0.40	-15.1	-17.3	-13.9	-16.3
L7	4	open + barley	6	0.22	-25.6	-15.8	-21.8	-14.3
L8	4	closed + barley	4	0.40	-22.6	-17.4	-20.1	-16.3

Open – open crucible; closed – bone wrapped in aluminium foil and buried in a crucible filled with sand; all isotopic data is measured in ‰ versus VPDB standards; common acid bath results from Snoeck (2011)

4.2 LAB 2

The results obtained for the LAB 1 samples questioned the validity of the common acid bath mass spectrometry. To test this, a calcined and a charred sample were analysed and ten

aliquots of each sample were measured successively in two different runs (Run 1 and Run 2). The ten aliquots of calcined samples were analysed directly after the internal standard (NOCZ) followed by the ten charred sample aliquots (Figure A.5). The results for the calcined bone aliquots are very variable and the values are highest the beginning of the run, or, in other words, in the samples that follow the internal standards. The charred samples that still contain significant amounts of carbon compared to calcined bone, show much smaller variation in the isotopic measurements. Both runs show very similar results.

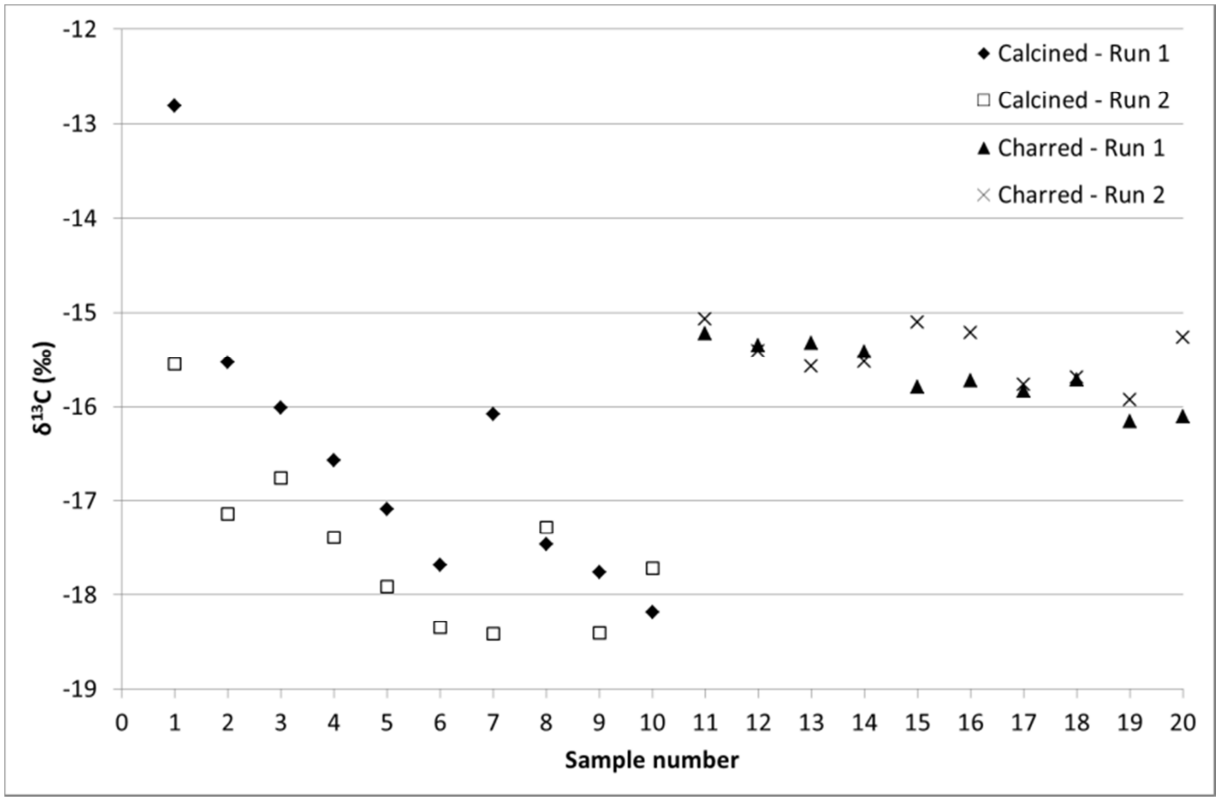

Figure A.5 – Stable carbon isotope values of calcined and charred samples as a function of their position in the run (sample number); ten aliquots of calcined and charred samples were measured successively in two different runs

4.3 Samples analysed on different mass spectrometers

Initially, calcined bone samples were analysed at the department of Earth Sciences at the University of Oxford using a common acid bath. The results likely showed a memory effect. Since calcined bone fragments contain only a very limited amount of carbonates for isotope

analyses, a small amount of carbon dioxide left from the reaction of the previous sample (or standard) with phosphoric acid in the common acid bath will have a significant impact on the isotope values. As shown for the results of LAB 1, the two samples that were measured directly after the internal standard have values that are not following the linear correlation observed for all the other samples. Furthermore, once these samples have been considered as outliers, even though the correlation between the samples measured in common acid bath and using a carbonate device are very good ($R^2 > 0.96$ for both carbon and oxygen), there is an offset of about 2 ‰ in carbon and 1.2 ‰ in oxygen questioning the comparability of the results obtained using different methods. The memory effect was also observed in the repeated measurements carried out on LAB 2 samples (Figure A.5). In order to exclude both problems of isotopic memory effect and comparability, most samples were analysed using a carbonate device on the same mass spectrometer.

5 Note on the use of Attenuated Total Reflectance (ATR) Mode

An important development in FTIR methodology over the last decade has been the introduction of FTIR-ATR (Attenuated Total Reflectance). Prior to this, it had been common practice to carry out FTIR measurements using the transmission mode (KBr pellets). The results obtained via ATR are not directly comparable with those obtained with the KBr method and are less quantitative (Thompson et al. 2009; Beasley et al. 2014). The ATR mode, however, allows fast and efficient screening of bone samples, making possible the measurement of more than 30 samples in triplicate each day. In transmission mode (KBr), the size of the analysed particles has an impact on the spectra (Surovell & Stiner, 2001), while in ATR mode, the particle size is of no significance (Thompson et al. 2009). In ATR mode, the samples need to be pressured onto the diamond crystal, and the amount of pressure has an impact on the maximum absorbance intensity. It is important when using ATR that enough pressure is applied onto the sample: at lower intensity, the reproducibility of the measurements decreases.

To illustrate the impact of the pressure applied onto the samples on the different infrared indices, the same set of archaeological cremated human remains from Knowth (Co. Meath, Ireland) was analysed twice, and the carbonate to phosphate ratio (CO_3/PO_4) measured. Lower pressure was applied the first time and the same samples were then submitted to higher pressure. Three aliquots were analysed for each sample both at low and high pressure and the standard deviation was measured for each triplicate. In Figure A.6, the maximum absorbance intensity is compared to the standard deviation of the CO_3/PO_4 measurements carried out on each three aliquots. The standard deviation is much more variable and generally higher when lower pressures are applied to the sample.

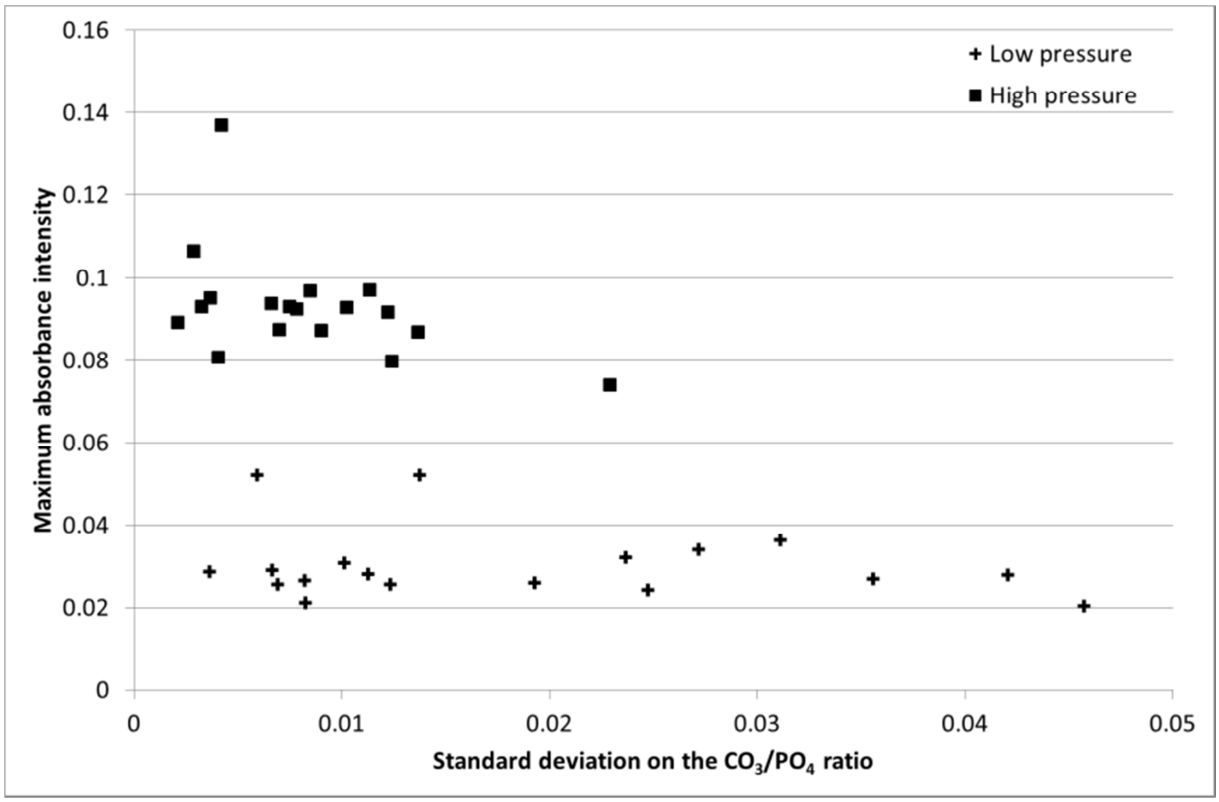

Figure A.6 – Maximum absorbance intensity versus the standard deviation measured on the CO_3/PO_4 ratio of archaeological calcined human bone from Knowth for low and high pressures applied to the sample

It can further be observed that at higher pressure, the carbonate to phosphate ratios are higher (Figure A.7a), highlighting the importance of pressing the samples with sufficiently high pressure onto the diamond crystal of the ATR-equipment. Figure A.7b shows that when the absorbance of the highest band (in the case of calcined bone, the phosphate band at 1035 cm^{-1}) is above 0.06 (the higher the pressure, the higher the maximum absorbance for a given sample), the calculated carbonate to phosphate ratio is much less variable and remains more or less constant with increasing pressure.

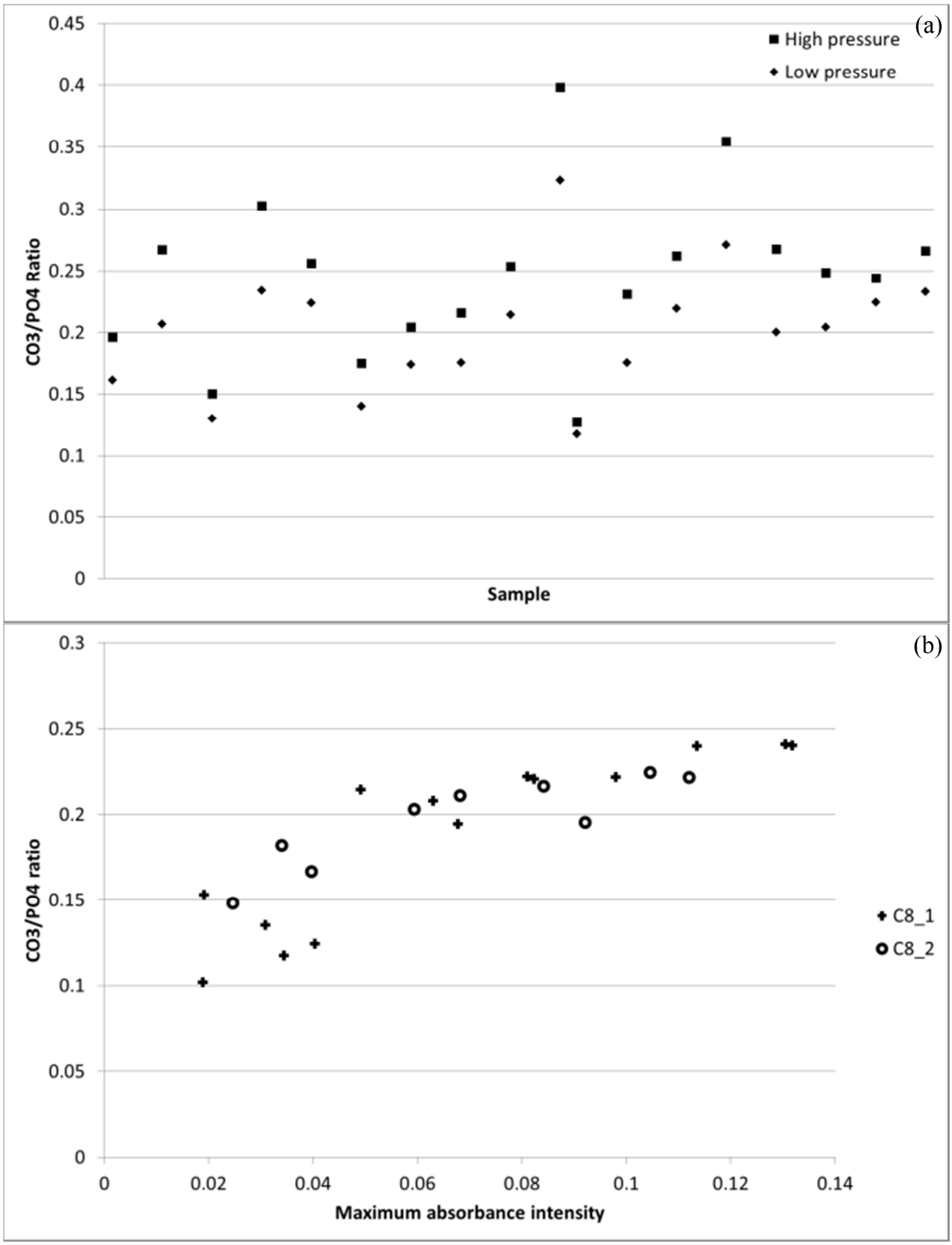

Figure A7 – (a) CO_3/PO_4 ratio of archaeological calcined human bone from Knowth for low and high pressure applied to the sample; (b) CO_3/PO_4 ratio of two different experimentally heated samples submitted to different pressures versus the maximum absorbance intensity

6 Raw data

For many samples the infrared results are presented before and after pre-treatment with sodium hypochlorite and acetic acid. Elementary analyses were performed on untreated samples while isotope analyses of bone apatite and tooth enamel samples were carried out after pre-treatment with sodium hypochlorite and acetic acid (see Chapter 3).

6.1 Laboratory heating experiment 1 (LAB 1)

6.1.1 Isotope analyses data

Table A.7 – Isotope analyses data for LAB 1

T (°C)	Time (h)	Sample	Colour Code	Setting	$\delta^{13}C$ (‰)	$\delta^{18}O$ (‰)	pCO_2/g of sample
0	0	/	0	/	-15.3	-4.1	2.31
700	0.5	L1	5	Open crucible	-21.3	-14.8	0.35
	1	L2	6	Open crucible	-21.7	-15.3	0.28
	2	L3	4	Bone placed in aluminium foil, and crucible filled with sand	-17.5	-14.2	0.68
	4	L4	6	Bone placed in aluminium foil, and crucible filled with sand	-20.8	-16.4	0.26
	4	L5	6	5g of millet seeds added into the open crucible	-14.6	-14.7	0.23
	4	L6	4	Bone placed together with 5g of millet seeds in aluminium foil, and crucible filled with sand	-15.1	-17.1	0.40
	4	L7	6	5g of barley seeds added into the open crucible	-25.6	-15.6	0.22
	4	L8	4	Bone placed together with 5g of barley seeds in aluminium foil, and crucible filled with sand	-22.6	-17.2	0.40

6.2 Laboratory heating experiment 2 (LAB 2)

6.2.1 Infrared data before pre-treatment

Table A.8 – Infrared data before pre-treatment for LAB 2

T (°C)	Time (h)	Sample	Colour Code	BPI	C/P 2	API	CO_3 /PO_4	IRSF	1060/ 1075	1030/ 1110	PPI	PSF	AB	C/C	OH/P	OHSF	CN/P	WAMPI
0	0	/	0	0.92	0.41	0.74	0.72	3.00	1.20	2.33	0.65	1.50	0.90	0.97	0.28	5.46	0.17	1.09
500	0.5	05_3	3	0.82	0.46	0.30	0.61	3.52	1.26	2.78	0.61	1.57	0.92	0.98	0.26	5.53	0.12	0.28
		10_4	3	0.71	0.37	0.23	0.53	3.73	1.28	3.02	0.60	1.66	0.92	0.98	0.28	5.13	0.15	0.20
	1	13_2	3	0.70	0.39	0.19	0.53	3.64	1.27	2.90	0.61	1.61	0.92	1.00	0.29	4.90	0.15	0.13
		15_1	3	0.66	0.41	0.17	0.51	3.61	1.26	2.78	0.63	1.60	0.92	1.03	0.31	4.67	0.13	0.13
	2	05_4	4	0.57	0.35	0.14	0.44	3.80	1.28	2.99	0.62	1.66	0.94	1.01	0.33	4.29	0.15	0.09
		15_4	4	0.58	0.33	0.13	0.45	3.79	1.27	2.90	0.63	1.68	0.94	1.01	0.33	4.31	0.13	0.09
	4	13_3	3.5	0.55	0.33	0.14	0.42	3.91	1.28	3.01	0.61	1.69	0.94	1.04	0.32	4.38	0.17	0.09
		14_4	3.5	0.57	0.35	0.14	0.45	3.76	1.26	2.80	0.63	1.63	0.94	1.02	0.34	4.24	0.16	0.09
	8	01_2	3.5	0.56	0.34	0.13	0.43	3.84	1.27	3.01	0.62	1.65	0.94	1.02	0.34	4.13	0.14	0.08
		05_2	3.5	0.56	0.34	0.14	0.43	3.85	1.27	2.96	0.62	1.65	0.94	1.01	0.34	4.12	0.17	0.09
	12	07_2	3.5	0.51	0.32	0.13	0.40	3.96	1.27	3.04	0.62	1.69	0.95	1.04	0.35	4.03	0.16	0.08
		11_1	3.5	0.53	0.33	0.13	0.42	3.82	1.27	2.95	0.62	1.67	0.94	1.03	0.34	4.13	0.14	0.08
	18	01_4	3.5	0.50	0.29	0.13	0.39	3.94	1.27	3.01	0.63	1.72	0.94	1.01	0.35	3.98	0.13	0.09
		20_2	3.5	0.52	0.26	0.13	0.40	4.12	1.28	3.05	0.62	1.83	0.92	1.00	0.34	4.06	0.17	0.09
	24	04_4	Failed															
		20_4																
600	0.5	03_1	3.5	0.63	0.42	0.19	0.49	3.69	1.27	2.93	0.62	1.58	0.93	1.05	0.30	4.74	0.17	0.15
		16_1	3.5	0.55	0.33	0.14	0.43	3.88	1.27	2.98	0.63	1.70	0.93	1.04	0.32	4.43	0.14	0.10
	1	01_1	4	0.49	0.32	0.11	0.39	3.98	1.27	3.02	0.63	1.68	0.95	1.04	0.35	3.99	0.15	0.08
		10_2	4	0.43	0.25	0.12	0.34	4.22	1.28	3.11	0.64	1.81	0.95	1.06	0.37	3.74	0.16	0.07
	2	02_4	4	0.45	0.30	0.12	0.36	4.08	1.27	3.14	0.62	1.72	0.95	1.06	0.36	3.84	0.16	0.07
		04_3	4	0.44	0.29	0.12	0.35	4.05	1.27	3.02	0.64	1.72	0.96	1.05	0.37	3.76	0.17	0.07
	4	14_1	5	0.34	0.22	0.09	0.27	4.59	1.31	3.13	0.65	1.96	0.95	1.05	0.42	3.82	0.11	0.05
		16_2	5	0.34	0.19	0.09	0.27	4.96	1.34	3.44	0.63	2.17	0.95	1.01	0.48	3.93	0.12	0.04

Table A.8 (*continued*)

T (°C)	Time (h)	Sample	Colour Code	BPI	C/P 2	API	CO_3 /PO_4	IRSF	1060/ 1075	1030/ 1110	PPI	PSF	AB	C/C	OH/P	OHSF	CN/P	WAMPI
600	8	09_4	Failed															
		18_4																
	12	04_2	5	0.29	0.18	0.08	0.23	4.95	1.38	3.34	0.65	2.08	0.96	1.03	0.54	4.20	0.13	0.04
		08_2	5	0.27	0.17	0.10	0.22	5.24	1.40	3.51	0.64	2.22	0.98	1.08	0.58	4.42	0.13	0.05
	18	08_4	5.5	0.29	0.11	0.06	0.15	6.68	1.61	5.47	0.54	3.13	0.99	1.15	0.57	5.74	0.12	0.01
		14_3	5	0.19	0.16	0.08	0.23	5.15	1.40	3.60	0.63	2.23	0.98	1.05	0.67	4.27	0.11	0.04
	24	02_2	6	0.12	0.08	0.05	0.09	6.30	1.52	4.56	0.58	2.75	1.03	1.07	0.71	5.91	0.10	0.02
		18_1	6	0.15	0.08	0.06	0.11	6.68	1.57	5.53	0.54	3.15	1.03	1.09	0.71	6.09	0.10	0.02
700	0.5	08_1	4.5	0.29	0.18	0.11	0.24	4.95	1.39	3.62	0.64	2.11	0.98	1.19	0.47	4.32	0.19	0.05
		12_1	4.5	0.32	0.22	0.10	0.27	4.63	1.35	3.28	0.66	1.92	0.97	1.13	0.45	4.16	0.23	0.05
	1	05_1	5	0.15	0.10	0.06	0.13	5.46	1.49	4.04	0.63	2.34	1.05	1.17	0.66	5.02	0.12	0.02
		10_1	5	0.18	0.10	0.07	0.14	6.11	1.60	4.88	0.59	2.54	1.04	1.15	0.66	5.59	0.14	0.03
	2	06_3	6	0.15	0.09	0.06	0.12	5.91	1.54	4.63	0.59	2.50	1.05	1.15	0.71	5.71	0.11	0.02
		15_2	6	0.16	0.10	0.06	0.13	5.86	1.54	4.72	0.60	2.45	1.07	1.15	0.72	5.76	0.11	0.02
	4	12_2	6	0.13	0.08	0.05	0.10	6.06	1.56	5.07	0.58	2.70	1.05	1.06	0.73	5.93	0.10	0.02
		13_4	6	0.12	0.08	0.05	0.09	5.93	1.55	4.97	0.57	2.61	1.05	1.18	0.68	5.57	0.11	0.02
	8	12_3	6	0.16	0.09	0.05	0.13	5.86	1.55	4.94	0.59	2.42	1.06	1.16	0.71	5.78	0.10	0.01
		15_3	6	0.12	0.07	0.04	0.09	6.17	1.57	5.02	0.56	2.67	1.10	1.04	0.76	6.15	0.10	0.01
	12	17_2	6	0.11	0.07	0.04	0.09	6.53	1.57	5.44	0.54	2.85	1.10	1.12	0.72	6.22	0.10	0.01
		18_2	6	0.11	0.10	0.04	0.09	6.47	1.69	4.32	0.57	2.17	1.07	1.20	0.71	5.49	0.11	0.01
	18	17_4	Failed															
		19_3																
	24	03_3	6	0.09	0.06	0.03	0.07	6.55	1.56	5.50	0.53	2.91	1.07	1.14	0.73	6.10	0.10	0.01
		03_4	6	0.12	0.07	0.04	0.09	6.49	1.55	5.34	0.53	2.70	1.10	1.16	0.71	6.09	0.11	0.01
800	0.5	02_1	4.5	0.22	0.17	0.09	0.21	4.97	1.42	3.70	0.66	2.00	1.05	1.34	0.47	4.71	0.32	0.03
		20_1	4.5	0.22	0.13	0.07	0.20	5.42	1.44	4.25	0.64	2.27	1.09	1.41	0.35	5.25	0.54	0.02
	1	07_3	5	0.15	0.10	0.05	0.13	5.78	1.55	4.96	0.59	2.34	1.10	1.31	0.66	5.44	0.11	0.02
		19_2	5.5	0.24	0.20	0.06	0.21	5.35	1.52	3.66	0.61	2.03	1.03	1.36	0.52	4.57	0.22	0.02
	2	09_2	6	0.14	0.14	0.07	0.12	5.22	1.54	4.46	0.62	2.01	1.17	1.30	0.71	5.48	0.11	0.02
		17_1	6	0.17	0.13	0.05	0.16	5.01	1.50	4.10	0.64	1.94	1.14	1.34	0.66	5.02	0.12	0.01

Table A.8 (*continued*)

T (°C)	Time (h)	Sample	Colour Code	BPI	C/P 2	API	CO_3 /PO_4	IRSF	1060/ 1075	1030/ 1110	PPI	PSF	AB	C/C	OH/P	OHSF	CN/P	WAMPI
800	4	02_3	6	0.18	0.16	0.06	0.16	5.36	1.54	4.85	0.59	2.02	1.13	1.36	0.67	5.24	0.11	0.02
		11_2	6	0.12	0.09	0.04	0.11	5.65	1.51	4.58	0.59	2.26	1.10	1.54	0.62	5.02	0.11	0.01
	8	01_3	6	0.13	0.13	0.04	0.12	5.30	1.53	4.24	0.62	2.02	1.08	1.44	0.66	5.12	0.11	0.01
		17_3	6	0.08	0.09	0.04	0.07	6.08	1.56	4.83	0.55	2.23	1.19	1.57	0.63	5.28	0.09	0.01
	12	16_3	6	0.09	0.10	0.05	0.09	5.50	1.51	4.52	0.57	2.09	1.21	1.57	0.64	5.07	0.11	0.01
		20_3	6	0.12	0.18	0.05	0.11	5.31	1.54	4.28	0.60	1.99	1.15	1.61	0.64	4.95	0.11	0.01
	18	03_2	6	0.06	0.08	0.03	0.05	5.87	1.58	4.74	0.58	2.24	1.09	1.30	0.76	5.93	0.10	0.01
		18_3	6	0.13	0.18	0.06	0.13	5.22	1.55	3.83	0.61	2.03	1.13	1.58	0.63	4.70	0.12	0.01
	24	06_4	6	0.10	0.10	0.04	0.09	5.66	1.52	4.64	0.57	2.19	1.15	1.40	0.69	5.52	0.10	0.01
		11_3	6	0.10	0.10	0.04	0.09	5.62	1.59	4.72	0.59	2.14	1.07	1.26	0.77	5.85	0.11	0.02
900	0.5	11_4	5.5	0.15	0.28	0.11	0.17	4.35	1.44	3.85	0.64	1.78	1.22	1.91	0.57	4.33	0.12	0.02
		19_4	5.5	0.18	0.30	0.08	0.18	4.47	1.46	3.51	0.65	1.80	1.15	1.56	0.51	4.41	0.18	0.02
	1	04_1	6	0.12	0.18	0.06	0.13	4.67	1.48	3.68	0.66	1.89	1.14	1.63	0.64	4.70	0.12	0.02
		13_1	6	0.15	0.20	0.06	0.15	4.51	1.45	3.69	0.66	1.83	1.12	1.52	0.65	4.54	0.13	0.02
	2	10_3	6	0.05	0.17	0.05	0.06	4.44	1.46	3.50	0.66	1.86	1.17	1.83	0.60	4.37	0.13	0.01
		14_2	6	0.12	0.17	0.06	0.12	5.02	1.53	4.34	0.62	1.95	1.19	1.69	0.65	4.94	0.10	0.02
	4	06_2	6	0.11	0.20	0.07	0.11	4.94	1.53	3.63	0.65	2.03	1.12	1.53	0.64	5.00	0.10	0.02
		07_4	6	0.12	0.14	0.05	0.11	5.07	1.52	4.33	0.61	1.94	1.18	1.62	0.63	4.93	0.11	0.02
	8	08_3	6	0.10	0.13	0.05	0.11	4.81	1.50	3.85	0.65	1.93	1.15	1.71	0.65	4.66	0.11	0.01
		09_3	6	0.10	0.21	0.06	0.11	4.60	1.51	3.76	0.65	1.86	1.16	1.78	0.66	4.72	0.12	0.01
	12	07_1	6	0.09	0.23	0.05	0.10	4.68	1.51	3.75	0.64	1.87	1.13	1.77	0.69	4.86	0.12	0.02
		09_1	6	0.07	0.15	0.04	0.08	4.78	1.50	4.01	0.63	1.88	1.16	1.83	0.62	4.48	0.11	0.01
	18	06_1	6	0.07	0.18	0.03	0.07	4.67	1.53	3.72	0.65	1.91	1.11	1.64	0.70	4.75	0.11	0.01
		19_1	6	0.08	0.12	0.04	0.08	5.29	1.56	4.41	0.60	1.99	1.14	1.74	0.68	5.03	0.10	0.01
	24	12_4	6	0.11	0.22	0.05	0.12	4.25	1.46	3.50	0.67	1.81	1.12	1.78	0.63	4.29	0.13	0.02
		16_4	6	0.10	0.26	0.05	0.12	4.35	1.47	3.47	0.67	1.79	1.12	1.83	0.66	4.41	0.14	0.02

6.2.2 Infrared data after pre-treatment

Table A.9 – Infrared data after pre-treatment for LAB 2

T (°C)	Time (h)	Sample	Colour Code	BPI	C/P 2	API	CO_3 /PO_4	IRSF	1060/ 1075	1030/ 1110	PPI	PSF	AB	C/C	OH/P	OHSF	CN/P	WAMPI
0	0	/	0	/	/	/	/	/	/	/	/	/	/	/	/	/	/	/
500	0.5	05_3	3	0.84	0.49	0.34	0.63	3.60	1.26	2.84	0.61	1.64	0.94	0.99	0.25	5.80	0.16	0.42
		10_4	3	0.71	0.48	0.24	0.54	3.73	1.27	3.00	0.61	1.68	0.95	1.02	0.26	5.28	0.18	0.30
	1	13_2	3	0.61	0.40	0.16	0.47	3.95	1.27	3.15	0.60	1.84	0.96	1.07	0.28	4.92	0.14	0.14
		15_1	3	0.57	0.37	0.16	0.45	3.98	1.28	3.12	0.61	1.85	0.97	1.11	0.29	4.73	0.16	0.15
	2	05_4	4	0.50	0.37	0.13	0.41	3.94	1.28	3.10	0.62	1.78	0.98	1.11	0.32	4.28	0.16	0.12
		15_4	4	0.51	0.36	0.13	0.41	3.99	1.27	3.05	0.62	1.85	0.97	1.11	0.32	4.37	0.17	0.12
	4	13_3	3.5	0.48	0.33	0.13	0.39	4.15	1.28	3.20	0.61	1.90	0.97	1.14	0.32	4.33	0.17	0.12
		14_4	3.5	0.51	0.38	0.13	0.41	3.94	1.27	3.05	0.62	1.78	0.98	1.12	0.32	4.26	0.15	0.11
	8	01_2	3.5	0.46	0.34	0.13	0.38	4.07	1.29	3.27	0.61	1.85	0.99	1.14	0.33	4.12	0.17	0.12
		05_2	3.5	0.45	0.32	0.11	0.36	4.19	1.30	3.30	0.60	1.92	0.97	1.11	0.33	4.09	0.15	0.10
	12	07_2	3.5	0.40	0.30	0.11	0.34	4.25	1.30	3.30	0.62	1.97	0.99	1.17	0.34	4.01	0.15	0.10
		11_1	3.5	0.47	0.36	0.12	0.39	4.01	1.28	3.14	0.62	1.80	0.98	1.13	0.34	4.07	0.16	0.11
	18	01_4	3.5	0.37	0.27	0.10	0.30	4.44	1.31	3.39	0.61	2.10	0.98	1.13	0.33	4.05	0.14	0.10
		20_2	3.5	0.36	0.26	0.10	0.30	4.45	1.31	3.47	0.61	2.10	0.98	1.15	0.32	4.21	0.19	0.13
	24	04_4	Failed															
		20_4																
600	0.5	03_1	3.5	0.55	0.38	0.19	0.44	3.97	1.29	3.19	0.61	1.79	0.97	1.12	0.29	4.78	0.18	0.21
		16_1	3.5	0.45	0.31	0.13	0.36	4.21	1.29	3.25	0.61	1.92	0.98	1.15	0.30	4.45	0.19	0.14
	1	01_1	4	0.38	0.29	0.12	0.32	4.32	1.31	3.38	0.63	1.97	0.98	1.18	0.35	3.99	0.17	0.12
		10_2	4	0.31	0.24	0.08	0.26	4.52	1.33	3.53	0.62	2.05	0.98	1.19	0.38	3.97	0.17	0.08
	2	02_4	4	0.33	0.26	0.10	0.28	4.40	1.31	3.34	0.63	2.01	0.99	1.19	0.36	3.96	0.16	0.09
		04_3	4	0.29	0.23	0.09	0.25	4.45	1.33	3.44	0.63	2.03	1.00	1.23	0.37	4.01	0.16	0.08
	4	14_1	5	0.20	0.17	0.06	0.18	5.03	1.41	3.84	0.64	2.43	1.00	1.27	0.50	4.40	0.17	0.07
		16_2	5	0.22	0.18	0.05	0.18	5.14	1.41	3.98	0.62	2.42	0.99	1.19	0.50	4.27	0.11	0.05
	8	09_4	Failed															
		18_4																

Table A.9 (*continued*)

T (°C)	Time (h)	Sample	Colour Code	BPI	C/P 2	API	CO_3 /PO_4	IRSF	1060/ 1075	1030/ 1110	PPI	PSF	AB	C/C	OH/P	OHSF	CN/P	WAMPI
600	12	04_2	5	0.15	0.15	0.04	0.13	5.27	1.48	4.01	0.64	2.43	1.01	1.25	0.59	4.77	0.14	0.04
		08_2	5	0.13	0.13	0.03	0.11	5.43	1.48	3.92	0.65	2.58	1.01	1.28	0.61	4.95	0.12	0.03
	18	08_4	5.5	0.06	0.07	0.01	0.05	6.00	1.61	4.99	0.61	2.94	1.05	1.31	0.70	5.89	0.10	0.02
		14_3	5	0.12	0.11	0.03	0.10	5.55	1.54	4.58	0.62	2.61	1.03	1.32	0.64	5.24	0.13	0.03
	24	02_2	6	0.06	0.08	0.01	0.06	5.93	1.58	4.67	0.62	2.83	1.07	1.37	0.69	5.91	0.11	0.01
		18_1	6	0.08	0.08	0.02	0.07	6.79	1.74	6.24	0.53	2.90	1.08	1.35	0.71	6.12	0.10	0.02
700	0.5	08_1	4.5	0.15	0.15	0.06	0.15	5.09	1.45	4.16	0.63	2.35	1.04	1.46	0.52	4.61	0.17	0.05
		12_1	4.5	0.21	0.20	0.07	0.20	4.74	1.42	3.90	0.65	2.11	1.02	1.40	0.49	4.38	0.22	0.07
	1	05_1	5	0.07	0.09	0.02	0.07	5.72	1.61	5.03	0.62	2.64	1.10	1.60	0.66	5.73	0.13	0.02
		10_1	5	0.07	0.07	0.02	0.06	5.90	1.67	5.00	0.62	2.71	1.10	1.41	0.69	5.91	0.11	0.01
	2	06_3	6	0.06	0.07	0.02	0.06	5.87	1.67	6.35	0.54	2.72	1.11	1.48	0.74	6.05	0.11	0.02
		15_2	6	0.07	0.07	0.02	0.06	5.97	1.66	6.01	0.57	2.79	1.10	1.45	0.73	6.07	0.10	0.01
	4	12_2	6	0.05	0.06	0.01	0.04	5.80	1.69	5.99	0.59	2.77	1.12	1.29	0.76	6.49	0.10	0.01
		13_4	6	0.06	0.07	0.01	0.05	6.05	1.67	6.73	0.53	2.67	1.12	1.51	0.76	6.41	0.11	0.02
	8	12_3	6	0.06	0.07	0.01	0.05	5.70	1.65	6.08	0.56	2.40	1.13	1.39	0.78	6.32	0.10	0.01
		15_3	6	0.05	0.07	0.01	0.05	5.80	1.68	6.15	0.57	2.58	1.12	1.43	0.77	6.36	0.10	0.01
	12	17_2	6	0.05	0.08	0.01	0.05	6.65	1.76	6.40	0.53	2.63	1.15	1.46	0.73	6.14	0.10	0.01
		18_2	6	0.05	0.07	0.01	0.05	6.45	1.76	5.53	0.57	2.48	1.12	1.44	0.73	6.08	0.10	0.01
	18	17_4	Failed															
		19_3																
	24	03_3	6	0.05	0.06	0.01	0.04	5.94	1.67	5.96	0.57	2.61	1.13	1.46	0.76	6.38	0.10	0.01
		03_4	6	0.05	0.08	0.01	0.05	6.06	1.69	6.54	0.54	2.63	1.13	1.51	0.76	6.31	0.09	0.01
800	0.5	02_1	4.5	0.13	0.14	0.04	0.14	5.08	1.49	4.57	0.65	2.12	1.13	1.76	0.49	4.91	0.30	0.02
		20_1	4.5	0.14	0.12	0.04	0.15	5.37	1.48	4.94	0.64	2.23	1.14	1.77	0.34	5.53	0.61	0.01
	1	07_3	5	0.06	0.08	0.03	0.06	5.74	1.62	5.65	0.58	2.51	1.22	1.79	0.67	5.65	0.11	0.01
		19_2	5.5	0.10	0.09	0.02	0.11	5.77	1.62	4.96	0.61	2.28	1.13	1.74	0.58	5.20	0.11	0.01
	2	09_2	6	0.04	0.09	0.03	0.04	5.53	1.64	5.62	0.59	2.24	1.28	2.05	0.75	5.93	0.10	0.01
		17_1	6	0.09	0.09	0.02	0.09	6.04	1.64	5.54	0.57	2.19	1.20	1.83	0.61	5.44	0.11	0.01
	4	02_3	6	0.07	0.09	0.02	0.08	5.54	1.61	5.14	0.61	2.33	1.15	1.70	0.69	5.77	0.10	0.01
		11_2	6	0.07	0.10	0.03	0.08	5.63	1.62	5.54	0.58	2.28	1.20	1.88	0.70	5.70	0.10	0.01

Table A.9 (*continued*)

T (°C)	Time (h)	Sample	Colour Code	BPI	C/P 2	API	CO_3 /PO_4	IRSF	1060/ 1075	1030/ 1110	PPI	PSF	AB	C/C	OH/P	OHSF	CN/P	WAMPI
800	8	01_3	6	0.07	0.11	0.02	0.07	5.58	1.60	5.66	0.56	2.17	1.18	1.88	0.73	5.66	0.10	0.01
		17_3	6	0.06	0.08	0.02	0.06	6.01	1.63	5.16	0.57	2.24	1.18	1.79	0.67	5.67	0.10	0.01
	12	16_3	6	0.05	0.08	0.03	0.05	5.76	1.62	5.15	0.58	2.17	1.22	1.89	0.71	5.75	0.10	0.01
		20_3	6	0.05	0.14	0.03	0.06	5.47	1.62	4.42	0.62	2.08	1.20	2.12	0.66	5.33	0.11	0.01
	18	03_2	6	0.04	0.08	0.02	0.04	5.56	1.65	5.06	0.60	2.17	1.16	1.81	0.77	6.02	0.10	0.01
		18_3	6	0.07	0.10	0.03	0.07	5.99	1.60	5.22	0.56	2.33	1.23	2.05	0.60	5.19	0.10	0.01
	24	06_4	6	0.06	0.08	0.02	0.06	5.84	1.63	4.94	0.59	2.26	1.16	1.73	0.71	5.86	0.10	0.01
		11_3	6	0.05	0.08	0.02	0.04	5.67	1.67	5.13	0.60	2.23	1.15	1.64	0.77	6.21	0.11	0.01
900	0.5	11_4	5.5	0.13	0.24	0.10	0.16	4.48	1.46	4.30	0.64	1.87	1.29	2.32	0.54	4.53	0.13	0.01
		19_4	5.5	0.11	0.17	0.05	0.13	5.08	1.51	4.40	0.65	1.98	1.19	2.03	0.45	5.04	0.36	0.01
	1	04_1	6	0.07	0.14	0.05	0.09	4.93	1.54	4.85	0.62	1.95	1.26	2.13	0.67	5.00	0.11	0.01
		13_1	6	0.07	0.13	0.04	0.08	5.16	1.57	5.50	0.59	2.07	1.25	2.04	0.69	5.22	0.09	0.01
	2	10_3	6	0.06	0.14	0.04	0.08	5.23	1.58	4.66	0.62	2.03	1.23	2.22	0.66	5.22	0.11	0.00
		14_2	6	0.08	0.14	0.05	0.09	5.04	1.56	4.46	0.64	2.00	1.26	2.21	0.64	5.05	0.10	0.01
	4	06_2	6	0.06	0.15	0.04	0.08	5.16	1.59	4.69	0.62	2.01	1.23	2.21	0.68	5.20	0.11	0.01
		07_4	6	0.07	0.14	0.04	0.09	5.14	1.55	4.92	0.59	1.94	1.26	2.16	0.65	4.95	0.10	0.00
	8	08_3	6	0.07	0.12	0.04	0.08	5.29	1.59	4.62	0.62	2.01	1.22	2.00	0.65	5.21	0.11	0.01
		09_3	6	0.06	0.13	0.04	0.07	4.98	1.57	4.45	0.62	1.96	1.22	2.17	0.64	4.90	0.10	0.01
	12	07_1	6	0.05	0.14	0.03	0.06	5.06	1.60	4.55	0.63	2.01	1.18	2.04	0.70	5.22	0.10	0.01
		09_1	6	0.06	0.13	0.04	0.07	5.20	1.60	4.55	0.63	2.00	1.21	2.07	0.65	5.19	0.11	0.01
	18	06_1	6	0.05	0.12	0.02	0.06	5.33	1.64	4.61	0.62	2.05	1.16	1.93	0.73	5.55	0.11	0.01
		19_1	6	0.06	0.12	0.04	0.07	5.70	1.61	5.02	0.58	2.07	1.23	2.02	0.66	5.24	0.10	0.01
	24	12_4	6	0.08	0.18	0.04	0.09	4.95	1.57	4.59	0.61	1.90	1.17	2.06	0.70	5.06	0.11	0.02
		16_4	6	0.05	0.11	0.03	0.06	5.47	1.61	5.07	0.58	1.99	1.21	2.11	0.70	5.35	0.11	0.01

6.2.3 Isotope analyses and elementary analyses data

Table A.10 – Infrared analyses and elementary analyses data for LAB 2

T (°C)	Time (h)	Sample	Colour Code	%N	%C	$\delta^{13}C$ (‰)	$\delta^{18}O$ (‰)	pCO_2/g of sample
0	0	/	0	/	/	-12.4	-3.3	/
500	0.5	05_3	3	0.90	4.83	-16.4	-5.4	1.55
		10_4	3	0.50	3.42	-16.0	-5.6	1.54
	1	13_2	3	0.16	1.63	-15.2	-6.1	1.56
		15_1	3	0.18	1.74	-17.4	-7.1	1.51
	2	05_4	4	0.08	1.20	-16.7	-7.4	1.42
		15_4	4	0.06	1.14	-17.2	-7.1	1.47
	4	13_3	3.5	0.08	1.17	-17.1	-6.9	1.47
		14_4	3.5	0.06	1.11	-17.3	-6.9	1.54
	8	01_2	3.5	0.08	1.10	-17.9	-7.9	1.27
		05_2	3.5	0.05	1.08	-17.2	-7.3	1.37
	12	07_2	3.5	0.06	1.03	-17.3	-7.2	1.40
		11_1	3.5	0.06	1.10	-17.4	-7.5	1.52
	18	01_4	3.5	0.04	0.97	-15.7	-7.0	1.27
		20_2	3.5	/	/	-16.5	-7.6	1.42
	24	04_4	Failed					
		20_4						
600	0.5	03_1	3.5	0.29	2.05	-18.0	-7.8	1.47
		16_1	3.5	0.15	1.62	-16.8	-8.1	1.45
	1	01_1	4	0.08	1.21	-18.2	-8.7	1.37
		10_2	4	0.04	0.96	-17.1	-9.0	1.27
	2	02_4	4	0.05	0.96	-18.0	-8.5	1.43
		04_3	4	0.04	0.88	-18.1	-8.3	1.27
	4	14_1	5	0.04	0.83	-18.4	-8.3	1.01
		16_2	5	/	/	-17.1	-8.8	0.89
	8	09_4	Failed					
		18_4						

Table A.10 (*continued*)

T (°C)	Time (h)	Sample	Colour Code	%N	%C	$\delta^{13}C$ (‰)	$\delta^{18}O$ (‰)	pCO_2/g of sample
600	12	04_2	5	bLoD	0.65	-18.0	-9.0	0.74
		08_2	5	bLoD	0.56	-17.8	-9.4	0.65
	18	08_4	5.5	bLoD	0.36	-17.3	-9.7	0.32
		14_3	5	/	/	-17.7	-8.7	0.63
	24	02_2	6	bLoD	0.39	-17.3	-9.1	0.19
		18_1	6	bLoD	0.36	-17.8	-12.0	0.14
700	0.5	08_1	4.5	0.08	0.80	-19.0	-11.8	0.90
		12_1	4.5	/	/	-18.7	-10.6	1.06
	1	05_1	5	bLoD	0.44	-19.4	-13.8	0.29
		10_1	5	bLoD	0.35	-21.3	-14.6	0.17
	2	06_3	6	bLoD	0.35	-19.8	-12.0	0.16
		15_2	6	bLoD	0.36	-20.1	-12.1	0.14
	4	12_2	6	/	/	-19.8	-13.1	0.11
		13_4	6	bLoD	0.31	-20.0	-12.4	0.12
	8	12_3	6	bLoD	0.28	-20.1	-12.4	0.12
		15_3	6	/	/	-20.1	-12.6	0.12
	12	17_2	6	/	/	-21.8	-13.4	0.12
		18_2	6	bLoD	0.24	-21.3	-12.4	0.12
	18	17_4	Failed					
		19_3						
	24	03_3	6	bLoD	0.26	-18.6	-11.7	0.10
		03_4	6	bLoD	0.23	-19.8	-11.4	0.11
800	0.5	02_1	4.5	0.20	0.63	-20.7	-14.0	0.56
		20_1	4.5	0.26	0.46	-20.7	-15.3	0.63
	1	07_3	5	0.03	0.27	-21.6	-15.3	0.23
		19_2	5.5	bLoD	0.22	-23.4	-14.6	0.42
	2	09_2	6	bLoD	0.24	-21.5	-13.0	0.12
		17_1	6	0.04	0.25	-22.5	-15.5	0.33
	4	02_3	6	bLoD	0.30	-20.9	-11.1	0.15
		11_2	6	bLoD	0.25	-19.9	-11.8	0.23

Table A.10 (*continued*)

T (°C)	Time (h)	Sample	Colour Code	%N	%C	$\delta^{13}C$ (‰)	$\delta^{18}O$ (‰)	pCO_2/g of sample
800	8	01_3	6	bLoD	0.20	-20.1	-13.4	0.23
		17_3	6	bLoD	0.19	-23.3	-14.3	0.18
	12	16_3	6	/	/	-21.3	-11.6	0.16
		20_3	6	0.03	0.17	-20.9	-13.5	0.17
	18	03_2	6	bLoD	0.17	-20.0	-13.1	0.10
		18_3	6	/	/	-21.6	-13.4	0.39
	24	06_4	6	bLoD	0.21	-19.3	-11.8	0.16
		11_3	6	bLoD	0.21	-21.5	-12.5	0.11
900	0.5	11_4	5.5	0.09	0.33	-17.2	-12.4	0.58
		19_4	5.5	0.17	0.36	-22.4	-15.8	0.50
	1	04_1	6	0.04	0.24	-19.5	-13.1	0.30
		13_1	6	bLoD	0.18	-19.4	-14.0	0.28
	2	10_3	6	0.03	0.21	-19.4	-13.1	0.21
		14_2	6	/	/	-18.4	-12.4	0.35
	4	06_2	6	bLoD	0.17	-18.8	-10.8	0.18
		07_4	6	bLoD	0.15	-20.3	-13.1	0.35
	8	08_3	6	bLoD	0.19	-21.0	-12.9	0.19
		09_3	6	bLoD	0.15	-21.5	-11.2	0.20
	12	07_1	6	bLoD	0.14	-19.2	-10.4	0.16
		09_1	6	bLoD	0.19	-21.6	-12.8	0.19
	18	06_1	6	bLoD	0.18	-20.1	-11.2	0.13
		19_1	6	bLoD	0.14	-18.5	-10.7	0.18
	24	12_4	6	bLoD	0.15	-17.9	-11.4	0.31
		16_4	6	bLoD	0.12	-18.2	-11.0	0.21

bLoD – below level of detection

6.3 Laboratory heating experiment 3 (LAB 3)

All samples were heated for four hours at 800°C in a muffle furnace. All were fully calcined (colour code 6). The codes correspond to those in Table 3.3

6.3.1 Infrared data before pre-treatment

Table A.11 – Infrared data before pre-treatment for LAB 3

Sample	Codes	BPI	C/P 2	API	CO_3/PO_4	IRSF	1060/1075	1030/1110	PPI	PSF	AB	C/C	OH/P	OHSF	CN/P	WAMPI
Pig rib	A0	1.00	0.34	0.93	0.80	2.84	1.18	2.23	0.68	1.52	0.89	0.98	0.33	4.63	0.12	1.38
	A1	0.10	0.15	0.06	0.09	4.86	1.45	4.67	0.57	2.10	1.17	1.66	0.54	4.50	0.11	0.02
	A2	0.04	0.07	0.02	0.03	5.84	1.57	5.42	0.52	2.54	1.21	1.52	0.70	5.53	0.09	0.01
	A3	0.03	0.14	0.05	0.04	4.04	1.28	3.98	0.66	1.97	1.31	2.48	0.33	4.41	0.12	0.01
	A4	0.04	0.09	0.06	0.05	4.45	1.42	4.19	0.62	2.06	1.41	2.60	0.53	4.38	0.11	0.01
	B0	2.62	0.71	2.78	2.11	2.81	1.17	2.08	0.68	1.46	0.88	0.99	0.28	5.33	0.11	4.05
	B1	0.07	0.07	0.04	0.06	5.13	1.49	4.56	0.60	2.52	1.13	1.40	0.63	5.11	0.10	0.02
	B2	0.03	0.07	0.03	0.03	5.23	1.50	4.83	0.58	2.61	1.21	1.51	0.61	4.87	0.11	0.01
	B3	0.10	0.12	0.04	0.10	4.51	1.40	4.29	0.63	2.09	1.15	1.64	0.50	4.29	0.10	0.02
	B4	0.06	0.10	0.05	0.07	4.68	1.46	4.04	0.62	2.10	1.24	1.77	0.62	4.78	0.11	0.02
	C0	1.36	0.68	0.61	0.98	3.08	1.24	2.76	0.61	1.51	0.91	0.90	0.21	7.22	0.17	0.64
	C1	0.03	0.07	0.02	0.02	5.64	1.56	4.50	0.57	2.53	1.10	1.03	0.68	5.22	0.11	0.01
	C2	0.06	0.09	0.03	0.05	5.40	1.56	4.58	0.57	2.31	1.12	1.13	0.74	5.33	0.12	0.02
	C3	0.02	0.06	0.02	0.02	4.93	1.46	4.47	0.64	2.60	1.18	1.50	0.47	4.43	0.09	0.01
	C4	0.10	0.12	0.05	0.09	4.84	1.52	4.19	0.60	2.04	1.13	1.40	0.71	4.84	0.11	0.02
	D0	1.37	0.67	0.64	0.98	3.08	1.24	2.81	0.61	1.50	0.90	0.89	0.22	6.87	0.15	0.75
	D1	0.05	0.09	0.03	0.04	5.61	1.57	4.89	0.54	2.34	1.12	1.12	0.72	5.27	0.12	0.02
	D2	0.04	0.07	0.02	0.03	5.82	1.58	4.76	0.56	2.55	1.10	1.09	0.71	5.58	0.13	0.01
	D3	0.04	0.08	0.03	0.05	4.95	1.47	4.57	0.62	2.40	1.16	1.70	0.51	4.36	0.11	0.02
	D4	0.03	0.07	0.02	0.02	4.68	1.46	4.22	0.64	2.34	1.15	1.50	0.57	4.33	0.11	0.02

Table A.11 (*continued*)

Sample	Codes	BPI	C/P 2	API	CO_3/PO_4	IRSF	1060/1075	1030/1110	PPI	PSF	AB	C/C	OH/P	OHSF	CN/P	WAMPI
Seal bone	A0	1.58	0.71	0.94	1.16	3.06	1.22	2.64	0.64	1.49	0.87	0.87	0.13	12.36	0.16	1.44
	A1	0.19	0.32	0.03	0.18	4.85	1.46	3.08	0.70	1.85	1.01	1.21	0.23	9.11	0.11	0.02
	A2	0.36	0.47	0.04	0.33	4.18	1.41	3.35	0.68	1.74	0.98	1.31	0.21	7.22	0.11	0.02
	A3	0.09	0.15	0.03	0.10	4.78	1.44	3.45	0.70	1.77	1.12	1.67	0.19	6.71	0.11	0.01
	A4	0.34	0.38	0.04	0.33	4.24	1.42	3.52	0.67	1.73	0.98	1.39	0.21	7.33	0.17	0.02
	B0	2.39	1.02	1.46	1.82	2.90	1.19	2.27	0.68	1.48	0.89	0.88	0.13	11.71	0.22	2.24
	B1	0.30	0.44	0.04	0.27	4.25	1.44	3.40	0.69	1.77	1.00	1.29	0.26	6.99	0.13	0.01
	B2	0.43	0.52	0.05	0.40	4.02	1.39	3.34	0.68	1.72	0.96	1.29	0.21	7.27	0.14	0.02
	B3	0.34	0.45	0.05	0.33	4.14	1.41	3.42	0.68	1.73	0.98	1.39	0.19	7.63	0.16	0.02
	B4	0.35	0.42	0.05	0.34	4.04	1.40	3.28	0.70	1.73	0.99	1.36	0.21	7.30	0.22	0.03
	C0	1.36	0.63	0.46	0.98	3.22	1.24	2.85	0.63	1.50	0.86	0.85	0.18	8.59	0.16	0.51
	C1	0.21	0.23	0.04	0.19	4.48	1.46	3.85	0.69	1.87	1.02	1.21	0.29	7.61	0.11	0.01
	C2	0.34	0.43	0.04	0.32	4.07	1.41	3.48	0.69	1.75	0.99	1.28	0.25	7.17	0.12	0.02
	C3	0.46	0.54	0.06	0.43	3.81	1.38	3.24	0.71	1.71	0.94	1.28	0.20	7.12	0.14	0.01
	C4	0.37	0.43	0.05	0.34	3.92	1.40	3.43	0.70	1.72	0.98	1.27	0.26	7.03	0.13	0.02
	D0	1.53	0.69	0.55	1.11	3.11	1.23	2.77	0.64	1.51	0.87	0.86	0.17	8.87	0.10	0.63
	D1	0.47	0.61	0.06	0.42	3.79	1.39	3.33	0.69	1.71	0.96	1.21	0.27	6.41	0.14	0.02
	D2	0.34	0.47	0.04	0.31	3.99	1.42	3.55	0.69	1.76	1.00	1.22	0.27	7.22	0.12	0.02
	D3	0.53	0.65	0.08	0.50	3.74	1.37	3.21	0.71	1.69	0.94	1.25	0.19	7.87	0.30	0.03
	D4	0.42	0.48	0.05	0.39	3.80	1.39	3.32	0.71	1.71	0.96	1.26	0.25	6.75	0.17	0.03

6.3.2 Infrared data after pre-treatment

Table A.12 – Infrared data after pre-treatment for LAB 3

Sample	Codes	BPI	C/P 2	API	CO_3/PO_4	IRSF	1060/1075	1030/1110	PPI	PSF	AB	C/C	OH/P	OHSF	CN/P	WAMPI
Pig rib	A0	n/a														
	A1	0.07	0.11	0.04	0.08	5.08	1.52	4.61	0.62	2.23	1.26	2.00	0.57	4.87	0.11	0.01
	A2	0.02	0.06	0.03	0.03	5.95	1.67	5.72	0.54	2.50	1.29	2.10	0.74	5.87	0.09	0.01
	A3	0.02	0.10	0.05	0.04	3.96	1.34	3.40	0.75	1.93	1.42	4.27	0.37	4.29	0.11	0.01
	A4	0.02	0.09	0.06	0.04	4.58	1.48	4.14	0.66	2.15	1.44	4.28	0.57	4.61	0.09	0.01
	B0	n/a														
	B1	0.04	0.08	0.02	0.05	5.28	1.62	5.28	0.60	2.43	1.23	1.82	0.69	5.54	0.10	0.01
	B2	0.01	0.08	0.03	0.02	4.77	1.55	3.90	0.68	2.29	1.23	2.75	0.66	4.88	0.10	0.01
	B3	0.10	0.12	0.04	0.12	4.47	1.48	4.33	0.67	2.05	1.16	1.84	0.54	4.57	0.10	0.02
	B4	0.06	0.10	0.04	0.07	4.90	1.56	4.41	0.64	2.05	1.29	2.02	0.68	5.25	0.11	0.02
	C0	n/a														
	C1	0.01	0.07	0.02	0.01	5.48	1.65	4.59	0.61	2.49	1.13	1.56	0.70	5.25	0.10	0.02
	C2	0.02	0.07	0.02	0.02	5.68	1.68	4.62	0.61	2.50	1.12	1.33	0.75	5.82	0.11	0.02
	C3	0.02	0.08	0.03	0.02	4.29	1.46	3.68	0.72	2.25	1.24	2.08	0.49	4.31	0.10	0.02
	C4	0.06	0.09	0.02	0.06	5.38	1.64	5.20	0.59	2.32	1.18	1.85	0.72	5.47	0.11	0.01
	D0	n/a														
	D1	0.02	0.07	0.01	0.02	5.43	1.66	4.66	0.62	2.53	1.15	1.30	0.74	5.63	0.10	0.02
	D2	0.02	0.06	0.01	0.02	5.62	1.70	4.48	0.63	2.45	1.15	1.39	0.77	5.96	0.10	0.02
	D3	0.04	0.08	0.03	0.05	4.65	1.49	4.04	0.68	2.22	1.18	1.93	0.55	4.50	0.10	0.02
	D4	0.01	0.07	0.02	0.02	4.82	1.56	4.41	0.65	2.47	1.19	1.96	0.58	4.61	0.09	0.01

Table A.12 (*continued*)

Sample	Codes	BPI	C/P 2	API	CO_3/PO_4	IRSF	1060/1075	1030/1110	PPI	PSF	AB	C/C	OH/P	OHSF	CN/P	WAMPI
Seal bone	A0	n/a														
	A1	0.18	0.35	0.02	0.18	4.74	1.47	3.15	0.71	1.84	1.01	1.36	0.28	8.03	0.11	0.01
	A2	0.29	0.36	0.02	0.29	4.48	1.44	3.44	0.70	1.78	0.98	1.43	0.21	7.66	0.12	0.02
	A3	0.22	0.29	0.02	0.22	4.94	1.44	3.27	0.70	1.85	1.00	1.49	0.18	8.32	0.12	0.01
	A4	0.31	0.36	0.03	0.32	4.29	1.42	3.28	0.71	1.72	0.98	1.50	0.21	7.63	0.17	0.02
	B0	n/a														
	B1	0.25	0.34	0.03	0.26	4.23	1.45	3.23	0.73	1.77	1.01	1.47	0.28	6.80	0.11	0.02
	B2	0.38	0.42	0.03	0.39	4.05	1.39	3.14	0.74	1.71	0.97	1.44	0.22	7.22	0.12	0.02
	B3	0.28	0.35	0.03	0.29	4.46	1.43	3.61	0.68	1.75	0.99	1.51	0.17	8.65	0.17	0.01
	B4	0.29	0.36	0.03	0.30	4.33	1.43	3.44	0.71	1.75	1.00	1.50	0.21	7.99	0.20	0.02
	C0	n/a														
	C1	0.16	0.17	0.02	0.16	4.46	1.52	3.71	0.76	1.85	1.04	1.37	0.30	8.18	0.11	0.01
	C2	0.27	0.35	0.04	0.30	3.94	1.42	3.08	0.79	1.78	1.00	1.48	0.29	6.45	0.11	0.03
	C3	0.37	0.40	0.03	0.38	3.96	1.39	3.21	0.74	1.69	0.95	1.41	0.21	7.05	0.13	0.01
	C4	0.26	0.30	0.03	0.28	4.06	1.43	3.30	0.77	1.78	1.00	1.46	0.28	6.77	0.11	0.02
	D0	n/a														
	D1	0.34	0.43	0.03	0.34	3.95	1.42	3.38	0.73	1.73	0.98	1.38	0.29	6.19	0.10	0.02
	D2	0.24	0.32	0.02	0.24	4.26	1.47	3.70	0.72	1.80	1.00	1.39	0.28	7.32	0.11	0.01
	D3	0.42	0.47	0.04	0.42	3.83	1.39	3.18	0.76	1.72	0.96	1.37	0.20	7.35	0.30	0.02
	D4	0.34	0.41	0.04	0.36	3.84	1.41	3.29	0.76	1.73	0.98	1.45	0.27	6.47	0.13	0.03

6.3.3 Isotope analyses data

Unfortunately, some samples released very little amount of carbon dioxide for reliable isotopic measurements (red values in following table); these samples were also those with the lowest BPI (see Chapter 4).

Table A.13 – Isotope analyses data for LAB 3

	Code	Treatment	Additives	$\delta^{13}C$ (‰)	$\delta^{18}O$ (‰)	pCO_2/g of sample
Pig rib	A0	/	Unburned	-10.8	-5.4	2.81
	A1		/	-20.3	-16.6	0.20
	A2		Lard	-21.2	-15.6	0.09
	A3		Barley seeds	-21	-17.7	0.14
	A4		Corn flower	-16.3	-18.5	0.13
	B1	Fat removal	/	-18.5	-14.4	0.14
	B2		Lard	-23	-16.9	0.09
	B3		Barley seeds	-26.4	-15.5	0.20
	B4		Corn flower	-14.8	-17.4	0.16
	C1	Organic removal	/	-20.3	-23.8	0.02
	C2		Lard	-20.2	-17.8	0.03
	C3		Barley seeds	-24.2	-17.5	0.08
	C4		Corn flower	-13.1	-14.9	0.15
	D1	Fat + organic removal	/	-16.9	-16.4	0.04
	D2		Lard	-18.2	-16.8	0.04
	D3		Barley seeds	-26.2	-13.8	0.14
	D4		Corn flower	-15.1	-18.9	0.06

Table A.13 (*continued*)

	Code	Treatment	Additives	$\delta^{13}C$ (‰)	$\delta^{18}O$ (‰)	pCO_2/g of sample
Seal bone	A0	/	Unburned	-9.6	-1.7	2.23
	A1		/	-11.3	-11.7	0.49
	A2		Lard	-11.2	-11.7	0.34
	A3		Barley seeds	-24.3	-13.8	0.60
	A4		Corn flower	-8.2	-12.9	0.38
	B1	Fat removal	/	-15.5	-11.5	0.27
	B2		Lard	-10.1	-11.7	0.38
	B3		Barley seeds	-22.6	-13.6	0.35
	B4		Corn flower	-7.3	-13.6	0.36
	C1	Organic removal	/	-10.5	-9.6	0.29
	C2		Lard	-11.8	-10.6	0.26
	C3		Barley seeds	-25.5	-13	0.37
	C4		Corn flower	-9.4	-12.5	0.34
	D1	Fat + organic removal	/	-8.3	-10.8	0.43
	D2		Lard	-11.7	-10.5	0.33
	D3		Barley seeds	-23.3	-13	0.36
	D4		Corn flower	-10.2	-12.2	0.35

6.4 Outdoor burning experiments (OUT)

6.4.1 Infrared data before pre-treatment

Table A.14 – Infrared data before pre-treatment for OUT

#	BPI	C/P 2	API	CO_3/PO_4	IRSF	1060/1075	1030/1110	PPI	PSF	AB	C/C	OH/P	OHSF	CN/P	WAMPI
L1_A	0.19	0.20	0.06	0.17	4.55	1.46	3.52	0.66	1.80	1.04	1.37	0.50	4.74	0.31	0.01
L1_B	/	/	/	/	/	/	/	/	/	/	/	/	/	/	/
L1_D	/	/	/	/	/	/	/	/	/	/	/	/	/	/	/
L2_A	0.11	0.10	0.04	0.10	4.72	1.37	3.79	0.71	2.35	1.08	1.22	0.43	4.13	0.12	0.02
L3	0.07	0.07	0.04	0.06	5.02	1.48	4.07	0.65	2.47	1.09	1.19	0.46	4.39	0.16	0.02
P1	0.25	0.17	0.04	0.23	5.15	1.38	2.71	0.73	2.03	0.92	1.20	0.26	5.50	0.08	0.01
P2	0.17	0.14	0.07	0.15	4.69	1.43	3.48	0.68	2.22	1.08	1.18	0.45	4.53	0.20	0.02
P3	0.17	0.17	0.07	0.15	4.35	1.39	3.79	0.67	2.15	1.15	1.20	0.37	4.54	0.23	0.02
P4	0.13	0.09	0.05	0.13	4.69	1.38	2.70	0.73	2.04	1.01	1.34	0.41	4.65	0.18	0.02
P5	0.21	0.14	0.07	0.20	5.10	1.48	4.06	0.65	2.26	1.00	1.36	0.50	4.50	0.15	0.02
P6	0.23	0.12	0.08	0.20	5.71	1.49	4.16	0.62	2.65	0.96	1.27	0.51	4.61	0.13	0.02
P7	0.25	0.16	0.06	0.23	5.54	1.46	3.89	0.63	2.28	1.06	1.40	0.43	4.72	0.28	0.02
C1	0.20	0.17	0.06	0.19	5.19	1.48	3.93	0.65	2.16	1.05	1.36	0.53	4.91	0.21	0.02
C2	0.14	0.12	0.06	0.12	5.28	1.49	3.67	0.67	2.34	1.03	1.26	0.59	4.73	0.17	0.02
Ch1	0.09	0.10	0.05	0.07	4.91	1.44	3.84	0.64	2.13	1.12	1.11	0.29	4.96	0.25	0.02

6.4.2 Infrared data after pre-treatment

Table A.15 – Infrared data after pre-treatment for OUT

#	BPI	C/P 2	API	CO_3/PO_4	IRSF	1060/1075	1030/1110	PPI	PSF	AB	C/C	OH/P	OHSF	CN/P	WAMPI
L1_A	0.06	0.08	0.03	0.05	6.07	1.63	5.43	0.56	2.31	1.13	1.60	0.56	5.22	0.15	0.01
L1_B	/	/	/	/	/	/	/	/	/	/	/	/	/	/	/
L1_D	/	/	/	/	/	/	/	/	/	/	/	/	/	/	/
L2_A	0.08	0.14	0.04	0.09	4.30	1.44	3.66	0.73	2.00	1.10	1.71	0.43	4.60	0.17	0.02
L3	0.02	0.06	0.02	0.02	4.93	1.55	4.44	0.66	2.38	1.21	2.05	0.49	4.74	0.17	0.01
P1	/	/	/	/	/	/	/	/	/	/	/	/	/	/	/
P2	0.05	0.08	0.02	0.05	4.83	1.51	4.51	0.67	2.44	1.11	1.56	0.45	4.82	0.23	0.02
P3	0.04	0.10	0.02	0.04	4.38	1.43	4.19	0.71	2.26	1.17	1.75	0.40	4.71	0.27	0.02
P4	0.11	0.11	0.02	0.12	5.04	1.50	4.84	0.66	2.37	1.09	1.70	0.43	4.95	0.28	0.01
P5	0.13	0.11	0.02	0.13	5.01	1.55	5.13	0.64	2.32	1.09	1.71	0.51	4.76	0.15	0.01
P6	0.13	0.11	0.02	0.13	5.58	1.57	5.14	0.61	2.58	1.02	1.55	0.52	4.85	0.13	0.02
P7	0.16	0.13	0.02	0.17	5.57	1.52	4.71	0.64	2.23	1.04	1.65	0.41	4.99	0.33	0.01
C1	0.14	0.14	0.02	0.15	5.23	1.55	5.09	0.63	2.05	1.06	1.65	0.56	4.97	0.20	0.01
C2	0.06	0.09	0.02	0.07	5.35	1.59	4.37	0.67	2.30	1.09	1.62	0.58	5.15	0.18	0.01
Ch1	0.02	0.06	0.01	0.02	5.23	1.51	4.19	0.66	2.34	1.18	1.76	0.33	4.91	0.25	0.01

6.4.3 Isotope analyses and radiocarbon dating data

Table A.16 – Isotope analyses and radiocarbon dating data for OUT

#	Sample	Fuel	Time	$\delta^{13}C$ (‰)	$\delta^{18}O$ (‰)	pCO_2/g of sample	$F^{14}C$ (OxA)
L1_A	Defleshed lamb leg	Wood 3	1h	-25.5	-16.4	0.17	/
L1_B	Defleshed lamb leg	Coal 1	50 min	-24.5	-14.9	0.18	/
L1_D	Defleshed lamb leg	Coal 1 + millet seeds	2h	-19.9	-17.7	0.28	/
L2_A	Defleshed lamb leg	Coal 1	1h 30 min	-24.5	-15.8	0.27	0.6298 ± 0.0022 (24941)
L3	Defleshed lamb leg	Wood 1	1h 30 min	-23.3	-18.2	0.18	/
P1	Defleshed and dried pig scapula	Coal 2	4h	/	/	/	/
P2	Defleshed pig rib	Wood 2	1h 15 min	-26.4	-15.5	0.25	0.9896 ± 0.0028 (27257)
P3	Defleshed pig rib	Wood 1	1h	-28.1	-15.6	0.30	1.0030 ± 0.0029 (27258)
P4	Defleshed pig rib (within the corn fed chicken)	Wood 2	2h 30 min	-23.1	-17.2	0.38	/
P5	Defleshed pig leg	Wood 2	1h 45 min	-25.1	-14.9	0.34	/
P6	Pig trotter with flesh and skin	Wood 1	1h 30 min	-28.1	-15.8	0.41	0.9602 ± 0.0027 (27261)
P7	Pig scapula with flesh and skin	Wood 1	1h 30 min	-25.2	-17.8	0.42	0.9961 ± 0.0030 (27262)
C1	Defleshed cow tibia	Wood 2	1h 15 min	-24.7	-13.8	0.22	1.0218 ± 0.0028 (27259)
C2	Defleshed cow tibia	Wood 1	1h	-24.4	-15.5	0.20	1.0158 ± 0.0031 (27260)
Ch1	Whole corn-fed chicken	Wood 2	2h 30 min	-20.1	-19.1	0.14	/

6.5 Archaeological cremated bone samples

6.5.1 Infrared data before pre-treatment

Table A.17 – Infrared data before pre-treatment for archaeological calcined bone samples

#	Colour code	BPI	C/P 2	API	CO_3/PO_4	IRSF	1060/1075	1030/1110	PPI	PSF	AB	C/C	OH/P	OHSF	CN/P	WAMPI
A1	5	0.26	0.30	0.03	0.24	4.83	1.50	3.50	0.63	1.99	0.99	1.35	0.52	4.18	0.09	0.04
A2	5.5	0.22	0.24	0.02	0.21	4.72	1.47	3.55	0.66	1.74	0.99	1.42	0.42	4.64	0.23	0.02
Asf1	6	0.25	0.27	0.01	0.25	4.63	1.52	3.43	0.68	1.87	1.00	1.49	0.51	4.22	0.11	0.01
Asf2	6	0.21	0.27	0.02	0.21	4.96	1.56	4.19	0.66	1.97	1.02	1.58	0.53	4.59	0.10	0.02
BM1a	6	0.17	0.21	0.01	0.16	5.18	1.57	3.74	0.62	1.93	1.02	1.43	0.58	4.56	0.09	0.01
BM1b	6	0.10	0.15	0.03	0.10	5.67	1.62	3.86	0.63	2.20	1.09	1.56	0.54	5.04	0.30	0.02
BM2a	6	0.14	0.22	0.01	0.13	4.92	1.58	3.50	0.63	1.74	1.03	1.44	0.54	4.70	0.14	0.01
BM2b	6	0.16	0.22	0.01	0.15	4.99	1.56	3.72	0.62	1.82	1.03	1.47	0.52	4.69	0.17	0.01
BM3a	6	0.13	0.16	0.02	0.12	5.43	1.62	4.21	0.59	2.01	1.06	1.47	0.56	4.78	0.14	0.01
BM3b	6	0.13	0.19	0.01	0.13	5.18	1.59	3.62	0.64	1.74	1.04	1.50	0.51	5.06	0.24	0.01
BN1	6	0.15	0.24	0.02	0.14	4.94	1.56	3.86	0.63	1.86	1.04	1.43	0.52	4.83	0.20	0.01
BN2	5.5	0.23	0.29	0.02	0.23	4.56	1.48	3.47	0.67	1.83	1.01	1.49	0.46	4.45	0.23	0.02
BN3	6	0.23	0.29	0.02	0.22	4.57	1.49	3.41	0.66	1.79	0.99	1.38	0.46	4.53	0.16	0.01
BN4	6	0.30	0.31	0.02	0.28	4.49	1.47	3.70	0.66	1.82	0.96	1.40	0.39	4.52	0.11	0.01
C1	5.5	0.25	0.19	0.04	0.22	5.37	1.49	3.99	0.60	2.02	1.00	1.38	0.53	4.33	0.11	0.06
C2	6	0.27	0.16	0.04	0.23	5.75	1.54	4.41	0.59	2.28	0.98	1.33	0.50	4.32	0.08	0.07
C3	5.5	0.23	0.18	0.05	0.20	5.45	1.55	4.15	0.62	2.01	1.00	1.34	0.48	4.70	0.28	0.07
CL1	6	0.12	0.24	0.02	0.13	4.79	1.56	3.64	0.68	1.78	1.07	1.61	0.42	5.52	0.45	0.01
CL2	5	0.15	0.18	0.04	0.14	5.39	1.56	4.33	0.61	2.00	1.07	1.58	0.39	5.32	0.60	0.02
CL3	6	0.07	0.22	0.04	0.08	5.05	1.59	3.66	0.68	1.97	1.14	1.81	0.54	5.00	0.41	0.02
CL4	6	0.16	0.25	0.02	0.16	5.05	1.58	3.94	0.66	1.96	1.05	1.52	0.53	4.81	0.33	0.01
CL5	6	0.14	0.23	0.02	0.14	4.89	1.57	3.62	0.67	1.83	1.05	1.54	0.52	4.94	0.18	0.01
GH1	6	0.35	0.46	0.03	0.33	4.54	1.47	2.92	0.69	1.95	0.97	1.33	0.49	4.11	0.12	0.01
GH2	5.5	0.32	0.43	0.03	0.31	4.37	1.48	3.32	0.70	1.85	0.99	1.31	0.53	4.16	0.19	0.01
IoM1	6	0.15	0.27	0.02	0.15	4.53	1.51	3.22	0.71	1.79	1.03	1.52	0.36	5.59	0.47	0.03
IoM10	5.5	0.27	0.37	0.02	0.26	4.65	1.51	3.63	0.69	1.89	0.98	1.37	0.45	4.54	0.43	0.01
IoM2	6	0.18	0.28	0.03	0.17	4.77	1.55	3.57	0.70	1.95	1.02	1.38	0.47	5.10	0.36	0.03
IoM3	6	0.14	0.29	0.02	0.14	4.68	1.56	3.27	0.67	1.75	1.03	1.44	0.54	4.85	0.15	0.02

Table A.17 (*continued*)

#	Colour code	BPI	C/P 2	API	CO_3/PO_4	IRSF	1060/1075	1030/1110	PPI	PSF	AB	C/C	OH/P	OHSF	CN/P	WAMPI
IoM4	6	0.20	0.36	0.02	0.20	4.65	1.51	3.21	0.69	1.93	0.99	1.38	0.37	5.30	0.54	0.02
IoM5	5	0.26	0.39	0.02	0.26	4.39	1.45	2.88	0.74	1.85	0.98	1.31	0.36	4.99	0.56	0.03
IoM6	5	0.32	0.39	0.04	0.31	4.26	1.42	2.95	0.71	1.80	0.97	1.32	0.49	4.02	0.13	0.06
IoM7	6	0.24	0.33	0.01	0.23	4.57	1.50	3.57	0.64	1.69	0.98	1.42	0.45	4.31	0.13	0.01
IoM8	6	0.23	0.30	0.02	0.21	5.15	1.54	3.60	0.65	2.03	0.99	1.39	0.52	4.48	0.12	0.02
IoM9	6	0.16	0.27	0.01	0.16	4.71	1.53	3.48	0.70	1.77	1.02	1.45	0.34	5.89	0.54	0.01
K01	5.5	0.20	0.41	0.02	0.20	4.62	1.44	3.08	0.71	1.77	1.02	1.39	0.34	5.79	0.68	0.02
K02	6	0.29	0.45	0.01	0.27	4.53	1.47	3.32	0.66	1.88	0.97	1.35	0.50	4.14	0.18	0.01
K03	4.5	0.16	0.41	0.02	0.15	4.49	1.53	3.59	0.72	1.90	1.02	1.33	0.30	6.59	1.13	0.01
K04	4.5	0.34	0.46	0.02	0.31	4.33	1.44	3.24	0.67	1.81	0.96	1.29	0.41	4.37	0.23	0.02
K05	6	0.28	0.42	0.02	0.26	4.60	1.47	3.16	0.65	1.96	0.97	1.34	0.45	4.31	0.21	0.02
K06	6	0.17	0.26	0.02	0.18	4.91	1.51	3.52	0.70	1.94	1.01	1.51	0.32	5.95	0.60	0.01
K07	6	0.21	0.34	0.02	0.21	4.67	1.51	3.31	0.70	1.95	0.99	1.40	0.35	5.79	0.56	0.01
K08	5.5	0.23	0.37	0.01	0.22	4.81	1.47	3.07	0.66	1.95	0.99	1.38	0.42	4.78	0.38	0.01
K09	5.5	0.28	0.46	0.02	0.26	4.61	1.44	2.98	0.66	1.84	0.99	1.29	0.44	4.65	0.35	0.03
K10	5	0.43	0.64	0.02	0.40	4.00	1.34	2.68	0.70	1.67	0.95	1.28	0.36	4.40	0.22	0.02
K11	5	0.12	0.26	0.03	0.13	5.04	1.52	4.07	0.69	1.90	1.08	1.58	0.35	5.92	0.77	0.02
K12	5	0.24	0.45	0.02	0.23	4.40	1.46	3.27	0.72	1.81	1.00	1.36	0.32	6.01	0.81	0.02
K13	5	0.27	0.48	0.01	0.27	4.32	1.43	3.06	0.70	1.78	0.99	1.37	0.46	4.32	0.22	0.02
K14	5.5	0.38	0.53	0.02	0.36	4.25	1.41	3.06	0.67	1.79	0.97	1.34	0.43	4.04	0.13	0.02
K15	6	0.28	0.40	0.03	0.27	4.22	1.44	3.03	0.71	1.78	0.98	1.29	0.35	5.21	0.46	0.03
K16	5.5	0.28	0.43	0.02	0.25	4.69	1.46	3.11	0.65	1.92	0.98	1.33	0.49	4.26	0.18	0.02
K17	4.5	0.26	0.50	0.02	0.25	4.35	1.44	3.03	0.71	1.80	0.99	1.29	0.37	5.24	0.68	0.02
K18	6	0.29	0.43	0.02	0.27	4.67	1.44	3.04	0.65	1.92	0.98	1.34	0.47	4.17	0.11	0.02
K30	5	0.15	0.29	0.01	0.15	4.74	1.53	3.73	0.69	1.89	1.03	1.42	0.35	5.74	0.71	0.01
K31	5	0.24	0.31	0.02	0.22	4.85	1.50	3.47	0.66	1.95	0.98	1.37	0.49	4.35	0.18	0.02
K32	5	0.20	0.27	0.02	0.19	4.75	1.52	3.65	0.66	1.90	1.00	1.43	0.46	4.71	0.30	0.02
K33	5	0.23	0.31	0.02	0.22	4.97	1.51	3.66	0.64	2.00	0.98	1.39	0.44	4.66	0.35	0.01
K34	5	0.17	0.30	0.02	0.17	4.58	1.53	3.49	0.70	1.86	1.02	1.37	0.47	4.96	0.48	0.02
K35	4.5	0.17	0.24	0.02	0.17	4.89	1.54	3.63	0.68	1.93	1.01	1.38	0.36	5.74	0.69	0.02
K36	3.5	0.19	0.27	0.02	0.19	4.74	1.50	3.88	0.69	1.90	1.00	1.50	0.33	5.86	0.64	0.02
K37	4.5	0.39	0.52	0.04	0.37	4.10	1.39	2.99	0.70	1.69	0.93	1.29	0.32	5.03	0.42	0.03
K38	6	0.18	0.46	0.04	0.17	5.19	1.39	2.81	0.67	1.71	1.08	1.37	0.27	7.49	1.04	0.08
K39	5	0.16	0.32	0.03	0.16	4.56	1.52	3.45	0.70	1.87	1.04	1.44	0.44	5.41	0.46	0.02

Table A.17 (*continued*)

#	Colour code	BPI	C/P 2	API	CO_3/PO_4	IRSF	1060/1075	1030/1110	PPI	PSF	AB	C/C	OH/P	OHSF	CN/P	WAMPI
K40	3.5	0.28	0.39	0.03	0.26	4.59	1.45	3.11	0.67	1.86	0.98	1.34	0.41	4.79	0.47	0.03
K41	5	0.50	0.31	0.09	0.44	4.18	1.35	3.10	0.70	1.77	0.91	1.15	0.37	4.15	0.23	0.09
K42	5.5	0.18	0.26	0.02	0.17	4.71	1.50	3.62	0.70	1.83	1.01	1.40	0.34	5.77	0.67	0.02
K43	5	0.18	0.23	0.02	0.19	4.99	1.50	3.75	0.67	1.88	1.03	1.57	0.38	5.18	0.32	0.02
K44	6	0.18	0.30	0.01	0.17	4.43	1.47	2.91	0.67	1.62	1.01	1.42	0.44	4.84	0.15	0.01
L1	5.5	0.20	0.17	0.03	0.19	5.26	1.51	3.58	0.66	2.06	1.01	1.47	0.43	4.93	0.38	0.04
L2	5.5	0.20	0.12	0.04	0.17	6.18	1.53	4.52	0.56	2.30	1.02	1.36	0.55	4.68	0.16	0.06
P1	5.5	0.17	0.22	0.03	0.16	4.69	1.54	3.76	0.68	1.89	1.02	1.34	0.42	5.25	0.55	0.03
P2	5.5	0.39	0.44	0.04	0.36	4.18	1.42	3.38	0.66	1.75	0.93	1.33	0.39	4.13	0.08	0.02
P3a	6	0.43	0.24	0.05	0.38	4.93	1.45	4.10	0.63	1.90	0.93	1.29	0.41	4.12	0.09	0.03
P3b	6	0.49	0.26	0.06	0.44	4.77	1.42	4.17	0.63	1.99	0.94	1.34	0.36	4.19	0.10	0.03
P3c	6	0.49	0.27	0.07	0.43	4.77	1.44	4.01	0.64	1.90	0.91	1.23	0.41	4.15	0.09	0.05
P4	4.5	0.18	0.29	0.02	0.17	4.58	1.50	3.65	0.71	1.82	1.01	1.34	0.29	6.86	0.99	0.02
St01	6	0.26	0.36	0.02	0.26	4.41	1.50	3.22	0.69	1.72	1.02	1.39	0.43	4.65	0.20	0.01
St02	6	0.33	0.40	0.03	0.31	4.50	1.49	3.23	0.68	1.71	1.02	1.30	0.44	4.70	0.20	0.00
St03	6	0.49	0.54	0.06	0.43	4.49	1.47	2.91	0.68	1.94	0.96	1.16	0.48	4.13	0.12	0.01
St04	6	0.34	0.38	0.05	0.31	4.83	1.57	3.39	0.68	1.84	1.02	1.27	0.51	4.77	0.18	0.01
St05	6	0.24	0.33	0.05	0.24	4.63	1.57	3.62	0.69	1.89	1.08	1.44	0.55	4.68	0.16	0.01
St06	6	0.46	0.49	0.05	0.43	4.41	1.48	3.18	0.70	1.90	0.97	1.27	0.47	4.20	0.12	0.01
St07	6	0.31	0.37	0.03	0.29	4.42	1.48	3.27	0.69	1.68	0.99	1.33	0.38	4.90	0.23	0.01
St08	5.5	0.87	0.71	0.10	0.78	4.08	1.40	2.79	0.73	1.80	0.95	1.12	0.35	4.33	0.20	0.02
St09	6	0.27	0.36	0.01	0.27	4.21	1.46	3.31	0.68	1.66	0.99	1.42	0.41	4.46	0.16	0.01
St10	6	0.30	0.35	0.04	0.28	4.78	1.55	3.54	0.68	1.91	1.02	1.33	0.51	4.64	0.22	0.01
St11	6	0.35	0.42	0.03	0.31	4.67	1.50	3.27	0.66	2.00	0.96	1.23	0.50	4.28	0.18	0.01
St12	6	0.40	0.39	0.04	0.36	4.71	1.48	3.35	0.65	1.95	0.97	1.30	0.49	4.11	0.10	0.01
St13	6	0.32	0.35	0.03	0.29	4.75	1.52	3.39	0.65	2.01	0.98	1.33	0.51	4.16	0.11	0.01
St14	5.5	0.19	0.36	0.03	0.19	4.32	1.49	3.37	0.68	1.79	1.03	1.48	0.55	4.37	0.17	0.02
St15	6	0.29	0.38	0.08	0.28	4.42	1.52	3.36	0.67	1.89	1.06	1.41	0.54	4.26	0.16	0.01
St16	6	0.26	0.38	0.04	0.25	4.56	1.56	3.27	0.68	1.76	1.04	1.32	0.52	4.76	0.19	0.01
St17	5.5	0.24	0.32	0.04	0.23	4.73	1.55	3.51	0.69	1.90	1.04	1.36	0.49	4.82	0.28	0.03
St18	6	0.23	0.39	0.01	0.22	4.18	1.46	3.15	0.66	1.63	0.98	1.40	0.38	4.81	0.22	0.01
St19	5.5	0.24	0.33	0.02	0.23	4.64	1.51	3.46	0.67	1.87	1.01	1.31	0.45	4.87	0.42	0.01
St20	6	0.31	0.38	0.04	0.28	4.75	1.57	3.45	0.67	1.86	1.04	1.29	0.51	4.75	0.22	0.01
St21	6	0.44	0.44	0.09	0.38	4.72	1.57	3.36	0.67	1.94	0.97	1.14	0.53	4.54	0.13	0.01

Table A.17 (*continued*)

#	Colour code	BPI	C/P 2	API	CO_3/PO_4	IRSF	1060/1075	1030/1110	PPI	PSF	AB	C/C	OH/P	OHSF	CN/P	WAMPI
St22	5	0.37	0.34	0.06	0.34	5.03	1.55	3.02	0.69	2.02	1.01	1.22	0.43	5.24	0.37	0.06
St23	5.5	0.17	0.26	0.03	0.16	4.86	1.57	3.36	0.67	1.80	1.07	1.43	0.50	4.91	0.21	0.01
St24	5.5	0.64	0.55	0.09	0.54	4.80	1.50	3.09	0.67	2.04	0.96	1.07	0.55	4.28	0.14	0.02
St25	6	0.30	0.39	0.03	0.27	4.33	1.49	3.47	0.64	1.64	1.03	1.30	0.45	4.61	0.24	0.01
St26	6	0.24	0.41	0.05	0.24	3.95	1.45	3.21	0.69	1.74	1.03	1.42	0.53	4.10	0.22	0.03
St27	6	0.69	0.55	0.13	0.60	4.94	1.49	3.47	0.66	1.95	0.99	1.19	0.47	4.30	0.17	0.02
St28	6	0.28	0.35	0.06	0.26	4.59	1.53	3.87	0.65	1.83	1.07	1.34	0.55	4.52	0.18	0.02
St29	6	0.43	0.47	0.06	0.39	4.37	1.47	3.82	0.63	1.84	0.95	1.31	0.48	4.08	0.10	0.02
St30	6	0.71	0.61	0.08	0.61	3.90	1.37	3.39	0.68	1.68	0.93	1.13	0.35	4.15	0.21	0.02
St31	6	0.22	0.34	0.02	0.20	4.42	1.52	3.50	0.65	1.67	1.03	1.35	0.43	4.95	0.38	0.01
WC1	6	0.11	0.27	0.02	0.11	4.94	1.61	3.50	0.65	1.87	1.07	1.51	0.64	5.03	0.12	0.01
WC2	6	0.18	0.32	0.02	0.18	4.74	1.53	3.22	0.68	1.91	1.02	1.47	0.48	4.73	0.33	0.02
WC3	6	0.15	0.28	0.02	0.16	4.75	1.57	3.49	0.67	1.91	1.05	1.62	0.61	4.62	0.14	0.01
WC4	5.5	0.21	0.26	0.02	0.22	4.75	1.50	3.51	0.69	1.93	1.02	1.58	0.51	4.43	0.13	0.02
WC5	5	0.24	0.24	0.03	0.24	4.81	1.46	3.03	0.71	2.03	0.99	1.41	0.45	4.48	0.22	0.05

6.5.2 Infrared data after pre-treatment

Table A.18 – Infrared data after pre-treatment for archaeological calcined bone samples

#	Colour code	BPI	C/P 2	API	CO_3/PO_4	IRSF	1060/1075	1030/1110	PPI	PSF	AB	C/C	OH/P	OHSF	CN/P	WAMPI
A1	5	0.30	0.37	0.02	0.28	4.52	1.46	3.37	0.65	1.87	1.00	1.38	0.53	4.05	0.13	0.02
A2	5.5	0.22	0.25	0.01	0.21	4.80	1.49	3.69	0.65	1.77	0.99	1.43	0.40	4.72	0.29	0.01
BM1a	6	0.17	0.19	0.00	0.16	5.50	1.59	4.02	0.63	2.03	1.01	1.46	0.57	4.62	0.10	0.00
BM1b	6	0.10	0.12	0.02	0.10	6.17	1.63	4.69	0.58	2.16	1.10	1.57	0.53	5.18	0.35	0.01
BM2a	6	0.15	0.22	0.01	0.14	5.00	1.58	3.42	0.66	1.77	1.03	1.45	0.54	4.75	0.15	0.01
BM2b	6	0.15	0.20	0.01	0.14	5.13	1.58	3.62	0.64	1.82	1.03	1.49	0.53	4.78	0.21	0.01
BM3a	6	0.13	0.14	0.01	0.12	5.75	1.63	4.14	0.62	2.18	1.07	1.49	0.55	4.85	0.16	0.01
BM3b	6	0.13	0.20	0.01	0.13	5.09	1.58	3.60	0.65	1.74	1.04	1.50	0.52	5.01	0.26	0.01
BN1	6	0.16	0.26	0.02	0.17	4.60	1.53	3.78	0.68	1.82	1.05	1.50	0.55	4.72	0.27	0.01
BN2	5.5	0.24	0.32	0.02	0.24	4.59	1.49	3.30	0.68	1.91	1.00	1.52	0.46	4.43	0.24	0.01
BN3	6	0.27	0.36	0.01	0.27	4.21	1.46	3.22	0.70	1.74	0.99	1.41	0.47	4.34	0.23	0.01
BN4	6	0.31	0.36	0.02	0.31	4.34	1.46	3.49	0.69	1.82	0.97	1.42	0.40	4.46	0.15	0.01
C1	5.5	0.23	0.20	0.01	0.22	5.21	1.49	3.39	0.65	2.06	1.00	1.44	0.54	4.26	0.13	0.01
C2	6	0.31	0.22	0.03	0.30	4.93	1.46	3.38	0.67	1.95	0.99	1.38	0.54	3.99	0.13	0.03
C3	5.5	0.24	0.23	0.02	0.23	4.88	1.48	3.44	0.67	1.88	1.01	1.40	0.51	4.42	0.34	0.02
K01	5.5	0.23	0.42	0.02	0.24	4.30	1.43	3.13	0.74	1.75	1.01	1.41	0.36	5.43	0.81	0.02
K02	6	0.32	0.41	0.02	0.30	4.48	1.47	3.74	0.66	1.84	0.98	1.37	0.51	4.11	0.19	0.01
K03	4.5	0.14	0.38	0.02	0.14	4.63	1.54	4.01	0.72	1.89	1.04	1.41	0.30	7.06	1.38	0.01
K04	4.5	0.37	0.43	0.02	0.35	4.32	1.44	3.42	0.69	1.80	0.97	1.33	0.43	4.29	0.32	0.01
K05	6	0.33	0.46	0.02	0.32	4.26	1.45	3.31	0.68	1.85	0.98	1.37	0.48	4.10	0.29	0.01
K06	6	0.20	0.34	0.02	0.21	4.41	1.45	3.48	0.71	1.78	1.01	1.52	0.34	5.71	0.76	0.01
K07	6	0.19	0.33	0.02	0.19	4.60	1.50	3.61	0.71	1.84	1.02	1.45	0.37	5.77	0.73	0.01
K08	5.5	0.30	0.50	0.02	0.30	4.13	1.42	3.12	0.69	1.76	1.00	1.40	0.46	4.40	0.54	0.02
K09	5.5	0.34	0.55	0.02	0.32	4.13	1.41	3.15	0.68	1.73	0.99	1.31	0.47	4.30	0.45	0.02
K10	5	0.47	0.60	0.03	0.44	3.96	1.36	3.08	0.70	1.67	0.95	1.29	0.37	4.30	0.27	0.02
K11	5	0.13	0.28	0.04	0.15	4.60	1.43	3.56	0.73	1.73	1.10	1.65	0.38	5.63	0.94	0.02
K12	5	0.26	0.44	0.02	0.27	4.27	1.43	3.46	0.73	1.75	1.00	1.39	0.32	5.88	1.09	0.02
K13	5	0.32	0.56	0.02	0.31	4.24	1.42	3.33	0.69	1.71	0.98	1.39	0.48	4.25	0.27	0.02
K14	5.5	0.38	0.50	0.02	0.36	4.28	1.43	3.08	0.68	1.79	0.96	1.36	0.43	4.05	0.13	0.01
K15	6	0.24	0.40	0.02	0.25	4.26	1.46	3.32	0.71	1.77	1.00	1.44	0.37	5.22	0.54	0.02
K16	5.5	0.30	0.44	0.02	0.29	4.46	1.45	3.14	0.67	1.84	0.99	1.37	0.51	4.17	0.21	0.02
K17	4.5	0.30	0.55	0.02	0.28	4.24	1.43	3.38	0.70	1.74	0.99	1.31	0.39	5.09	0.81	0.02

Table A.18 (*continued*)

#	Colour code	BPI	C/P 2	API	CO_3/PO_4	IRSF	1060/1075	1030/1110	PPI	PSF	AB	C/C	OH/P	OHSF	CN/P	WAMPI
K18	6	0.35	0.48	0.02	0.34	4.26	1.41	3.17	0.68	1.75	0.99	1.37	0.49	3.97	0.12	0.01
K30	5	0.15	0.30	0.02	0.16	4.52	1.48	3.99	0.74	1.85	1.04	1.50	0.35	6.14	1.13	0.01
K31	5	0.29	0.39	0.02	0.27	4.53	1.47	3.38	0.68	1.83	0.99	1.38	0.51	4.19	0.24	0.01
K32	5	0.25	0.42	0.02	0.25	4.12	1.46	3.32	0.71	1.77	1.01	1.42	0.49	4.40	0.42	0.02
K33	5	/		/	/	/	/	/	/	/	/	/	/	/	/	/
K34	5	/	/	/	/	/	/	/	/	/	/	/	/	/	/	/
K35	4.5	0.15	0.26	0.01	0.15	5.00	1.58	3.88	0.69	1.99	1.02	1.46	0.39	5.80	0.64	0.01
K36	3.5	0.19	0.31	0.01	0.20	4.50	1.48	3.70	0.74	1.86	1.00	1.52	0.32	6.13	0.80	0.01
K37	4.5	0.45	0.63	0.03	0.44	3.86	1.37	3.12	0.72	1.68	0.95	1.33	0.34	4.70	0.58	0.02
K38	6	0.21	0.75	0.04	0.21	4.65	1.32	2.69	0.70	1.66	1.07	1.40	0.29	7.22	1.39	0.08
K39	5	0.13	0.37	0.03	0.14	4.48	1.53	3.58	0.73	1.83	1.06	1.62	0.48	5.34	0.64	0.02
K40	3.5	0.16	0.27	0.02	0.16	4.92	1.55	3.45	0.69	1.89	1.03	1.48	0.45	5.14	0.46	0.01
K41	5	0.51	0.41	0.06	0.45	4.18	1.35	3.34	0.69	1.77	0.93	1.20	0.40	4.04	0.31	0.06
K42	5.5	0.31	0.49	0.02	0.29	4.49	1.44	3.32	0.65	1.82	0.99	1.35	0.52	4.11	0.13	0.02
K43	5	0.22	0.34	0.06	0.25	4.42	1.45	3.25	0.73	1.77	1.03	1.68	0.40	4.91	0.48	0.04
K44	6	0.21	0.40	0.01	0.21	4.19	1.46	2.89	0.70	1.66	1.00	1.46	0.45	4.66	0.22	0.01
L1	5.5	0.19	0.15	0.02	0.18	5.67	1.53	4.17	0.62	2.20	1.03	1.51	0.43	5.07	0.40	0.01
L2	5.5	0.19	0.12	0.01	0.17	5.87	1.52	3.53	0.63	2.27	1.01	1.43	0.56	4.58	0.18	0.02
P1	5.5	0.21	0.38	0.02	0.21	4.17	1.48	3.56	0.71	1.81	1.04	1.48	0.50	4.36	0.52	0.02
P2	5.5	0.49	0.59	0.04	0.48	3.76	1.38	3.14	0.72	1.72	0.95	1.38	0.42	3.83	0.12	0.02
P3a	6	0.40	0.27	0.03	0.39	4.62	1.42	3.52	0.69	1.82	0.96	1.38	0.44	4.03	0.12	0.02
P3b	6	0.45	0.28	0.04	0.43	4.69	1.42	3.98	0.65	1.93	0.97	1.43	0.37	4.16	0.13	0.03
P3c	6	0.48	0.32	0.05	0.47	4.36	1.39	3.36	0.70	1.76	0.97	1.36	0.43	4.05	0.12	0.05
P4	4.5	0.18	0.36	0.02	0.19	4.29	1.49	3.47	0.76	1.81	1.03	1.47	0.31	6.59	1.34	0.02

6.5.3 Isotope analyses data

Table A.19 – Isotope analyses data for archaeological calcined bone samples

#	Colour code	Geological carbonate content	$\delta^{13}C$ (‰)	$\delta^{18}O$ (‰)	pCO_2/g of sample	$^{87}Sr/^{86}Sr$ (± 2σ)
A1	5	Low	-25.8	-15.9	0.39	0.710551 ± 9
A2	5.5		-20.6	-17.6	0.50	0.709003 ± 6
BM1a	6	Low	-26.4	-16.4	0.37	0.707072 ± 8
BM1b	6		-23.3	-21.0	0.30	0.707232 ± 8
BM2a	6		-25.6	-18.4	0.36	0.706603 ± 9
BM2b	6		-25.4	-16.2	0.35	0.706628 ± 10
BM3a	6		-23.7	-18.1	0.40	0.706899 ± 7
BM3b	6		-24.4	-17.6	0.33	0.706883 ± 8
BN1	6	Low	-23.3	-17.0	0.31	0.710377 ± 9
BN2	5.5		-22.2	-17.4	0.38	0.709410 ± 7
BN3	6		-22.7	-17.4	0.37	0.710258 ± 8
BN4	6		-25.0	-16.4	0.43	0.710338 ± 8
C1	5.5	Low	-25.3	-18.0	0.44	0.709006 ± 9
C2	6		-28.9	-14.8	0.44	0.709271 ± 8
C3	5.5		-23.7	-15.8	0.41	0.709291 ± 9
K01	5.5	High	-21.0	-16.3	0.40	0.710165 ± 9
K02	6		-23.3	-16.4	0.47	0.709944 ± 11
K03	4.5		-20.0	-15.0	0.32	0.710261 ± 11
K04	4.5		-23.0	-15.8	0.51	0.709611 ± 10
K05	6		-21.6	-18.3	0.47	0.709280 ± 7
K06	6		-20.6	-13.8	0.47	0.709268 ± 9
K07	6		-20.3	-16.1	0.43	0.709950 ± 8
K08	5.5		-20.4	-16.2	0.35	0.709251 ± 8
K09	5.5		-21.9	-17.5	0.44	0.709515 ± 8
K10	5		-23.8	-14.5	0.51	0.709230 ± 8
K11	5		-22.7	-16.3	0.37	0.709893 ± 9
K12	5		-19.7	-14.7	0.36	0.709580 ± 11
K13	5		-23.3	-18.9	0.50	0.709685 ± 8
K14	5.5		-25.6	-15.7	0.48	0.709366 ± 8
K15	6		-19.9	-14.8	0.45	0.709344 ± 10
K16	5.5		-22.8	-16.7	0.43	0.709652 ± 11
K17	4.5		-18.7	-15.3	0.41	0.710135 ± 10
K18	6		-24.0	-17.3	0.43	0.709457 ± 11

Table A.19 (*continued*)

#	Colour code	Geological carbonate content	$\delta^{13}C$ (‰)	$\delta^{18}O$ (‰)	pCO_2/g of sample	$^{87}Sr/^{86}Sr$ (± 2σ)
K30	5		-21.5	-15.0	0.42	0.709345 ± 7
K31	5		-23.9	-17.4	0.47	0.709615 ± 8
K32	5		-21.8	-16.4	0.47	0.709672 ± 8
K33	5		/	/	/	0.709974 ± 9
K34	5		/	/	/	0.710180 ± 8
K35	4.5		-22.3	-15.1	0.41	0.709760 ± 8
K36	3.5		-20.0	-12.5	0.39	0.710399 ± 8
K37	4.5	High	-20.6	-15.4	0.58	0.709921 ± 10
K38	6		-23.1	-16.9	0.32	0.710026 ± 10
K39	5		-22.9	-16.1	0.37	0.711192 ± 7
K40	3.5		-23.4	-15.3	0.44	0.709379 ± 9
K41	5		-20.9	-16.8	0.57	0.710052 ± 9
K42	5.5		-23.8	-16.3	0.46	0.709526 ± 6
K43	5		-26.1	-13.6	0.46	0.709438 ± 7
K44	6		-22.4	-17.4	0.41	0.709541 ± 9
L1	5.5	Low	-22.9	-15.1	0.42	0.709896 ± 12
L2	5.5		-28.0	-15.0	0.38	0.713614 ± 8
P1	5.5		-20.8	-15.3	0.31	0.711166 ± 10
P2	5.5		-28.4	-13.6	0.73	0.709881 ± 8
P3a	6	High	-25.3	-16.3	0.42	0.710134 ± 7
P3b	6		-26.1	-15.2	0.46	0.709818 ± 7
P3c	6		-28.0	-15.0	0.41	0.710212 ± 10
P4	4.5		-18.0	-14.9	0.40	0.711371 ± 8
St01	6		-21.7	-18.5	0.34	/
St02	6		-23.9	-16.3	0.33	/
St03	6		-24.0	-17.0	0.36	/
St04	6		-22.6	-14.8	0.33	/
St05	6		-22.2	-13.7	0.21	/
St06	6		-24.6	-15.8	0.31	/
St07	6	High	-11.8	-7.4	0.37	/
St08	5.5		-19.2	-17.7	0.35	/
St09	6		-20.9	-16.0	0.36	/
St10	6		-24.7	-15.2	0.29	/
St11	6		-23.9	-17.6	0.36	/
St12	6		/	/	/	/

Table A.19 (*continued*)

#	Colour code	Geological carbonate content	$\delta^{13}C$ (‰)	$\delta^{18}O$ (‰)	pCO_2/g of sample	$^{87}Sr/^{86}Sr$ (± 2σ)
St13	6		-25.2	-17.8	0.38	/
St14	5.5		/	/	/	/
St15	6		-23.9	-19.5	0.29	/
St16	6		-22.5	-16.4	0.22	/
St17	5.5		-23.0	-17.0	0.27	/
St18	6		-19.5	-18.3	0.40	/
St19	5.5		-20.4	-18.0	0.28	/
St20	6		-20.4	-19.1	0.26	/
St21	6		-23.2	-21.7	0.26	/
St22	5	High	-23.5	-18.5	0.26	/
St23	5.5		-23.4	-17.9	0.32	/
St24	5.5		-25.1	-17.1	0.40	/
St25	6		-21.1	-19.9	0.32	/
St26	6		-22.6	-17.6	0.35	/
St27	6		-24.5	-16.2	0.40	/
St28	6		-21.6	-14.7	0.31	/
St29	6		-23.8	-18.1	0.35	/
St30	6		-20.8	-17.4	0.42	/
St31	6		-21.5	-17.3	0.33	/

6.6 Archaeological unburned tooth samples

6.6.1 Isotope analyses data

Table A.20 – Isotope analyses data for archaeological unburned tooth samples

#	$\delta^{13}C$ (‰)	$\delta^{18}O$ (‰)	$^{87}Sr/^{86}Sr$ (± 2σ)
BNT1	-17.3	-3.3	0.708455 ± 29
BNT2	/	/	0.708610 ± 8
BNT3	-17.1	-3.5	0.708962 ± 8
PT1	-16.7	-3.2	0.710142 ± 7
PT2	-16.2	-2.9	0.709612 ± 11
PT3	-16.7	-2.8	0.708883 ± 7
PT4	-16.9	-2.2	0.708728 ± 8
KT1	-16.6	-3.2	0.709671 ± 9
KT2	-16.5	-3.4	0.709073 ± 10
KT3	-16.6	-3.0	0.709588 ± 9
KT4	-15.9	-2.8	0.710215 ± 7
KT5	-14.8	-4.3	0.712358 ± 8
KT6	-16.6	-3.7	0.709055 ± 9
KT7	-18.1	-3.3	0.710594 ± 8
KT8	-16.0	-3.7	0.709410 ± 7

6.7 Modern unburned bone samples

6.7.1 Infrared data (no pre-treatment)

Table A.21 – Infrared data for modern unburned bone samples

#	BPI	C/P 2	API	CO_3/PO_4	IRSF	1060/1075	1030/1110	PPI	PSF	AB	C/C	OH/P	OHSF	CN/P	WAMPI
L1	/	/	/	/	/	/	/	/	/	/	/	/	/	/	/
L2	/	/	/	/	/	/	/	/	/	/	/	/	/	/	/
L3	/	/	/	/	/	/	/	/	/	/	/	/	/	/	/
P1	/	/	/	/	/	/	/	/	/	/	/	/	/	/	/
P2	1.00	0.34	0.93	0.80	2.84	1.18	2.23	0.68	1.52	0.89	0.98	0.33	4.63	0.12	1.38
P3	/	/	/	/	/	/	/	/	/	/	/	/	/	/	/
P4	1.00	0.35	0.91	0.79	2.81	1.17	2.16	0.67	1.50	0.86	0.98	0.35	4.48	0.15	1.34
P5	0.96	0.33	0.84	0.77	2.78	1.18	2.18	0.68	1.51	0.89	0.97	0.34	4.47	0.16	1.25
C	0.92	0.41	0.74	0.72	3.00	1.20	2.33	0.65	1.50	0.90	0.97	0.28	5.46	0.17	1.09
Ch	/	/	/	/	/	/	/	/	/	/	/	/	/	/	/
Seal	1.58	0.71	0.94	1.16	3.06	1.22	2.64	0.64	1.49	0.87	0.87	0.13	12.36	0.16	1.44

6.7.2 Isotope analyses data

Table A.22 – Isotope analyses data for modern unburned bone samples

#	Corresponding heated fragments	$\delta^{13}C$ (‰) – collagen	$\delta^{13}C$ (‰) – apatite	$\delta^{18}O$ (‰) – apatite
L1	LAB 1, L1_A, L1_B, L1_D	-22.6	-15.3	-4.3
L2	L2_A	-22.4	-15.9	-5.4
L3	L3	/	/	/
P1	P1	-22.8	/	/
P2	LAB 3 (pig rib), P2, P3, P4	-20.3	-10.8	-5.4
P3	P5	-22.9	-13.3	-5.3
P4	P6	-23.1	-12.7	-4.5
P5	P7	-23.5	-12.8	-4.6
C	LAB2, C1, C2	-23.2	-12.4	-3.3
Ch	Ch1	-12.2	-11.5	-3.9
Seal	LAB 3 (seal bone)	-19.0	-9.6	-1.7

6.8 Archaeological unburned bone samples

These samples are archaeological unburned bone fragments from Haddenham Causewayed Enclosure (HAD), Wally Corner (Berinsfield – BER) and Imperial College Sports Ground (IC), Sipson Lane (Brock et al. 2007; 2010a).

6.8.1 Infrared data (no pre-treatment)

Table A.23 – Infrared data for archaeological unburned bone samples

#	BPI	C/P 2	API	CO_3/PO_4	IRSF	1060/1075	1030/1110	PPI	PSF	AB	C/C	OH/P	OHSF	CN/P	WAMPI
BER1	1.11	0.48	0.35	0.82	3.42	1.27	2.95	0.65	1.55	0.82	0.87	0.20	7.11	0.16	0.26
BER2	1.15	0.50	0.36	0.84	3.54	1.28	3.02	0.64	1.60	0.82	0.87	0.20	7.13	0.13	0.28
BER3	1.19	0.51	0.40	0.87	3.35	1.27	2.89	0.65	1.55	0.84	0.86	0.18	8.30	0.14	0.38
BER4	1.10	0.46	0.34	0.81	3.44	1.28	2.93	0.65	1.59	0.81	0.86	0.20	7.46	0.14	0.27
BER5	1.18	0.49	0.39	0.87	3.32	1.26	2.86	0.65	1.55	0.83	0.86	0.20	7.33	0.17	0.35
BER6	1.05	0.45	0.32	0.77	3.50	1.28	3.03	0.64	1.60	0.83	0.88	0.20	7.11	0.14	0.27
BER7	1.14	0.54	0.40	0.83	3.23	1.27	2.94	0.64	1.50	0.84	0.87	0.21	6.73	0.16	0.36
BER8	1.07	0.50	0.33	0.77	3.40	1.27	3.03	0.63	1.54	0.84	0.87	0.20	7.10	0.13	0.28
BER9	1.02	0.47	0.30	0.75	3.48	1.28	3.04	0.64	1.58	0.84	0.87	0.19	7.43	0.14	0.25
BER10	1.07	0.47	0.36	0.78	3.49	1.27	2.92	0.64	1.59	0.86	0.86	0.18	8.35	0.14	0.36
BER11	1.32	0.67	0.38	0.98	3.64	1.24	2.61	0.67	1.66	0.88	0.84	0.15	10.32	0.24	0.31
BER12	1.02	0.50	0.34	0.74	3.49	1.27	2.96	0.64	1.58	0.87	0.87	0.16	9.03	0.15	0.33
IC01	1.03	0.67	0.38	0.76	3.46	1.25	2.78	0.63	1.60	0.96	0.90	0.19	7.75	0.18	0.33
IC02	0.80	0.42	0.27	0.61	3.48	1.25	2.79	0.63	1.65	0.94	0.94	0.27	5.45	0.16	0.21
IC03	0.87	0.48	0.30	0.67	3.44	1.25	2.74	0.65	1.63	0.94	0.95	0.28	5.24	0.16	0.22
IC04	0.74	0.40	0.25	0.56	3.77	1.27	2.95	0.62	1.68	0.95	0.96	0.23	6.23	0.16	0.24
IC05	0.92	0.77	0.31	0.66	3.78	1.26	2.97	0.59	1.60	0.99	0.94	0.17	8.77	0.19	0.33
IC06	0.68	0.40	0.22	0.52	3.70	1.26	2.78	0.64	1.71	0.97	0.97	0.24	6.03	0.15	0.23
IC07	0.78	0.52	0.26	0.58	3.59	1.25	2.74	0.62	1.65	0.98	0.94	0.23	6.27	0.14	0.28
IC08	0.87	0.55	0.28	0.64	3.52	1.25	2.73	0.62	1.65	0.96	0.90	0.21	6.94	0.16	0.31
IC09	1.08	2.52	0.48	0.67	3.71	1.24	2.78	0.48	1.56	1.06	0.92	0.12	12.70	0.30	0.84
IC10	0.73	0.36	0.24	0.56	3.87	1.29	3.23	0.62	1.72	0.94	1.00	0.25	5.45	0.14	0.18
IC11	0.76	0.43	0.28	0.57	3.95	1.28	3.04	0.62	1.72	0.96	0.97	0.20	7.01	0.14	0.27
IC12	0.75	0.49	0.28	0.56	3.60	1.25	2.75	0.63	1.64	0.98	0.95	0.23	6.16	0.16	0.30
IC13	0.81	0.44	0.26	0.61	3.70	1.27	2.96	0.64	1.68	0.96	0.93	0.20	7.21	0.14	0.26

Table A.23 (*continued*)

#	BPI	C/P 2	API	CO_3/PO_4	IRSF	1060/1075	1030/1110	PPI	PSF	AB	C/C	OH/P	OHSF	CN/P	WAMPI
IC14	0.98	1.14	0.39	0.66	3.51	1.24	2.76	0.55	1.59	1.03	0.91	0.21	7.21	0.22	0.50
IC15	0.98	1.19	0.37	0.66	3.52	1.23	2.73	0.55	1.59	1.02	0.90	0.19	7.63	0.24	0.49
IC16	1.02	1.08	0.38	0.68	3.64	1.24	2.87	0.54	1.61	1.02	0.91	0.19	7.77	0.19	0.48
IC17	1.02	1.47	0.43	0.67	3.61	1.23	2.71	0.52	1.59	1.04	0.91	0.19	7.86	0.23	0.63
IC18	0.80	0.47	0.30	0.61	3.63	1.27	3.03	0.63	1.61	0.94	0.97	0.22	6.39	0.16	0.30
IC19	1.09	0.64	0.57	0.80	3.45	1.26	2.88	0.63	1.54	0.93	0.90	0.13	11.11	0.15	0.79
IC20	0.88	0.56	0.32	0.66	3.79	1.26	2.90	0.63	1.62	0.97	0.96	0.17	8.14	0.15	0.34
HAD1	0.84	0.35	0.34	0.64	3.55	1.26	2.66	0.69	1.71	0.91	0.88	0.19	7.62	0.14	0.32
HAD2	0.82	0.63	0.33	0.63	3.54	1.23	2.45	0.66	1.63	0.99	0.91	0.19	7.72	0.18	0.37
HAD3	0.78	0.31	0.27	0.60	3.51	1.27	2.76	0.69	1.71	0.84	0.88	0.17	8.56	0.14	0.21
HAD4	0.72	0.36	0.25	0.55	3.68	1.27	2.77	0.69	1.76	0.92	0.88	0.17	8.61	0.14	0.24
HAD5	0.74	0.30	0.23	0.56	3.90	1.30	3.09	0.66	1.78	0.87	0.90	0.18	7.66	0.12	0.17
HAD6	0.69	0.30	0.23	0.53	4.23	1.28	2.93	0.65	1.87	0.92	0.97	0.17	8.43	0.15	0.19
HAD7	0.85	0.33	0.31	0.64	3.74	1.27	2.83	0.68	1.74	0.88	0.87	0.18	8.27	0.13	0.26
HAD8	1.19	0.47	0.35	0.90	3.31	1.26	2.69	0.71	1.62	0.81	0.81	0.18	8.59	0.12	0.24
HAD9	0.99	0.47	0.45	0.75	3.90	1.25	2.55	0.69	1.71	0.95	0.87	0.11	13.63	0.19	0.40
HAD10	0.98	0.43	0.35	0.76	3.63	1.28	2.70	0.74	1.72	0.86	0.82	0.13	12.30	0.17	0.35
HAD11	1.13	0.38	0.38	0.81	3.50	1.29	3.06	0.66	1.75	0.77	0.81	0.19	7.70	0.14	0.32
HAD12	1.05	0.63	0.43	0.79	3.86	1.25	2.57	0.68	1.65	0.95	0.84	0.10	15.96	0.20	0.43
HAD13	1.52	0.61	0.37	1.17	3.35	1.26	2.67	0.72	1.68	0.86	0.85	0.20	7.70	0.14	0.21
HAD14	0.92	0.36	0.34	0.72	3.42	1.27	2.67	0.73	1.67	0.82	0.85	0.18	7.83	0.11	0.31
HAD15	0.83	0.30	0.29	0.65	3.89	1.29	2.82	0.72	1.89	0.81	0.86	0.15	9.85	0.13	0.22
HAD16	0.75	0.30	0.28	0.58	3.72	1.27	2.84	0.68	1.80	0.88	0.89	0.20	7.18	0.16	0.26
HAD17	0.93	0.36	0.29	0.70	3.43	1.27	2.76	0.71	1.69	0.79	0.83	0.19	7.89	0.13	0.27
HAD18	0.84	0.30	0.33	0.62	3.72	1.29	2.98	0.66	1.80	0.83	0.86	0.23	6.37	0.16	0.28
HAD19	1.00	0.46	0.43	0.72	3.74	1.27	2.79	0.65	1.77	0.91	0.85	0.17	8.58	0.18	0.46
HAD20	0.90	0.32	0.35	0.66	3.72	1.28	2.99	0.65	1.80	0.84	0.86	0.22	6.67	0.15	0.34

6.9 Modern plant samples

For each measurement, the 2σ values are calculated following the equation: 2 x mean of the 60 ratio measurements x standard error. Red values represent outliers (see Chapter 7).

Table A.24 – GPS location and strontium isotope measurements of modern plant samples

Site	GPS-location		Values (± 2σ)		
	North	West	Grass	Shrubs	Trees
Formation 0 – Coastal Zone					
I16	54-02-697	006-11-279	/	0.709889 ± 7	0.710759 ± 9
I17	53-58-788	006-11-439	/	0.709449 ± 13	0.709373 ± 6
I20	53-46-110	006-14-657	0.709397 ± 7 0.709177 ± 10 0.709179 ± 9	/	/
I21	53-44-126	006-15-717	/	0.709235 ± 15	0.709566 ± 8
I65	52-50-492	009-25-934	0.709265 ± 9 0.709241 ± 10 0.709412 ± 9	/	/
I85	55-14-084	006-30-914	0.707537 ± 9	0.708212 ± 8	/
Formation 5 – Lower Palaeozoic gabbro, dolerite and diorite (416–542 Ma)					
A03(1)	54-37-159	007-00-040	0.709500 ± 10 **0.712242 ± 10**	0.709789 ± 9	/
A03(2-bog)	54-37-055	006-59-735	0.709752 ± 10	/	/
Formation 8 – Caledonian (Silurian - Devonian) granite and granodiorite (359–444 Ma)					
I38	53-13-527	006-14-710	/	0.710125 ± 10	/
I44	53-08-216	006-18-584	/	**0.720011 ± 10**	/
I46	53-13-527	006-14-710	0.709628 ± 8	0.712058 ± 12	/
I54	53-15-788	009-10-633	/	0.709794 ± 11	0.709599 ± 9
I93	54-19-382	006-01-209	**0.766315 ± 95**	0.711756 ± 9	/

Table A.24 (*continued*)

Site	GPS-location		Values (± 2σ)		
	North	**West**	**Grass**	**Shrubs**	**Trees**
Formation 9 –Tertiary (Palaeogene) granite, felsite and granophyre (23–65 Ma)					
A18 – C	54-06-737	006-19-257	/	0.713011 ± 9	0.710335 ± 9
I94	54-11-394	006-04-566	0.713979 ± 8	0.716419 ± 41	0.712585 ± 11
I95	54-02-995	006-16-226	0.711108 ± 8	0.719498 ± 25	/
Formation 10 – Tertiary (Palaeogene) rhyolite (23–65 Ma)					
I06	54-46-718	006-09-100	/	0.707862 ± 7	0.708582 ± 7
Formation 11 – Tertiary (Palaeogene) basic intrusion, dolerite and gabbro (23–65 Ma)					
I15	54-03-435	006-16-174	/	0.708154 ± 12	0.708157 ± 6
Formation 19 – Slishwood Division (Neoproterozoic); Quartzo-feldspathic paragneiss (>542 Ma)					
A10	54-31-094	007-56-861	/	0.710009 ± 9	0.709352 ± 14
Formation 27 – Dalradian Argyll group; Psammitic and pelitic schist, marble, amphibolite, diamictite (>542 Ma)					
A08 – L	54-40-234	007-25-063	/	0.714330 ± 12	0.712345 ± 9
A09	54-40-844	007-27-526	/	0.711579 ± 12	0.709974 ± 7
Formation 29 – Sperrins Dalradian Southern Highland Group; Pelitic & psammitic schist, phyllite & marble (>542 Ma)					
I88	55-07-211	006-06-594	0.712568 ± 10	0.714015 ± 12	0.712568 ± 10
I89	55-01-443	006-56-216	/	0.708649 ± 10	0.708385 ±10
Formation 32 – Cambrian marine greywacke, shale, sandstone and quartzite (488–542 Ma)					
I40	53-08-730	006-09-254	0.711603 ± 8	0.708830 ± 10	/
Formation 33 – Lower-Mid Ordovician basic volcanic basalt (444–488 Ma)					
A04	54-36-956	007-04-698	0.709147 ± 11	0.708897 ± 12	0.711065 ± 11
A05	54-36-831	007-08-523	0.710569 ± 9	0.712146 ± 9	/
Formation 35 – Lower-Mid Ordovician slate (444–488 Ma)					
I43	53-06-462	006-13-33	0.709892 ± 7	0.708801 ± 12	/
Formation 39 – Mid-Upper Ordovician slate (444–488 Ma)					
I82	52-22-102	006-44-245	0.712728 ± 8	0.711154 ± 9	0.712577 ± 9
Formation 40 –Mid-Upper Ordovician Derryveeny formation; Marine to fluvial; Greywacke, shale, sandstone & conglomerate (444–488 Ma)					
A01 – BN	54-32-428	005-57-107	/	0.708457 ± 6	0.708310 ± 9
A16	54-13-862	006-52-225	/	0.712152 ± 11	0.712751 ± 7

Table A.24 (*continued*)

Site	GPS-location		Values (± 2σ)		
	North	**West**	**Grass**	**Shrubs**	**Trees**
Formation 42 – Ordovician - Silurian Rathkenny formation; "Moffat shale" facies; Shale and greywacke (416–488 Ma)					
I24	53-43-219	006-35-922	0.710787 ± 8	/	/
Formation 49 – Silurian deep marine turbidite sequence; mudstone, sandstone, greywacke, shale and conglomerate (416–444 Ma)					
A02	54-31-183	005-57-646	/	0.710811 ± 8	0.710373 ± 8
A17 – A	54-05-391	006-36-648	/	0.711202 ± 6	0.710512 ± 7
I19	53-48-127	006-22-125	0.711762 ± 7 0.710486 ± 8	/	/
I27	53-97-678	007-02-930	0.710315 ± 7 **0.708119 ± 8**	**0.708328 ± 12**	/
I35	53-36-770	006-19-048	/	0.709302 ± 14	0.709377 ± 9
I48	52-50-008	008-27-873	/	0.710889 ± 11	0.710786 ± 8
I80	52-19-552	007-34-591	/	0.711228 ± 11	0.710779 ± 7
I87	53-12-566	006-31-205	/	0.708757 ± 14	0.708914 ± 8
I91	53-47-584	006-17-304	0.711300 ± 9 0.711027 ± 8	0.711445 ± 11	/
I92	53-47-291	006-18-867	**0.714687 ± 11** 0.710293 ± 9	/	/
Formation 52 – Upper Silurian – lower Devonian continental redbed facies; Sandstone, siltstone & mudstone (359–444 Ma)					
A13	54-28-704	007-44-037	0.708946 ± 8	0.710409 ± 8	/
Formation 54 – Upper Devonian -Lower Carboniferous continental redbed facies; Sandstone, conglomerate & siltstone (299–416 Ma)					
I50	53-00-373	008-38-931	**0.719715 ± 8**	0.712282 ± 12	/
I79	52-19-750	007-43-688	0.709322 ± 8	0.711539 ± 12	0.711228 ± 11
Formation 56 – Carboniferous volcanic and minor intrusions; Basalt, trachyte, syenite & tuff					
I73	52-33-042	008-23-602	**0.714479 ± 11**	0.707709 ± 9 0.707619 ± 12	/
Formation 59 – Carboniferous shallow marine & coastal plain (basal clastics); Sandstone, mudstone and conglomerate (299–359 Ma)					
A06	54-38-672	007-19-694	/	0.709748 ± 11	0.710950 ± 7

Table A.24 (*continued*)

Site	GPS-location		Values (± 2σ)		
	North	West	Grass	Shrubs	Trees
Formation 63 – Carboniferous shallow marine & coastal plain (Basal Clastics); Sandstone, mudstone & conglomerate (299–359 Ma)					
A07	54-38-504	007-23-282	0.709613 ± 8	**0.712556 ± 11**	/
Formation 64 – Carboniferous marine shelf facies; Limestone & calcareous shale (299–359 Ma)					
A12	54-30-613	007-40-158	/	0.708305 ± 7	0.708167 ± 8
I22	53-43-471	006-25-639	/	0.709521 ± 14	0.709682 ± 5
I51	53-01-038	008-55-629	/	0.708490 ± 10	0.708320 ± 10
I97	53-02-962	009-08-451	0.708813 ± 7	0.708725 ± 15	/
I98 – P	52-59-289	009-05-736	0.708971 ± 8	/	0.708545 ± 8
Formation 65 – Carboniferous Visean basinal limestone; Marine basinal facies (Tobercolleen and Lucan Formations); Dark-grey argillaceous and cherty limestone & shale (299–359 Ma)					
I26	53-50-313	006-40-346	/	0.709575 ± 9	0.709248 ± 6
I28	53-46-909	007-19-785	0.708228 ± 7	0.708305 ± 13	/
I37	54-32-346	006-21-000	/	0.708884 ± 8	/
Formation 66 – Carboniferous Tyrone GP; Visean mudstone, sandstone and evaporite; Marginal marine (Mullaghmore, Downpatrick & Clogher Valley Formations) (299–359 Ma)					
A11	54-30-842	007-49-981	/	0.710056 ± 10	0.708650 ± 9
Formation 68 – Carboniferous Leitrim GP; Visean mudstone, sandstone and evaporite; Marginal marine (Meenymore Formation) (299–359 Ma)					
A15	54-15-992	007-23-407	/	0.708212 ± 9	0.708897 ± 9
Formation 70 – Carboniferous (Late Visean-Westphalian) continental redbed; Sandstone, conglomerate & mudstone (299–359 Ma)					
A14	54-24-437	007-35-923	/	0.709173 ± 12	0.712266 ± 9

Table A.24 (*continued*)

Site	GPS-location		Values (± 2σ)		
	North	**West**	**Grass**	**Shrubs**	**Trees**
Formation 71 – Carboniferous Namurian sandstone, shale; Fluvio-deltaic & basinal marine (Turbiditic); Shale, sandstone, siltstone & coal (299–359 Ma)					
I61	52-52-347	009-11-054	0.709795 ± 10	0.709871 ± 14	0.709516 ± 9
I62	52-52-879	009-17-547	0.710820 ± 12	0.710544 ± 14	0.710495 ± 8
I63	52-51-734	009-21-123	**0.718632 ± 9**	0.711837 ± 11	0.710106 ± 9
I64	52-48-201	009-27-171	0.711017 ± 10 0.710774 ± 8	0.709836 ± 10	/
I96	53-41-136	006-28-973	0.708677 ± 10	0.708911 ± 14	0.708937 ± 7
Knowth – K	53-42-076	006-29-478	**0.710756 ± 14**	0.708692 ± 8	/
Newgrange	53-41-683	006-28-535	0.709201 ± 8	/	/
Formation 75 – Triassic sandstone and mudstone with evaporite; Continental redbed facies, lagoonal & shallow marine (200–251 Ma)					
I31	53-54-574	006-47-298	0.710008 ± 8	0.708955 ± 8	/
Formation 79 – Palaeocene Lower Basalt Formation; Olivine basalt lava (56–65 Ma)					
I01 – BM	55-00-106	006-24-266	0.706915 ± 8	0.707287 ± 12	0.706485 ± 13
Formation 82 – Palaeocene Upper Basalt Formation; Olivine basalt lava (56–65 Ma)					
I03	55-06-749	006-40-060	0.710448 ± 9	0.709116 ± 14	0.709987 ± 12
I05	54-43-869	006-12-243	/	0.706724 ± 12	0.707360 ± 8
Formation 83 – Oligocene Lacustrine; Clay, sand & lignite (23–34 Ma)					
I02	55-06-617	006-26-261	/	0.707089 ± 12	0.707743 ± 7
I04	54-33-359	006-17-596	/	0.718187 ± 13	0.708123 ± 7

6.10 Fuels and additives

Various fuels and additives were used in the laboratory heating and outdoor burning experiments. Several fresh animal joints were burned (OUT) using different types of fuel, three of which were not modern and were chosen especially to combine stable carbon isotope analyses and radiocarbon dating. These three fuels were manufactured coal briquettes (Homefire Smokeless Fuel from CPL Products, UK) and two timbers whose age had been assessed by dendrochronology. The manufactured coal was radiocarbon dated. However, because it is manufactured coal (potentially heterogeneous), the age range could be much larger than shown by a single date. The two timbers gave ages as follows: Wood 1 (1730–1805 AD) and Wood 2 (1453–1607 AD). These dates were compared to the radiocarbon calibration curve (IntCal13 – Reimer et al. 2013) to obtain fraction modern carbon values ($F^{14}C$). The carbon isotope composition of the fuel samples were also measured before burning.

Table A.25 – Isotope analyses and chronological data for fuels and additives

Fuel/additive	Type	Dendrochronological date	$F^{14}C$	$\delta^{13}C$ (‰)
Wood 1 (208–283 yrs)	Old wood	1730–1805 AD	0.9787 ± 0.0029	-24.8
Wood 2 (406–560 yrs)	Old wood	1453–1607 AD	0.9554 ± 0.0029	-27.0
Wood 3	Modern wood	Modern		/
'Coal' 1 (OxA-24943)	Manufactured coal briquettes	/	0.0543 ± 0.0007	-24.3
'Coal' 2	Charcoal	/	/	/
BAR	Barley seeds	Modern		-26.8
MIL	Millet seeds	Modern		-12.9
CORN	Cornflour	Modern		-11.5
LARD	Pig lard	Modern		/